Targeting hepatic stellate cells to prevent or reverse liver fibrosis

Zhang, Mengfan

DOI:
10.33612/diss.146692010

university of groningen

Targeting hepatic stellate cells to prevent or reverse liver fibrosis

PhD thesis

to obtain the degree of PhD at the
University of Groningen
on the authority of the
Rector Magnificus Prof. C. Wijmenga
and in accordance with
the decision by the College of Deans.

This thesis will be defended in public on

Monday 23 November 2020 at 9.00 hours

by

Mengfan Zhang

born on 15 July 1989
in Henan, China

Supervisors
Prof. Dr. A.J. Moshage
Prof. Dr. K.N. Faber

Assessment Committee
Prof. Dr. M.C. Harmsen
Prof. Dr. J.K. Burgess
Prof. Dr. D.A. Mann

Paranimfen
Sandra Serna Salas
Zongmei Wu

Contents

Chapter 1

General Introduction

General introduction

Liver cirrhosis is the end stage of chronic liver diseases and causes more than 1 million deaths per year worldwide (1). In liver cirrhosis, the lobular architecture and vasculature are disrupted by excessive deposition of scar tissue. Variceal hemorrhage, hepatic encephalopathy and hepatic failure are the main lethal complications of decompensated liver cirrhosis. Additionally, cirrhosis is a risk factor for the development of hepatocellular carcinoma (2). To date, no medication is available to prevent or reverse liver cirrhosis. Patients with liver cirrhosis can only be cured by liver transplantation.

Chronic liver diseases of various etiology lead to cirrhosis, including liver damage induced by toxins, alcohol, viral infection, autoimmune disorders, metabolic and genetic disorders (2). According to recent epidemiological surveys, non-alcoholic fatty liver disease (NAFLD) is emerging as the leading cause of chronic liver disease in developed countries, whereas viral hepatitis is the prevailing etiology of cirrhosis in developing countries (1, 3). Based on advancing knowledge, NAFLD has been suggested to be termed Metabolic Associated Fatty Liver Disease (MAFLD) (4). Regardless of the etiology, the pathogenic mechanisms leading to liver cirrhosis are similar and start with chronic inflammation and the development of fibrosis. Liver fibrosis is defined as an intermediate stage in chronic liver diseases and, histologically, varies from fibrous expansion of portal tracts to bridging fibrosis. The histological alterations in the progression of chronic liver diseases is shown in Figure 1. These histopathological phenomena are the basis of the pathological scoring systems, e.g. the Ishak score and NAFLD activity score from the Non-alcoholic Steatohepatitis Clinical Research Network (NAS CRN) (5, 6).

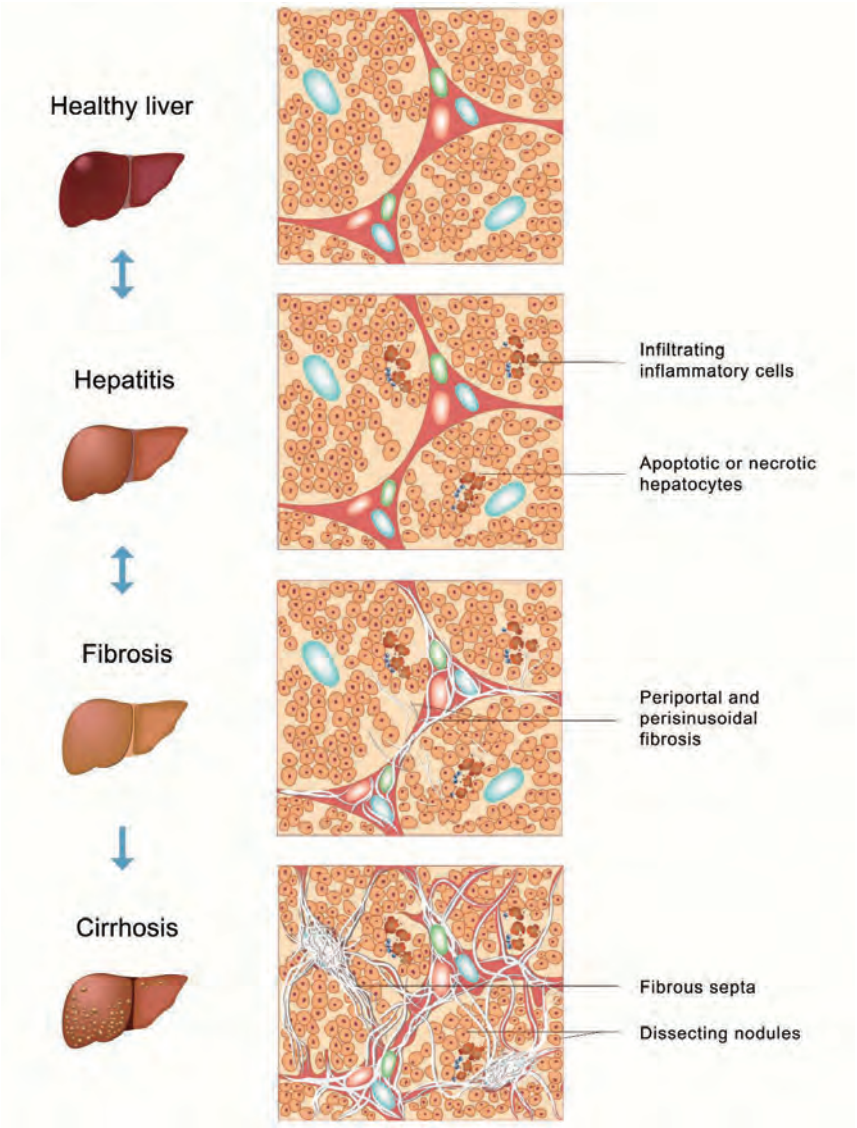

Figure 1. Histology of different stages of chronic liver diseases.

In the stage of hepatitis, apoptotic and necrotic hepatocytes recruit infiltrating inflammatory cells. Unresolved hepatic inflammation induces activation of hepatic stellate cells, which form the fibrous tissue. Liver fibrosis is a dynamic process and varies from periportal or perisinusoidal fibrosis to bridging fibrosis. With the progression of fibrosis and regeneration of hepatocytes, liver lobules are segmented by fibrous septa, forming dissecting nodules.

Excessive extracellular matrix (ECM) deposition is the hallmark of fibrosis. Important components of ECM are collagens, laminin, fibronectin and proteoglycans (7). Among the components of ECM, collagens are the most abundant. Collagens are mainly secreted by

profibrogenic myofibroblasts (7, 8). Collagen fibers have a triple-helix structure and contain the repeated peptide motif Gly-X-Y. Gly is glycine and X and Y can be any amino acid, although X is commonly a proline and Y is a hydroxyproline. The Gly-X-Y structure confers rigidity to collagen fibers, shown in Figure 2 (9). A cohort study demonstrated that the fibrosis stage, evaluated with the NASH Clinical Research Network (NASH CRN) Feature Scoring System, negatively correlates with long-term prognosis of patients with fibrosis (10). Therefore, it is important to diagnose and start therapy of fibrosis at an early stage to prevent progression of chronic liver disease. Multiple cell types are involved in the pathogenesis of liver fibrosis, making it difficult to select the right target cell type in the development of therapeutics for liver fibrosis. However, since myofibroblasts account for the pathological formation of fibrous tissue in the liver, inactivation and clearance of myofibroblasts are likely to alleviate liver fibrosis (11).

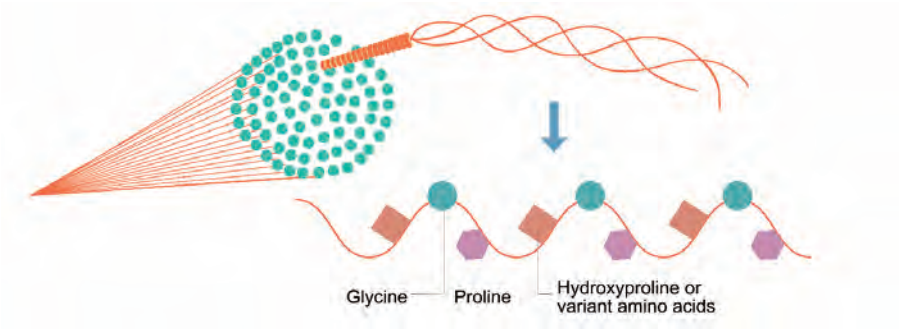

Figure 2. Collagen structure.

Collagens have a triple helix structure. Each chain of collagen contains the abundantly repeated peptide motif Gly-X-Y. Gly is glycine. X is commonly proline and Y is commonly hydroxyproline.

Pathogenic myofibroblasts can originate from hepatic stellate cells (HSCs), portal fibroblasts, circulating monocytes and bone marrow-derived mesenchymal cells and hepatocytes might also transdifferentiate to fibroblast-like cells during epithelial-to-mesenchymal transition (12, 13). Studies in animal models of liver fibrosis suggest that HSC are main precursors of myofibroblasts (14). HSC are the most abundant non-parenchymal cells in the liver and account for 5%-8% of the total cell population in the healthy liver (15). HSCs originate from mesothelial cells during embryonic development (16). HSCs are located in the space of Disse, which is the space between the sinusoidal endothelium and hepatocytes. In the healthy state, HSCs maintain a lipocyte-like phenotype and store retinyl esters. These HSCs are termed quiescent HSCs (qHSCs). About 80% of vitamin A in the human body is stored in qHSCs in large intracellular lipid droplets (17). Upon liver injury, qHSCs are stimulated by various stimuli and transdifferentiate into myofibroblast-like cells. The process of transdifferentiation of HSCs is termed activation and

transdifferentiated HSCs are termed activated HSCs. Activated HSCs (aHSCs) lose the ability to store retinyl esters, their lipid droplets disappear and they acquire a stretched morphology during activation (18). In contrast to qHSC, aHSCs show an increased ability to proliferate, migrate and contract and start secreting high amounts of ECM (11). HSCs are highly responsive to pro-inflammatory signals from inflammatory cells, but in addition, they also secrete various cytokines and chemokines themselves. In turn, these HSC-derived factors act on inflammatory cells during the pathogenesis of liver fibrosis, thereby forming an pathogenic amplifying loop (19, 20). During activation, HSCs lose the expression of the transcription factor peroxisome proliferator-activated receptor-gamma (PPARγ) and lecithin retinol acyltransferase (LRAT), but acquire expression of alpha-smooth muscle actin (αSMA) and collagen type 1 alpha-1 (COL1A1) (12). The differential expression of these proteins and distinct morphologies are common biomarkers used to differentiate between qHSC and aHSC.

Mechanisms involved in the activation of hepatic stellate cells

Activation of HSCs can be triggered by various endogenous and exogenous factors. Exogenous cytokines secreted from inflammatory cells or aHSCs themselves, including Transforming growth factor beta (TGF-β), Platelet-derived growth factor (PDGF) and Connective tissue growth factor (CTGF), have been demonstrated to activate HSCs (21, 22). In addition to cytokines, toxic compounds like ethanol and the released contents of necrotic cells are also activators of HSCs (22, 23). Furthermore, physical factors can contribute to the activation of HSCs, e.g. hypoxia and mechanical force have been demonstrated to contribute to the activation of HSCs (24, 25).

TGF-β is a well-known cytokine that activates HSCs and promotes fibrogenesis. SMADs are the canonical downstream signaling proteins of TGF-β (26). Activation of TGF-β signaling *in vivo* consists of a series of complex processes. TGF-β is synthesized as a latent precursor that needs to be cleaved by proteases to be activated. The C-terminus of TGF-β binds to the N-terminus of the Latency Associated Protein (LAP) to form the TGF-β latent complex, which is released and deposited in the surrounding ECM. Various factors induce the release of active TGF-β from the ECM. Upon binding of TGF-β to the TGF-β type Ⅱ receptor, the TGF-β type Ⅰ receptor is phosphorylated by the type Ⅱ receptor, leading to a conformational change in the TGF-β type Ⅰ receptor, which leads tophosphorylation of downstream targets, such as SMAD2 and SMAD3 (27). TGF-β/SMAD3 promotes the transdifferentiation of HSC and enhances the gene expression of COL1A1. Subsequently, aHSCs acquire the ability to secrete cytokines, including TGF-β, that in turn activate qHSCs in a paracrine manner (28, 29). Recent evidence has revealed the interaction between

TGF-β and mammalian target of rapamycin (mTOR) in the regulation of the inflammatory response and metabolism (30). mTOR is the important subunit of two complexes, mTORC1 and mTORC2. Over-activation of the mTORC1/p70S6K axis exacerbates liver fibrosis (31). The mTORC1/4E-BP1 axis has an important role in TGF-β-dependent collagen production (30). In HSCs, activation of mTOR signaling inhibits autophagy and increases HSC-derived extracellular vesicles release and fibrosis (32). These observations indicate an essential role of mTOR in the activation of HSCs.

Dysregulated intracellular signal transduction and metabolism can generate HSC activating signals as well (33). Nitric oxide (NO) is the first discovered gasotransmitter and is involved in many physiological processes. NO is produced by Nitric Oxide Synthases (NOS) that convert arginine into citrulline. Three isoforms of NOS are known: neuronal NOS (nNOS), inducible NOS (iNOS) and endothelial NOS (eNOS), which are encoded by NOS1, NOS2 and NOS3, respectively. NOS isoforms are expressed or can be induced (iNOS) in a wide variety of cell types. NO is a direct scavenger of ROS and can alleviate oxidative stress (34). As a gasotransmitter, NO activates soluble guanylate cyclase (sGC) increasing the intracellular concentration of cyclic guanosine monophosphate (cGMP). Several studies have demonstrated that the activation of sGC suppresses the activation of HSCs (35, 36). Inhibition of iNOS activity promotes the activation of fibroblasts and prevents the reversal of liver fibrosis (37, 38), supporting a role for the NOS-dependent NO-sGC pathway in the activation of HSC.

Arginase competes with NOS for the use of arginine as substrate in the cytoplasm. Arginase has two isoforms: Arginase-1 (ARG1) and Arginase-2 (ARG2). ARG1 is predominantly expressed in the cytoplasm of liver cells whereas ARG2 is localized in mitochondria of e.g. kidney cells (39). Differential arginine catabolism in macrophages is a well-known biomarker and regulator of macrophage polarization. Macrophage polarization is a process in which macrophages acquire different phenotypes in response to specific signals or stimuli. There are 2 distinct phenotypes of polarized macrophages: M1 phenotype: the classically activated pro-inflammatory macrophages, stimulated by e.g. lipopolysaccharide and the M2 phenotype: the alternatively activated pro-fibrogenic macrophages, stimulated by e.g. interleukin-4 (IL-4). M1 macrophages are characterized by iNOS expression, whereas M2 macrophages are characterized by ARG1 expression. Polarization of macrophages plays an important role in the modulation of fibrogenesis (40). Arginase converts arginine into ornithine, which is an amino acid that is not incorporated into proteins. In turn, ornithine can be converted by ornithine decarboxylase (ODC) into polyamines and by ornithine aminotransferase (OAT) into proline. Polyamines are necessary to maintain normal cell division and proline is the most abundant amino acid in

collagens and therefore essential in collagen synthesis (41). Since ornithine synthesis is dependent on arginase, it is very likely that arginase activity is involved in the activation of HSCs.

Hydrogen sulfide (H_2S) is another important gasotransmitter participating in a variety of physiological processes. H_2S is generated by three enzymes: cystathionine γ-lyase (CSE), cystathionine β-synthase (CBS) and 3-mercaptopyruvate sulfurtransferase (3-MST). L-cysteine and L-homocysteine are the main substrates for H_2S biosynthesis. H_2S modulates the Phosphoinositide 3-kinases (PI3K)-Akt, STAT3, Protein kinase C (PKC), Nuclear factor E2-related factor 2 (Nrf2) and Nuclear factor kappa B (NF-κB) signaling pathways (42). Dysregulated H_2S production is associated with liver fibrosis (43). H_2S protects hepatocytes against apoptosis via inhibiting the JNK/MAPK pathway (44). Endogenously generated H_2S promotes the bioenergetics of mitochondria and stimulates proliferation of HSCs (45). The heterogeneity in the observed effects of H_2S probably derives from differential expression of H_2S-producing enzymes in different cell types (44, 45).

Although the factors and mechanisms discussed above are key regulators of HSC activation, the full complexity of HSC activation, especially *in vivo*, is not completely elucidated yet.

Mechanisms that reverse hepatic stellate cell activation

Spontaneous resolution and regression of liver fibrosis has been observed in some cases upon removal of the injury (e.g. after hepatitis virus clearance). This phenomenon has also been demonstrated in experimental models of liver fibrosis (38). Once toxic stimuli are removed, most of the aHSCs are inactivated and revert to a quiescence-like phenotype without proliferation and collagen production. However, inactivated HSCs (iHSCs) have a gene expression profile that is different from both qHSCs and aHSCs. In addition, iHSCs are more sensitive to novel toxic stimuli, showing a stronger pro-fibrogenic response compared to aHSCs and qHSCs (46). A recent transcriptomic study demonstrated that some transcription factors, including members of the SRY-related HMG-box (SOX) and Signal Transducer and Activator of Transcription (STAT) families, are highly expressed in iHSCs (47). However, the reason why iHSCs exhibit a stronger response to injury remains unclear.

Cellular senescence is described as a terminal cell fate in which proliferating cells acquire a permanent cell cycle arrest (48). HSC senescence has been observed both in pre-clinical fibrosis models as well as in clinical samples (49-51). Senescent cells are characterized by a high activity of senescence-associated β-galactosidase (SA-β-Gal), high expression of cell cycle arrest genes, including CDKN1A ($P21^{CIP1}$), P53 and CDKN2A

($P16^{INK4A}$) and the expression of a senescence-associated secretory phenotype (SASP) (52). Senescent HSCs display reduced collagen production and cell proliferation. This suggests that induction of senescence in HSCs may be a promising strategy to resolve fibrosis (53). In experimental models of liver fibrosis, impaired senescence of HSCs in p53/p21 knockout mice has been shown to accelerate the progression of fibrogenesis (50). Senescent HSCs express MICA/ULBP2, which is a ligand for the NK cell receptor NKG2D that facilitates HSC clearance (54). Considering the advantages of cellular senescence, therapy-induced senescence has been proposed as a strategy to prevent or reverse liver fibrosis. Recently, curcumin, interleukin-22 and interleukin-10 have been demonstrated to alleviate liver fibrosis via inducing senescence of HSCs (55-57). However, it should be noted that accumulation of senescent cells and hepatocyte senescence may form a pro-inflammatory micro-environment that induces aging-related liver dysfunction. To avoid the disadvantages of senescence, clearing senescent cells, a process called senolysis, should be considered as a second-stage strategy (48, 58).

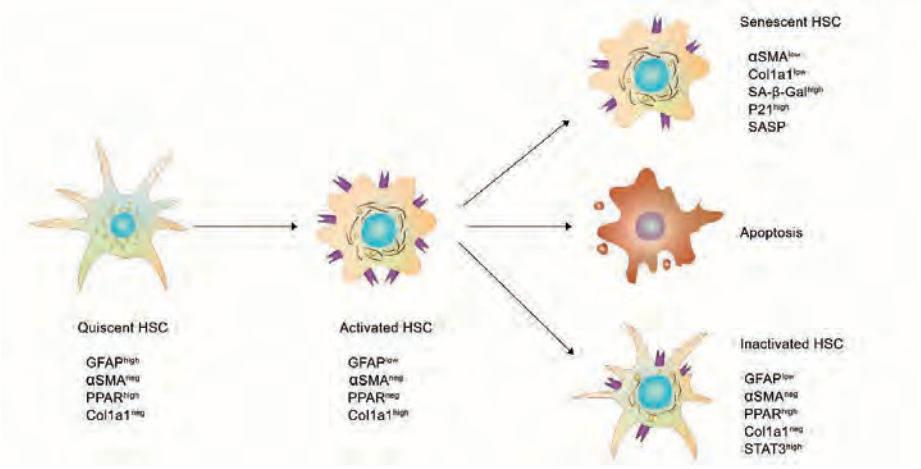

Figure 3. Different markers of hepatic stellate cells (HSCs).

During liver fibrosis, quiescent HSCs transdifferentiate into activated HSCs. Upon the removal of injurious stimuli, activated HSCs are inactivated into a quiescent-like phenotype (inactivated HSCs), but are highly responsive to novel injurious stimuli. Senescent HSCs acquire a less pro-fibrogenic phenotype, characterized by distinct markers like Senescence Associated β-Galactosidase (SA-β-Gal) activity, P21 and Senescence-Associated Secretory Phenotype (SASP).

The scope of this thesis

Chapter 1

In this chapter, we present a general introduction to liver fibrosis and hepatic stellate cells and discuss in more detail the various mechanisms and factors that are the subject of this thesis: cellular senescence, the gasotransmitters hydrogen sulfide and nitric oxide, arginine metabolism and TGF-β signaling.

Chapter 2

In this chapter, we review the current literature on senescence in hepatic stellate cells and the potential of induction of senescence as a therapeutic intervention to inhibit or reverse HSC activation and attenuate liver fibrosis.

Chapter 3

In this chapter, we study the potential of the bioactive coumarin-like compound esculetin to induce senescence in HSC. Biomarkers of HSC activation, proliferation and senescence were investigated to elucidate the association between cellular senescence and HSC inactivation. The PI3K-Akt signaling pathway was investigated in detail, since it proved to be a target of esculetin.

Chapter 4

In this chapter, differential expression of H_2S-producing enzymes and production of H_2S were investigated during HSC activation. Inhibitors of H_2S-producing enzymes, e.g. DL-PAG and AOAA, were used to elucidate the role of H_2S on HSC activation. In addition, we used the H_2S donor GYY4137 to elucidate the effect of exogenous H_2S on the activation of HSCs. Mitochondrial activity was analyzed to investigate the association between H_2S and cellular bioenergetics.

Chapter 5

In chapters 3 and 4, we showed an association between H_2S and HSC activation and an association between cellular senescence and HSC activation, respectively. In chapter 5, we combine this knowledge and investigated the association between induction of cellular senescence and decreased H_2S production.

Chapter 6

Pirfenidone is a broad-spectrum anti-fibrotic drug that has been approved for the clinical

treatment of idiopathic pulmonary fibrosis. In addition, preclinical evidence has demonstrated an anti-fibrotic effect of pirfenidone on hepatic and nephrotic fibrogenesis. In view of the similar mechanisms of fibrogenesis, the effect of pirfenidone on primary human intestinal fibroblasts, as an *in vitro* model of intestinal fibrogenesis, was investigated. The TGF-β/mTOR signaling pathway was investigated to elucidate the mechanism of the anti-fibrotic effect of pirfenidone.

Chapter 7

In this chapter, differential expression of arginine-catabolizing enzymes was analyzed in HSC at different states of activation. The arginase inhibitor Nor-NOHA was used to block the arginase activity of HSCs to investigate its effect on collagen synthesis and HSC proliferation.

Chapter 8

The results of this thesis and future perspectives are discussed in this chapter.

References

1. Sepanlou SG, Safiri S, Bisignano C, Ikuta KS, Merat S, Saberifiroozi M, Poustchi H, et al. The global, regional, and national burden of cirrhosis by cause in 195 countries and territories, 1990–2017: a systematic analysis for the Global Burden of Disease Study 2017. The Lancet Gastroenterology & Hepatology 2020;5:245-266.

2. Schuppan D, Afdhal NH. Liver Cirrhosis. Lancet 2008;371:838-851.

3. Simeone JC, Bae JP, Hoogwerf BJ, Li Q, Haupt A, Ali AK, Boardman MK, et al. Clinical course of nonalcoholic fatty liver disease: an assessment of severity, progression, and outcomes. Clin Epidemiol 2017;9:679-688.

4. Eslam M, Sanyal AJ, George J, International Consensus P. MAFLD: A Consensus-Driven Proposed Nomenclature for Metabolic Associated Fatty Liver Disease. Gastroenterology 2020;158:1999-2014 e1991.

5. Goodman ZD. Grading and staging systems for inflammation and fibrosis in chronic liver diseases. J Hepatol 2007;47:598-607.

6. Kleiner DE, Brunt EM, Van Natta M, Behling C, Contos MJ, Cummings OW, Ferrell LD, et al. Design and validation of a histological scoring system for nonalcoholic fatty liver disease. Hepatology 2005;41:1313-1321.

7. Iredale JP, Thompson A, Henderson NC. Extracellular matrix degradation in liver fibrosis: Biochemistry and regulation. Biochim Biophys Acta 2013;1832:876-883.

8. Baiocchini A, Montaldo C, Conigliaro A, Grimaldi A, Correani V, Mura F, Ciccosanti F, et al. Extracellular Matrix Molecular Remodeling in Human Liver Fibrosis Evolution. PLoS One 2016;11:e0151736.

9. Shoulders MD, Raines RT. Collagen structure and stability. Annu Rev Biochem 2009;78:929-958.

10. Angulo P, Kleiner DE, Dam-Larsen S, Adams LA, Bjornsson ES, Charatcharoenwitthaya P, Mills PR, et al. Liver Fibrosis, but No Other Histologic Features, Is Associated With Long-term Outcomes of Patients With Nonalcoholic Fatty Liver Disease. Gastroenterology 2015;149:389-397 e310.

11. Tsuchida T, Friedman SL. Mechanisms of hepatic stellate cell activation. Nat Rev Gastroenterol Hepatol 2017.

12. Kisseleva T. The origin of fibrogenic myofibroblasts in fibrotic liver. Hepatology

2017;65:1039-1043.

13. Taura K, Iwaisako K, Hatano E, Uemoto S. Controversies over the Epithelial-to-Mesenchymal Transition in Liver Fibrosis. J Clin Med 2016;5.

14. Iwaisako K, Jiang C, Zhang M, Cong M, Moore-Morris TJ, Park TJ, Liu X, et al. Origin of myofibroblasts in the fibrotic liver in mice. Proc Natl Acad Sci U S A 2014;111:E3297-3305.

15. Yin C, Evason KJ, Asahina K, Stainier DY. Hepatic stellate cells in liver development, regeneration, and cancer. J Clin Invest 2013;123:1902-1910.

16. Asahina K, Zhou B, Pu WT, Tsukamoto H. Septum transversum-derived mesothelium gives rise to hepatic stellate cells and perivascular mesenchymal cells in developing mouse liver. Hepatology 2011;53:983-995.

17. Bobowski-Gerard M, Zummo FP, Staels B, Lefebvre P, Eeckhoute J. Retinoids Issued from Hepatic Stellate Cell Lipid Droplet Loss as Potential Signaling Molecules Orchestrating a Multicellular Liver Injury Response. Cells 2018;7.

18. Shang L, Hosseini M, Liu X, Kisseleva T, Brenner DA. Human hepatic stellate cell isolation and characterization. J Gastroenterol 2018;53:6-17.

19. Fujita T, Narumiya S. Roles of hepatic stellate cells in liver inflammation: a new perspective. Inflamm Regen 2016;36:1.

20. Li Y, Kim BG, Qian S, Letterio JJ, Fung JJ, Lu L, Lin F. Hepatic Stellate Cells Inhibit T Cells through Active TGF-beta1 from a Cell Surface-Bound Latent TGF-beta1/GARP Complex. J Immunol 2015;195:2648-2656.

21. Kocabayoglu P, Lade A, Lee YA, Dragomir AC, Sun X, Fiel MI, Thung S, et al. beta-PDGF receptor expressed by hepatic stellate cells regulates fibrosis in murine liver injury, but not carcinogenesis. J Hepatol 2015;63:141-147.

22. Chen L, Charrier AL, Leask A, French SW, Brigstock DR. Ethanol-stimulated differentiated functions of human or mouse hepatic stellate cells are mediated by connective tissue growth factor. J Hepatol 2011;55:399-406.

23. Zhan S-S, Jiang JX, Wu J, Halsted C, Friedman SL, Zern MA, Torok NJ. Phagocytosis of apoptotic bodies by hepatic stellate cells induces NADPH oxidase and is associated with liver fibrosisin vivo. Hepatology 2006;43:435-443.

24. Yu F, Dong B, Dong P, He Y, Zheng J, Xu P. Hypoxia induces the activation of hepatic stellate cells through the PVT1-miR-152-ATG14 signaling pathway. Mol Cell Biochem 2020;465:115-123.

25. Olsen AL, Bloomer SA, Chan EP, Gaca MD, Georges PC, Sackey B, Uemura M, et al. Hepatic stellate cells require a stiff environment for myofibroblastic differentiation. Am J Physiol Gastrointest Liver Physiol 2011;301:G110-118.

26. Yoshida K, Matsuzaki K. Differential Regulation of TGF-beta/Smad Signaling in Hepatic Stellate Cells between Acute and Chronic Liver Injuries. Front Physiol 2012;3:53.

27. Dewidar B, Meyer C, Dooley S, Meindl-Beinker AN. TGF-beta in Hepatic Stellate Cell Activation and Liver Fibrogenesis-Updated 2019. Cells 2019;8.

28. Xu MY, Hu JJ, Shen J, Wang ML, Zhang QQ, Qu Y, Lu LG. Stat3 signaling activation crosslinking of TGF-beta1 in hepatic stellate cell exacerbates liver injury and fibrosis. Biochim Biophys Acta 2014;1842:2237-2245.

29. Wright JH, Johnson MM, Shimizu-Albergine M, Bauer RL, Hayes BJ, Surapisitchat J, Hudkins KL, et al. Paracrine activation of hepatic stellate cells in platelet-derived growth factor C transgenic mice: evidence for stromal induction of hepatocellular carcinoma. Int J Cancer 2014;134:778-788.

30. Woodcock HV, Eley JD, Guillotin D, Platé M, Nanthakumar CB, Martufi M, Peace S, et al. The mTORC1/4E-BP1 axis represents a critical signaling node during fibrogenesis. Nature Communications 2019;10.

31. Shan L, Ding Y, Fu Y, Zhou L, Dong X, Chen S, Wu H, et al. mTOR Overactivation in Mesenchymal cells Aggravates CCl4- Induced liver Fibrosis. Sci Rep 2016;6:36037.

32. Gao J, Wei B, de Assuncao TM, Liu Z, Hu X, Ibrahim S, Cooper SA, et al. Hepatic stellate cell autophagy inhibits extracellular vesicle release to attenuate liver fibrosis. J Hepatol 2020.

33. Hou W, Syn WK. Role of Metabolism in Hepatic Stellate Cell Activation and Fibrogenesis. Front Cell Dev Biol 2018;6:150.

34. Iwakiri Y, Kim MY. Nitric oxide in liver diseases. Trends Pharmacol Sci 2015;36:524-536.

35. Sandner P, Stasch JP. Anti-fibrotic effects of soluble guanylate cyclase stimulators and activators: A review of the preclinical evidence. Respir Med 2017;122 Suppl 1:S1-S9.

36. Hall KC, Bernier SG, Jacobson S, Liu G, Zhang PY, Sarno R, Catanzano V, et al. sGC stimulator praliciguat suppresses stellate cell fibrotic transformation and inhibits fibrosis and inflammation in models of NASH. Proc Natl Acad Sci U S A 2019;116:11057-11062.

37. Sciacca M, Belgorosky D, Zambrano M, Gomez Escalante JI, Roca F, Langle YV, Sandes EO, et al. Inhibition of breast tumor growth by N(G)-nitro-l-arginine methyl ester (l-NAME) is accompanied by activation of fibroblasts. Nitric Oxide 2019;93:34-43.

38. Lukivskaya O, Patsenker E, Lis R, Buko VU. Inhibition of inducible nitric oxide synthase activity prevents liver recovery in rat thioacetamide-induced fibrosis reversal. Eur J Clin Invest 2008;38:317-325.

39. Pernow J, Jung C. Arginase as a potential target in the treatment of cardiovascular disease: reversal of arginine steal? Cardiovasc Res 2013;98:334-343.

40. Tacke F. Targeting hepatic macrophages to treat liver diseases. J Hepatol 2017;66:1300-1312.

41. Bronte V, Zanovello P. Regulation of immune responses by L-arginine metabolism. Nat Rev Immunol 2005;5:641-654.

42. Li L, Rose P, Moore PK. Hydrogen sulfide and cell signaling. Annu Rev Pharmacol Toxicol 2011;51:169-187.

43. Wu DD, Wang DY, Li HM, Guo JC, Duan SF, Ji XY. Hydrogen Sulfide as a Novel Regulatory Factor in Liver Health and Disease. Oxid Med Cell Longev 2019;2019:3831713.

44. Li X, Lin J, Lin Y, Huang Z, Pan Y, Cui P, Yu C, et al. Hydrogen sulfide protects against acetaminophen-induced acute liver injury by inhibiting apoptosis via the JNK/MAPK signaling pathway. J Cell Biochem 2019;120:4385-4397.

45. Damba T, Zhang M, Buist-Homan M, van Goor H, Faber KN, Moshage H. Hydrogen sulfide stimulates activation of hepatic stellate cells through increased cellular bio-energetics. Nitric Oxide 2019;92:26-33.

46. Troeger JS, Mederacke I, Gwak GY, Dapito DH, Mu X, Hsu CC, Pradere JP, et al. Deactivation of hepatic stellate cells during liver fibrosis resolution in mice. Gastroenterology 2012;143:1073-1083 e1022.

47. Liu X, Xu J, Rosenthal S, Zhang LJ, McCubbin R, Meshgin N, Shang L, et al. Identification of Lineage-Specific Transcription Factors That Prevent Activation of Hepatic Stellate Cells and Promote Fibrosis Resolution. Gastroenterology 2020;158:1728-1744 e1714.

48. Aravinthan AD, Alexander GJ. Senescence in chronic liver disease: Is the future in aging? J Hepatol 2016;65:825-834.

49. Gutierrez-Reyes G, del Carmen Garcia de Leon M, Varela-Fascinetto G, Valencia P, Perez Tamayo R, Rosado CG, Labonne BF, et al. Cellular senescence in livers from children with end stage liver disease. PLoS One 2010;5:e10231.

50. Krizhanovsky V, Yon M, Dickins RA, Hearn S, Simon J, Miething C, Yee H, et al. Senescence of activated stellate cells limits liver fibrosis. Cell 2008;134:657-667.

51. Paradis V, Youssef N, Dargere D, Ba N, Bonvoust F, Deschatrette J, Bedossa P. Replicative senescence in normal liver, chronic hepatitis C, and hepatocellular carcinomas. Hum Pathol 2001;32:327-332.

52. Sharpless NE, Sherr CJ. Forging a signature of in vivo senescence. Nat Rev Cancer 2015;15:397-408.

53. Schnabl B, Purbeck CA, Choi YH, Hagedorn CH, Brenner D. Replicative senescence of activated human hepatic stellate cells is accompanied by a pronounced inflammatory but less fibrogenic phenotype. Hepatology 2003;37:653-664.

54. Jin H, Jia Y, Yao Z, Huang J, Hao M, Yao S, Lian N, et al. Hepatic stellate cell interferes with NK cell regulation of fibrogenesis via curcumin induced senescence of hepatic stellate cell. Cell Signal 2017;33:79-85.

55. Jin H, Lian N, Zhang F, Chen L, Chen Q, Lu C, Bian M, et al. Activation of PPARgamma/P53 signaling is required for curcumin to induce hepatic stellate cell senescence. Cell Death Dis 2016;7:e2189.

56. Kong X, Feng D, Wang H, Hong F, Bertola A, Wang FS, Gao B. Interleukin-22 induces hepatic stellate cell senescence and restricts liver fibrosis in mice. Hepatology 2012;56:1150-1159.

57. Huang YH, Chen MH, Guo QL, Chen YX, Zhang LJ, Chen ZX, Wang XZ. Interleukin10 promotes primary rat hepatic stellate cell senescence by upregulating the expression levels of p53 and p21. Mol Med Rep 2018;17:5700-5707.

58. Amor C, Feucht J, Leibold J, Ho YJ, Zhu C, Alonso-Curbelo D, Mansilla-Soto J, et al. Senolytic CAR T cells reverse senescence-associated pathologies. Nature 2020.

Chapter 2

Cellular Senescence of Hepatic Stellate Cell in Liver Fibrosis: characteristics, Mechanisms and Perspectives

Mengfan Zhang[1], Sandra Serna-Salas[1] ,Turtushikh Damba[1], Michaela Borghesan[2], Marco Demaria[2], Han Moshage[1]

[1]Dept. of Gastroenterology and Hepatology and [2]European Research Institute on the Biology of Aging (ERIBA), University Medical Center Groningen, University of Groningen, Groningen, the Netherlands

Correspondence: Han Moshage, PhD

E mail address: a.j.moshage@umcg.nl

1.Introduction

Chronic liver diseases of diverse etiology, including toxic injury, viral infection, autoimmune disorders, metabolic and genetic disorders can evolve into liver fibrosis. Liver fibrosis is characterized by excessive accumulation of extracellular matrix (ECM) and is considered an intermediate stage which can still be reversed or advance to cirrhosis and end-stage liver disease (1). Epidemiological data demonstrate that cirrhosis leads to 1.03 million deaths per year worldwide (2). Interventions at the stage of fibrosis are aimed to limit disease progression and prevent progression to cirrhosis.

The main characteristic of liver fibrosis is the excessive production of ECM. ECM is produced by fibrogenic myofibroblast (3). Myofibroblasts are (almost) absent in normal tissue and only transiently activated during tissue injury to produce ECM and scar tissue in the process of controlled wound healing (4). The source of myofibroblasts can be epithelial cells, mesenchymal stromal cells (MSCs), fibrocytes, mesothelial cells, hepatic stellate cells (HSCs) and portal fibroblasts (PFs) (3). Among these, HSCs are the predominant source of myofibroblasts in various models of experimental fibrosis (3, 5, 6).

The hepatic stellate cell is the most abundant non-parenchymal cell type in the liver (4). HSCs originate from mesothelial cells during embryonic development and reside in the subendothelial space of Disse (7). In normal healthy liver, HSCs store vitamin A and do not proliferate. These HSCs are termed quiescent hepatic stellate cells (qHSCs) and are characterized by the presence of lipid droplets containing vitamin A and the expression of platelet-derived growth factor receptor‐β (PDGFRβ), lecithin retinol acyltransferase (LRAT), desmin and glial fibrillary acidic protein (GFAP) (4). In response to profibrotic stimuli, qHSCs activate and transdifferentiate into myofibroblast-like cells and play an essential role in tissue repair. Compared to qHSCs, activated HSC (aHSC) acquire novel characteristics including proliferation, contractility, enhanced ECM synthesis, chemotaxis and generation of inflammatory signals (4). Activation of HSCs can be self-driven, e.g. when cultured *in vitro* on tissue culture plastic. Activated HSCs lose their cytoplasmic vitamin A droplets, acquire a stretched morphology and contractile properties and have different transcriptional characteristics, including increased expression of alpha actin 2 (ACTA2) and collagen type 1 alpha 1 (COL1A1) and reduced expression of peroxisome proliferator-activated receptor gamma (PPARG) and GFAP (3).

In experimental hepatic fibrosis, the fibrotic liver can revert to the normal state upon removal of the pro-fibrotic stimuli, a process known as fibrosis resolution (8, 9). During fibrosis resolution, aHSCs spontaneously initiate apoptosis or revert to the inactive phenotype. HSC apoptosis partially contributes to early resolution while inactivation of surviving aHSC accounts for mid to late stages of resolution (8-10). Inactivated HSCs

(iHSCs) downregulate expression of activation markers including COL1A1, ACATA2 and TIMP1, re-express quiescence markers like PPARG and restore vitamin A droplets. However, iHSCs are not identical to qHSCs since they do not completely revert to the quiescent phenotype. E.g. iHSCs do not restore transcription of GFAP and are more responsive to repeated fibrogenic stimuli compared to qHSCs (9).

Cellular senescence is a physiological process in which proliferating cells enter a state of permanent or stable cell cycle arrest and do not respond to mitogens (11). Besides apoptosis, senescence is another fate of aHSCs in the reversal of fibrosis (12). Senescent HSCs acquire a less fibrogenic phenotype, thereby limiting the progression of fibrosis (12, 13). Hence, induction of senescence in HSCs may serve as a promising anti-fibrotic strategy. In the following paragraphs, we review the characteristics, mechanisms and possible effects of cellular senescence on liver fibrosis.

2.Characteristics of senescent cells

Cellular senescence is a stable cell cycle arrest program, first described in primary human fibroblasts that had reached replicative exhaustion *in vitro* (14, 15). Replicative senescence was already associated with telomere length regulation. Due to the 'end-replication problem' of DNA polymerase, telomeres become progressively shorter with every cell division (16, 17). Eventually, short telomeres are sensed as double-strand breaks (DSBs) by the DNA Damage Response (DDR) machinery leading to senescence via activation of the tumor suppressor protein p53 (18). Loss of proliferation is accompanied by changes in gene expression and cell morphology, consistently used as principle determinants of senescence in cell culture. Specifically, senescent cells display loss of DNA synthesis, enlarged and flattened cell morphology, enhanced β-galactosidase (SA-β-gal) activity, accumulation of heterochromatin foci (SAHFs) and a hypersecretory phenotype (Figure 1) (19). Senescence was originally thought to be an intrinsic cellular mechanism. Although this might be the case for replicative senescence, it is now established that other stressors may induce an indistinguishable senescence phenotype termed stress-induced senescence or premature senescence (19, 20). As the list of senescence types and effector pathways grows, it becomes more evident that the phenotypic markers of senescence vary depending on the context, the stimuli and the cell type (11, 21). Endogenous β galactosidase is a lysosomal enzyme, with maximum activity at pH 4.0-4.5 (15). SA-β gal activity is usually measured at pH 6.0 with the artificial substrate X-Gal and this assay is most commonly used to determine senescence. Determination of β- galactosidase activity at the suboptimal pH 6.0 demonstrates a high level of expression in senescent cells (16). However, this activity can also be detected in cells with increased lysosomal number and size, e.g. during autophagy. Contact inhibition in long-term cell cultures also induces

β-galactosidase activity in quiescent cells (14). Therefore, a high β-galactosidase activity is not specific for senescent cells and a combinatorial marker strategy for the identification of senescent cells should be preferred. Several studies have identified senescence-associated gene expression signatures (21-24), which revealed changes in cell-cycle regulators as expected. Two cell-cycle inhibitors that are often expressed by senescent cells are the cyclin-dependent kinase inhibitors (CDKIs) CDKN1a (also termed Waf1, encodes p21Cip1) and INK4a (also termed CDKN2a, encodes p16INK4a). On the other hand, senescent cells repress genes that encode proteins involved in cell-cycle progression; some of them are E2F targets (for example, replication-dependent histones, c-FOS, cyclin A, cyclin B and PCNA) (25, 26). Interestingly, the quest for senescence-specific gene expression signatures also revealed that besides changes in cell-cycle regulators, senescent cells exhibited changes in genes that appeared to be unrelated with growth arrest (21, 22, 27). These include the upregulation of multiple secreted factors that are known to alter the tissue microenvironment and are thought to contribute to age-related pathologies. The senescent-associated secretory phenotype (SASP) can trigger different and, sometimes, opposing effects in the microenvironment and surrounding cells. Work by Campisi's group suggests that factors secreted by senescent fibroblasts promote cancer progression (28-30), however, besides its implication in tumor clearance by the immune system (31), several studies suggest that the SASP also has an important role in establishing and maintaining the senescent state itself. Some of the factors secreted by senescent cells were shown to have tumor suppressive roles. The plasminogen activator inhibitor (PAI)-1 is necessary and sufficient for the induction of senescence (32). Insulin-like growth factor-binding protein 7 (IGFBP7) was shown to mediate senescence induced by oncogenic BRAF (33). Likewise, pro-inflammatory cytokines and chemokines secreted by senescent cells, such as IL-8, CXCL1, IL-6, and their receptors have been shown to be upregulated during senescence and their depletion partially bypasses replicative and oncogene-induced senescence (34, 35). Recent finding also described the SASP as a highly heterogeneous plethora of circulating factors, including cell-derived small extracellular vesicles or sEV (36). Facultative heterochromatin are condensed, transcriptionally silent chromatin regions that can reverse condensation to allow gene transcription (37). SAHF was first described in nuclei of senescent cells containing 30–50 bright, punctate DNA-dense foci that can be distinguished from chromatin of normal cells (38). SAHF are specialized domains of facultative heterochromatin, characterized by heterochromatic histone modifications and the presence of heterochromatic proteins, histone variant macro H2A, high-mobility group A (HMGA) proteins and late replicating regions in the genome (39). Histone methylation, specifically histone 3 lysine 4 trimethylation (H3K4me3) (activating) and H3K27me3 (repressing) are epigenetic modifications that are highly associated with gene transcription and linked to

lifespan regulation in many organisms (40). More than 30% of chromatin is reorganized in senescent cells. This reorganization includes the formation of large-scale domains (mesas) of H3K4me3 and H3K27me3 over lamin-associated domains (LADs), as well as depletion (canyons) of H3K27me3 outside of LADs, indicating profound changes in the transcriptional profile of senescent cells (41).

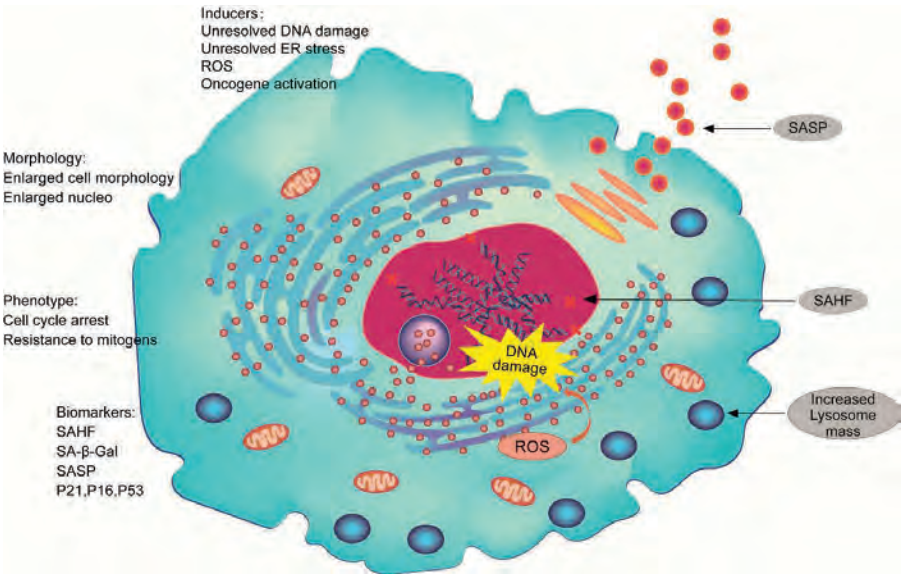

Figure 1, Characteristics of senescent cells.

The triggers, morphology, phenotype and biomarkers of cellular senescence are illustrated. ROS, reactive oxygen species; SASP, senescence associated secretory phenotype; SAHF, senescence associated heterochromatin foci; SA-β-Gal, senescence associated β galactosidase.

3.Mechanisms that regulate hepatic stellate cell senescence

3.1. DNA damage response

Isolated primary HSCs can only be cultured for a limited number of passages and eventually undergo replicative senescence (42, 43). In addition, cellular senescence can be triggered by a variety of intrinsic stressors, e.g. lysosomal stress, the unfolded protein response (UPR), oncogene activation and reactive oxygen species (ROS) generation leading to unresolved DNA damage (44, 45).

In a typical mammalian cell, the incidence of spontaneous DNA damage is estimated to be less than 2×10^5 lesions per day (46). The majority of damaged DNA can be repaired and is unlikely to drive the senescence process. However, a persistent DDR can drive cell senescence (47). Single-stranded and/or double-stranded DNA breaks (SSBs or DSBs,

respectively) are activators of the DDR (48). The Mre11-Rad50-Nbs1 (MRN) complex is the sensor of double-stranded DNA damage (49). Upon DSB, MRN complexes recruit and activate Ataxia-Telangiectasia Mutated (ATM) or ATM- and Rad3-related (ATR) kinases that activate CHK1 and CHK2 (check point kinase 1 and 2, respectively) (18, 50). Activated CHK1 promotes the degradation of CDC25A, a phosphatase that removes inhibitory modifications from cyclin dependent kinases (CDKs). ATM can phosphorylate p53 on multiple sites, including S15, which has been demonstrated to inhibit its interaction with the ubiquitin ligase MDM2, resulting in p53 stabilization and initiation of senescence (50). Upon SSB, poly-(ADP)ribose polymerase (PARP), predominantly PARP1, which senses the breaks, initiates DDR and probably induces p16-dependent cellular senescence (51).

Senescence has a heterogeneous phenotype and is driven by multiple stressors. It is a highly coordinated and regulated process (Figure 2). A summary of the main regulators and pathways of senescence is presented in the subsequent paragraphs.

3.2. NF-κB signaling

The hierarchy of the networks inducing a secretory phenotype is still unclear. Yet the transcription of several SASP genes primarily depends on two transcription factors (TFs): nuclear factor-kappa B (NF-κB) and CCAAT/enhancer binding protein beta (C/EBPβ) (34, 35, 52).

The NF-κB transcription factor family consists of five proteins: p65 (RelA), RelB, c-Rel, p105/p50 (NF-κB1), and p100/52 (NF-κB2) that associate with each other to form distinct transcriptionally active homo- and heterodimeric protein complexes. In most cells, NF-κB dimers are sequestrated in an inactive form in the cytosol through their interaction with IκB proteins. Degradation of these inhibitors upon their phosphorylation by the IκB kinase (IKK) complex leads to nuclear translocation of NF-κB dimers and induces transcription of their target genes (53). NF-κB activation includes two major signaling pathways: the canonical and the non-canonical NF-κB signaling pathways. The canonical pathway is induced by inflammatory stimuli including TNFα, IL-1 or LPS and uses a large variety of signaling adaptors to engage IKK activity. The non-canonical pathway depends on NIK (NF-κB-inducing kinase)-induced activation of IKKα. The canonical pathway mediates the activation of NF-κB1/p50, RelA/p65 and c-Rel, whereas the non-canonical NF-κB pathway selectively activates p100-sequestered NF-κB members, predominantly NF-κB2/p52 and RelB (54). Among all the dimers, the p50/65 heterodimer is the most abundant. The proportion of NF-κB dimers varies depending on the cell type. In addition, not all combinations of NF-κB dimers are transcriptionally active. Only p65, RelB and c-Rel contain carboxy-terminal transactivation domains to induce NF-κB dependent gene transcription.

Homo- and heterodimers of p50 and p52 inhibit NF-κB dependent gene transcription via competition with other dimers to bind to the κB sites of genes (53).

As mentioned before, the DNA damage response is essential for the induction of senescence. NF-κB is a master regulator of the genotoxic stress-induced cell response and both of the canonical and the non-canonical pathway can be activated by the DNA damage response (55). E.g., NF-κB-regulated gene expression increases in fibroblasts in response to UVA or UVB irradiation-induced DNA damage (56). Following DNA damage, ATM is activated and causes sustained NF-κB activation, independent of p53 signaling (57). In addition, the DNA damage response kinases ATM and ATR activate GATA4 which in turn activates NF-κB to facilitate senescence induction thus constituting a positive feedback loop (58). NF-κB and C/EBPβ are activated and enriched in the chromatin fraction in oncogene-induced senescent cells (35, 52). NF-κB also showed increased DNA-binding activity in replicative-, irradiation- and chemotherapy-induced senescent cells (52, 59-61). Depletion of the NF-κB subunit p65 reduced expression of many pro-inflammatory SASP factors in OIS and IR-induced senescence (52, 59). NF-κB directly controls transcription by binding to promoters of SASP components including IL-8, IL-6 and GM-CSF (59). C/EBPβ on the other hand is recruited specifically to the IL-6 promoter and C/EBPβ knockdown caused a collapse of the whole inflammatory network mainly due to disruption of IL-6 autocrine signaling (35). NF-κB and C/EBPβ are critical regulators of the SASP. In fact it seems that DDR and p38 signaling converge to NF-κB activation (59).

Sustained activation of NF-κB is required for the progression of senescence. In a mouse model of aging driven by *Ercc1* deficiency and presenting as the failure to repair stochastic endogenous DNA damage, additional genetic depletion of p65 attenuates aging symptoms (62). Oxidative stress is well-known to induce DNA damage in cells (63). Over-activation of NF-κB via deletion of its inhibitor c-*abl* increases fibroblast resistance to apoptosis, indicating that NF-κB activation contributes to the anti-apoptotic phenotype of senescent cells (64). In line with this, loss of *Nfkb1*, one of the canonical NF-κB subunits, promotes nuclear translocation of the p65/p65 homodimer, leading to reduced apoptosis and increased accumulation of senescent cells with DNA damage (65). In addition, NF-κB signaling is known to control the senescence associated secretory phenotype and may play a key role in SASP-induced paracrine senescence (66, 67). In contrast, knockdown or pharmacological inhibition of NF-κB reduces the number of senescent cells (68, 69).

3.3. PI3K-Akt pathway

The phosphatidylinositol-3-kinase (PI3K) pathway regulates a wide range of target proteins and Akt is one of the main downstream targets of PI3K. The PI3K-Akt axis

modulates a variety of cellular process, including survival and proliferation and is also involved in cellular senescence. During induction of senescence, Akt phospho-Ser473 (pS473) and phospho-Thr308 (pT308) are increased and accompanied by increased P53 expression (70, 71). Hyperactivation of the PI3K-Akt pathway via PTEN depletion or PIK3CA mutant expression induces cellular senescence in the absence of DNA damage (72). Pharmacological inhibition of Akt by the PI3K inhibitor LY294002 reduces $P21^{CIP1}$ expression and SA-β-Gal positivity in fibroblasts (70).

Akt has a variety of substrates, including Glycogen Synthase Kinase 3 (GSK3), Forkhead box O family transcription factors and Tuberous Sclerosis Complex 2, mTORC1 etc (73). These downstream targets of Akt also influence cellular senescence in various ways. GSK3 is one of the main targets of Akt and is phosphorylated by active Akt at its two subunits GSK3α (Ser21) and GSK3β (Ser9) (73). Ser9 phosphorylated GSK3β increases stability of $P21^{CIP1}$ post-translationally. Conversely, overexpression of a mutant GSK3β unable to phosphorylate Ser9 decreases P21CIP1 protein expression (74). Inability to phosphorylate FOXO3a by Akt inhibits transcription of the antioxidant enzyme SOD2 and consequently promotes ROS production, leading to DNA damage and cellular senescence (75). PI3K-Akt activation triggers mTOR and P53 activation (72). Significant activation of Akt-mTOR is also observed in replicative senescence (76). Furthermore, SASP components are regulated by the Akt-mTOR pathway in premature senescent cells (77).

3.4. mTOR complexes

mTOR is a serine/threonine protein kinase belonging to the PI3K-related kinase (PIKK) family. It is composed of two different protein complexes mTORC1 and mTORC2. mTORC1 consists of three core components: mTOR, Raptor (regulatory protein associated with mTOR) and mLST8 (mammalian lethal with Sec13 protein 8, also known as GßL). mTORC2 also contains mTOR and mLST8 but contains Rictor (rapamycin insensitive companion of mTOR) instead of Raptor (78). The two mTOR complexes regulate different cellular processes because they target different downstream kinases. mTORC1 promotes protein synthesis largely through the phosphorylation of two downstream kinases, p70S6 Kinase 1 (S6K1) and eIF4E Binding Protein (4EBP) (79, 80). mTORC1 activates the sterol responsive element binding protein (SREBP) in response to low sterol levels to promote *de novo* lipogenesis (81). PGC1α (Peroxisome proliferator-activated receptor gamma coactivator 1-alpha), a key regulator of mitochondria biogenesis is also regulated by mTORC1 (82). The mTORC2 complex mainly controls proliferation and survival, primarily by phosphorylating several members of the AGC (PKA/PKG/PKC) family of protein kinases (78). The most well-documented role of mTORC2 is to activate Akt via phosphorylation of Ser473 (83).

Recent research also suggested a positive feedback loop between Akt and mTORC2 (84). Furthermore, Akt-dependent phosphorylation of specific kinases including FoxO1/3a and TSC2 is also required for mTORC2 activation (78, 85).

In senescent cells, mTORC1 signaling is dysregulated (82, 86). In normal cells, the removal of mitogenic cues such as growth factors and amino acids inactivates mTORC1. However, in senescent cells, mTORC1 acquires resistance to inactivation by nutrient starvation and growth factor removal (86, 87). Sensitivity of mTORC1 to amino acids is increased in replicative senescent cells (88). This phenomenon is in line with evidence that the Ras-related small GTP-binding protein Rag is activated by amino acids and in turn activates mTORC1 (78). Palmitate-induced lipotoxicity and accumulation of lipids is accompanied by increased expression of senescence markers, suggesting a link between lipogenesis and senescence (89, 90). It has also been demonstrated that high glucose-induced cellular senescence promotes intracellular lipid accumulation via the PI3K-Akt-mTOR pathway (91). In addition, mTORC1 directly regulates phosphorylation of p53 in PTEN-loss induced senescence (92). In contrast to the clear evidence of dysregulation of mTOR signaling in senescence, the results of mTORC1 inhibition to decrease senescence are inconsistent. Rapamycin has been reported to reduce oxidative stress-induced senescence by inhibiting SASP (93). However, although rapamycin and Torins decrease the number of SA-β-Gal positive cells they fail to restore the proliferation ability of senescent fibroblasts (94). Knockdown of Raptor decreases phosphorylation of S6K and expression of senescent markers including $P16^{INK4A}$ and SA-β-Gal (95). But S6K and 4EBP1 activities seem to be dispensable in PTEN-loss induced senescence (92). The interpretation of the heterogeneous effects of mTORC2 on senescence may be hampered by the lack of detailed knowledge of the role of mTORC2 on senescence (78, 96, 97). Another layer of complexity in understanding the role of mTOR in senescence is the role of mTOR in regulating autophagy (see next section).

3.5. Autophagy

Autophagy is an evolutionary conserved, dynamic process that involves the scavenging of intracellular components and facilitates the turn-over of long-lived proteins. Macroautophagy is the most investigated type of autophagy. It begins with the formation of autophagosomes and ends with the fusion of the autophagosomes with lysosomes. Macroautophagy (which is usually referred to as autophagy) is essential to maintain intracellular homeostasis (98). The role of macroautophagy in senescence is complex. The complexity of macroautophagy in senescence is underscored by the phenomenon that both increasing as well as decreasing autophagy induces senescence. Macroautophagy is

enhanced in senescent cells (45). Nevertheless, impaired macroautophagy is sufficient to induce cellular senescence, which can be attenuated by mTOR inhibitors (99). Adding to the complexity is that macroautophagy interacts with various signaling transduction pathways that regulate senescence (98, 100). P38α activation triggers macroautophagosome formation and autophagic flux (101). Accumulation of P62 as a result of deficient macroautophagy increases activation of P38 (102). In $CD8^+$ T cells, P38 inhibition increases macroautophagy independent of mTOR activity and decreases senescence (103).

Selective autophagy is the selective degradation of specific cargos, such as organelles and proteins. The mechanisms and molecules used in selective autophagy are diverse and specific for each cargo (organelle) (104). Selective autophagy is also linked to senescence (105). Dysfunctional mitochondria are degraded by mitophagy, which involves recognition of poly-ubiquitinated mitochondria by the autophagy receptors P62 and Optineurin (OPTN) or NDP52 (106). Impaired mitophagy increases mitochondrial ROS production and is involved in cellular senescence (107). Improving mitophagy by supplementation of NAD+ attenuated senescence and aging (108).

Chaperone-mediated autophagy (CMA) is one of the main pathways of the lysosome-autophagy proteolytic system. CMA is a special kind of selective autophagy that requires the proteins targeted for degradation to contain a specific pentapeptide motif that is recognized by the heat shock cognate protein 71kDa (HSC70/HSPA8) (109). The chaperone-bound proteins are then transported to lysosomes, where they are recognized by the lysosome-associated membrane protein type 2a (LAMP2a) receptor (110). CMA delivers individual proteins for lysosomal degradation one at a time. In contrast, in macroautophagy, autophagosomes engulf and deliver larger structures for bulk degradation of cargo (110). Genetic ablation of growth hormone receptor in mice increases hepatic CMA and confers a longer life span to mice (111). CMA dysfunction is accompanied by aging and leads to an imbalance of proteostasis (112, 113). Defective CMA also leads to accumulation of CHK1 in response to cellular stress and potentiates genomic instability (114). In addition, NEF2L2/NRF2 has been demonstrated to be regulated by CMA which suggests a connection between redox balance and CMA (115).

3.6. Hydrogen sulfide and redox homeostasis

Excessive ROS generation is known to induce genetic instability leading to cellular senescence (45). Endogenous ROS can be generated by several sources. Mitochondria are the major source of ROS. Under normal physiological conditions most oxygen (O_2) in organisms will acquire four electrons and four protons to form water by cytochrome c oxidase in the electron transport system of mitochondria. However, if molecular oxygen

undergoes sequential univalent reduction, highly reactive $\cdot O_2^-$, $HO\cdot$ and H_2O_2 will be formed (116).

Hydrogen sulfide is one of various gasotransmitters that regulate a variety of cellular processes. The antioxidant effect of H_2S has been extensively investigated. The desulfhydration of cysteine is considered to be the major source of H_2S in mammals. The process is catalyzed by two pyridoxal-5'-phosphate- (PLP-) dependent enzymes, cystathionine β-synthase (CBS) and cystathionine γ-lyase (CTH/CSE) (117). H_2S improves redox homeostasis in various ways. In physiological conditions, the concentration of H_2S is in the submicromolar range and not sufficient to serve as a direct reductant (117). It is speculated that H_2S can be a direct scavenger of ROS at much higher concentrations, e.g. by exogenous administration of H_2S or chemical H_2S donors (118). H2S producing enzymes CSE and CBS can be upregulated by long-term supplementation of H_2S donors in vivo (119). H_2S increases glutathione biosynthetic pathways, increases the cellular glutathione pool and decreases homocysteine levels (120). Furthermore, increased H_2S levels promote post-translational sulfhydration of KEAP1 to facilitate the release of NRF2, which is a transcription factor that increases transcription of various antioxidant genes (121).

It has been demonstrated that H_2S production is increased during activation of hepatic stellate cells and increases the bioenergetics of mitochondria (122). Genetic ablation of CSE in mouse embryonic fibroblasts stimulates cellular senescence by increasing oxidative stress. In these fibroblasts, H_2S production is significantly reduced (123). Supplementation of H_2S reduces senescence by scavenging intracellular ROS (124). Decreased levels of nicotinamide adenine dinucleotide (NAD^+) are considered to be a cause of senescence and aging (125). Supplementation of exogenous H_2S restores intracellular NAD^+ level and induces SIRT1 expression to reduce senescence (126). Sirt1 is a member of the mammalian class III histone deacetylases and regulates PGC-1α activity in mitochondrial biogenesis (127). In addition, H_2S has been shown to modulate various kinases involved in senescence (128). This evidence suggests that H_2S regulates cellular senescence via various mechanisms.

3.7. STAT3 pathway

STAT3 is a member of the STAT (Signal Transducers and Activators of Transcription) family that has DNA binding activity and stimulates expression of innate immune mediators in the liver in response to interferon (129). It has been demonstrated that numerous cytokines and growth factors including IL-6, IL-10 family members, G-CSF (Granulocyte colony-stimulating factor) and growth factors that act through protein tyrosine kinase receptors (e.g. epidermal growth factor) are capable to activate STAT3 (130-132). In

addition to its transcriptional activities, non-transcriptional functions of STAT3 have been described as well. Mitochondrial STAT3 associates with mitochondria and regulates electron transport chain function as well as glycolysis and oxidative phosphorylation independent of its transcriptional action (133). Furthermore, STAT3 directly interacts with EIF2AK2 (Eukaryotic Translation Initiation Factor 2 Alpha Kinase 2) to inhibit autophagy (134).

STAT3 is activated by extracellular inflammatory signals derived from SASP and regulates senescence. IL-6 is one of the well-established SASP components that regulates cellular senescence via activation of STAT3 (135). IL-22, a member of the IL-10 family, induces hepatic stellate cell senescence via phosphorylation of STAT3 and upregulation of SOCS3 (suppressor of cytokine signaling 3) (136). IL-10 is also able to promote hepatic stellate cell senescence via STAT3 (137, 138). Oxidative stress-induced senescence is accompanied by hyperactivity of the STAT3 pathway and disruption of the IL-6-STAT3 axis reduces cellular senescence (139). In addition, STAT3 interacts with mTOR to negatively regulate autophagy during cellular senescence (140).

3.8. Adrenergic receptors signaling and cell proliferation

Adrenergic receptors (AR) are a family of transmembran receptors coupled to G-proteins. Three types have been identified: alpha-1, alpha-2 and beta, each one characterized by its structure and function (156). Alpha-1 AR is coupled to the Gq protein and regulates PKC activation via diacylglycerol synthesis as well as calcium fluxes via PLC signaling and IP3 generation (157-161). Previous studies demonstrated an important relationship between intracellular calcium levels and senescence, which could be related to the alpha-1 AR response. It has been demonstrated that calcium levels increase in response to different inducers of senescence inducers like telomere shortening and oxidative stress. This dysregulation of intracellular calcium homeostasis was linked to the PLC/IP3/IP3R pathway in human mammary epithelial cells during the induction of senescence (162). In addition, the use of BAPTA-AM, a calcium chelator, reduces the number of cells with a senescent phenotype (163). Calmodulin (CaM), a calcium-dependent enzyme, controls different processes including cell division (164). This enzyme is required for G1 transit by regulating the activity of calcineurin a Ca^{2+}/ CaM-dependent protein, which increases the synthesis of cyclin D1 in fibroblasts (165). Thus,Ca^{2+} appears to be important for both cell proliferation and senescence and its precise effects depends on the intracellular concentration and location which is associated with the activation and regulation of alpha 1 AR. Protein kinase C (PKC) is part of the family of serine/threonine protein kinases and can modulate cell cycle progression (166), PKCη has been related to cell cycle arrest during G1

phase, since it induces the phosphorylation of p21 at Ser146 and the dephosphorylation of Thr160 of Cdk2 in keratinocytes, (167). PKCα also showed and effect on the cell cycle during the transition from G1 to S phase, by decreasing the expression of cyclin D1 (168-169) and increasing the expression of p21 (168, 170, 171). PKCδ is also able to promote cellular senescence in TIG-1 cells, increasing the activity of β-galactosidase (172). However, in addition to the role of some PKC isoforms in senescence, PKC isoforms are also important for cell growth. PKCα has growth-stimulatory effects which has been observed in different cell types including hepatocytes (173-174). Apparently, the effect of protein kinase C depends mainly on the isoform as well as the cell type in which it is present. Beta AR are coupled to the Gs protein and regulate cAMP production and protein kinase A activation. It has been demonstrated that the β AR agonist isoproterenol promotes proliferation of U251 cells and this effect was inhibited bypropranolol, a selective antagonist of beta AR.However, the mechanism of the antagonism of beta AR has not been fully elucidated yet (175). Moreover, it has also been demonstrated that propranolol decreases the proliferation of breast cancer cells by increasing expression of p53, reducing expression of bcl-2 and increasing apoptosis (176). In hepatic stellate cells, activation of ARs is mainly related to proliferation (177). This proliferative effect is mainly linked to the activation of alpha-1 AR and the downstream response involves PI3K and the Erk family of mitogen activated protein kinases. In addition, hepatic stellate cells are able to produce and release catecholamines, including norepinephrine, which is important for autocrine stimulation of their proliferation (178-179). Doxazosin, a selective alpha 1 AR antagonist, has antifibrotic properties in the liver by reducing the deposition of the extracellular matrix and reduction of the stellate cell marker α-smooth muscle actin. (180). However, whether doxazosin has a direct effect on alpha 1 AR on HSCs remains to be elucidated. We hypothesize that the antagonism of adrenergic receptors may be linked to the resolution of fibrosis via the induction of senescence of HSC since decreased collagen production and decreased proliferation have been observed in senescent HSCs.

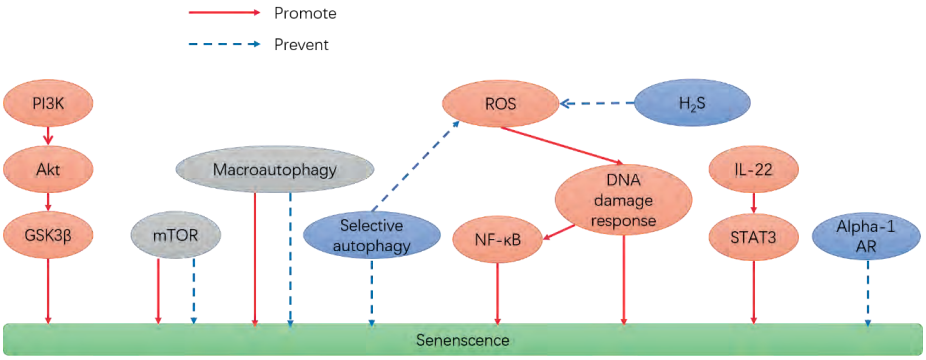

Figure 2. The major pathways that regulate cellular senescence.

PI3K, Phosphoinositide 3-kinase. GSK3β, Glycogen synthase kinase 3 beta. mTOR, The mammalian target of rapamycin. ROS, Reactive oxygen species. NF-κB, Nuclear factor kappa B. H_2S, Hydrogen sulfide. IL-22, Interleuikin-22. STAT3, Signal transducer and activator of transcription 3.

4. Consequences of cellular senescence in liver fibrosis

In the CCl_4 (carbon tetrachloride) model of liver fibrosis, senescent cells mainly derive from activated hepatic stellate cells (12). Activated hepatic stellate cells that undergo replicative senescence exhibit a less fibrogenic phenotype and are prone to spontaneous apoptosis (13). Induced premature senescence of aHSCs decreases fibrogenesis *in vivo* (12, 136, 141). Senescent HSCs express cell surface ligands for receptors on NK cells that promote the elimination of senescent HSCs (142). It has been suggested that the SASP of senescent HSCs initiates cellular senescence of surrounding non-senescent HSCs (143, 144). These data underscore the biological rationale of therapy-induced HSC senescence as a strategy to treat liver fibrosis. Accumulation of senescent cells is termed chronic senescence and has a significant impact on the microenvironment and tissue homeostasis. Excessive SASP secreted by accumulating senescent cells in tissue may induce senescence in neighboring non-senescent cells and cause infiltration of inflammatory cells, exacerbating local inflammation (45). Hence, in view of the long-term disadvantages of senescence, the induction of senescence in non-HSC liver cell types should be considered and, if possible, avoided.

Senescence of hepatocytes has been observed in various liver diseases including chronic viral hepatitis, alcohol-related liver disease, non-alcoholic fatty liver disease (NAFLD) and genetic haemochromatosis (45). Replicative senescence of hepatocytes has been described in both normal and fibrotic liver. In fibrotic liver, the number ofsenescent cells is higher than in non-fibrotic liver (145). In biopsies of NAFLD patients, $P21^{CIP1}$ positive hepatocytes are present and correlate with the grade of fibrosis (146). Apart from direct injury or aging, cytokine-induced senescence of hepatocytes appears to be the most

important cause of senescence in hepatocytes (147, 148). Hepatocyte senescence is involved in the pathogenesis of chronic liver diseases. Hepatocyte-specific senescence promotes intracellular fat accumulation in hepatocytes in experimental NAFLD models and positively correlates with the grade of steatosis (149). In contrast, senescent hepatocytes in chronic alcohol-induced injury appears to be more resistant to apoptosis and steatosis (148). Since the accumulation of senescent cells is the cause of aging-related disorders, the specific removal of senescent cells may help to attenuate these symptoms and increase life-span. Senolytics are (therapeutic) agents that selectively target senescent cells and induce death of senescent cells only, a phenomenon termed senolysis (150). Senolysis of senescent hepatocytes has been shown to improve liver regeneration and decrease the expression of $P21^{CIP1}$ and SASP (151). Nevertheless, genetic ablation of P21 in the liver enhances DNA damage, cholestasis and carcinogenesis (152). The effect of hepatocyte senescence in carcinogenesis is bidirectional. Hepatocyte senescence is considered as a tumor-suppressing mechanism because of the accompanying permanent proliferation arrest (153). On the other hand, senescent hepatocytes that escape from the senescent state and re-enter the cell cycle are pre-malignant and promote tumorigenesis (154).

It is not clear whether senescent HSCs drive hepatocyte senescence but senescent HSCs interact with macrophages to create a tumor-suppressing microenvironment (144). IL-10 and IL-22 have been shown to induce senescence of HSCs (136, 138). Senescent HSCs promote recruitment of NK cells in the liver (142). Whereas infiltrating B-lymphocytes inhibit senescence of HSCs, they exacerbate fibrogenesis and maintain a tumorigenic inflammatory microenvironment (155). These data suggest that the immune microenvironment of liver cells is to a large extent determined by the interaction of senescent HSCs and (infiltrating) immune cells.

5. Conclusions and future perspectives

Hepatic stellate cell activation is involved in the pathogenesis of liver fibrosis. Senescent HSCs acquire a less fibrogenic phenotype and exhibit permanent proliferation arrest. This phenomenon favors resolution of fibrosis. HSC senescence can be triggered by various stimuli. Different stimuli induce slightly different biomarkers of senescence in HSCs. Among the biomarkers, $P21^{CIP1}$, P53, SA-β-Gal and SASP can be used to identify senescent HSCs in vivo and in vitro.

Senescent HSCs acquire genetic and epigenetic changes that profoundly alter their cellular signaling pathways and intracellular biological processes. For instance, both increased as well as decreased autophagy are involved in senescence induction. mTOR inhibitors failed to reverse all aspects of the senescent phenotype, suggesting a complex regulation of signaling pathways leading to senescence.

Evidence that promoting HSC senescence reduces fibrogenesis is the rationale for exploring induction of senescence as a strategy for the treatment of liver fibrosis. However, it should be noted that accumulation of senescent hepatocytes may lead to hepatic dysfunction. This potential detrimental consequence requires a comprehensive evaluation of the effects of inducing HSC senescence in the liver. Furthermore, the interaction between senescent HSCs and immune cells, including macrophages, lymphocytes and NK cells, demonstrates that the elimination of senescent HSCs is determined to a large extent by immune cells. This indicates that maintaining the proper micro-environment in the liver is key to the success of immune clearance of senescent HSCs. Finally, in the end, inducers of senescence may only be successfully applied in combination with senolytics to minimize the disadvantages and detrimental effects of accumulated senescent cells. In conclusion, more studies should be conducted to clarify role of HSC senescence in liver fibrosis.

References

1. Zoubek ME, Trautwein C, Strnad P. Reversal of liver fibrosis: From fiction to reality. Best Pract Res Clin Gastroenterol 2017;31:129-141.

2. Tsochatzis EA, Bosch J, Burroughs AK. Liver cirrhosis. The Lancet 2014;383:1749-1761.

3. Kisseleva T. The origin of fibrogenic myofibroblasts in fibrotic liver. Hepatology 2017;65:1039-1043.

4. Tsuchida T, Friedman SL. Mechanisms of hepatic stellate cell activation. Nat Rev Gastroenterol Hepatol 2017;14:397-411.

5. Lua I, Li Y, Zagory JA, Wang KS, French SW, Sevigny J, Asahina K. Characterization of hepatic stellate cells, portal fibroblasts, and mesothelial cells in normal and fibrotic livers. J Hepatol 2016;64:1137-1146.

6. Iwaisako K, Jiang C, Zhang M, Cong M, Moore-Morris TJ, Park TJ, Liu X, et al. Origin of myofibroblasts in the fibrotic liver in mice. Proc Natl Acad Sci U S A 2014;111:E3297-3305.

7. Rinkevich Y, Mori T, Sahoo D, Xu P-X, Bermingham JR, Weissman IL. Identification and prospective isolation of a mesothelial precursor lineage giving rise to smooth muscle cells and fibroblasts for mammalian internal organs, and their vasculature. Nature Cell Biology 2012;14:1251-1260.

8. Troeger JS, Mederacke I, Gwak GY, Dapito DH, Mu X, Hsu CC, Pradere JP, et al. Deactivation of hepatic stellate cells during liver fibrosis resolution in mice. Gastroenterology 2012;143:1073-1083 e1022.

9. Kisseleva T, Cong M, Paik Y, Scholten D, Jiang C, Benner C, Iwaisako K, et al. Myofibroblasts revert to an inactive phenotype during regression of liver fibrosis. Proc Natl Acad Sci U S A 2012;109:9448-9453.

10. Issa R, Williams E, Trim N, Kendall T, Arthur MJ, Reichen J, Benyon RC, et al. Apoptosis of hepatic stellate cells: involvement in resolution of biliary fibrosis and regulation by soluble growth factors. Gut 2001;48:548-557.

11. Gorgoulis V, Adams PD, Alimonti A, Bennett DC, Bischof O, Bishop C, Campisi J, et al. Cellular Senescence: Defining a Path Forward. Cell 2019;179:813-827.

12. Krizhanovsky V, Yon M, Dickins RA, Hearn S, Simon J, Miething C, Yee H, et al. Senescence of activated stellate cells limits liver fibrosis. Cell 2008;134:657-667.

13. Schnabl B, Purbeck CA, Choi YH, Hagedorn CH, Brenner D. Replicative senescence of activated human hepatic stellate cells is accompanied by a pronounced inflammatory but less

fibrogenic phenotype. Hepatology 2003;37:653-664.

14. Hayflick L, Moorhead PS. The serial cultivation of human diploid cell strains. Experimental Cell Research 1961;25:585-621.

15. Hayflick L. The limited in vitro lifetime of human diploid cell strains. Experimental Cell Research 1965;37:614-636.

16. Olovnikov AM. A theory of marginotomy. The incomplete copying of template margin in enzymic synthesis of polynucleotides and biological significance of the phenomenon. J Theor Biol 1973;41:181-190.

17. Watson JD. Origin of concatemeric T7 DNA. Nat New Biol 1972;239:197-201.

18. d'Adda di Fagagna F, Reaper PM, Clay-Farrace L, Fiegler H, Carr P, Von Zglinicki T, Saretzki G, et al. A DNA damage checkpoint response in telomere-initiated senescence. Nature 2003;426:194-198.

19. Kuilman T, Michaloglou C, Mooi WJ, Peeper DS. The essence of senescence. Genes Dev 2010;24:2463-2479.

20. Serrano M, Blasco MA. Putting the stress on senescence. Curr Opin Cell Biol 2001;13:748-753.

21. Hernandez-Segura A, de Jong TV, Melov S, Guryev V, Campisi J, Demaria M. Unmasking Transcriptional Heterogeneity in Senescent Cells. Curr Biol 2017;27:2652-2660 e2654.

22. Mason JM, Ransom J, Konev AY. A deficiency screen for dominant suppressors of telomeric silencing in Drosophila. Genetics 2004;168:1353-1370.

23. Trougakos IP, Saridaki A, Panayotou G, Gonos ES. Identification of differentially expressed proteins in senescent human embryonic fibroblasts. Mech Ageing Dev 2006;127:88-92.

24. Yoon IK, Kim HK, Kim YK, Song IH, Kim W, Kim S, Baek SH, et al. Exploration of replicative senescence-associated genes in human dermal fibroblasts by cDNA microarray technology. Exp Gerontol 2004;39:1369-1378.

25. Pang JH, Chen KY. Global change of gene expression at late G1/S boundary may occur in human IMR-90 diploid fibroblasts during senescence. J Cell Physiol 1994;160:531-538.

26. Seshadri T, Campisi J. Repression of c-fos transcription and an altered genetic program in senescent human fibroblasts. Science 1990;247:205-209.

27. Shelton DN, Chang E, Whittier PS, Choi D, Funk WD. Microarray analysis of replicative senescence. Curr Biol 1999;9:939-945.

28. Krtolica A, Parrinello S, Lockett S, Desprez PY, Campisi J. Senescent fibroblasts promote epithelial cell growth and tumorigenesis: a link between cancer and aging. Proc Natl Acad Sci U S A

2001;98:12072-12077.

29. Parrinello S, Coppe JP, Krtolica A, Campisi J. Stromal-epithelial interactions in aging and cancer: senescent fibroblasts alter epithelial cell differentiation. J Cell Sci 2005;118:485-496.

30. Demaria M, O'Leary MN, Chang J, Shao L, Liu S, Alimirah F, Koenig K, et al. Cellular Senescence Promotes Adverse Effects of Chemotherapy and Cancer Relapse. Cancer Discov 2017;7:165-176.

31. Xue W, Zender L, Miething C, Dickins RA, Hernando E, Krizhanovsky V, Cordon-Cardo C, et al. Senescence and tumour clearance is triggered by p53 restoration in murine liver carcinomas. Nature 2007;445:656-660.

32. Kortlever RM, Higgins PJ, Bernards R. Plasminogen activator inhibitor-1 is a critical downstream target of p53 in the induction of replicative senescence. Nat Cell Biol 2006;8:877-884.

33. Wajapeyee N, Serra RW, Zhu X, Mahalingam M, Green MR. Oncogenic BRAF induces senescence and apoptosis through pathways mediated by the secreted protein IGFBP7. Cell 2008;132:363-374.

34. Acosta JC, O'Loghlen A, Banito A, Guijarro MV, Augert A, Raguz S, Fumagalli M, et al. Chemokine signaling via the CXCR2 receptor reinforces senescence. Cell 2008;133:1006-1018.

35. Kuilman T, Michaloglou C, Vredeveld LC, Douma S, van Doorn R, Desmet CJ, Aarden LA, et al. Oncogene-induced senescence relayed by an interleukin-dependent inflammatory network. Cell 2008;133:1019-1031.

36. Basisty N, Kale A, Jeon OH, Kuehnemann C, Payne T, Rao C, Holtz A, et al. A proteomic atlas of senescence-associated secretomes for aging biomarker development. PLoS Biol 2020;18:e3000599.

37. Trojer P, Reinberg D. Facultative Heterochromatin: Is There a Distinctive Molecular Signature? Molecular Cell 2007;28:1-13.

38. Narita M, Nuñez S, Heard E, Narita M, Lin AW, Hearn SA, Spector DL, et al. Rb-Mediated Heterochromatin Formation and Silencing of E2F Target Genes during Cellular Senescence. Cell 2003;113:703-716.

39. Nacarelli T, Liu P, Zhang R. Epigenetic Basis of Cellular Senescence and Its Implications in Aging. Genes (Basel) 2017;8.

40. Sen P, Shah PP, Nativio R, Berger SL. Epigenetic Mechanisms of Longevity and Aging. Cell 2016;166:822-839.

41. Shah PP, Donahue G, Otte GL, Capell BC, Nelson DM, Cao K, Aggarwala V, et al. Lamin B1 depletion in senescent cells triggers large-scale changes in gene expression and the chromatin

landscape. Genes Dev 2013;27:1787-1799.

42. Knittel T, Kobold D, Saile B, Grundmann A, Neubauer K, Piscaglia F, Ramadori G. Rat liver myofibroblasts and hepatic stellate cells: different cell populations of the fibroblast lineage with fibrogenic potential. Gastroenterology 1999;117:1205-1221.

43. Saile B, Matthes N, Neubauer K, Eisenbach C, El-Armouche H, Dudas J, Ramadori G. Rat liver myofibroblasts and hepatic stellate cells differ in CD95-mediated apoptosis and response to TNF-alpha. Am J Physiol Gastrointest Liver Physiol 2002;283:G435-444.

44. Gonzalez LC, Ghadaouia S, Martinez A, Rodier F. Premature aging/senescence in cancer cells facing therapy: good or bad? Biogerontology 2016;17:71-87.

45. Aravinthan AD, Alexander GJ. Senescence in chronic liver disease: Is the future in aging? J Hepatol 2016;65:825-834.

46. Ciccia A, Elledge SJ. The DNA Damage Response: Making It Safe to Play with Knives. Molecular Cell 2010;40:179-204.

47. White RR, Vijg J. Do DNA Double-Strand Breaks Drive Aging? Mol Cell 2016;63:729-738.

48. Bielak-Zmijewska A, Mosieniak G, Sikora E. Is DNA damage indispensable for stress-induced senescence? Mech Ageing Dev 2018;170:13-21.

49. Lamarche BJ, Orazio NI, Weitzman MD. The MRN complex in double-strand break repair and telomere maintenance. FEBS Lett 2010;584:3682-3695.

50. Blackford AN, Jackson SP. ATM, ATR, and DNA-PK: The Trinity at the Heart of the DNA Damage Response. Mol Cell 2017;66:801-817.

51. Nassour J, Abbadie C. A novel role for DNA single-strand breaks in senescence and neoplastic escape of epithelial cells. Mol Cell Oncol 2016;3:e1190885.

52. Chien Y, Scuoppo C, Wang X, Fang X, Balgley B, Bolden JE, Premsrirut P, et al. Control of the senescence-associated secretory phenotype by NF-kappaB promotes senescence and enhances chemosensitivity. Genes Dev 2011;25:2125-2136.

53. Oeckinghaus A, Ghosh S. The NF-kappaB family of transcription factors and its regulation. Cold Spring Harb Perspect Biol 2009;1:a000034.

54. Sun SC. The non-canonical NF-kappaB pathway in immunity and inflammation. Nat Rev Immunol 2017;17:545-558.

55. McCool KW, Miyamoto S. DNA damage-dependent NF-kappaB activation: NEMO turns nuclear signaling inside out. Immunol Rev 2012;246:311-326.

56. Vile GF, Tanew-Ilitschew A Fau - Tyrrell RM, Tyrrell RM. Activation of NF-kappa B in human skin fibroblasts by the oxidative stress generated by UVA radiation.

57. Piret B, Schoonbroodt S, Piette J. The ATM protein is required for sustained activation of NF-kappaB following DNA damage. Oncogene 1999;18:2261-2271.

58. Kang C, Xu Q, Martin TD, Li MZ, Demaria M, Aron L, Lu T, et al. The DNA damage response induces inflammation and senescence by inhibiting autophagy of GATA4. Science 2015;349:aaa5612.

59. Freund A, Patil CK, Campisi J. p38MAPK is a novel DNA damage response-independent regulator of the senescence-associated secretory phenotype. EMBO J 2011;30:1536-1548.

60. Jing H, Lee S. NF-kappaB in cellular senescence and cancer treatment. Mol Cells 2014;37:189-195.

61. Jing H, Kase J, Dorr JR, Milanovic M, Lenze D, Grau M, Beuster G, et al. Opposing roles of NF-kappaB in anti-cancer treatment outcome unveiled by cross-species investigations. Genes Dev 2011;25:2137-2146.

62. Tilstra JS, Robinson AR, Wang J, Gregg SQ, Clauson CL, Reay DP, Nasto LA, et al. NF-kappaB inhibition delays DNA damage-induced senescence and aging in mice. J Clin Invest 2012;122:2601-2612.

63. Venkatachalam G, Surana U, Clement MV. Replication stress-induced endogenous DNA damage drives cellular senescence induced by a sub-lethal oxidative stress. Nucleic Acids Res 2017;45:10564-10582.

64. Liberatore RA, Goff SP, Nunes I. NF-kappaB activity is constitutively elevated in c-Abl null fibroblasts. Proc Natl Acad Sci U S A 2009;106:17823-17828.

65. Bernal GM, Wahlstrom JS, Crawley CD, Cahill KE, Pytel P, Liang H, Kang S, et al. Loss of Nfkb1 leads to early onset aging. Aging (Albany NY) 2014;6:931-943.

66. Lopes-Paciencia S, Saint-Germain E, Rowell MC, Ruiz AF, Kalegari P, Ferbeyre G. The senescence-associated secretory phenotype and its regulation. Cytokine 2019;117:15-22.

67. Malaquin N, Martinez A, Rodier F. Keeping the senescence secretome under control: Molecular reins on the senescence-associated secretory phenotype. Exp Gerontol 2016;82:39-49.

68. Tian Y, Li H, Qiu T, Dai J, Zhang Y, Chen J, Cai H. Loss of PTEN induces lung fibrosis via alveolar epithelial cell senescence depending on NF-kappaB activation. Aging Cell 2019;18:e12858.

69. Xu W, Li Y, Yuan WW, Yin Y, Song WW, Wang Y, Huang QQ, et al. Membrane-Bound CD40L Promotes Senescence and Initiates Senescence-Associated Secretory Phenotype via NF-kappaB Activation in Lung Adenocarcinoma. Cell Physiol Biochem 2018;48:1793-1803.

70. Kim YY, Jee HJ, Um JH, Kim YM, Bae SS, Yun J. Cooperation between p21 and Akt is required for p53-dependent cellular senescence. Aging Cell 2017;16:1094-1103.

71. Boichuck M, Zorea J, Elkabets M, Wolfson M, Fraifeld VE. c-Met as a new marker of cellular senescence. Aging (Albany NY) 2019;11:2889-2897.

72. Astle MV, Hannan KM, Ng PY, Lee RS, George AJ, Hsu AK, Haupt Y, et al. AKT induces senescence in human cells via mTORC1 and p53 in the absence of DNA damage: implications for targeting mTOR during malignancy. Oncogene 2012;31:1949-1962.

73. Manning BD, Toker A. AKT/PKB Signaling: Navigating the Network. Cell 2017;169:381-405.

74. Rossig L, Badorff C, Holzmann Y, Zeiher AM, Dimmeler S. Glycogen synthase kinase-3 couples AKT-dependent signaling to the regulation of $p21^{Cip1}$ degradation. J Biol Chem 2002;277:9684-9689.

75. Imai Y, Takahashi A, Hanyu A, Hori S, Sato S, Naka K, Hirao A, et al. Crosstalk between the Rb pathway and AKT signaling forms a quiescence-senescence switch. Cell Rep 2014;7:194-207.

76. Tan P, Wang YJ, Li S, Wang Y, He JY, Chen YY, Deng HQ, et al. The PI3K/Akt/mTOR pathway regulates the replicative senescence of human VSMCs. Mol Cell Biochem 2016;422:1-10.

77. Bent EH, Gilbert LA, Hemann MT. A senescence secretory switch mediated by PI3K/AKT/mTOR activation controls chemoprotective endothelial secretory responses. Genes Dev 2016;30:1811-1821.

78. Saxton RA, Sabatini DM. mTOR Signaling in Growth, Metabolism, and Disease. Cell 2017;168:960-976.

79. Lipton JO, Yuan ED, Boyle LM, Ebrahimi-Fakhari D, Kwiatkowski E, Nathan A, Guttler T, et al. The Circadian Protein BMAL1 Regulates Translation in Response to S6K1-Mediated Phosphorylation. Cell 2015;161:1138-1151.

80. Morita M, Gravel SP, Hulea L, Larsson O, Pollak M, St-Pierre J, Topisirovic I. mTOR coordinates protein synthesis, mitochondrial activity and proliferation. Cell Cycle 2015;14:473-480.

81. Porstmann T, Santos CR, Griffiths B, Cully M, Wu M, Leevers S, Griffiths JR, et al. SREBP activity is regulated by mTORC1 and contributes to Akt-dependent cell growth. Cell Metab 2008;8:224-236.

82. Summer R, Shaghaghi H, Schriner D, Roque W, Sales D, Cuevas-Mora K, Desai V, et al. Activation of the mTORC1/PGC-1 axis promotes mitochondrial biogenesis and induces cellular senescence in the lung epithelium. Am J Physiol Lung Cell Mol Physiol 2019;316:L1049-L1060.

83. Sarbassov DD, Guertin DA, Ali SM, Sabatini DM. Phosphorylation and regulation of Akt/PKB by the rictor-mTOR complex. Science 2005;307:1098-1101.

84. Yang G, Murashige DS, Humphrey SJ, James DE. A Positive Feedback Loop between Akt

and mTORC2 via SIN1 Phosphorylation. Cell Rep 2015;12:937-943.

85. Jacinto E, Facchinetti V, Liu D, Soto N, Wei S, Jung SY, Huang Q, et al. SIN1/MIP1 Maintains rictor-mTOR Complex Integrity and Regulates Akt Phosphorylation and Substrate Specificity. Cell 2006;127:125-137.

86. Carroll B, Nelson G, Rabanal-Ruiz Y, Kucheryavenko O, Dunhill-Turner NA, Chesterman CC, Zahari Q, et al. Persistent mTORC1 signaling in cell senescence results from defects in amino acid and growth factor sensing. J Cell Biol 2017;216:1949-1957.

87. Zhang H, Hoff H, Marinucci T, Cristofalo VJ, Sell C. Mitogen-independent phosphorylation of S6K1 and decreased ribosomal S6 phosphorylation in senescent human fibroblasts. Exp Cell Res 2000;259:284-292.

88. Chen Y, Wang J, Cai J, Sternberg P. Altered mTOR signaling in senescent retinal pigment epithelium. Invest Ophthalmol Vis Sci 2010;51:5314-5319.

89. Inoue C, Zhao C, Tsuduki Y, Udono M, Wang L, Nomura M, Katakura Y. SMARCD1 regulates senescence-associated lipid accumulation in hepatocytes. NPJ Aging Mech Dis 2017;3:11.

90. Chang Y-C, Liu H-W, Chen Y-T, Chen Y-A, Chen Y-J, Chang S-J. Resveratrol protects muscle cells against palmitate-induced cellular senescence and insulin resistance through ameliorating autophagic flux. Journal of Food and Drug Analysis 2018;26:1066-1074.

91. Chen Q, Tang L, Xin G, Li S, Ma L, Xu Y, Zhuang M, et al. Oxidative stress mediated by lipid metabolism contributes to high glucose-induced senescence in retinal pigment epithelium. Free Radic Biol Med 2019;130:48-58.

92. Jung SH, Hwang HJ, Kang D, Park HA, Lee HC, Jeong D, Lee K, et al. mTOR kinase leads to PTEN-loss-induced cellular senescence by phosphorylating p53. Oncogene 2019;38:1639-1650.

93. Wang R, Yu Z, Sunchu B, Shoaf J, Dang I, Zhao S, Caples K, et al. Rapamycin inhibits the secretory phenotype of senescent cells by a Nrf2-independent mechanism. Aging Cell 2017;16:564-574.

94. Leontieva OV, Blagosklonny MV. While reinforcing cell cycle arrest, rapamycin and Torins suppress senescence in UVA-irradiated fibroblasts. Oncotarget 2017;8:109848-109856.

95. Ito M, Yurube T, Kakutani K, Maeno K, Takada T, Terashima Y, Kakiuchi Y, et al. Selective interference of mTORC1/RAPTOR protects against human disc cellular apoptosis, senescence, and extracellular matrix catabolism with Akt and autophagy induction. Osteoarthritis Cartilage 2017;25:2134-2146.

96. Schreiber KH, Ortiz D, Academia EC, Anies AC, Liao CY, Kennedy BK. Rapamycin-mediated mTORC2 inhibition is determined by the relative expression of FK506-binding

proteins. Aging Cell 2015;14:265-273.

97. Sarbassov DD, Ali SM, Sengupta S, Sheen JH, Hsu PP, Bagley AF, Markhard AL, et al. Prolonged rapamycin treatment inhibits mTORC2 assembly and Akt/PKB. Mol Cell 2006;22:159-168.

98. Kang C, Elledge SJ. How autophagy both activates and inhibits cellular senescence. Autophagy 2016;12:898-899.

99. Tai H, Wang Z, Gong H, Han X, Zhou J, Wang X, Wei X, et al. Autophagy impairment with lysosomal and mitochondrial dysfunction is an important characteristic of oxidative stress-induced senescence. Autophagy 2017;13:99-113.

100. Zhang H, Puleston DJ, Simon AK. Autophagy and Immune Senescence. Trends Mol Med 2016;22:671-686.

101. Slobodnyuk K, Radic N, Ivanova S, Llado A, Trempolec N, Zorzano A, Nebreda AR. Autophagy-induced senescence is regulated by p38alpha signaling. Cell Death Dis 2019;10:376.

102. Qiang L, Wu C, Ming M, Viollet B, He YY. Autophagy controls p38 activation to promote cell survival under genotoxic stress. J Biol Chem 2013;288:1603-1611.

103. Henson SM, Lanna A, Riddell NE, Franzese O, Macaulay R, Griffiths SJ, Puleston DJ, et al. p38 signaling inhibits mTORC1-independent autophagy in senescent human CD8(+) T cells. J Clin Invest 2014;124:4004-4016.

104. Anding AL, Baehrecke EH. Cleaning House: Selective Autophagy of Organelles. Dev Cell 2017;41:10-22.

105. Zheng K, He Z, Kitazato K, Wang Y. Selective Autophagy Regulates Cell Cycle in Cancer Therapy. Theranostics 2019;9:104-125.

106. Gatica D, Lahiri V, Klionsky DJ. Cargo recognition and degradation by selective autophagy. Nat Cell Biol 2018;20:233-242.

107. Ito S, Araya J, Kurita Y, Kobayashi K, Takasaka N, Yoshida M, Hara H, et al. PARK2-mediated mitophagy is involved in regulation of HBEC senescence in COPD pathogenesis. Autophagy 2015;11:547-559.

108. Fang EF, Hou Y, Lautrup S, Jensen MB, Yang B, SenGupta T, Caponio D, et al. NAD(+) augmentation restores mitophagy and limits accelerated aging in Werner syndrome. Nat Commun 2019;10:5284.

109. Moreno-Blas D, Gorostieta-Salas E, Castro-Obregon S. Connecting chaperone-mediated autophagy dysfunction to cellular senescence. Ageing Res Rev 2018;41:34-41.

110. Kaushik S, Cuervo AM. The coming of age of chaperone-mediated autophagy. Nat Rev Mol Cell Biol 2018.

111. Endicott SJ, Boynton DN, Jr., Beckmann LJ, Miller RA. Long-lived mice with reduced growth hormone signaling have a constitutive upregulation of hepatic chaperone-mediated autophagy. Autophagy 2020:1-14.

112. Schneider JL, Villarroya J, Diaz-Carretero A, Patel B, Urbanska AM, Thi MM, Villarroya F, et al. Loss of hepatic chaperone-mediated autophagy accelerates proteostasis failure in aging. Aging Cell 2015;14:249-264.

113. Zhou J, Chong SY, Lim A, Singh BK, Sinha RA, Salmon AB, Yen PM. Changes in macroautophagy, chaperone-mediated autophagy, and mitochondrial metabolism in murine skeletal and cardiac muscle during aging. Aging (Albany NY) 2017;9:583-599.

114. Park C, Suh Y, Cuervo AM. Regulated degradation of Chk1 by chaperone-mediated autophagy in response to DNA damage. Nat Commun 2015;6:6823.

115. Pajares M, Rojo AI, Arias E, Diaz-Carretero A, Cuervo AM, Cuadrado A. Transcription factor NFE2L2/NRF2 modulates chaperone-mediated autophagy through the regulation of LAMP2A. Autophagy 2018;14:1310-1322.

116. Murphy MP. How mitochondria produce reactive oxygen species. Biochem J 2009;417:1-13.

117. Xie ZZ, Liu Y, Bian JS. Hydrogen Sulfide and Cellular Redox Homeostasis. Oxid Med Cell Longev 2016;2016:6043038.

118. Lan A, Liao X, Mo L, Yang C, Yang Z, Wang X, Hu F, et al. Hydrogen sulfide protects against chemical hypoxia-induced injury by inhibiting ROS-activated ERK1/2 and p38MAPK signaling pathways in PC12 cells. PLoS One 2011;6:e25921.

119. Wu W, Hou CL, Mu XP, Sun C, Zhu YC, Wang MJ, Lv QZ. H_2S Donor NaHS Changes the Production of Endogenous H_2S and NO in D-Galactose-Induced Accelerated Ageing. Oxid Med Cell Longev 2017;2017:5707830.

120. Parsanathan R, Jain SK. Hydrogen sulfide increases glutathione biosynthesis, and glucose uptake and utilisation in C2C12 mouse myotubes. Free Radic Res 2018;52:288-303.

121. Corsello T, Komaravelli N, Casola A. Role of Hydrogen Sulfide in NRF2- and Sirtuin-Dependent Maintenance of Cellular Redox Balance. Antioxidants (Basel) 2018;7.

122. Damba T, Zhang M, Buist-Homan M, van Goor H, Faber KN, Moshage H. Hydrogen sulfide stimulates activation of hepatic stellate cells through increased cellular bio-energetics. Nitric Oxide 2019;92:26-33.

123. Yang G, Zhao K, Ju Y, Mani S, Cao Q, Puukila S, Khaper N, et al. Hydrogen sulfide protects against cellular senescence via S-sulfhydration of Keap1 and activation of Nrf2. Antioxid Redox

Signal 2013;18:1906-1919.

124. Zhang W, Huang C, Sun A, Qiao L, Zhang X, Huang J, Sun X, et al. Hydrogen alleviates cellular senescence via regulation of ROS/p53/p21 pathway in bone marrow-derived mesenchymal stem cells in vivo. Biomed Pharmacother 2018;106:1126-1134.

125. Nacarelli T, Lau L, Fukumoto T, Zundell J, Fatkhutdinov N, Wu S, Aird KM, et al. NAD(+) metabolism governs the proinflammatory senescence-associated secretome. Nat Cell Biol 2019;21:397-407.

126. Das A, Huang GX, Bonkowski MS, Longchamp A, Li C, Schultz MB, Kim LJ, et al. Impairment of an Endothelial NAD(+)-H_2S Signaling Network Is a Reversible Cause of Vascular Aging. Cell 2018;173:74-89 e20.

127. Tang BL. Sirt1 and the Mitochondria. Mol Cells 2016;39:87-95.

128. Lee HJ, Feliers D, Barnes JL, Oh S, Choudhury GG, Diaz V, Galvan V, et al. Hydrogen sulfide ameliorates aging-associated changes in the kidney. Geroscience 2018;40:163-176.

129. Hillmer EJ, Zhang H, Li HS, Watowich SS. STAT3 signaling in immunity. Cytokine Growth Factor Rev 2016;31:1-15.

130. Hutchins AP, Diez D, Miranda-Saavedra D. The IL-10/STAT3-mediated anti-inflammatory response: recent developments and future challenges. Brief Funct Genomics 2013;12:489-498.

131. Nguyen-Jackson HT, Li HS, Zhang H, Ohashi E, Watowich SS. G-CSF-activated STAT3 enhances production of the chemokine MIP-2 in bone marrow neutrophils. J Leukoc Biol 2012;92:1215-1225.

132. Lo HW, Hsu SC, Ali-Seyed M, Gunduz M, Xia W, Wei Y, Bartholomeusz G, et al. Nuclear interaction of EGFR and STAT3 in the activation of the iNOS/NO pathway. Cancer Cell 2005;7:575-589.

133. Wegrzyn J, Potla R, Chwae YJ, Sepuri NB, Zhang Q, Koeck T, Derecka M, et al. Function of mitochondrial Stat3 in cellular respiration. Science 2009;323:793-797.

134. Niso-Santano M, Shen S, Adjemian S, Malik SA, Marino G, Lachkar S, Senovilla L, et al. Direct interaction between STAT3 and EIF2AK2 controls fatty acid-induced autophagy. Autophagy 2013;9:415-417.

135. Kojima H, Inoue T, Kunimoto H, Nakajima K. IL-6-STAT3 signaling and premature senescence. JAKSTAT 2013;2:e25763.

136. Kong X, Feng D, Wang H, Hong F, Bertola A, Wang FS, Gao B. Interleukin-22 induces hepatic stellate cell senescence and restricts liver fibrosis in mice. Hepatology 2012;56:1150-1159.

137. Huang YH, Chen MH, Guo QL, Chen YX, Zhang LJ, Chen ZX, Wang XZ. Interleukin10

promotes primary rat hepatic stellate cell senescence by upregulating the expression levels of p53 and p21. Mol Med Rep 2018;17:5700-5707.

138. Huang YH, Chen MH, Guo QL, Chen ZX, Chen QD, Wang XZ. Interleukin-10 induces senescence of activated hepatic stellate cells via STAT3-p53 pathway to attenuate liver fibrosis. Cell Signal 2020;66:109445.

139. Waters DW, Blokland KEC, Pathinayake PS, Wei L, Schuliga M, Jaffar J, Westall GP, et al. STAT3 Regulates the Onset of Oxidant-induced Senescence in Lung Fibroblasts. Am J Respir Cell Mol Biol 2019;61:61-73.

140. Yang S, Sun D, Wang L, Wang X, Shi M, Jiang X, Gao X. The role of STAT3/mTOR-regulated autophagy in angiotensin II-induced senescence of human glomerular mesangial cells. Cell Signal 2019;53:327-338.

141. Jin H, Lian N, Zhang F, Chen L, Chen Q, Lu C, Bian M, et al. Activation of PPARgamma/P53 signaling is required for curcumin to induce hepatic stellate cell senescence. Cell Death Dis 2016;7:e2189.

142. Jin H, Jia Y, Yao Z, Huang J, Hao M, Yao S, Lian N, et al. Hepatic stellate cell interferes with NK cell regulation of fibrogenesis via curcumin induced senescence of hepatic stellate cell. Cell Signal 2017;33:79-85.

143. Sugihara H, Teramoto N, Yamanouchi K, Matsuwaki T, Nishihara M. Oxidative stress-mediated senescence in mesenchymal progenitor cells causes the loss of their fibro/adipogenic potential and abrogates myoblast fusion. Aging (Albany NY) 2018;10:747-763.

144. Lujambio A, Akkari L, Simon J, Grace D, Tschaharganeh DF, Bolden JE, Zhao Z, et al. Non-cell-autonomous tumor suppression by p53. Cell 2013;153:449-460.

145. Paradis V, Youssef N, Dargere D, Ba N, Bonvoust F, Deschatrette J, Bedossa P. Replicative senescence in normal liver, chronic hepatitis C, and hepatocellular carcinomas. Hum Pathol 2001;32:327-332.

146. Richardson MM, Jonsson JR, Powell EE, Brunt EM, Neuschwander-Tetri BA, Bhathal PS, Dixon JB, et al. Progressive fibrosis in nonalcoholic steatohepatitis: association with altered regeneration and a ductular reaction. Gastroenterology 2007;133:80-90.

147. Kandhaya-Pillai R, Miro-Mur F, Alijotas-Reig J, Tchkonia T, Kirkland JL, Schwartz S. TNFalpha-senescence initiates a STAT-dependent positive feedback loop, leading to a sustained interferon signature, DNA damage, and cytokine secretion. Aging (Albany NY) 2017;9:2411-2435.

148. Wan J, Benkdane M, Alons E, Lotersztajn S, Pavoine C. M2 kupffer cells promote hepatocyte senescence: an IL-6-dependent protective mechanism against alcoholic liver disease.

Am J Pathol 2014;184:1763-1772.

149. Ogrodnik M, Miwa S, Tchkonia T, Tiniakos D, Wilson CL, Lahat A, Day CP, et al. Cellular senescence drives age-dependent hepatic steatosis. Nat Commun 2017;8:15691.

150. Pignolo RJ, Passos JF, Khosla S, Tchkonia T, Kirkland JL. Reducing Senescent Cell Burden in Aging and Disease. Trends Mol Med 2020;26:630-638.

151. Ritschka B, Knauer-Meyer T, Goncalves DS, Mas A, Plassat JL, Durik M, Jacobs H, et al. The senotherapeutic drug ABT-737 disrupts aberrant p21 expression to restore liver regeneration in adult mice. Genes Dev 2020;34:489-494.

152. Ehedego H, Boekschoten MV, Hu W, Doler C, Haybaeck J, Gabetaler N, Muller M, et al. p21 ablation in liver enhances DNA damage, cholestasis, and carcinogenesis. Cancer Res 2015;75:1144-1155.

153. Papatheodoridi AM, Chrysavgis L, Koutsilieris M, Chatzigeorgiou A. The Role of Senescence in the Development of Nonalcoholic Fatty Liver Disease and Progression to Nonalcoholic Steatohepatitis. Hepatology 2020;71:363-374.

154. Chan ASL, Narita M. Short-term gain, long-term pain: the senescence life cycle and cancer. Genes Dev 2019;33:127-143.

155. Faggioli F, Palagano E, Di Tommaso L, Donadon M, Marrella V, Recordati C, Mantero S, et al. B lymphocytes limit senescence-driven fibrosis resolution and favor hepatocarcinogenesis in mouse liver injury. Hepatology 2018;67:1970-1985.

156. Strosberg AD. Structure, function, and regulation of adrenergic receptors. Protein Science 1993; 2: 1198-1209.

157.Suzuki E, Tsujimoto G, Tamura K, Hashimoto K. Two pharmacologically distinct al-adrenoceptor subtypes in the contraction of rabbit aorta: each subtype couples with a different Ca + signalling mechanism and plays a different physiological role. Mol Pharmacal. 1990; 38:725-36.

158. van Breemen C, Saida K. Cellular mechanisms regulating [Ca2+]i smooth muscle. Annu. Rev. Physiol. 1989; 51:315-29.

159. Burch RM, Luini A, Axelrod J. Phospholipase A_2 and phospholipase C are activated by distinct GTP binding proteins in response to α1-adrenergic stimulation in FRTL-5 thyroid cells. Proc. Natl. Acad. Sci. 1986; 83:7201-05

160. Han C, Wilson KM, Minneman KP. α1-Adrenergic receptor subtypes and formation of inositol phosphates in dispersed hepatocytes and renal cells. Mol. Pharmacal. 1990; 37:903-10

161. Wilson KM, Minneman KP. Different pathways of [^{3}H] inositol phosphate formation

mediated by α1a and α1b-adrenergic receptors. J. Bioi. Chem. 1990; 265: 17601-06.

162. C. Wiel, H. Lallet-Daher, D. Gitenay, et al. Endoplasmic reticulum calcium release through ITPR2 channels leads to mitochondrial calcium accumulation and senescence. Nat. Commun. 2014; 5: 3792.

163. A.V. Borodkina, A.N. Shatrova, P.I. Deryabin, et al., Calcium alterations signal either to senescence or to autophagy induction in stem cells upon oxidative stress. Aging (Albany NY). 2016; 8;8(12):3400-3418.

164. Rasmussen CD, Means AR. Calmodulin is required for cell-cycle progression during G1 and mitosis. Embo J. 1989; 8:73–82.

165. Kahl CR,Means AR, Calcineurin regulates cyclin D1 accumulation in growth-stimulated fibroblasts, Mol. Biol. Cell. 2004;15:1833–1842.

166. Nishizuka Y. The role of protein kinase C in cell surface signal transduction and tumour promotion. Nature. 1984; 308:693–698.

167. Kashiwagi M, Ohba M, Watanabe H, Ishino K, Kasahara K, Sanai Y, et al. PKCeta associates with cyclin E/cdk2/p21 complex, phosphorylates p21 and inhibits cdk2 kinase in keratinocytes. Oncogene. 2000; 19:6334–6341.

168. Detjen KM, Brembeck FH, Welzel M, Kaiser A, Haller H, Wiedenmann B, et al.Activation of protein kinase Calpha inhibits growth of pancreatic cancer cells via p21(cip)-mediated G(1) arrest. J. Cell Sci. 2000; 113(17): 3025– 3035

169. Hizli A A, Black AR, Pysz MA, Black JD. Protein kinase C alpha signaling inhibits cyclin D1 translation in intestinal epithelial cells. J. BioI. Chem. 2006; 281: 14596–14603.

170. Tibudan SS, Wang Y, Denning MF. Activation of protein kinase C triggers irreversible cell cycle withdrawal in human keratinocytes. J. Invest. Dermatol. 2002; 119:1282–1289.

171. Clark JA, Black AR, Leontieva OV, Frey MR, Pysz MA, Kunneva L, et al. Involvement of the ERK signaling cascade in protein kinase C- mediated cell cycle arrest in intestinal epithelial cells. J. Biol. Chem. 2004; 279:9233–9247.

172. Katakura Y, Udono M, Katsuki K, Nishide H, Tabira Y, Ikei T, et al. Protein Kinase C δ Plays a Key Role in Cellular Senescence Programs of Human Normal Diploid Cells. J. Biochem. 2009;146(1)87–93.

173. Liu Y, Lin JK, Chen WK, Liu C, Wang C, et al. Augmentation of prtein kinase C activity and liver cell proliferation in lead nitrate treated rats.Biochemistryand Molecular Biology International. 1997; 43:355-364.

174. Alisi A, Spagnuolo S, Napoletano S, Spaziani A, Leoni S. Thyroid hormones regulate DNA-synthesis and cell-cycle proteins by activation of PKCalpha and p42/44 MAPK in chick embryo hepatocytes. J Cell Physiol. 2004;201(2):259-65.

175. He JJ, Zhang WZ,Liu SL, Chen YF, Liao SX, Shen Q, et al. Activation of β-adrenergic receptor promotes cellular proliferation in human glioblastoma. Oncoloy letters. 2017; 14: 3846-3852.

176. Montoya A, Varela-Ramirez A, Dickerson E, Pasquier E, Torabi A, Aguilera R, et al. The beta adrenergic receptor antagonist propranolol alters mitogenic and apoptotic signaling in late stage breast cancer. Biomedical Journal. 2019; 42:155-165.

177. Oben JA, Yang S, Lin H, Ono M, Diehl AM. Norepinephrine and neuropeptide Y promote proliferation and collagen gene expression ofhepatic myofibroblastic stellate cells. Biochemical and Biophysical Research Communications. 2003; 302 (4):685–690.

178. Oben JA, Roskams T, Yang S, Lin H, Sinelli N, Torbenson, et al. Hepatic fibrogenesis requires sympathetic neurotransmitters. Gut. 2004; 53: 438–445.

179. Sigala B, McKee C, Soeda J, Pazienza V, Morgan M, Lin C, et al. Sympathetic Nervous System Catecholamines and Neuropeptide Y Neurotransmitters Are Upregulated in Human NAFLD and Modulate the Fibrogenic Function of Hepatic Stellate Cells. PLoS ONE, 2013, 8(9): e72928.

180. Serna-Salas SA, Navarro-González Y, Martinez-Hernández SL, Barba-Gallardo LF, Sánchez-Alemán E, et al. Doxazosin and Carvedilol Treatment Improves Hepatic Regeneration in a Hamster Model of Cirrhosis. Biomed Res Int. 2018; 12:4706976.

Chapter 3

Bioactive coumarin-derivative esculetin decreases hepatic stellate cell activation via induction of cellular senescence via the PI3K-Akt-GSK3β pathway

Mengfan Zhang, Turtushikh Damba, Manon Buist-Homan, Klaas Nico Faber, Han Moshage

Department of Gastroenterology and Hepatology, University Medical Center Groningen, University of Groningen, the Netherlands

Correspondence: Han Moshage; a.j.moshage@umcg.nl

Key words: Fibrosis, Esculetin, Hepatic stellate cell, Senescence, P21, Akt

Abstract

Background: Activation of hepatic stellate cells (HSC) leads to initiation and progression of liver fibrosis. HSC senescence is inversely correlated with HSC proliferation and activation. Therefore, induction of HSC senescence may be a strategy to treat liver fibrosis. The natural compound esculetin, a coumarin-derivative, has been shown to inhibit HSC activation and proliferation, however its effect on senescence is unknown. Aim: to investigate the effect of esculetin on HSC activation and senescence. Methods Primary rat HSCs were used in all experiments. Real-time cell analyzer and BrdU incorporation assay were used to determine HSC proliferation. Gene expression of the senescence-associated genes Cdkn1a (p21), P53, activation markers Acta2, Col1a1 and quiescence markers Pparg and Lrat were measured by RT-qPCR. Senescence associated β-Galactosidase (SA-β-Gal) staining was used to identify senescent HSCs. Akt/GSK3β phosphorylation and $P21^{Cip1}$ expression was probed by Western blotting. **Results:** Esculetin increased percentage of SA-β-Gal positive cells and mRNA level of Cdkn1a and Il6 in HSCs. Proliferation of HSCs was inhibited and mRNA expression of fibrogenic genes Acta2 and Col1a1 was reduced by esculetin, while Pparg mRNA expression was restored in esculetin-treated HSCs. Activated HSCs pre-treated with esculetin followed by washout still exhibited less proliferation and activation and increased expression of senescence markers and SA-β-Gal staining. Protein expression of $P21^{Cip1}$, accompanied by phosphorylation of Ser473 Akt and Ser9 GSK3β was increased by esculetin. The effect of esculetin was dependent on PI3K-Akt signaling. **Conclusions:** Esculetin induces HSC senescence and reverses the fibrogenic phenotype of HSCs. The induction of senescence depends on PI3K-Akt-GSK3β signaling. Inadequate induction of senescence preserves fibrogenic phenotype of HSCs. Esculetin could be a potential therapeutic drug for liver fibrosis by the novel mechanism of inducing senescence.

Introduction

Liver fibrosis is a dynamic pathological process characterized by the accumulation of excessive extracellular matrix (ECM) resulting from chronic liver injury of any etiology, including chronic viral hepatitis, alcoholic liver disease (ALD) and non-alcoholic fatty liver disease (NAFLD). The prevalence of liver fibrosis varies from 0.7% to 25.7% in different cohorts (1). Advanced liver fibrosis has a high risk to progress to cirrhosis, which is estimated to result in 1.03 million deaths per year worldwide (2). Activation of hepatic stellate cells (HSC) plays a pivotal role in the initiation and progression of hepatic fibrosis in experimental and human liver injury (3). Activated HSCs acquire a myofibroblast-like phenotype with enhanced proliferation, contractility, matrix synthesis, altered matrix degradation and pro-inflammatory signaling to form scar tissue in injured liver (3, 4). It is a consensus that if activation of HSCs is prevented or reversed, liver fibrosis can be slowed down or even reversed.

Currently, there is a strong interest in bioactive natural compounds that are able to prevent or reverse HSC activation. Esculetin, a coumarin derivative, has been demonstrated to attenuate hepatic steatosis and inflammation (5, 6). Esculetin has been shown to inhibit proliferation of vascular smooth muscle cell and cancer cells (7, 8). Moreover, esculetin has been demonstrated to attenuate liver fibrosis via inhibition of the activation of hepatic stellate cells (Bai et al; in preparation). Interestingly, cell cycle arrest, which is a characteristic of cellular senescence, has also been observed in esculetin-treated cells (9).

Cellular senescence is a specific phenomenon characterized by the induction of permanent growth arrest of proliferating cells in response to various cellular stresses (10). It has been shown that induction of cellular senescence is negatively correlated with proliferation and activation of HSCs (11, 12). In addition, there is a specific set of secretory proteins released by senescent cells, collectively defined as the senescence associated secretory phenotype (SASP). SASP displays a characteristic secretory proteome, including specific cytokines and chemokines, to promote tissue regeneration through the induction of cell plasticity and stemness (13). Inadequate senescence induction in experimental models of fibrosis exacerbate progression of fibrosis (11, 14). Therefore, induction of stellate cell senescence can be a therapeutic strategy for liver fibrosis.

Several studies have demonstrated that natural compounds can induce HSC senescence and attenuate experimental liver fibrosis (15, 16). In view of the reported effects of esculetin on cell proliferation, we hypothesized that esculetin can induce HSC senescence and consequently alleviate liver fibrosis. *In vitro* experiments were conceived and performed on primary rat HSC to verify our hypothesis.

Materials and Methods

Rats and cell isolation

Primary rat HSCs were isolated from 350-500g specified pathogen-free male Wistar rats (Charles River, Wilmington, MA, USA). Rats were housed under standard animal laboratory conditions with free access to food and drinking water. All experiments were carried out according to the guidelines for welfare of laboratory animals from the Committee for Care and Use of laboratory animals of the University of Groningen. Cells were isolated via portal vein perfusion with Pronase-E (Merck, Amsterdam, the Netherlands) and Collagenase-P (Roche, Almere, the Netherlands) until complete digestion of the liver, followed by gradient centrifugation on 13% (w/v) Nycodenz (Axis-Shield POC, Oslo, Norway). Isolated cells were cultured in Iscove's Modified Dulbecco's Medium supplemented with Glutamax (Thermo Fisher Scientific, Waltham, MA, USA), 20% heat inactivated fetal calf serum (Thermo Fisher Scientific), 1% MEM Non Essential Amino Acids (Thermo Fisher Scientific), 1% Sodium Pyruvate (Thermo Fisher Scientific) and antibiotics: 50 µg/mL gentamycin (Thermo Fisher Scientific), 100 U/mL penicillin (Lonza, Vervier, Belgium), 10 µg/mL streptomycin (Lonza) and 250 ng/mL fungizone (Lonza) in an incubator containing 5% CO_2 at a 37°C.

Experimental design

Isolated quiescent HSCs were cultured in culture medium for 7 days for culture-activation. Activated HSCs were then seeded at 70% confluency in plates. Unless otherwise stated, all treatments were performed in fresh medium. Esculetin (Alfa Aesar, MA, USA) and the pan-PI3k inhibitor LY294002 (Calbiochem, Darmstadt, Germany) were diluted in DMSO to prepare stock solutions. Each experimental condition was performed in duplicate and repeated at least 3 times.

Quantitative Real-Time Polymerase Chain Reaction

Gene expression levels were quantified by real-time reverse transcription polymerase chain reaction. Total mRNA was isolated from cells using Tri-reagent (Sigma Aldrich) according to the manufacturer's protocol. Concentration of RNA was determined by Nano-Drop 2000c (Thermo Fisher Scientific). cDNA was synthesized from 0.5-2.5 µg RNA by MLV reverse transcriptase and RNase Out (Sigma-Aldrich). Gene expression was determined by TaqMan probes and primers by real-time polymerase chain reaction on the QuantStudioTM 3 system (Thermo Fisher Scientific). Relative gene expression was

calculated via the $2^{-\Delta\Delta Ct}$ method. The primers and probes are shown in Table 1. All samples were measured in duplicate using 36b4 as housekeeping gene.

Table 1.

Gene	Sense 5'-3'	Antisense 5'-3'	Probe 5'-3'
36b4	GCTTCATTGTGGGAGCAGACA	CATGGTGTTCTTGCCCATCAG	TCCAAGCAGATGCAGCAGATCCGC
Col1α1	TGGTGAACGTGGTGTACAAGGT	CAGTATCACCCTTGGCACCAT	TCCTGCTGGTCCCCGAGGAAACA
Acta2	GCCAGTCGCCATCAGGAAC	CACACCAGAGCTGTGCTGTCTT	CTTCACACATAGCTGGAGCAGCTTCTCGA
Cdkn1a ($P21^{Cip1}$)	TTGTCGCTGTCTTGCACTCTG	CGCTTGGAGTGATAGAAATCTGTTA	CTGCCTCCGTTTTCGGCCCTG
Il-6	CCGGAGAGGAGACTTCACAGA	AGAATTGCCATTGCACAACTCTT	ACCACTTCACAAGTCGGAGGCTTAATTACA
Tp53	CCATGAGCGTTGCTCTGATG	CAGATACTCAGCATACGGATTTCCT	CGGCCTGGCTCCTCCCCAAC
Pparg	GACCCCAGAGTCACCAAATGA	GGCCTGCAGTTCCAGAGAGT	CCCCATTTGAGAACAAGACTATTGAGCGAACC
Lrat	ACTGTGGAACAACTGCGAACAC	AGGCCTGTGTAGATAATAGACACTAATCC	TTGTGACCTACTGCAGATACGGCTC
Mmp9	CCCTCTGCATGAAGACGACAT	GGAGGTGCAGTGGGACACA	TCCAGCATCTGTATGGTCGTGGCTCTAAAC

Senescence-associated β-galactosidase staining

Senescent cells were identified by Senescence-associated β-galactosidase staining kit (Cell Signaling Technology, Danvers, Massachusetts, USA) according to the supplier's instruction. Briefly, after treatment, activated HSCs were fixated and stained by X-gal solution (pH= 5.9-6.1) for 24 hr at 37^0C in a dry incubator. After incubation, the β-galactosidase staining solution was removed and wells were rinsed in 70% glycerol and images were evaluated on the EVOS xl cell imaging (Thermo Fisher Scientific) microscope (200x magnification).

Cell proliferation assay

Cell proliferation was determined by Real Time Cell Analysis system xCELLigence (RTCA DP; ACEA Biosciences, Inc., CA, USA) and results were confirmed using the BrdU incorporation assay (Roche Diagnostic Almere, the Netherlands). Using the xCELLigence system, cell confluence was monitored in real-time and cell index was measured in E-plates. Cells were seeded in 96 well plates and treated as described before. Incorporation of BrdU

in proliferating cells was detected by chemiluminescence using Synergy-4 (Bio-Tek).

Western blot analysis

Protein samples were prepared in lysis buffer (HEPES 25 mmol/L, KAc 150 mmol/L, EDTA pH 8.0 2mmol/L, NP-40 0.1%, NaF 10 mmol/L, PMSF 50 mmol/L, aprotinin 1 μg/μL, pepstatin 1 μg/μL, leupeptin 1 μg/μL, DTT 1 mmol/L). Protein concentration was quantified by Bio-Rad protein assay (Bio-Rad; Hercules, CA, USA) according to the manufacturer's protocol using bovine serum albumin (BSA) to prepare a standard curve. Gel electrophoresis was performed with 10-20 μg protein using the Mini-Protein® TGX™ precast 4-15% gels (Bio-Rad), followed by transblotting to 0.2 μm nitrocellulose membrane (Bio-Rad). Proteins were detected using the primary antibodies listed in table 2. Protein band intensities were determined and detected using the Chemidoc MR (Bio-Rad) system.

Table 2.

Protein	Species	Dilution	Company
β-Actin	Polyclonal rabbit	1:1000	4970, Cell Signaling
COL1α1	Polyclonal goat	1:2000	1310-01, Southern Biotech
ACTA2	Polyclonal rabbit	1:2000	Ab5694, Abcam
Phospho-AKT (Ser473)	Polyclonal rabbit	1:1000	9271L, Cell Signaling
Phospho-AKT (Thr 308)	Polyclonal rabbit	1:1000	sc-16646-R, Santa Cruz
Total AKT	Polyclonal rabbit	1:2000	9272, Cell Signaling
Phospho-GSK3β(Ser9)	Polyclonal rabbit	1:1000	9336, Cell Signaling
Total GSK3β	Monoclonal rabbit	1:2000	9315, Cell Signaling
P21(Gene is *Cdkn1a*)	Monoclonal rabbit	1:1000	ab109199, Abcam
GAPDH	Monoclonal mouse	1:1000	CB1001, Calbiochem

Statistical analysis

Data are presented as mean ± standard deviation (mean±SD) and mean ± standard error of means (mean±sem). Each result was obtained from at least three independent experiments. Statistical significance was determined by Mann-Whitney U test between the two groups, one-way ANOVA or Kruskal-Wallis followed by post-hoc Dunnet's test for multiple comparison test and two-way ANOVA followed by Tukey's multiple comparison. $P<0.05$ was considered statistically significant (*: $p<0.05$, **: $p<0.01$, ***: $p<0.001$, ****: $p<0.001$, ns: $p>0.05$). Data analysis was performed using GraphPad Prism 7 (GraphPad Software, San Diego, CA, USA).

Results

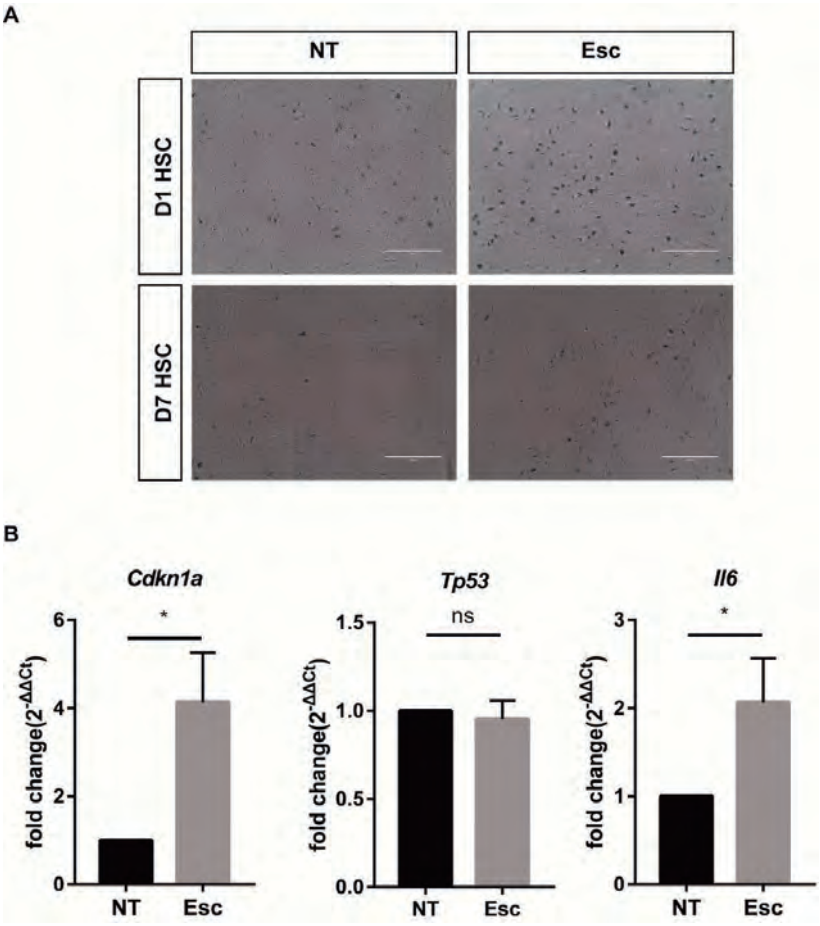

Figure 1. Esculetin induces senescence of primary HSCs.

A. Senescence Associated β-Galactosidase staining. Quiescent qHSCs (D1) and activated aHSCs (D7) were treated with 50 μmol/L esculetin or vehicle for 48 hr. Magnification: 200x. **B.** aHSCs were treated with 50 μmol/L esculetin or vehicle for 48 hr and mRNA expression of Cdkn1a, Tp53 and Il6 was determined and shown as mean±sem.

Freshly isolated quiescent HSCs become activated during cell culture (17). D1 and D7 cultured HSCs represent quiescent HSCs (qHSC) and activated HSCs (aHSC), respectively. Senescence associated β-Galactosidase (SA-β-Gal) staining was used to determine cell senescence. As shown in Figure 1A, esculetin treatment increased the number of β-Gal positive cells in both qHSCs and aHSCs. Senescence associated genes Cdkn1a, Tp53 and Il6 mRNA expression were measured as markers of senescence, shown in Figure 1B. Expression of Cdkn1a and Il6 was increased four-fold and two-fold, respectively, in

esculetin-treated aHSCs. In contrast, Tp53 mRNA expression was not affected by esculetin.

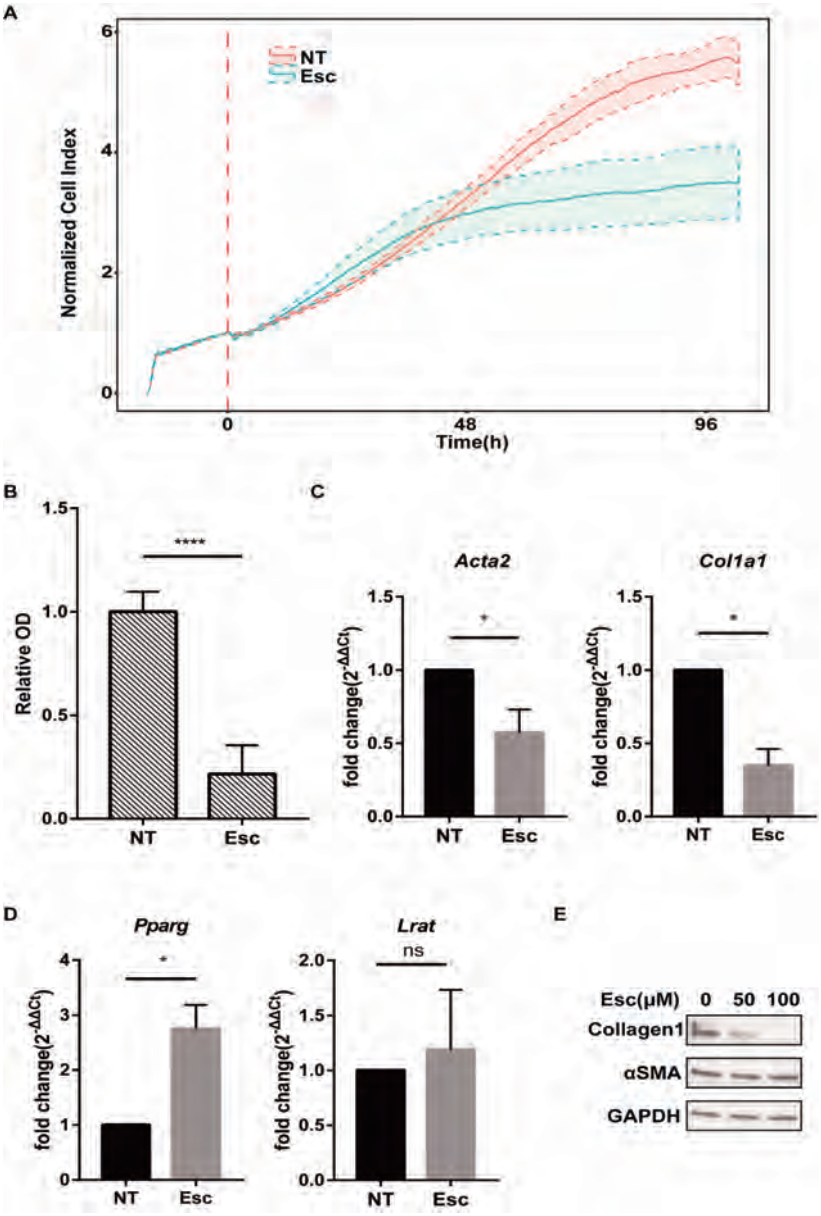

Figure 2. Esculetin inhibits proliferation and activation of primary hepatic stellate cells.

A. xCELLigence proliferation assay. Activated primary HSCs were cultured and treated with 50 μmol/L esculetin or vehicle for 96 hr. Normalized cell index is shown as mean±sd. **B.** BrdU incorporation assay. Activated primary HSCs were cultured in 96-well plates and treated by 50 μmol/L esculetin or vehicle for 72 hr. Data are shown as mean±sem, n = 3. **C, D.** Quiescent primary HSCs were treated by 50 μmol/L

esculetin or vehicle for 48 hr. Data are shown as mean±sem, n = 4. **E.** Expression of collagen type I and αSMA protein was determined by Western blotting in aHSCs treated for 72 hr with 0, 50 and 100 μmol/L esculetin, respectively.

Uncontrolled proliferation of aHSCs is one of most important characteristics during fibrosis progression (3). Therefor we investigated whether esculetin had anti-proliferative effects. As shown in **Figure 2A**, esculetin inhibited the proliferation of aHSCs significantly after 48 hr of incubation. To verify whether the decreased cell index was the result of inhibition of proliferation, we performed the BrdU incorporation assay. As shown in **Figure 2B**, incorporation of BrdU in proliferating HSCs was reduced by 70% in esculetin-treated cells, which demonstrated that esculetin inhibited DNA replication in S-phase cells. Next, we examined whether esculetin could prevent activation of qHSCs. As shown in **Figure 2C**, expression of the activation markers *Acta2* and *Col1a1* was decreased by about 40% and 60%, respectively upon treatment with esculetin. In contrast, esculetin-treated qHSCs had more than two-fold higher expression of the quiescence marker *Pparg* than vehicle treated cells. *Lrat* expression did not change upon esculetin treatment as shown in **Figure 2D**. Collagen type1 but not αSMA protein expression in aHSCs was inhibited by esculetin in a dose-dependent manner. Moreover, we performed immunofluorescence microcopy to determine intracellular collagen expression. The result was in line with the Western blotting results of **Figure 2D** as shown in supplemental **Figure S1**.

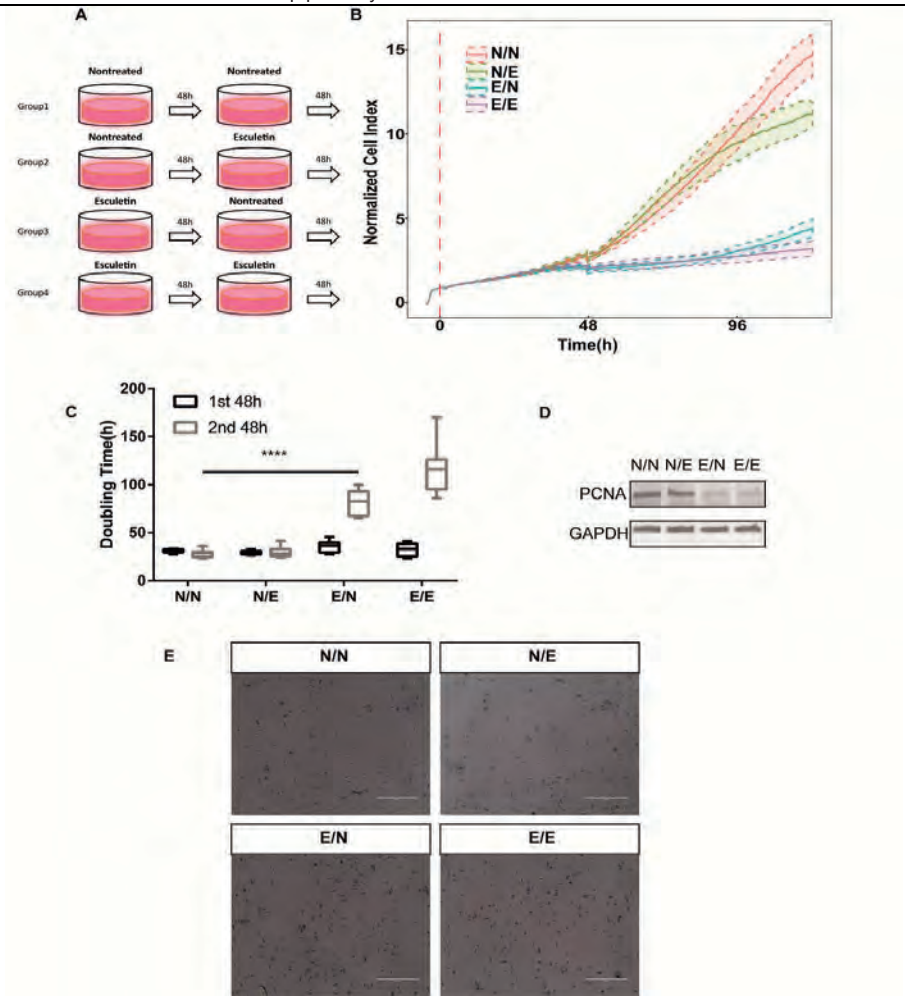

Figure 3. Esculetin induced long-lasting senescence of primary HSCs.

A. Graphical illustration of wash-out strategy of different groups. **B.** xCELLigence proliferation assay. Primary HSCs were seeded into plates and treated by wash-out strategy as indicated. **C.** Doubling time of cell index before and after wash-out was calculated and depicted as mean±sd. **D.** PCNA protein expression, determined by Western blotting using GAPDH as loading control. **E.** SA-β-Gal staining. Magnification 200X.

Since cellular senescence is characterized as stable cell-cycle arrest, we designed a wash-out strategy to determine the proliferation potential of HSCs as illustrated in **Figure 3A**. aHSCs pretreated with esculetin for 48 hr exhibited much lower proliferation ability compared to vehicle-treated ones in the subsequent 48 hr wash-out period as shown in **Figure 3B**. Furthermore, doubling time was sharply increased in esculetin pre-treated groups after wash-out as shown in **Figure 3C**. Proliferating cell nuclear antigen (PCNA)

stimulates DNA polymerases and promotes DNA synthesis and its expression is used as a marker for cell replication (18, 19). In line with the proliferation data, expression of PCNA in esculetin pre-treated groups was significantly lower than in non-pretreated ones after the 48 hr wash-out period as shown in **Figure 3D**. In addition, the number of β-Galactosidase positive cells in esculetin pre-treated groups remained higher than non-treated groups in spite of the wash-out as shown in **Figure 3E**.

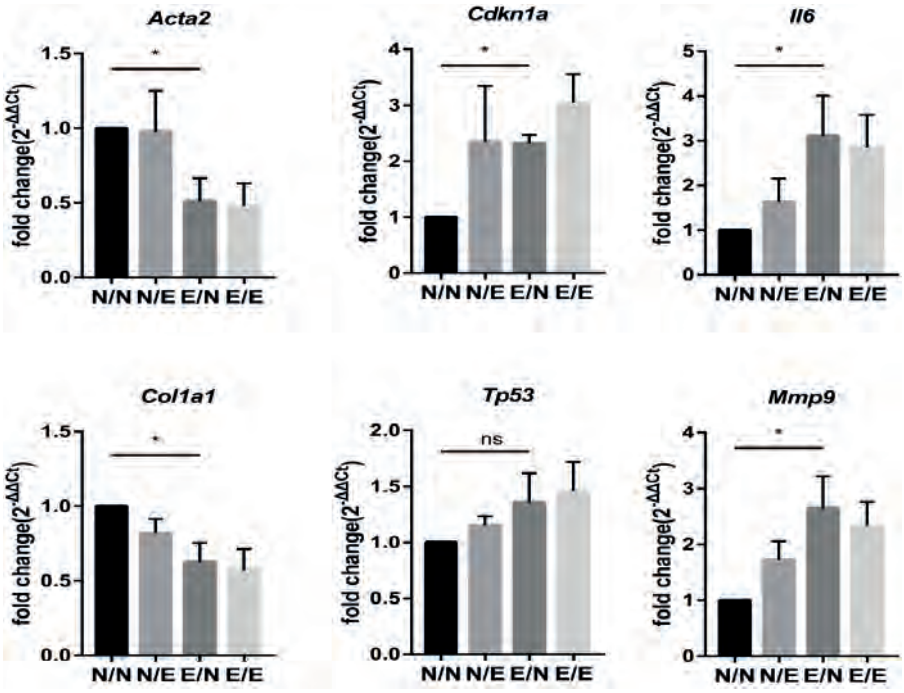

Figure 4. Esculetin induces senescence progression in aHSCs.

aHSCs were treated with esculetin, followed by wash-out protocol and mRNA levels were measured by RT-qPCR. Data are shown as mean±sem; n=3.

As shown in **Figure 4**, aHSCs pre-treated by esculetin following wash-out generally maintained a similar transcription profile compared to cells continuously treated with esculetin. However, compared to non-treated cells, pre-treated aHSCs demonstrated a 50% and 40% reduction of expression of *Acta2* and *Col1a1*, respectively. Additionally, expression of *Cdkn1a, Il6* and *Mmp9* mRNA was increased 2-3 fold while *Tp53* tended to increase but not significantly in esculetin pre-treated aHSCs.

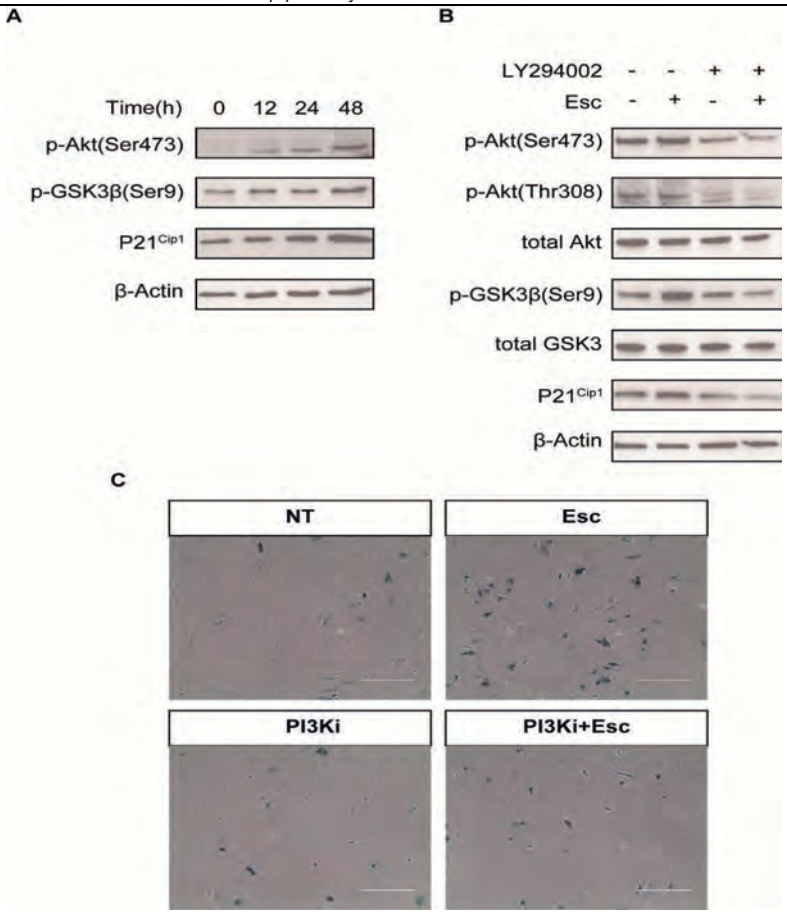

Figure 5. Esculetin induces senescence via the PI3K-Akt-GSK3β pathway.

A. aHSCs were treated with esculetin and harvested at 0, 12, 24 and 48 hr after treatment. **B**. aHSCs were treated with or without 2 μmol/L LY294002 followed by treatment with 50 μmol/L esculetin or vehicle for 24 hr. **C**. SA-β-Gal staining. aHSCs were treated with or without 2 μmol/L LY294002 followed by 50 μmol/L esculetin or vehicle for 48 hr.

Cooperation between intracellular Akt and $P21^{Cip1}$ is essential for the induction of senescence (20). Phosphorylation at the Ser473 site activates Akt kinase. GSK3β is its main target and is phosphorylated at Ser9 by active Akt (21). We hypothesized that esculetin treatment activates Akt in HSCs. Therefore, we investigated phosphorylation of Akt at Ser473 and phosphorylation of its downstream target GSK3β at Ser9 as well as $P21^{Cip1}$ by Western blot at different time points after esculetin treatment (**Figure 5A**). Phosphorylation of Akt-Ser473 and GSK3β-Ser9 was induced within 48 hr of esculetin treatment, in line with increased expression of $P21^{Cip1}$. PI3K is one of the kinases able to activate Akt and

LY294002 is a non-selective inhibitor of PI3K that is used to block Akt activity (20). As shown in **Figure 5B**, phosphorylation of Akt-Ser473 and Akt-Thr308 was efficiently inhibited in aHSCs treated with esculetin in combination with LY204002 compared to esculetin alone. Phosporylation of GSK3β-Ser9 and expression of $P21^{Cip1}$ were also downregulated by LY294002. While total Akt and total GSK3β amount were not changed in any of the experimental conditions, LY294002 decreased phosphorylation of Akt as expected. The number of β-Gal positive cells was markedly diminished in aHSCs treated by the combination of esculetin and LY294002 compared to esculetin alone, shown in **Figure 5C**.

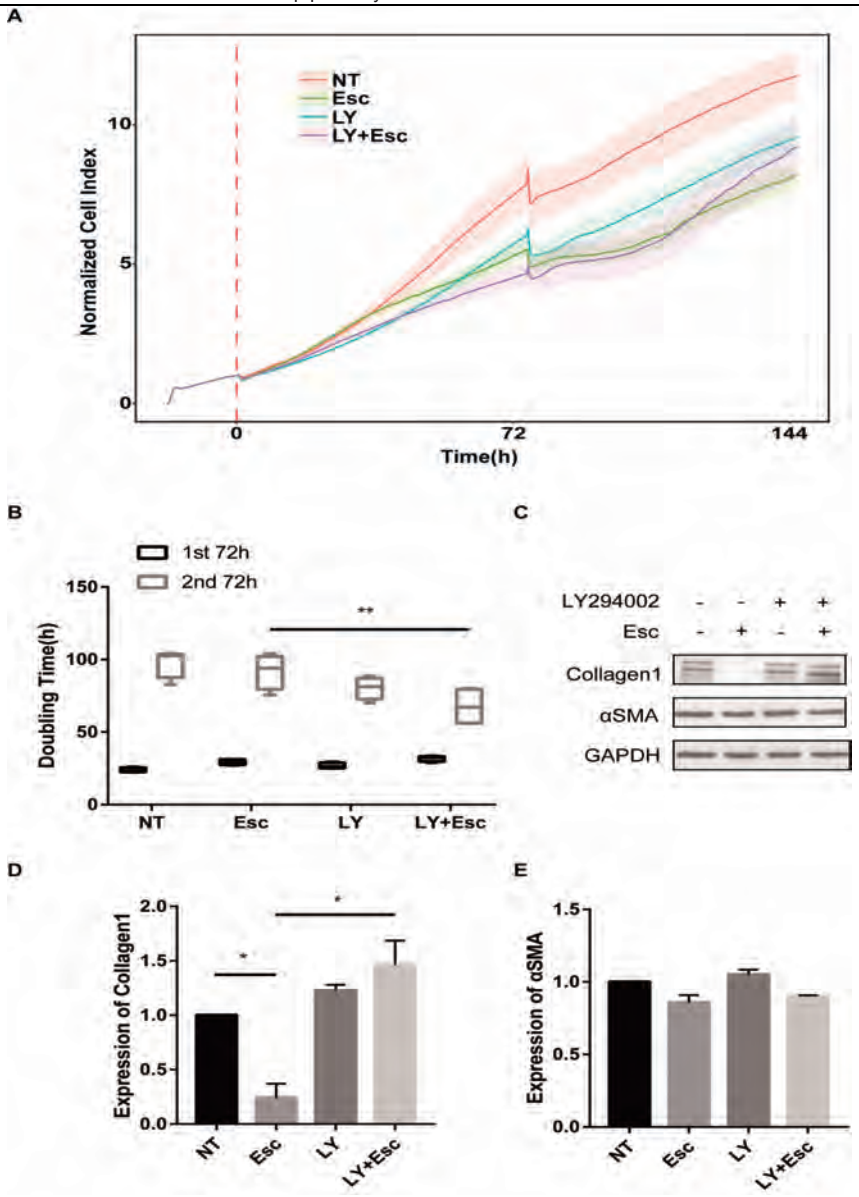

Figure 6. Inhibition of PI3K restores pro-fibrogenic phenotype in esculetin-treated aHSCs.

A. xCELLigence assay. aHSCs were treated with 2 μmol/L LY294002 or vehicle combined with or without esculetin for 72 hr after which medium was refreshed. **B.** Doubling time before and after wash-out (72 hr periods) were calculated and shown as median and quartile. **C-E.** aHSCs were treated by esculetin or vehicle with or without LY294002 for 72 hr. Collagen type I and αSMA were assessed by Western blotting.

Considering that the senescence phenotype is repressed by PI3K inhibitor, we

investigated whether the anti-senescent PI3K inhibitor could also affect the fibrogenic phenotype of HSCs which was suppressed by esculetin. In the first 72 hr, the PI3K inhibitor inhibited proliferation of aHSCs and did not rescue the impaired proliferation of esculetin-treated aHSCs. However, after wash-out and addition of fresh medium, aHSCs treated with esculetin in combination with PI3K inhibitor proliferated more rapidly than cells treated by esculetin or PI3K inhibitor alone as shown in **Figure 6A,B**. Likewise, collagen expression was restored by PI3K inhibitor in esculetin-treated aHSCs, as shown in **Figure 6C-D**, while expression of αSMA was not significantly changed in any of the experimental conditions.

Disscussion

Liver fibrosis is characterized by the excessive deposition of extracellular matrix (ECM) in the liver. Activated hepatic stellate cells are the main source of excessive matrix production in response to liver injury (2). Transdifferentiation of quiescent stellate cells into activated stellate cells is characterized by increased proliferation, contractility, chemotaxis and matrix synthesis (3). Activated HSCs have a specific phenotype, including increased expression of αSMA and collagen and decreased expression of PPARγ and LRAT (4). Cellular senescence of HSCs was observed in a model of experimental liver fibrosis and is thought to slow down the progression of fibrosis (11). Cellular senescence is characterized by a specific phenotype: $P21^{Cip1}$, $P16^{INK4A}$ and P53 are important effectors of the cell cycle arrest in senescence induction (10). Senescence-associated β-Galactosidase (SA-β-Gal) is increased as a consequence of lysosomal stress and is one of the well-established markers to identify senescent cells (22, 23). Senescent cells secrete a specific proteome consisting of cytokines, proteinases and chemokines, collectively known as senescence associated secretory phenotype (SASP). Among the components of the SASP is interleukin-6 (IL6), one of the essential cytokines that contribute to senescence in a paracrine manner (24). In contrast to fibrogenic HSCs, senescent HSCs exhibit decreased expression of αSMA and collagen and increased expression of inflammatory cell receptor ligands facilitating their clearance by the immune system (11, 16). The phenotype and biological properties of senescent HSCs suggest that inducing senescence of HSCs might be considered as a therapeutic strategy for liver fibrosis (12). In this study, we demonstrate that the coumarin-derivative esculetin induced a senescence-like phenotype in HSCs as demonstrated by increased mRNA expression of *Cdkn1a* (P21) and *Il6* and an increased number of SA-β-Gal positive cells. In our experimental protocol, an increase in P53 mRNA level was not observed. Because P21 is an established downstream target of and transcriptionally controlled by P53 (25), we assume that P53 might be changed in a

posttranslational manner to induce the expression of P21.

Since cellular senescence of HSCs was induced by esculetin, the fibrogenic phenotype of HSCs was also investigated to explore the association between senescence and fibrogenesis. P21, encoded by the gene CDKN1A, is the checkpoint of cell cycle progression in G1/S and G2/M transitions (26). Real-time xCELLigence assay as well as BrdU incorporation revealed that esculetin inhibited mitosis and DNA replication in HSCs. In line with this, P21 expression was increased upon treatment with esculetin in aHSCs.

Primary quiescent HSCs cultured *in vitro* on tissue culture plastic undergo activation into a fibrogenic phenotype characterized by active proliferation, increased expression of the fibrogenic markers *Acta2* and *Col1a1* and gradual loss of *Pparg* and *Lrat* (27). In our study, the increased expression of *Acta2* and *Col1a1* was inhibited by esculetin whereas expression of the quiescence marker *Pparg* was preserved. The expression of the quiescence marker *Lrat* was not affected by esculetin. Interestingly, it has been demonstrated that depletion of *Lrat* may not be an important factor in the acquisition of the fibrogenic phenotype (28). These results confirm the reciprocal regulation of the senescent and fibrogenic phenotype by esculetin in HSCs.

Cellular senescence has been described as a time-dependent process: initiation and maintenance of senescence are highly regulated by different signaling pathways (20, 29). The complete senescence phenotype depends on the combined action of various signaling pathways. For instance, $P21^{Cip1}$ initiates senescence whereas $P16^{INK4A}$ accounts for maintaining growth arrest (10). Permanent cell cycle arrest and non-responsiveness to mitogens and growth factors are essential to the senescent phenotype (10). We performed wash-out experiments to investigate the response of esculetin-treated HSCs to mitogens and growth factors in the absence of the senescence inducer. Our results show that the ability to proliferate remains inhibited in senescent cells. In line with this, protein expression of PCNA, which represents the S-phase of cells undergoing DNA replication (18), was also inhibited in senescent cells. Additionally, the SA-β-Gal staining demonstrated that during the wash-out period, the senescence phenotype did not reverse to the fibrogenic phenotype by the mitogens and growth factors present in medium. This phenomenon was also observed in co-cultures of senescent cells and proliferating cells (30). During the wash-out period, the expression levels of the senescence markers *Cdkn1a, Il6* and *Mmp9* remained at almost the same high level as in esculetin pre-treated cells with or without additional esculetin. These results indicate that the maintenance of the senescent phenotype is not dependent on the inducer itself (esculetin). This is in accordance with the mechanism described as SASP-induced non-cell-autonomous effect (14). Non-cell autonomous refers to the non-intrinsic mechanism and is attributed to e.g. the cell microenvironment (14, 31). The

mRNA expression of *Acta2* and *Col1a1* remained lower than in non-treated cells, demonstrating that the suppressed fibrogenic phenotype results from induced senescence.

Induction of senescence is a highly regulated biological process with different signaling pathways involved. Cooperation between Akt and P21 has been demonstrated to be essential in the initiation of cellular senescence (20, 32). Phosphorylation of Ser473 and Thr308 are well-known posttranslational modifications in the activation of Akt. GSK3β is the first downstream target of Akt and is phosphorylated by active Akt at Ser9. In addition, it has been demonstrated that phosphorylation at Ser9 of GSK3β is necessary to maintain protein expression of P21 (33) and that it correlates positively with cellular senescence (34). In our study, we observed that during the period of senescence induction, phosphorylation at Ser473 of Akt was accompanied by phosphorylation at Ser9 of GSK3β and increased gradually with time, indicating the existence of an Akt-GSK3β axis in senescence induction. PI3K is one of the main upstream activators of Akt and its non-selective inhibitor has been shown to reverse the inhibition of proliferation of fibroblasts in response to oncogene-induced senescence (20). LY294002 has been shown to inhibit phosphorylation at Ser9 of GSK3β and consequently to reduce P21 expression (33). Using PI3K inhibition, we could establish the importance of the PI3K-Akt-GSK3β pathway in the induction of senescence of esculetin-treated HSCs: LY294002 reduced phosphorylation at Ser473 and Thr308 of Akt and Ser9 of GSK3β as well as expression of P21 expression which was increased by esculetin treatment. In accordance with the reduced P21 expression, a sharp reduction in the number of SA-β-Gal positive cells was observed in esculetin-treated cells after LY294002 pretreatment. Therefore, it can be concluded that esculetin-induced HSC senescence depends on an intact PI3K-Akt-GSK3β pathway.

In addition to senescence induction, the PI3K-Akt pathway participates in a variety of biological processes including cell survival and proliferation (21). The PI3K inhibitor LY294002 failed to rescue the proliferative ability of HSC which was inhibited by esculetin. However, the ability of HSCs to respond to mitogens and growth factors was preserved during the wash-out period. Furthermore, collagen synthesis was completely rescued by the PI3K inhibitor. It should be noted that non-selective inhibition of PI3K also inhibited proliferation of HSC but did not affect collagen synthesis. These results suggest that concurrence of proliferation inhibition and loss of fibrogenic phenotype of HSCs is not indispensable for the induction of senescence.

In conclusion, esculetin induces HSC senescence and consequently inactivates HSC activation *in vitro*. The induction of senescence depends on an intact PI3K-Akt-GSK3β signaling pathway. In addition, our results demonstrate that inadequate induction of senescence can prevent inactivation and preserve the fibrogenic phenotype of HSCs. In this

regard, esculetin could be a potential therapeutic drug for liver fibrosis.

References

1. Harris R, Harman DJ, Card TR, Aithal GP, Guha IN. Prevalence of clinically significant liver disease within the general population, as defined by non-invasive markers of liver fibrosis: a systematic review. The Lancet Gastroenterology & Hepatology 2017;2:288-297.

2. Tsochatzis EA, Bosch J, Burroughs AK. Liver cirrhosis. The Lancet 2014;383:1749-1761.

3. Tsuchida T, Friedman SL. Mechanisms of hepatic stellate cell activation. Nat Rev Gastroenterol Hepatol 2017.

4. Bansal MB. Hepatic stellate cells: fibrogenic, regenerative or both? Heterogeneity and context are key. Hepatol Int 2016;10:902-908.

5. Choi RY, Ham JR, Lee MK. Esculetin prevents non-alcoholic fatty liver in diabetic mice fed high-fat diet. Chem Biol Interact 2016;260:13-21.

6. Pandey A, Raj P, Goru SK, Kadakol A, Malek V, Sharma N, Gaikwad AB. Esculetin ameliorates hepatic fibrosis in high fat diet induced non-alcoholic fatty liver disease by regulation of FoxO1 mediated pathway. Pharmacol Rep 2017;69:666-672.

7. Yun ES, Park SS, Shin HC, Choi YH, Kim WJ, Moon SK. p38 MAPK activation is required for esculetin-induced inhibition of vascular smooth muscle cells proliferation. Toxicol In Vitro 2011;25:1335-1342.

8. Lee SH, Park C, Jin CY, Kim GY, Moon SK, Hyun JW, Lee WH, et al. Involvement of extracellular signal-related kinase signaling in esculetin induced G1 arrest of human leukemia U937 cells. Biomed Pharmacother 2008;62:723-729.

9. Turkekul K, Colpan RD, Baykul T, Ozdemir MD, Erdogan S. Esculetin Inhibits the Survival of Human Prostate Cancer Cells by Inducing Apoptosis and Arresting the Cell Cycle. J Cancer Prev 2018;23:10-17.

10. Sharpless NE, Sherr CJ. Forging a signature of in vivo senescence. Nat Rev Cancer 2015;15:397-408.

11. Krizhanovsky V, Yon M, Dickins RA, Hearn S, Simon J, Miething C, Yee H, et al. Senescence of activated stellate cells limits liver fibrosis. Cell 2008;134:657-667.

12. Kong X, Feng D, Wang H, Hong F, Bertola A, Wang FS, Gao B. Interleukin-22 induces hepatic stellate cell senescence and restricts liver fibrosis in mice. Hepatology 2012;56:1150-1159.

13. Ritschka B, Storer M, Mas A, Heinzmann F, Ortells MC, Morton JP, Sansom OJ, et al. The senescence-associated secretory phenotype induces cellular plasticity and tissue regeneration. Genes & Development 2017;31:172-183.

14. Lujambio A, Akkari L, Simon J, Grace D, Tschaharganeh DF, Bolden JE, Zhao Z, et al. Non-cell-autonomous tumor suppression by p53. Cell 2013;153:449-460.

15. Jin H, Lian N, Zhang F, Chen L, Chen Q, Lu C, Bian M, et al. Activation of PPARgamma/P53

signaling is required for curcumin to induce hepatic stellate cell senescence. Cell Death Dis 2016;7:e2189.

16. Jin H, Jia Y, Yao Z, Huang J, Hao M, Yao S, Lian N, et al. Hepatic stellate cell interferes with NK cell regulation of fibrogenesis via curcumin induced senescence of hepatic stellate cell. Cell Signal 2017;33:79-85.

17. Dunning S, Ur Rehman A, Tiebosch MH, Hannivoort RA, Haijer FW, Woudenberg J, van den Heuvel FA, et al. Glutathione and antioxidant enzymes serve complementary roles in protecting activated hepatic stellate cells against hydrogen peroxide-induced cell death. Biochim Biophys Acta 2013;1832:2027-2034.

18. Boehm EM, Gildenberg MS, Washington MT. The Many Roles of PCNA in Eukaryotic DNA Replication. Enzymes 2016;39:231-254.

19. Goodlad RA. Quantification of epithelial cell proliferation, cell dynamics, and cell kineticsin vivo. Wiley Interdisciplinary Reviews: Developmental Biology 2017;6:e274.

20. Kim YY, Jee HJ, Um JH, Kim YM, Bae SS, Yun J. Cooperation between p21 and Akt is required for p53-dependent cellular senescence. Aging Cell 2017;16:1094-1103.

21. Manning BD, Toker A. AKT/PKB Signaling: Navigating the Network. Cell 2017;169:381-405.

22. Lee BY, Han JA, Im JS, Morrone A, Johung K, Goodwin EC, Kleijer WJ, et al. Senescence-associated beta-galactosidase is lysosomal beta-galactosidase. Aging Cell 2006;5:187-195.

23. Debacq-Chainiaux F, Erusalimsky JD, Campisi J, Toussaint O. Protocols to detect senescence-associated beta-galactosidase (SA-betagal) activity, a biomarker of senescent cells in culture and in vivo. Nat Protoc 2009;4:1798-1806.

24. Mosteiro L, Pantoja C, de Martino A, Serrano M. Senescence promotes in vivo reprogramming through p16(INK)(4a) and IL-6. Aging Cell 2018;17.

25. Rufini A, Tucci P, Celardo I, Melino G. Senescence and aging: the critical roles of p53. Oncogene 2013;32:5129-5143.

26. Karimian A, Ahmadi Y, Yousefi B. Multiple functions of p21 in cell cycle, apoptosis and transcriptional regulation after DNA damage. DNA Repair (Amst) 2016;42:63-71.

27. Lua I, Li Y, Zagory JA, Wang KS, French SW, Sevigny J, Asahina K. Characterization of hepatic stellate cells, portal fibroblasts, and mesothelial cells in normal and fibrotic livers. J Hepatol 2016;64:1137-1146.

28. Kluwe J, Wongsiriroj N, Troeger JS, Gwak GY, Dapito DH, Pradere JP, Jiang H, et al. Absence of hepatic stellate cell retinoid lipid droplets does not enhance hepatic fibrosis but decreases hepatic carcinogenesis. Gut 2011;60:1260-1268.

29. Young AR, Narita M, Ferreira M, Kirschner K, Sadaie M, Darot JF, Tavare S, et al. Autophagy mediates the mitotic senescence transition. Genes Dev 2009;23:798-803.

30. Sugihara H, Teramoto N, Yamanouchi K, Matsuwaki T, Nishihara M. Oxidative stress-mediated

senescence in mesenchymal progenitor cells causes the loss of their fibro/adipogenic potential and abrogates myoblast fusion. Aging (Albany NY) 2018;10:747-763.

31. Saleh T, Tyutynuk-Massey L, Cudjoe EK, Jr., Idowu MO, Landry JW, Gewirtz DA. Non-Cell Autonomous Effects of the Senescence-Associated Secretory Phenotype in Cancer Therapy. Front Oncol 2018;8:164.

32. Yang D, Zhang Q, Ma Y, Che Z, Zhang W, Wu M, Wu L, et al. Augmenting the therapeutic efficacy of adenosine against pancreatic cancer by switching the Akt/p21-dependent senescence to apoptosis. EBioMedicine 2019;47:114-127.

33. Rossig L, Badorff C, Holzmann Y, Zeiher AM, Dimmeler S. Glycogen synthase kinase-3 couples AKT-dependent signaling to the regulation of p21Cip1 degradation. J Biol Chem 2002;277:9684-9689.

34. Iwagami Y, Huang CK, Olsen MJ, Thomas JM, Jang G, Kim M, Lin Q, et al. Aspartate beta-hydroxylase modulates cellular senescence through glycogen synthase kinase 3beta in hepatocellular carcinoma. Hepatology 2016;63:1213-1226.

Supplement figures

S1

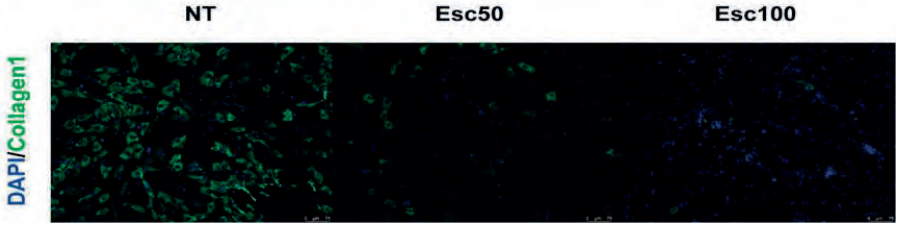

Supplementary figure 1, Immunofluorescence staining for collagen type I.

Primary quiescent HSCs were treated with different concentrations of esculetin for 72h. 100x magnification

Chapter 4

Hydrogen sulfide stimulates activation of hepatic stellate cells through increased cellular bio-energetics

Turtushikh Damba[1], Mengfan Zhang[1], Manon Buist-Homan[1,2], Harry van Goor[3], Klaas Nico Faber[1,2], Han Moshage[1,2]

[1]Dept. Gastroenterology and Hepatology, [2]Dept. Laboratory Medicine and [3]Dept. Pathology and Medical Biology, University of Groningen, University Medical Center Groningen, Groningen, the Netherlands

Correspondence: Han Moshage; a.j.moshage@umcg.nl

Acknowledgment: Mongolian State Training Fund

Published in *Nitric Oxide* 92 (2019) 26-33

Abbreviations: Acta2, alpha-actin-2; Akt, protein kinase B; AOAA, amino-oxyacetic acid; ATP, adenosine triphosphate; BDL, bile duct ligation; BrdU, 5-bromo-2'-deoxyuridine; CBS, cystathionine β-synthase; cDNA, complementary deoxyribonucleic acid; CO, carbon monoxide; CTH, cystathionine γ-lyase; Col1α1, collagen type 1 alpha 1; DL-PAG, DL-Propargylglycine; ECAR, Extra-cellular acidification rate; ECM, extracellular matrix; FCCP, trifluoromethoxy carbonylcyanide phenylhydrazone; GAPDH, glyceraldehyde 3-phosphate dehydrogenase; H_2O_2, hydrogen peroxide; HBSS, Hanks' balanced salt solution; H_2S, hydrogen sulfide; HSCs**,** hepatic stellate cells**;** MPST, 3-mercaptopyruvate sulfur transferase; NaHS, sodium hydrosulfide; NASH, nonalcoholic steatohepatitis; NO, nitric oxide; mRNA, messenger ribonucleic acid; OCR, Oxygen consumption rate; p38 MAP-Kinase, P38 mitogen-activated protein kinases; PDGF-BB, platelet-derived growth factor BB; PLP, Pyridoxal phosphate; TGFβ1, transforming growth factor beta 1;

Highlights

- *CTH* expression and H_2S production are increased during activation of hepatic stellate cells
- Exogenous H_2S increases hepatic stellate cell proliferation while inhibitors of H_2S production reduce proliferation and expression of fibrogenic markers
- The effect of H_2S on hepatic stellate cells correlated with increased cellular bioenergetics
- H_2S production in hepatic stellate cells is a potential target for anti-fibrotic intervention

Abstract

Hepatic fibrosis is caused by chronic inflammation and characterized as the excessive accumulation of extracellular matrix (ECM) by activated hepatic stellate cells (HSCs). Gasotransmitters like NO and CO are known to modulate inflammation and fibrosis, however, little is known about the role of the gasotransmitter hydrogen sulfide (H_2S) in liver fibrogenesis and stellate cell activation. Endogenous H_2S is produced by the enzymes cystathionine β-synthase (CBS), cystathionine γ-lyase (CTH) and 3-mercaptopyruvate sulfur transferase (MPST) (1). The aim of this study was to elucidate the role of endogenously produced and/or exogenously administered H_2S on rat hepatic stellate cell activation and fibrogenesis. Primary rat HSCs were culture-activated for 7 days and treated with different H_2S releasing donors (slow releasing donor GYY4137, fast releasing donor NaHS) or inhibitors of the H_2S producing enzymes CTH and CBS (DL-PAG, AOAA). The main message of our study is that mRNA and protein expression level of H_2S synthesizing enzymes are low in HSCs compared to hepatocytes and Kupffer cells. However, H_2S promotes hepatic stellate cell activation. This conclusion is based on the fact that production of H_2S and mRNA and protein expression of its producing enzyme CTH are increased during hepatic stellate cell activation. Furthermore, exogenous H_2S increased HSC proliferation while inhibitors of endogenous H_2S production reduce proliferation and fibrotic makers of HSCs. The effect of H_2S on stellate cell activation correlated with increased cellular bioenergetics. Our results indicate that the H_2S generation in hepatic stellate cells is a target for anti-fibrotic intervention and that systemic interventions with H_2S should take into account cell-specific effects of H_2S.

Key words: hydrogen sulfide, H_2S, cystathionine γ-lyase, CTH, CSE, hepatic fibrosis, hepatic stellate cells, HSCs

Introduction

Chronic inflammation occurs in many liver diseases, e.g. non-alcoholic steatohepatitis (NASH), viral infection or chronic alcohol consumption. Liver fibrosis can be viewed as an uncontrolled wound healing response. Hepatic stellate cells (HSCs) play an important role in the onset and perpetuation of liver fibrosis. Under normal conditions, HSCs are quiescent and are the principal vitamin A storing cells in the liver (1). In conditions of chronic inflammatory liver injury, quiescent hepatic stellate cells (qHSCs) transform into proliferative myofibroblast-like cells called activated HSCs (aHSCs). During activation, HSCs lose their vitamin A content and start to produce large amounts of extracellular matrix (ECM) (2). When the inflammatory response is not suppressed, the excessive accumulation of ECM can lead to hepatic fibrosis, cirrhosis and eventually hepatocellular carcinoma. At present, there is no effective treatment for hepatic fibrosis, leaving liver transplantation as the only viable treatment option. Therefore, it is important to understand the mechanisms that lead to hepatic stellate cell activation and hepatic fibrosis (3,4). Gasotransmitters like nitric oxide (NO) and carbon monoxide (CO) have been shown to play an important role in chronic liver inflammation and liver fibrosis (5,6). Recently, interest has been focused on another gasotransmitter, hydrogen sulfide (H_2S) (7–9).

In the last two decades, H_2S has been identified as a gasotransmitter that is generated in many mammalian cells and is involved in various physiological and pathophysiological processes as a signaling molecule similar to NO and CO (10). H_2S has also been implicated to modulate inflammation and fibrosis, although its role in liver fibrosis and hepatic stellate cell activation is still not completely elucidated.

H_2S is produced intracellularly from cysteine and methionine by the enzymes cystathionine β-synthase (CBS), cystathionine γ-lyase (CTH) and 3-mercaptopyruvate sulfur transferase (MPST) (11,12). It has been shown to regulate hepatic fibrosis via its anti-oxidative and anti-inflammatory properties and by inducing cell-cycle arrest, apoptosis, vasodilation and reduction of portal hypertension (8,9,13–16). However, most of these experiments were performed in in vivo conditions and did not focus directly on the process of fibrogenesis and HSCs activation. Furthermore, conflicting results have been reported depending on the concentration or type of H_2S donor used. Based on the H_2S release rate, H_2S releasing donors can be categorized as fast (NaHS; Na_2S) or slow (GYY4137; ADT-OH) releasing donors, often yielding contrasting results (17–19). For instance, some studies reported pro-inflammatory and anti-apoptotic properties of H_2S and in some studies H_2S was shown to increase mitochondrial bioenergetics and promote cell proliferation (20–23). Therefore, there are still major gaps in our understanding of the actual effects of H2S on HSCs and liver fibrosis.

The aim of the current study was to elucidate the effects of H_2S on HSCs by

investigating how endogenously produced and/or exogenously administered H_2S affects primary rat HSCs and its proliferation. Furthermore, we tried to elucidate the dynamics of endogenous production of H_2S and H_2S synthesizing enzymes during HSCs activation.

Materials and methods

Hepatic stellate cell isolation and culture

Specified pathogen-free male Wistar rats were purchased from Charles River (Wilmington, MA, USA) and housed in a 12hr light-dark cycle under standard animal housing conditions with free access to chow and water. HSCs were isolated from rats weighing 350 to 450 g, anesthetized by isoflurane and a mixture of Ketamine and Medetomidine. The liver was perfused via the portal vein with a buffer containing Pronase-E (Merck, Amsterdam, the Netherlands) and Collagenase-P (Roche, Almere, the Netherlands). The HSC population was isolated by density centrifugation using 13% Nycodenz (Axis-Shield POC, Oslo, Norway) solution. Isolated HSCs were cultured in Iscove's Modified Dulbecco's Medium supplemented with Glutamax (Thermo Fisher Scientific, Waltham, MA, USA), 20% heat inactivated fetal calf serum (Thermo Fisher Scientific), 1% MEM Non Essential Amino Acids (Thermo Fisher Scientific), 1% Sodium Pyruvate (Thermo Fisher Scientific, Waltham, MA, USA) and antibiotics: 50 µg/mL gentamycin (Thermo Fisher Scientific), 100 U/mL Penicillin (Lonza, Vervier, Belgium), 10 µg/mL streptomycin (Lonza) and 250 ng/mL Fungizone (Lonza) in an incubator containing 5% CO_2 at a 37°C (24). Quiescent HSCs (day 1) spontaneously activate when cultured on tissue culture plastic and reached complete activation (increased proliferation, loss of retinoids and increased synthesis of extracellular matrix components) after 7 days of culture. Day 3 cultured HSCs are considered intermediately activated.

Experimental design

Culture-activated HSCs (aHSCs) were treated with H_2S donors or inhibitors for 72 hrs. All treatments with H_2S donors and inhibitors were performed in fresh medium containing 20% FCS and other supplements. H_2S releasing donors GYY4137 (kind gift from Prof. Matt Whiteman, University of Exeter, United Kingdom) and NaHS (Sigma-Aldrich, Zwijndrecht, the Netherlands) were diluted in distilled water and prepared freshly. NaHS was added every 8 hrs to the cells because of its rapid evaporation. The CBS inhibitor O-(carboxymethyl) hydroxylamine, AOAA (Sigma-Aldrich) was prepared as a 200 mmol/L stock solution and diluted in distilled water at neutral pH. CTH inhibitor DL-propargylglycine, DL-PAG (Sigma-Aldrich) was freshly prepared.

Measurement of H_2S concentration

The accumulation of H_2S in the culture medium was measured as described previously (25,26). After 72 hrs incubation, medium samples were collected in 250 µL of 1% (wt/vol) zinc acetate and distilled water was added up to 500 µL. Next, 133 µl of 20 mmol/L N-dimethyl-p-phenylenediamine sulfate in 7.2 mmol/L hydrogen chloride and 133 µl 30 mmol/L ferric chloride in 1.2 mmol/L hydrogen chloride were added. After incubation for 10 minutes at room temperature, protein was removed by adding 250 µL trichloroacetic acid and centrifugation at 14000 g for 5 minutes. Spectrophotometry was performed at 670 nm light absorbance (BioTek Epoch2 microplate reader) in 96 well-plates. All samples were assayed in duplicate and normalized to the number of cells. Concentrations were calculated against a calibration curve of NaHS (5–400 µmol/L) in culture medium.

Quantitative Real-time Polymerase Chain Reaction

Hepatic stellate cell RNA was isolated using Tri-reagent (Sigma-Aldrich) according to the manufacturer's protocol. RNA concentrations were measured by Nano-Drop 2000c (Thermo Fisher Scientific, Waltham, MA, USA) and 1.5 µg of RNA was used for reverse transcription (Sigma-Aldrich). cDNA was diluted in RNAse-free water and used for real-time polymerase chain reaction on the QuantStudio™ 3 system (Thermo Fisher Scientific). All samples were analyzed in duplicate using 18S and 36b4 as housekeeping genes. The mRNA levels of *Cth*, *Cbs*, *Mpst* (Invitrogen) were quantified using SYBR Green (Applied Biosystems), other genes were quantified by TaqMan probes and primers. Relative gene expression was calculated via the $2^{-\Delta\Delta Ct}$ method. The primers and probes are shown in Table 1.

Table 1. Primer sequences

Gene	Sense 5'-3'	Antisense 5'-3'	Probe 5'-3'
18s	CGGCTACCACATCCAAGGA	CCAATTACAGGGCCTCGAAA	CGCGCAAATTACCCACTCCCGA
Col1α1	TGGTGAACGTGGTGTACAAGGT	CAGTATCACCCTTGGCACCAT	TCCTGCTGGTCCCCGAGGAAACA
Acta2	GCCAGTCGCCATCAGGAAC	CACACCAGAGCTGTGCTGTCTT	CTTCACACATAGCTGGAGCAGCTTCTCGA
Cth	TACTTCAGGAGGGTGGCATC	AGCACCCAGAGCCAAAG	no probe, qPCR with Sybr green
Cbs	GCGGTGGTGGATAGGTGGTT	CTTCACAGCCACGGCCATAG	no probe, qPCR with Sybr green
Mpst	TGGAACAGGCGTTGGATCTC	GGCATCGAACCTGGACACAT	no probe, qPCR with Sybr green
36b4	GCTTCATTGTGGGAGCAGACA	CATGGTGTTCTTGCCCATCAG	TCCAAGCAGATGCAGCAGATCCGC
Tgfβ1	GGG CTA CCA TGC CAA CTT CTG	GAG GGC AAG GAC CTT GCT GTA	CCT GCC CCT ACA TTT GGA GCC TGG A

Cell toxicity determination by Sytox Green

Cell necrosis was measured by Sytox Green nucleic acid staining (Invitrogen, the Netherlands) at a dilution of 1:40.000 in culture medium or HBSS for 15 minutes at a 37°C. Necrotic cells have ruptured plasma membranes, allowing entrance of non-permeable Sytox green into the cells. Sytox green then binds to nucleic acids. Fluorescent nuclei were visualized at an excitation wavelength of 450-490nm by a Leica microscope. Hydrogen peroxide 1 mmol/L was used as a positive control.

Cell proliferation measurement

Proliferation of aHSCs was measured by Real-Time xCELLigence system (RTCA DP; ACEA Biosciences, Inc., CA, USA) and by colorimetric BrdU cell proliferation ELISA kit (Roche Diagnostic Almere, the Netherlands). Cells were seeded in a 16-well E-plate and treated as indicated. Cell index was determined by measuring the change of impedance on the xCELLigence system.

For BrdU incorporation assay, aHSCs were seeded in a 96-well plate and treated as indicated. BrdU incorporation was determined according to manufacturer's instructions and quantified by light emission chemiluminiscence using the Synergy-4 machine (BioTek).

Western Blot analysis

Cells were seeded in 6-well plates and treated as described. Protein lysates were collected by scraping in cell lysis buffer (HEPES 25 mmol/L, KAc 150 mmol/L, EDTA pH 8.0 2mmol/L, NP-40 0.1%, NaF 10 mmol/L, PMSF 50 mmol/L, aprotinin 1 µg/µL, pepstatin 1 µg/µL, leupeptin 1 µg/µL, DTT 1 mmol/L). Total amount of protein in lysates was measured by Bio-Rad protein assay (Bio-Rad; Hercules, CA, USA). For Western blotting, 20-30 µg protein was loaded on SDS-PAGE gels. Proteins were transferred to nitrocellulose transfer membranes using Trans-Blot Turbo Blotting System for tank blotting. Proteins were detected using the following primary antibodies: monoclonal mouse anti-GAPDH 1:5000 (CB1001, Calbiochem), polyclonal goat anti-COL1α1 (1310-01, Southern Biotech), monoclonal mouse anti-ACTA2 1:5000 (A5228, Sigma Aldrich), polyconal rabbit anti-CTH 1:1000 (12217-1-AP, Proteintech), monoclonal mouse anti-CBS 1:1000 (sc-271886, Santa Cruz), monoclonal mouse anti-MPST 1:1000 (sc-374326, Santa Cruz) . Protein band intensities were determined and detected using the Chemidoc MR (Bio-Rad) system.

Cellular bioenergetics analysis

Mitochondrial activity and production of ATP was assessed by XF24 Extracellular Flux

Analyzer (Seahorse Bioscience, Agilent Technologies, Santa Clara SA, USA). aHSCs were seeded in Seahorse XF24 cell culture plates and treated as indicated for 48hrs. Oxygen Consumption Rate (OCR) and Extra-Cellular Acidification Rate (ECAR) were assessed after the addition of glucose (5 mmol/L), oligomycin (1 µmol/L), FCCP (0,25 µmol/L) and a mixture of antimycin (1 µmol/L), rotenone (1 µmol/L), 2-Deoxy-D-glucose (100 mmol/L). Results were normalized for the protein concentration of each sample.

Bile duct ligation

Male Wistar rats were anaesthetized with halothane/O_2/N_2O and subjected to bile duct ligation (BDL) as described by Kountouras J et al (27). At the indicated times after bile duct ligation (BDL), the rats (n = 4 per group) were sacrificed, livers were perfused with saline and removed. Control rats received a sham operation (SHAM). Specimens of these livers were snap-frozen in liquid nitrogen for isolation of mRNA and protein.

Statistical analysis

Results are presented as mean ± standard deviation (mean ± SD). Every experiment was repeated at least 3 times. Statistical significance was analyzed by Mann-Whitney test between the two groups and Kruskal-Wallis followed by post-hoc Dunn's test for multiple comparison test. Statistical analysis was performed with GraphPad Prism 7 (GraphPad Software, San Diego, CA, USA).

Results

Hydrogen sulfide production is increased upon activation of hepatic stellate cells

In order to determine the dynamics of H_2S production and H_2S producing enzymes during HSC activation, mRNA expression of H_2S synthesizing enzymes was measured in quiescent (q) and activated (a) HSCs and compared to the expression of these enzymes in hepatocytes and Kupffer cells. As shown in **Figure 1**, the H_2S producing enzymes Cth, Cbs and Mpst were expressed at low levels in qHSCs compared to hepatocytes and Kupffer cells. Upon activation, Cth gene expression increased in HSCs (**Fig 1A**) while Cbs and Mpst mRNA levels were not changed **(Fig 1B,C)**. In line with this, the accumulation of H_2S in culture medium was increased during HSC activation (**Fig 1D**). This result is denormalized due to comparable results with Figure 3. However, concentration of H_2S in quiescent and activated HSCs were similar when we normalized by the number of cells. Western blotting results showed similar trend as observed for the mRNA expression data. Protein expression of CTH was increased during HSCs activation (**Fig 1E**).

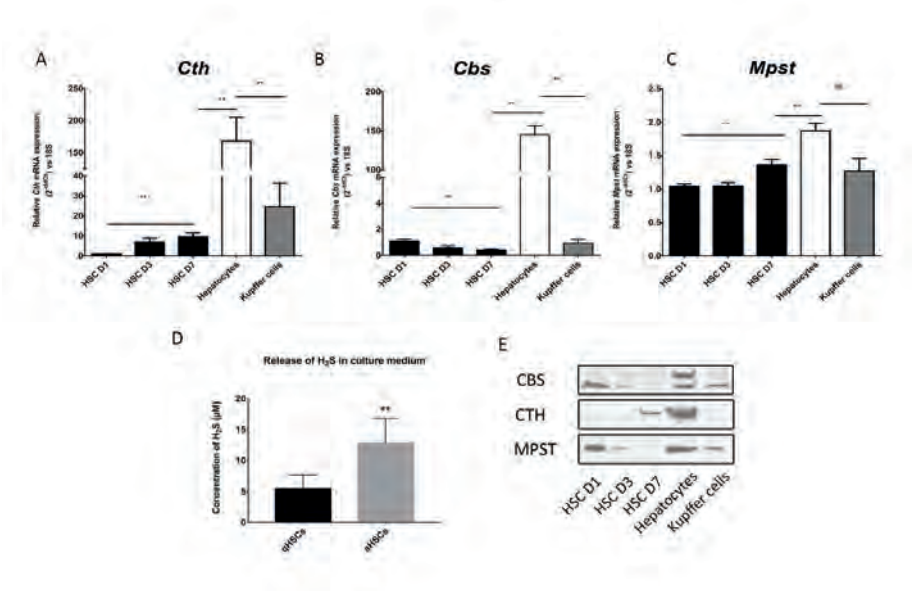

Figure 1. Expression of H_2S producing enzymes and H_2S production in hepatic stellate cells

Cth, *Cbs* and *Mpst* mRNA expression was determined in HSCs at day 1, 3, and 7 and compared to primary rat hepatocytes and Kupffer cells (**A-C**). The cytosolic enzymes *Cth* and *Cbs* were abundantly expressed in hepatocytes, while their expression was relatively low in HSCs. Upon HSCs activation, *Cth* expression was induced 7-fold, and *Mpst* slightly upregulated, whereas expression of *Cbs* was downregulated. Expression levels are relative to *18S* expression. **D.** Production of H_2S in activated and quiescent HSCs. The production of H_2S was increased upon activation of HSCs. Results were normalized with respect to the number of cells. **E.** Protein expressions of CTH, CBS, MPST of HSCs at different time point and hepatocytes and Kupffer cells. Equal protein loading was confirmed by Ponceau S staining and Western blot for GAPDH.

Effect of H_2S on activation markers in hepatic stellate cells

In order to avoid confounding effects of cell toxicity, we optimized the concentration of H_2S donors and inhibitors by Sytox green staining. At concentrations twice as high as used in the experiments, none of the donors or inhibitors were toxic to HSCs (**Figure 2**).

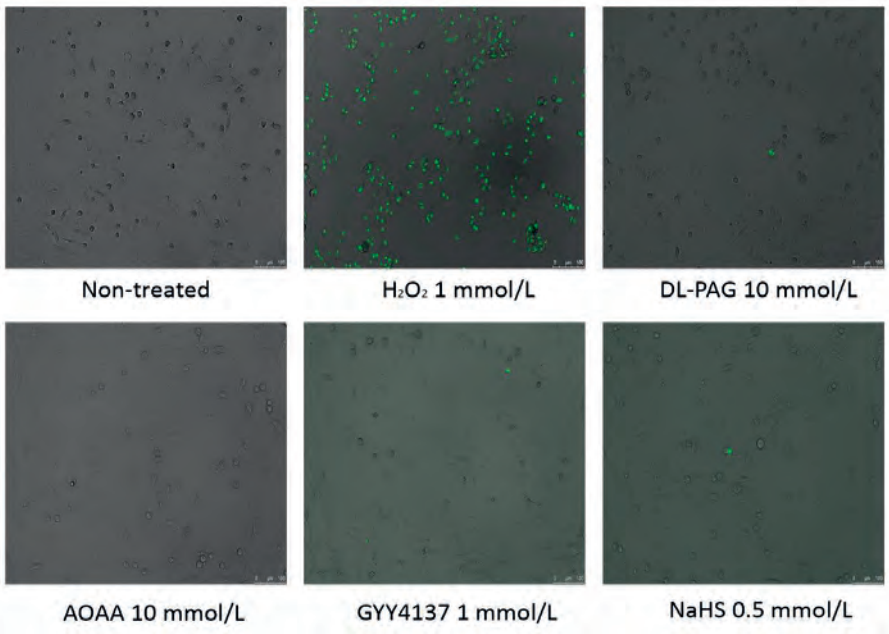

Figure 2. H_2S releasing donors and enzyme inhibitors are not toxic for hepatic stellate cells
Toxicity of the compounds was checked by Sytox Green staining. Hydrogen peroxide (1 mmol/L; 6 hr exposure) was used as a positive control. The compounds DL-PAG (Cth inhibitor), AOAA (Cbs inhibitor), GYY4137 (slow releasing donor) and NaHS (fast releasing donor) were not toxic for HSCs. Duration of the treatment was 24hrs.

We next evaluated the effect of H_2S on activation markers in aHSCs. Inhibitors of H_2S producing enzymes (DL-PAG, AOAA) decreased the expression of the fibrogenic markers *Col1α1* and *Acta2* (**Fig 3A**). The H_2S donors GYY4137 and NaHS did not affect the expression of *Col1α1*. However, GYY4137 slightly, but significantly, reduced *Acta2* mRNA expression (**Fig 3B**). Interestingly, both of the two enzyme inhibitors also downregulated the expression of *Cth* mRNA. The changes in mRNA expression were reflected in similar changes in protein expression of COL1α1 but not ACTA2 (**Fig 3C**). Accumulation of H_2S in culture medium was reduced by inhibitors, whereas GYY4137 increased H_2S accumulation. Because of the fast release, no accumulation of H_2S was measured in NaHS-treated group (**Fig 3D**).

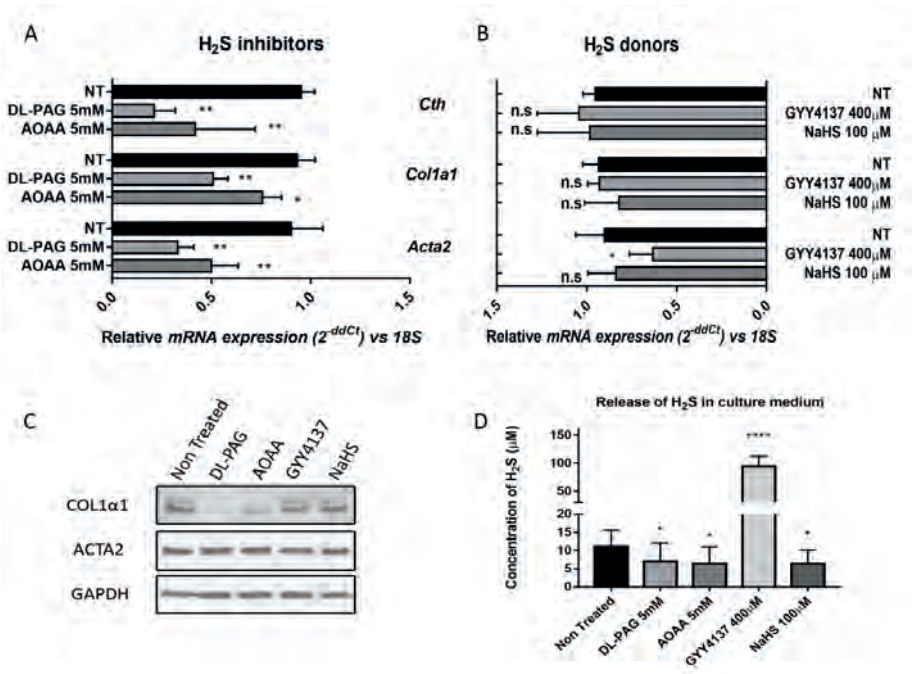

Figure 3. mRNA and protein expression of HSC activation markers in response to H_2S donors and enzyme inhibitors

The H_2S synthesizing enzyme inhibitors DL-PAG and AOAA downregulated *Col1α1*, *Acta2* and *Cth* mRNA expression while the H_2S donors GYY4137 and NaHS did not affect *Cth* and *Col1α1* mRNA expression (**A, B**). In contrast, GYY4137, but not NaHS reduced *Acta2* mRNA expression slightly. *18S* was used as a housekeeping gene. The inhibitors also reduced COL1α1 protein level but not ACTA2 protein level (**C**). GAPDH was used as loading control for protein analysis. The accumulation over 72 hr of H_2S in culture medium was measured in the experimental groups (**D**). DL-PAG and AOAA significantly reduced the accumulation of H_2S. Because of its fast release, no accumulation of H_2S was measured in the NaHS-treated group. Accumulation of H_2S was detected with the slow releasing donor GYY4137.

H_2S promotes hepatic stellate cell proliferation

The effect of H_2S on rat HSC proliferation was assessed using real-time cell analyzing xCelligence and BrdU incorporation ELISA assays. H_2S donors promote, whereas H_2S synthesizing enzyme inhibitors inhibit aHSCs proliferation, indicating a stimulatory effect of H_2S on HSC proliferation (**Figure 4**).

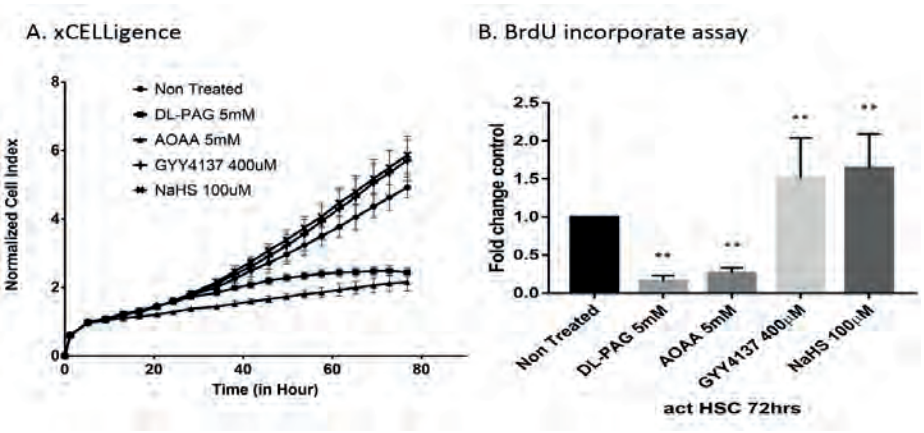

Figure 4. H_2S promotes the proliferation of activated hepatic stellate cells

Culture-activated HSCs were treated with H_2S donors and enzyme inhibitors over period of 72 hrs. Cell proliferation was monitored by real-time xCELLigence system (**A**) and confirmed with BrdU incorporation ELISA assay (**B**). Inhibition of endogenous production of H_2S suppressed cell proliferation, whereas H_2S donors increased aHSCs proliferation. Data are presented ±SD.

H_2S increases cell metabolic activity

H_2S at low concentrations can increase cellular bioenergetics as an electron donor in mitochondrial oxidative phosphorylation (20,28). Since enhanced bioenergetics is associated with HSC activation, we investigated the effect of H_2S on the bioenergetics of aHSCs. Two parameters of cellular metabolic activity, oxygen consumption rate (OCR) for mitochondrial oxidative phosphorylation and extracellular acidification rate (ECAR) for glycolysis, were determined using the Seahorse Extracellular Flux analyzer (**Figure 5**). The H_2S donors GYY4137 and NaHS increased both the OCR and ECAR and ATP production, whereas the enzyme inhibitors DL-PAG and AOAA decreased metabolic activity of HSCs and ATP production.

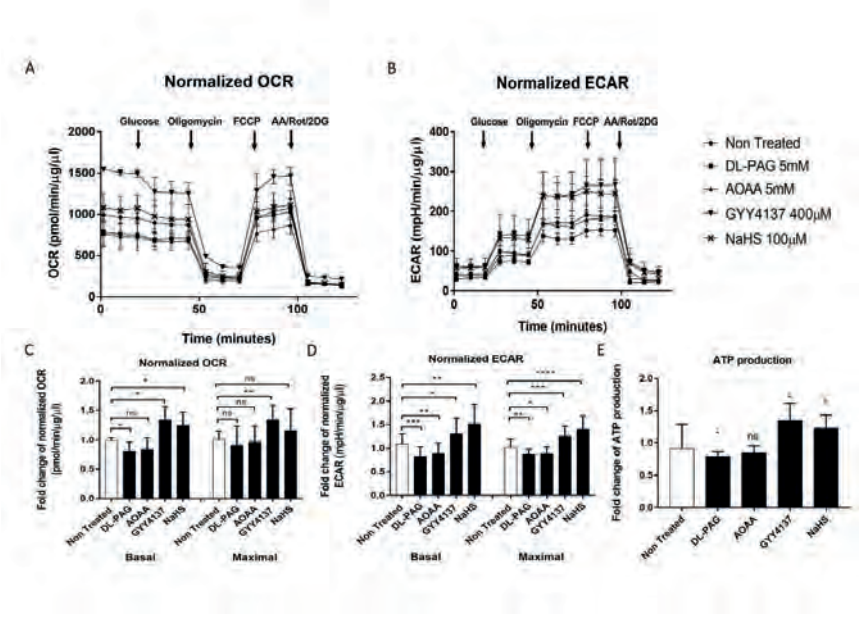

Figure 5. H_2S increases mitochondrial oxidative phosphorylation and glycolysis in aHSCs

Effect of H_2S donors and enzyme inhibitors on bioenergetics of aHSCs. Treatments with donors and inhibitors was for 48hrs. OCR and ECAR are represented as mean ± SEM of a representative experiment (**A, B**). Results were normalized with respect to the total amount of protein. Fold change of normalized maximal and basal level of OCR and ECAR between conditions were analyzed in 3 different experiments. For each experiment, every condition was repeated at least two times (**C, D**). Production of ATP was calculated using Seahorse XF Cell Mito Stress Test Report Generator software. Fold change of ATP production in experimental groups was calculated in 3 independent experiments (**E**).

Cth is specifically induced in hepatic stellate cells during fibrogenesis

We next evaluated the expression of H_2S synthesizing enzymes in the bile duct ligation model, an experimental model of chronic inflammation leading to fibrosis (29). mRNA levels of all H_2S synthesizing enzymes, Cth, Cbs and Mpst, decreased progressively in the bile duct ligation model (**Figure 6 A-C**). As expected, expression of the profibrogenic cytokine TGFβ1 increased progressively in the bile duct ligation model (**Figure 6D**). We next evaluated the effect of TGFβ1 on the mRNA expression of H_2S synthesizing enzymes in different liver cell populations. TGFβ1 decreased mRNA expression of all H_2S synthesizing enzymes in hepatocytes. In contrast, TGFβ1 increased mRNA expression of *Cth* in HSCs and did not change the mRNA expression of *Cbs* and *Mpst* in HSCs (**Figure 6 E-G**).

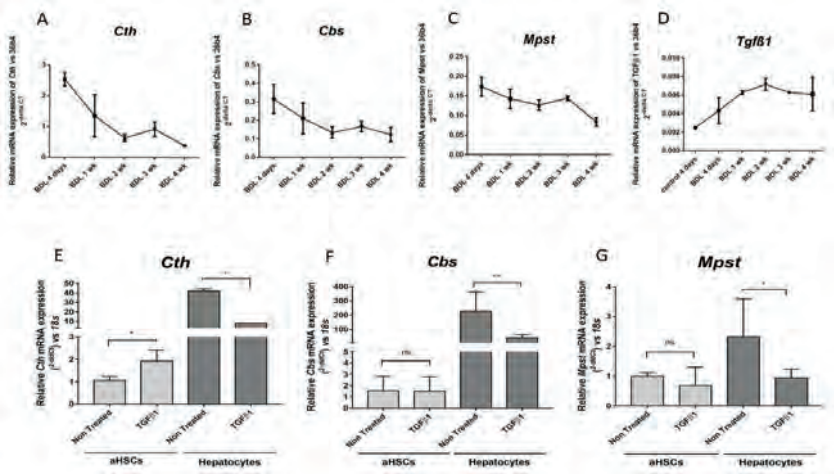

Figure 6. mRNA expression of Cth, Cbs and Mpst in the bile duct ligation model of liver fibrosis and their regulation by TGFβ1 in different liver cell populations

Comparison of H_2S synthesizing enzymes mRNA levels during fibrosis *in vivo* and *in vitro*. *Cth, Cbs, Mpst* were downregulated in total liver in the BDL model of liver fibrosis (**A,B,C**). *Tgfβ1* expression is increased in fibrosis (**D**). *36b4* was used as a housekeeping gene. TGFβ1 reduced the expression of H_2S synthesizing enzymes in hepatocytes (**F,G**), but it specifically induced *Cth* mRNA expression in HSCs *in vitro* (**E**).

Discussion

The main message of our study is that H_2S promotes hepatic stellate cell activation. This conclusion is based on the fact that production of H_2S and expression its producing enzyme cystathionine γ-lyase (CTH) expression are increased during hepatic stellate cell activation and on the fact that exogenous H_2S increased HSC proliferation while inhibitors of endogenous H_2S production reduce proliferation of HSCs. Although the inhibitors we used are not completely specific for one of the H_2S producing enzymes, e.g. the CBS inhibitor AOAA is also a potent inhibitor of CTH (30). it is important to note that reducing H_2S production leads to reduced stellate cell activation. In addition, since CTH is the sole enzyme to upregulated during HSCs activation, it is likely that the effect of AOAA is mediated via inhibition of CTH.

The effect of H_2S on stellate cell activation correlated with increased cellular bioenergetics. Previous *in vivo* studies reported that H_2S has anti-fibrotic properties due to its antioxidant and/or anti-inflammatory actions and its ability to reduce portal hypertension in the liver. In models of (experimental) fibrosis and cirrhosis, reduced expression of H_2S producing enzymes are observed and an anti-fibrotic effect as well as reduction of portal hypertension of systemically administered H_2S donors has been reported (7,13–15). In line with this, *in vitro* studies, using the fast-releasing H_2S donor NaHS have demonstrated that H_2S inhibits stellate cell proliferation, possibly via decreasing the phosphorylation of p38 MAP-Kinase and increasing the phosphorylation of Akt (9,15). In another study, the natural H_2S donor diallyl trisulfide suppressed activation of HSCs through cell cycle arrest at the G2/M checkpoint associated with downregulation of cyclin B1 and cyclin-dependent kinase 1 in primary rat HSCs (8). However, the results described above were obtained using potentially toxic, fast-releasing H_2S donors, which is not representative of the continuous production of low levels of H_2S by cells. Furthermore, the use of systemically administered donors or inhibitors does not allow to distinguish effects of H_2S on different cell types present within one organ. Therefore, we applied 2 different H_2S releasing donors, GYY4137 and NaHS at concentrations 5 times as lower as in some *in vitro* studies. Furthermore, most studies used exogenous H_2S donors to study the role of H_2S in stellate cell activation and fibrogenesis and the importance of endogenous production of H_2S in HSC activation has not been properly addressed. Therefore, we also used 2 inhibitors of H_2S synthesizing enzymes (DL-PAG and AOAA) and we determined H_2S production by HSCs during the process of activation (8,9).

Our observations of increased expression of H_2S synthesizing enzyme *CTH* and increased H_2S production during HSC activation indicates a role for H_2S in HSC activation and fibrogenesis. Indeed, inhibition of endogenous H_2S production in HSCs reduced

proliferation and expression of activation markers. These results are in line with the observation that platelet-derived growth factor BB (PDGF-BB) induced proliferation of rat mesangial cells via induction of CTH (31) and the observation that homocysteine, a precursor in H_2S synthesis, enhances activation of rat HSCs via activation of the PI3K/Akt pathway (32). In contrast, an anti-fibrotic role has been proposed for cystathionine-β-synthase (CBS), another PLP-dependent enzyme which is involved in H_2S synthesis in the liver (33).

Since our results demonstrated a pro-fibrogenic effect of H_2S on HSCs, whereas most *in vivo* studies reported an anti-fibrotic role for H_2S, we investigated in more detail the H_2S generating capacity in different liver cell types. First, we determined that expression of H_2S-synthesizing enzymes in hepatocytes and Kupffer cells is much higher than in HSCs. Next, we determined the expression of H_2S-synthesizing enzymes in the bile duct ligation model of liver fibrosis. We observed a down-regulation of total hepatic expression of both *Cth* and *Cbs* in our bile duct ligation model. As expected, the pro-fibrogenic cytokine *Tgfβ1* was increased in the bile duct ligation model. Finally, we studied the effect of TGFβ1 on the expression of H_2S-synthesizing enzymes in different liver cell types. Of note, we observed that TGFβ1 decreases *Cth* and *Cbs* mRNA expression in hepatocytes, but increased *Cth* mRNA expression in stellate cells. These findings could explain the contradictory results between *in vivo* and *in vitro* studies with regard to the role of H_2S in fibrogenesis: since hepatocytes are the major source of H_2S in total liver, the increased expression of Tgfβ1 will lead to an overall reduction in the hepatic expression of Cth and Cbs and H_2S production, whereas at the same time it will increase expression of Cth and H_2S production in hepatic stellate cells. The cell-specific and local increase in H_2S generation also explains the effect of H_2S donors and inhibitors of H_2S-synthesizing enzymes on HSC proliferation and activation. Recently, Szabo et al reported that a low exogenous dose of H_2S or endogenously produced H_2S increases mitochondrial oxidative phosphorylation (35,36). In accordance, Katalin et al described that low concentrations of H_2S stimulates mitochondrial bio-energetics via S-sulfhydration of ATP- synthase in HepG2 and HEK293 cell lines (20). Activation of stellate cells is also accompanied by increased bioenergetics (37). We have extended these findings by demonstrating that H_2S increases cellular bioenergetics in hepatic stellate cells.

In summary, we demonstrate that stellate cell activation is accompanied by increased generation of H_2S via induction of the H_2S-synthesizing enzyme CTH, leading to increased cellular bioenergetics and proliferation of HSCs. In addition, the response of H_2S-synthesizing enzymes to the fibrogenic cytokine Tgfβ1 is liver cell-type specific. Our results indicate that the H_2S generation in hepatic stellate cells is a target for anti-fibrotic intervention and that systemic interventions with H_2S should take into account cell-specific

responses to H_2S.

References

1. Kasparek MS, Linden DR, Kreis ME, Sarr MG. Gasotransmitters in the gastrointestinal tract. *Surgery*. 2008;143(4):455-459. doi:10.1016/j.surg.2007.10.017

2. Geerts A. History, heterogeneity, developmental biology, and functions of quiescent hepatic stellate cells. *Semin Liver Dis*. 2001;21(3):311-335. doi:10.1055/s-2001-17550

3. Wynn TA. Cellular and molecular mechanisms of fibrosis. *Nat Rev Immunol*. 2004;4(8):583-594. doi:10.1002/path.2277.Cellular

4. Hernandez-Gea V, Friedman SL. Pathogenesis of Liver Fibrosis. *Annu Rev Pathol Mech Dis*. 2011;6(1):425-456. doi:10.1146/annurev-pathol-011110-130246

5. Guo S Bin, Duan ZJ, Wang QM, Zhou Q, Li Q, Sun XY. Endogenous carbon monoxide downregulates hepatic cystathionine-γ-lyase in rats with liver cirrhosis. *Exp Ther Med*. 2015;10(6):2039-2046. doi:10.3892/etm.2015.2823

6. Zhang G, Li X, Sheng C, et al. Macrophages activate iNOS signaling in adventitial fibroblasts and contribute to adventitia fibrosis. *Nitric Oxide - Biol Chem*. 2016;61:20-28. doi:10.1016/j.niox.2016.09.006

7. Fiorucci S, Antonelli E, Mencarelli A, et al. The third gas: H_2S regulates perfusion pressure in both the isolated and perfused normal rat liver and in cirrhosis. *Hepatology*. 2005;42(3):539-548. doi:10.1002/hep.20817

8. Zhang F, Jin H, Wu L, et al. Diallyl trisulfide suppresses oxidative stress-induced activation of hepatic stellate cells through production of hydrogen sulfide. *Oxid Med Cell Longev*. 2017;2017. doi:10.1155/2017/1406726

9. Deng Y. Protective effects of hydrogen sulfide on oxidative stress and fibrosis in hepatic stellate cells. *Mol Med Rep*. 2012:247-253. doi:10.3892/mmr.2012.1153

10. Mani S, Cao W, Wu L, Wang R. Hydrogen sulfide and the liver. *Nitric Oxide - Biol Chem*. 2014;41:62-71. doi:10.1016/j.niox.2014.02.006

11. Li L, Rose P, Moore PK. Hydrogen Sulfide and Cell Signaling. *Annu Rev Pharmacol Toxicol*. 2011;51(1):169-187. doi:10.1146/annurev-pharmtox-010510-100505

12. Carter RN, Morton NM. Cysteine and hydrogen sulphide in the regulation of metabolism: Insights from genetics and pharmacology. *J Pathol*. 2016;238(2):321-332. doi:10.1002/path.4659

13. Wei W, Wang C, Li D. The content of hydrogen sulfide in plasma of cirrhosis rats combined with portal hypertension and the correlation with indexes of liver function and liver fibrosis. *Exp Ther Med*. 2017;14(5):5022-5026. doi:10.3892/etm.2017.5133

14. Tan G, Pan S, Li J, et al. Hydrogen sulfide attenuates carbon tetrachloride-induced hepatotoxicity, liver cirrhosis and portal hypertension in rats. *PLoS One*. 2011;6(10):1-10. doi:10.1371/journal.pone.0025943

15. Fan HN, Wang HJ, Ren L, et al. Decreased expression of p38 MAPK mediates protective effects

of hydrogen sulfide on hepatic fibrosis. *Eur Rev Med Pharmacol Sci*. 2013;17(5):644-652.

16. Majid ASA, Majid AMSA, Yin ZQ, Ji D. Slow regulated release of H_2S inhibits oxidative stress induced cell death by influencing certain key signaling molecules. *Neurochem Res*. 2013;38(7):1375-1393. doi:10.1007/s11064-013-1034-z

17. Wedmann R, Bertlein S, Macinkovic I, et al. Working with "H_2S": Facts and apparent artifacts. *Nitric Oxide - Biol Chem*. 2014;41:85-96. doi:10.1016/j.niox.2014.06.003

18. Zheng Y, Ji X, Ji K, Wang B. Hydrogen sulfide prodrugs-a review. *Acta Pharm Sin B*. 2015;5(5):367-377. doi:10.1016/j.apsb.2015.06.004

19. Zhao Y, Biggs TD, Xian M.ChemInform Abstract: Hydrogen Sulfide (H 2 S) Releasing Agents: Chemistry and Biological Applications . *ChemInform*. 2014;45(45):no-no. doi:10.1002/chin.201445292

20. Katalin Módisa, Young Jun Jua, Akbar Ahmadc, Ashley A. Untereinera, c ZA, Lingyun Wue, Csaba Szaboc,*, and Rui Wanga F. S-sulfhydration of ATP synthase by hydrogen sulfide stimulates mitochondrial bioenergetics. *Cell Rep*. 2015;11(10):1651-1666. doi:10.1080/10937404.2015.1051611.INHALATION

21. Xie X, Dai H, Zhuang B, Chai L, Xie Y, Li Y. Exogenous hydrogen sulfide promotes cell proliferation and differentiation by modulating autophagy in human keratinocytes. *Biochem Biophys Res Commun*. 2016;472(3):437-443. doi:10.1016/j.bbrc.2016.01.047

22. Sekiguchi F, Sekimoto T, Ogura A, Kawabata A. Endogenous Hydrogen Sulfide Enhances Cell Proliferation of Human Gastric Cancer AGS Cells. *Biol Pharm Bull*. 2016;39(5):887-890. doi:10.1248/bpb.b15-01015

23. Maskey M, Jawad MU, Chao C, et al. Upregulation of Cystathionine-β-Synthase in Colonic Epithelia Reprograms Metabolism and Promotes Carcinogenesis. *Cancer Res*. 2017;77(21):5741-5754. doi:10.1158/0008-5472.can-16-3480

24. Shajari S, Laliena A, Heegsma J, Tuñõn MJ, Moshage H, Faber KN. Melatonin suppresses activation of hepatic stellate cells through RORα-mediated inhibition of 5-lipoxygenase. *J Pineal Res*. 2015;59(3):391-404. doi:10.1111/jpi.12271

25. Zhu YZ, Wang ZJ, Ho P, et al. Hydrogen sulfide and its possible roles in myocardial ischemia in experimental rats. *J Appl Physiol*. 2006;102(1):261-268. doi:10.1152/japplphysiol.00096.2006

26. Mok YYP, Mohammed Atan MS Bin, Ping CY, et al. Role of hydrogen sulphide in haemorrhagic shock in the rat: Protective effect of inhibitors of hydrogen sulphide biosynthesis. *Br J Pharmacol*. 2004;143(7):881-889. doi:10.1038/sj.bjp.0706014

27. Kountouras J, Billing BH, Scheuer PJ. Prolonged bile duct obstruction: a new experimental model for cirrhosis in the rat. :305-311.

28. Vicente JB, Malagrinò F, Arese M, Forte E, Sarti P, Giuffrè A. Bioenergetic relevance of hydrogen sulfide and the interplay between gasotransmitters at human cystathionine β-synthase. *Biochim Biophys Acta - Bioenerg*. 2016. doi:10.1016/j.bbabio.2016.03.030

29. Schoemaker MH, Gommans WM, Conde De La Rosa L, et al. Resistance of rat hepatocytes

against bile acid-induced apoptosis in cholestatic liver injury is due to nuclear factor-kappa B activation. *J Hepatol*. 2003;39(2):153-161. doi:10.1016/S0168-8278(03)00214-9

30. Asimakopoulou A, Panopoulos P, Chasapis CT, et al. Selectivity of commonly used pharmacological inhibitors for cystathionine β synthase (CBS) and cystathionine γ lyase (CSE). *Br J Pharmacol*. 2013;169(4):922-932. doi:10.1111/bph.12171

31. Hassan MI, Boosen M, Schaefer L, et al. Platelet-derived growth factor-BB induces cystathionine Iγ-lyase expression in rat mesangial cells via a redox-dependent mechanism. *Br J Pharmacol*. 2012;166(8):2231-2242. doi:10.1111/j.1476-5381.2012.01949.x

32. Zou CG, Gao SY, Zhao YS, et al. Homocysteine enhances cell proliferation in hepatic myofibroblastic stellate cells. *J Mol Med*. 2009;87(1):75-84. doi:10.1007/s00109-008-0407-2

33. Renga B. Hydrogen Sulfide Generation in Mammals : The Molecular Biology of. *Allergy*. 2011:85-91.

34. Robert K, Nehmé J, Bourdon E, et al. Cystathionine β synthase deficiency promotes oxidative stress, fibrosis, and steatosis in mice liver. *Gastroenterology*. 2005;128(5):1405-1415. doi:10.1053/j.gastro.2005.02.034

35. Szabo C, Ransy C, Módis K, et al. Regulation of mitochondrial bioenergetic function by hydrogen sulfide. Part I. Biochemical and physiological mechanisms. *Br J Pharmacol*. 2014;171(8):2099-2122. doi:10.1111/bph.12369

36. Módis K, Bos EM, Calzia E, et al. Regulation of mitochondrial bioenergetic function by hydrogen sulfide. Part II Pathophysiological and therapeutic aspects. *Br J Pharmacol*. 2014;171(8):2123-2146. doi:10.1111/bph.12368

37. Gajendiran P, Vega LI, Itoh K, et al. Elevated mitochondrial activity distinguishes fibrogenic hepatic stellate cells and sensitizes for selective inhibition by mitotropic doxorubicin. *J Cell Mol Med*. 2018;22(4):2210-2219. doi:10.1111/jcmm.13501

Chapter 5

Inhibition of endogenous hydrogen sulfide production reduces activation of hepatic stellate cells via the induction of cellular senescence

Mengfan Zhang[1*], Turtushikh Damba[1*], Harry van Goor[3], Manon Buist-Homan[1,2], Han Moshage[1,2]

[1]Dept. of Gastroenterology and Hepatology, [2]Dept. of Laboratory Medicine, [3]Dept. of Pathology and Medical Biology, University Medical Center Groningen, University of Groningen, Groningen, the Netherlands

*: both authors contributed equally to this work

Correspondence: Han Moshage, PhD

Email address: a.j.moshage@umcg.nl

Abstract

Background: In fibrogenesis, quiescent hepatic stellate cells (HSCs) transdifferentiate into myofibroblast-like cells. These activated HSCs are the main producers of extracellular matrix during fibrogenesis. Recent studies indicate that the induction of cellular senescence in HSCs leads to the resolution of liver fibrosis. Cellular senescence is characterized by irreversible cell-cycle arrest, resulting in arrested cell proliferation and the acquisition of a senescence associated secretory phenotype (SASP). The PI3K-Akt signaling pathway is an important regulator of cellular senescence. Previously, we have shown that the gasotransmitter hydrogen sulfide (H_2S) promotes HSC activation and fibrogenesis. We hypothesize that the inhibition of endogenous H_2S production induces cellular senescence and reduces activation of HSCs. **Methods**: Rat HSCs were isolated and cultured for 7 days for complete activation and then treated with H_2S slow releasing donor GYY4137 and/or DL-propargylglycine (DL-PAG), an inhibitor of the H_2S producing enzyme CTH, as well as the PI3K inhibitor LY294002. **Results**: CTH expression was significantly increased in fully activated HSCs compared to quiescent HSCs. Inhibition of CTH by DL-PAG reduced proliferation and expression of fibrotic markers *Col1a1* and *Acta2* in HSCs. DL-PAG increased the expression of the cell-cycle arrest markers *Cdkn1a*, *p53* and increased the expression of the senescent associated secretory phenotype (SASP) marker *Il6.* Additionally, the number of senescent positive β-galactosidase HSCs was increased. The H_2S donor GYY4137 partially restored the proliferation of senescent HSCs and attenuated the DL-PAG-induced senescent phenotype. Induced senescence by DL-PAG was dependent on intact PI3K-Akt signaling. The non-selective PI3K inhibitor LY294002 partially reduced the senescence phenotype of HSCs induced by DL-PAG. **Conclusion:** Inhibition of endogenous H_2S production reduces hepatic stellate cell activation via induction of cellular senescence in a PI3K-Akt dependent manner. Our results suggest that cell specific inhibition of H_2S could be novel target for anti-fibrotic therapy via induced cell senescence.

Key words: hydrogen sulfide, H_2S, cystathionine γ-lyase, CTH, liver fibrosis, hepatic stellate cells, cellular senescence, TGFβ1

Abbreviations: HSCs, Hepatic Stellate Cells; SASP, Senescence Associated Secretory Phenotype; DL-PAG, DL-propargylglycine; CTH, Cystathionine γ-lyase; SA-β-gal, Senescence Associated β-Galactosidase staining;

Funding: This research did not receive any specific grant from funding agencies in the public, commercial, or not-for-profit sectors

Introduction

Liver fibrosis is characterized by the excessive deposition of extracellular matrix (ECM) in the liver. Activated hepatic stellate cells (HSCs) are the main producers of ECM in liver fibrogenesis. In physiological conditions, quiescent HSCs (qHSCs), located in the space of Disse, store 50-80% of whole-body vitamin A in the form of lipid droplets. In chronic inflammatory liver diseases, qHSCs transdifferentiate into myofibroblast-like cells, termed activated HSCs (aHSCs). Once activated, HSCs lose their vitamin A droplets, start to proliferate and produce excessive amounts of ECM (1, 2). In addition, the key fibrogenic cytokine transforming growth factor (TGFβ) is released and increases the production of ECM by HSCs (3). Reversal of activated HSCs into the quiescent stage and/or induction of apoptosis of activated HSCs are considered as potential strategies to cure liver fibrosis (4, 5).

Cell senescence is defined as irreversible cell cycle arrest accompanied by increased cytokine secretion, termed Senescence-Associated Secretory Phenotype (SASP) (6). Cellular senescence is regulated by various pathways including P53/$P21^{Cip1}$ and PI3K-AKT signaling. $P21^{Cip1}$ (mRNA: Cdkn1a) is an essential cell cycle checkpoint regulator that arrests cell proliferation at the G1 phase and initiates senescence (7). In the absence of Akt kinase activity, $P21^{Cip1}$ is unable to arrest the cell cycle and initiate senescence (8). It has been reported that induction of senescence in activated HSCs reverses the fibrogenic phenotype of activated HSCs (9). Therefore, recent interest has been focused on inducing cellular senescence as a new mechanism for the resolution of liver fibrosis (10). It has been reported that some bioactive anti-fibrotic compounds induce cellular senescence via P53 and YAP or via increased Natural Killer cell activation (4, 11). In addition, some anti-fibrotic proteins and cytokines, e.g. the matricellular protein CCN1 and the cytokines IL-10 and IL-22 have been reported to induce senescence via an integrin-dependent mechanism, via the generation of ROS or via the activation of p53 and/or $p21^{cip1}$ (12-14).

Hydrogen sulfide (H_2S) is one of the gaseous signaling molecules along with nitric oxide and carbon monoxide. The liver is an essential organ for H_2S production and clearance. Hepatic H_2S is involved in mitochondrial biogenesis and bioenergetics, insulin sensitivity, lipoprotein synthesis and glucose metabolism (15). Endogenous H_2S is synthesized by the enzymes cystathionine γ-lyase (CTH), cystathionine β-synthase (CBS) and 3-mercaptopyruvate sulfur transferase (MPST) (1). We previously reported that CTH expression and the generation of H_2S are increased during HSCs activation and that H_2S promotes activation of HSCs: inhibition of CTH decreased HSCs proliferation and showed anti-fibrotic effects (16). It has been demonstrated that the gasotransmitter hydrogen sulfide

(H_2S) has potent anti-senescence effects on endothelial cells via the induction of splicing factors *HNRNPD* and *SRSF2* (17). Therefore we hypothesized that the inhibition of endogenous production of H_2S in activated HSCs is anti-fibrogenic via the induction of senescence.

Materials and Methods

Rats

Primary hepatic stellate cells (HSCs) were isolated from 400-500 g specified pathogen-free male Wistar rats (Charles River, Wilmington, MA, USA). Animals were housed under standard condition in a 12 hr light-dark cycle with free access to chow and water. All experiments were approved by the Committee for Care and Use of laboratory animals of the University of Groningen.

Hepatic Stellate Cell isolation

In order to isolate the HSCs, rats were anesthetized and perfused via the portal vein with Pronase-E (Merck, Amsterdam, the Netherlands) and Collagenase-P (Roche, Almere, the Netherlands). After perfusion, the digested liver was removed and the cell suspension centrifuged on 13% w/v Nycodenz (Axis-Shield POC, Oslo, Norway) to obtain HSCs. Following isolation, HSCs were cultured in Iscove's Modified Dulbecco's Medium supplemented with Glutamax (Thermo Fisher Scientific, Waltham, MA, USA), 20% heat inactivated fetal calf serum (Thermo Fisher Scientific), 1% MEM Non Essential Amino Acids (Thermo Fisher Scientific), 1% Sodium Pyruvate (Thermo Fisher Scientific) and antibiotics: 50 µg/mL gentamycin (Thermo Fisher Scientific), 100 U/mL Penicillin (Lonza, Verviers, Belgium), 10 µg/mL streptomycin (Lonza) and 250 ng/mL Fungizone (Lonza) in an incubator containing 5% CO_2 at a 37°C. HSCs were culture-activated for seven days on tissue culture plastic.

Experimental design

Activated HSCs (aHSCs) were seeded at a density resulting in a confluency of around 90% at the end of each treatment. Depending on the assay, the duration of the treatments was 48 to 72 hr. Unless otherwise stated, all treatments were performed in fresh medium containing 20% FCS (v/v) and other supplements as described above. Hydrogen sulfide (H_2S) slow-releasing donor GYY4137 (kind gift of prof. Matt Whiteman, University of Exeter, United Kingdom) and the pharmacological inhibitor of CTH DL-propargylglycine (DL-PAG;

Sigma-Aldrich, Zwijndrecht, the Netherlands) were freshly prepared prior to administration. PI3K inhibitor LY294002 (Calbiochem, Darmstadt, Germany) was diluted in DMSO to prepare a stock solution. Each experimental condition was performed in duplicate wells and repeated at least 3 times.

Quantitative Real-Time Polymerase Chain Reaction

Cellular mRNA was isolated by Tri-reagent (Sigma Aldrich) according to manufacturer's protocol. Total RNA concentration was determined by Nano-Drop 2000c (Thermo Fisher Scientific). 0.5 to 2.5 µg of RNA was used for preparation of cDNA using MLV reverse transcriptase and RNase Out (Thermo). cDNA was diluted in RNAse-free water and used for real-time polymerase chain reaction on the QuantStudio™ 3 system (Thermo Fisher Scientific). All samples were analyzed in duplicate using 36b4 as housekeeping gene. The mRNA levels of *Cth*, *Cbs*, *Mpst* (Thermo Fisher Scientific) were quantified using SYBR Green (Applied Biosystems), other genes were quantified by TaqMan probes and primers. Relative gene expression was calculated via the $2^{-\Delta\Delta Ct}$ method. The primers and probes are shown in table 1.

Table 1.

Gene	Sense 5'-3'	Antisense 5'-3'	Probe 5'-3'
36b4	GCTTCATTGTGGGAGCAGACA	CATGGTGTTCTTGCCCATCAG	TCCAAGCAGATGCAGCAGATCCGC
Col1α1	TGGTGAACGTGGTGTACAAGGT	CAGTATCACCCTTGGCACCAT	TCCTGCTGGTCCCCGAGGAAACA
Acta2	GCCAGTCGCCATCAGGAAC	CACACCAGAGCTGTGCTGTCTT	CTTCACACATAGCTGGAGCAGCTTCTCGA
Cth	TACTTCAGGAGGGTGGCATC	AGCACCCAGAGCCAAAG	no probe, qPCR with Sybr green
Cbs	GCGGTGGTGGATAGGTGGTT	CTTCACAGCCACGGCCATAG	no probe, qPCR with Sybr green
Mpst	TGGAACAGGCGTTGGATCTC	GGCATCGAACCTGGACACAT	no probe, qPCR with Sybr green
Tgfβ1	GGG CTA CCA TGC CAA CTT CTG	GAG GGC AAG GAC CTT GCT GTA	CCT GCC CCT ACA TTT GGA GCC TGG A
Cdkn1a (p21)	TTGTCGCTGTCTTGCACTCTG	CGCTTGGAGTGATAGAAATCTGTTA	CTGCCTCCGTTTTCGGCCCTG
Il-6	CCGGAGAGGAGACTTCACAGA	AGAATTGCCATTGCACAACTCTT	ACCACTTCACAAGTCGGAGGCTTAATTACA
p53	CCATGAGCGTTGCTCTG	CAGATACTCAGCATACGG	CGGCCTGGCTCCTCCCCAAC

	ATG	ATTTCCT	

Senescence-associated β-galactosidase staining

Culture-activated HSCs were treated as described before. Cellular senescence was determined by Senescence-associated β-galactosidase staining kit (Cell Signaling Technology, Danvers, Massachusetts, USA) according to manufacturer's protocol. After fixation, senescent cells were stained by X-gal solution (pH= 5.9-6.1) for 24 hr at 37°C in a dry incubator. Images were captured by digital phase contrast microscopy.

Cell proliferation assay

Cell proliferation was determined by BrdU incorporation assay (Roche Diagnostic Almere, the Netherlands) and Real-Time xCelligence assay (RTCA DP; ACEA Biosciences, Inc., CA, USA). Cells were seeded in 96 well plates and treated as described. Incorporation of BrdU was detected by chemiluminescence using Synergy-4 (Bio-Tek). For xCelligence, aHSCs were seeded in 16 well E-plates. Real-time cell proliferation was measured as a cell index in the xCelligence system.

Western blot analysis

Cells were seeded and treated as described. Protein lysates were scraped in cell lysis buffer (HEPES 25 mmol/L, KAc 150 mmol/L, EDTA pH 8.0 2 mmol/L, NP-40 0.1%, NaF 10 mmol/L, PMSF 50 mmol/L, aprotinin 1 µg/µL, pepstatin 1 µg/µL, leupeptin 1 µg/µL, DTT 1 mmol/L). Concentration of protein was measured by Bio-Rad protein assay (Bio-Rad; Hercules, CA, USA). 10-20 µg protein was loaded on SDS-PAGE gels. Proteins were transferred to nitrocellulose transfer membranes using Trans-Blot Turbo Blotting System for tank blotting. Proteins were detected using the primary antibodies listed in table 2. Protein band intensities were determined and detected using the Chemidoc MR (Bio-Rad) system.

Table 2.

Protein	Species	Dilution	Company
β-Actin	Polyclonal rabbit	1:1000	4970, Cell Signaling
COL1α1	Polyclonal goat	1:2000	1310-01, Southern Biotech
ACTA2	Monoclonal mouse	1:5000	A5228, Sigma Aldrich
$P21^{Cip1}$ (CDKN1A)	Polyclonal rabbit	1:1000	Sc-471, Santa Cruz
CTH	Polyclonal rabbit	1:1000	12217-1-AP, Proteintech
CBS	Monoclonal mouse	1:1000	sc-271886, Santa Cruz
MPST	Monoclonal mouse	1:1000	sc-374326, Santa Cruz

GAPDH	Monoclonal mouse	1:1000	CB1001, Calbiochem
p-Akt(Ser473)	Polyclonal rabbit	1:1000	9271L, Cell Signaling
p-Akt(Thr308)	Polyclonal rabbit	1:1000	sc-16646-R, Santa Cruz
Total Akt	Polyclonal rabbit	1:1000	9272, Cell Signaling

Immunofluorescence microscopy

Cells were cultured on glass coverslips and fixed with 4% paraformaldehyde/PBS. 5 min incubation with 1% Triton X-100 was used to permeabilize cells. Nonspecific antibody binding sited were blocked by 0.5% BSA/PBS for 30 min. After blocking, cells were incubated by primary antibody against collagen type 1 (1310-01, Southern Biotech) 1:400 diluted in 0.5% BSA/PBS for 1 hr at room temperature.Coverslips were washed 3 times by PBS and then incubated with secondary antibody Alexa fluorophore (Molecular Probes) 1:400 diluted in 0.5% BSA/PBS for 1 hr at room temperature. Coverslips were mounted with fluorescence mounting medium containing DAPI (Vectashield, Burlingame, CA, USA). Images were captured by Zeiss 410 inverted laser scanning microscope.

Statistical analysis

Data are presented as mean ± standard deviation (mean ± SD) of at least three independent experiments. Statistical significance was analyzed by Mann-Whitney test between the two groups and one-way ANOVA or Kruskal-Wallis followed by post-hoc Dunn's test for multiple comparison test. $P<0.05$ was considered statistically significant. Analysis was performed using GraphPad Prism 7 (GraphPad Software, San Diego, CA, USA).

Results

TGFβ1 increases CTH expression in activated hepatic stellate cells

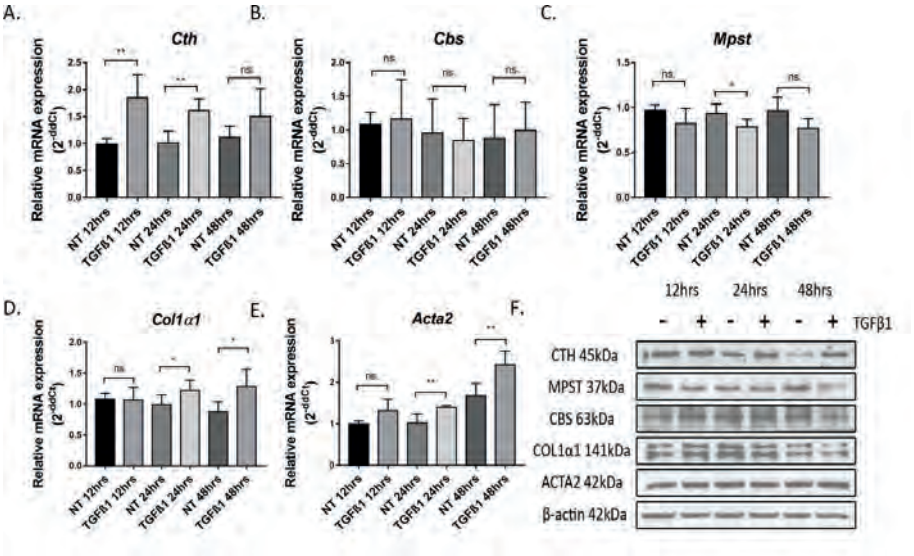

Figure 1. CTH mRNA and protein expression is increased by the pro-fibrogenic cytokine TGFβ1.
A-E. Relative gene expression of endogenous H_2S producing enzymes *Cth, Cbs, Mpst* and hepatic stellate cell activation markers *Col1α1, Acta2* (mean ± SD) were measured at 12, 24 and 48 hr in serum-free medium with or without treatment with 5 ng/ml TGFβ1. Expression levels were calculated relative to 36b4 house-keeping gene. **F**. Protein expression of CTH, CBS, MPST and stellate cell activation markers COL1α1 and ACTA2. β-actin was used as loading control. Results are represented as mean ± SD; **P*<0.05, ***P*<0.005.

We previously reported that the expression of the endogenous H_2S synthesizing enzyme cystathionine γ-lyase (CTH) and the production of H_2S (CTH/H_2S) were increased during transdifferentiation of quiescent hepatic stellate cells (qHSCs) into activated hepatic stellate cells (aHSCs) (16). Here, we investigated the effect of the pro-fibrogenic cytokine TGFβ1 on the expression of the H_2S producing enzymes CTH, CBS, and MPST (**Fig 1A-E**). The fibrogenic cytokine TGFβ1 significantly increased the mRNA and protein expression of CTH but not of CBS and MPST. As expected, the expression of the fibrogenic markers *Col1α1* and *Acta2* mRNA were increased upon treatment of HSCs with TGFβ1.

CTH inhibition reverses activation of hepatic stellate cells

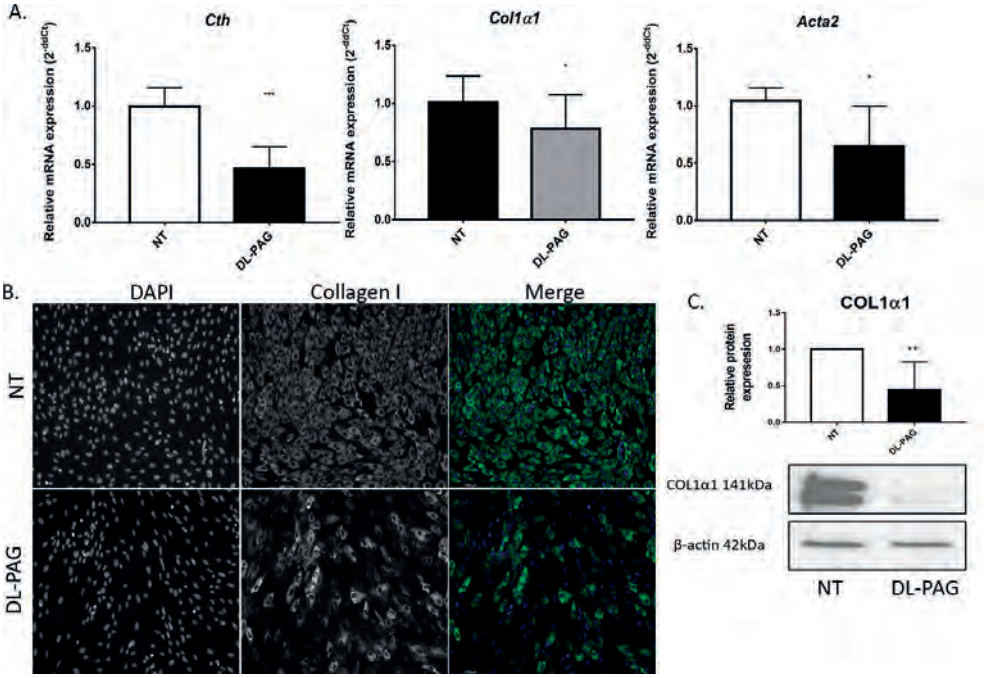

Figure 2. The CTH inhibitor DL-PAG reverses activation of HSCs.

A. mRNA levels of the activation markers *Col1α1* and *Acta2* were reduced in activated HSCs after 72 hr treatment with DL-PAG. *Cth* expression was also reduced by DL-PAG. 36b4 was used as housekeeping gene. **B, C.** Immunofluorescence staining and Western blotting of COL1α1 (magnification 200x) in activated HSCs. β-actin was used as loading control. Results are expressed as mean ± SD; **P*<0.05, ***P*<0.005, ****P*<0.0005.

Since CTH expression was increased by TGFβ1, we hypothesized that inhibition of CTH could inhibit TGFβ1-driven transdifferentiation of HSCs. As shown in **Fig. 2A**, inhibition of CTH reduced the expression of the fibrogenic markers Acta2 and Col1a1. In addition, protein level of collagen type 1 was also reduced by DL-PAG as shown by immunofluorescence and Western blot (**Fig. 2B-C**).

CTH inhibition induces cellular senescence in hepatic stellate cells

To determine whether the anti-fibrotic effect of CTH inhibition correlated with the induction of senescence, we investigated markers of senescence in DL-PAG treated HSCs. CTH inhibition decreased protein expression of CTH and $P21^{Cip1}$ (**Fig 3A**). The mRNA expression of the cell cycle arrest markers *Cdkn1α* and *p53* as well as the senescence

associated secretory phenotype (SASP) marker *IL-6* were increased upon CTH inhibition (**Fig 3B**). In addition, inhibition of CTH by DL-PAG increased the number of senescence associated β-galactosidase positive (SA-β-gal) cells (**Fig 3C**). In order to investigate whether the proliferation arrest induced by DL-PAG was irreversible, we performed wash-out experiments. In the first 48 hr, DL-PAG inhibited HSC proliferation. After refreshing the medium (and removing DL-PAG), the proliferation ability remained impaired compared to non-treated HSCs (**Fig 3D**).

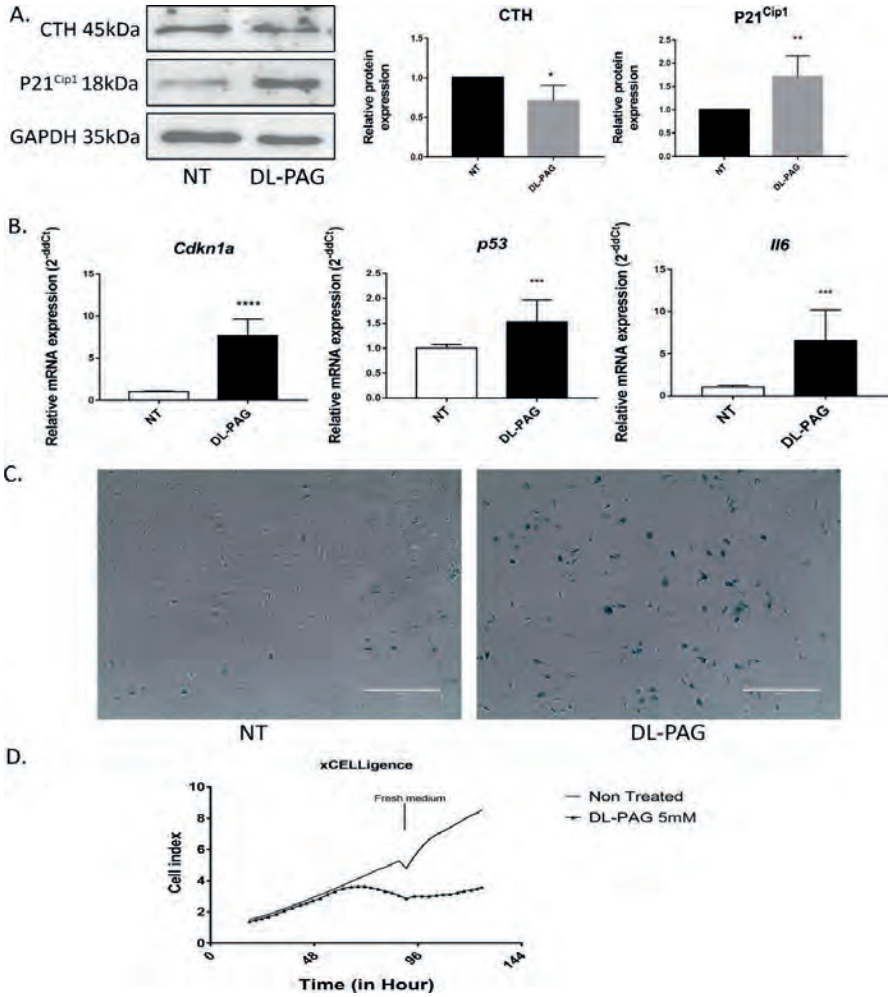

Figure 3. Inhibition of CTH induces cellular senescence.

A. Protein expression of H_2S synthesizing enzyme CTH is decreased and cell cycle arrest marker $P21^{Cip1}$ is increased upon CTH inhibition at 24 hr. GAPDH is used as loading control. **B.** mRNA expression of senescence markers *Cdkn1α*, *p53* and SASP marker *IL-6* after 72 hr treatment of aHSCs with DL-PAG.

36b4 was used as housekeeping gene. **C.** SA-β-gal staining (magnification 200x) after 48 hr treatment of HSCs with DL-PAG. **D.** Cell proliferation was measured by the xCELLigence system. Cells were treated for 48 hr followed by the addition of fresh medium. Cell proliferation is represented by cell index. Results are represented as mean ± SD; **P*<0.05, ***P*<0.005

H_2S donor GYY4137 restores proliferation ability of senescent HSCs

Since inhibition of the endogenous H_2S synthesizing enzyme CTH showed anti-fibrotic effects via the induction of cellular senescence, we hypothesized that supplementation of exogenous H_2S reverses induction of senescence. To test the hypothesis, HSCs were treated with both the inhibitor of CTH, DL-PAG and different concentrations of the H_2S slow-releasing donor GYY4137. $P21^{Cip1}$ expression, SA-β-galactosidase positive cell and mRNA expressions of *Cdkn1α, p53 and Il6* were does-dependently reduced by GYY4137 (**Fig 4A-C**). In addition, the impaired proliferation of HSCs treated with DL-PAG was improved by the H_2S donor GYY4137 (**Fig 4D**).

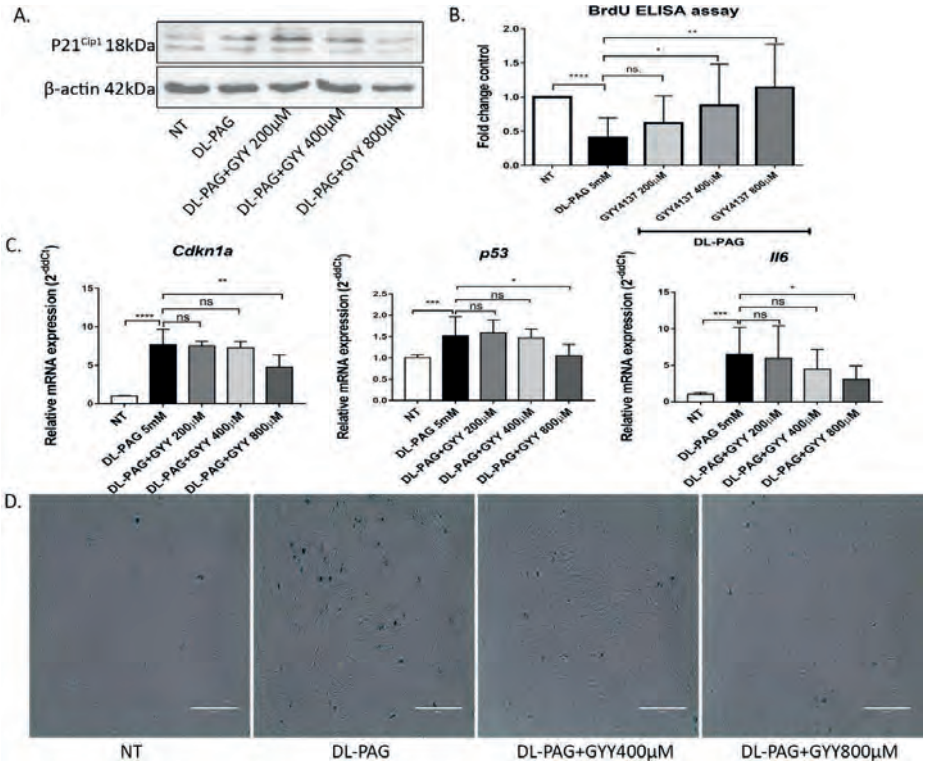

Figure 4. H_2S donor GYY4137 partially reversed the pro-senescence effect of DL-PAG.
A. $P21^{Cip1}$ expression in HSCs treated with DL-PAG with or without different concentrations of GYY4137 at 24 hr. **B.** Cell proliferation was measured by BrdU incorporation assay. **C.** mRNA expression of senescence markers *Cdkn1α*, *p53*, *IL-6*. 36b4 was used as housekeeping gene. **D.** SA-β-Gal staining of HSCs treated with DL-PAG with or without GYY4137 (magnification 200x). Results are represented as mean ± SD; **P*<0.05, ***P*<0.005. Abbreviation: GYY, GYY4137.

PI3K-Akt pathway is involved in DL-PAG induced senescence

We next investigated the signaling pathway involved in the anti-senescence effect of H_2S. Akt activity is essential for induction of $P21^{Cip1}$-dependent cellular senescence (6, 8, 18). In order to determine the role of Akt in DL-PAG induced senescence, the pan-PI3K inhibitor LY294002 was applied to block Akt activity in HSCs. LY294002 decreased the level of Akt phospho-Ser473 and Akt phospho-Thr308 in HSCs. At the same time, LY294002 attenuated the DL-PAG-induced increased expression of the senescence marker $P21^{cip1}$ (**Fig 5A**). In addition, the DL-PAG-induced increase in mRNA expression of cell cycle arrest markers *Cdkn1α*, *p53* and SASP marker *IL-6* which was attenuated by the PI3K inhibitor (**Fig 5B**). The downregulation of CTH expression by DL-PAG was not reversed by LY294002 (**Fig 5B**). The attenuation of DL-PAG-induced expression of $P21^{Cip1}$ by the PI3K inhibitor correlated with an attenuation of the DL-PAG-increased number of SA-β-Gal positive cells (**Fig 5C**). Also, the DL-PAG-induced downregulation of the pro-fibrotic marker *Acta2*, but not Col1a1, was reversed by PI3K inhibitor LY294002 (**Fig 5B**). Finally, the PI3K inhibitor LY294002 improved the proliferation ability of DL-PAG treated aHSCs (**Fig 5D**). Taken together, the results demonstrate that senescence induced by CTH/H_2S inhibition is mediated via PI3K-Akt signaling.

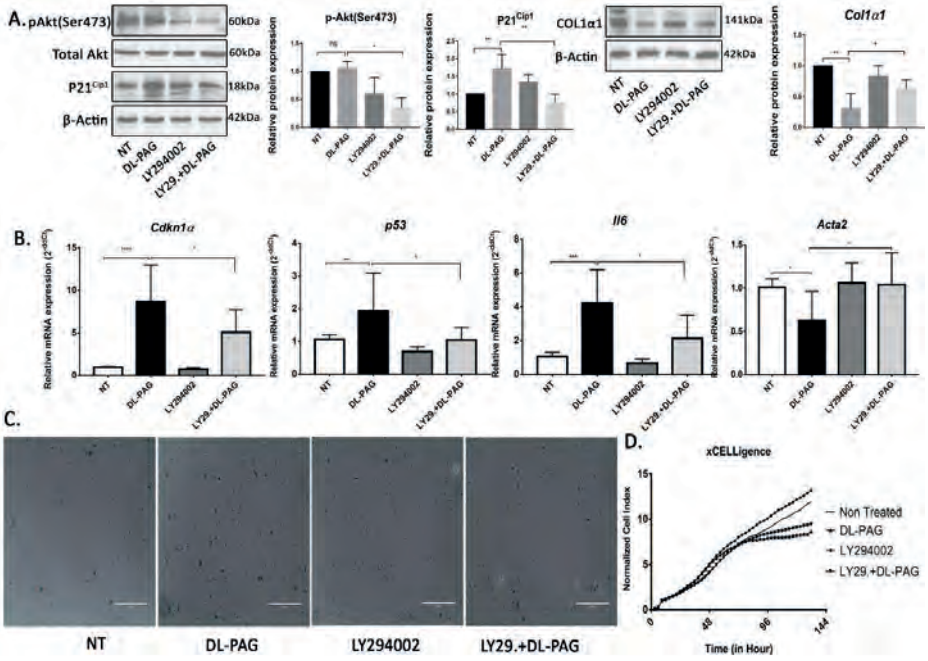

Figure 5. DL-PAG induced cellular senescence is mediated via PI3K-AKT signaling.

A. protein expression of Akt phosphorylation at Serine 471, total Akt and senescence marker $P21^{Cip1}$ at 24 hr. β-Actin was used as loading control. COL1α1 and β-actin protein expression at 72 hr. **B.** mRNA expression of senescence markers *Cdkn1α*, *p53*, *IL-6*, and fibrotic marker *Acta2*. 36b4 was used as housekeeping gene. **C**. SA-β-Gal staining of non-treated HSCs and HSCs treated by DL-PAG with or without PI3K inhibitor for 48 hr (magnification 200x). **D.** Real-time cell proliferation was measured using the xCELLigence system. Results are represented as mean ± SD; **P*<0.05, ***P*<0.005.Abbreviation: LY29., LY294002.

Discussion

Cellular senescence has been identified as a promising therapeutic strategy for the treatment of liver fibrosis due to its potential to inactivate HSCs (9, 19). Senescence can be induced in HSCs in response to a variety of stimuli, such as matricellular protein CCN1 and the cytokines IL-10 and IL-22. In addition, cell cycle arrest marker p53 double knockout ($p53^{-/-}$) mice contain more fibrotic tissue compared to wild type mice due to impaired cellular senescence (9, 11). However, the specific signaling pathways in HSCs that account for the induction of senescence remain to be fully elucidated. Previously, we have shown that hydrogen sulfide (H_2S) promotes stellate cell activation (16). It has also been shown that H_2S hampers senescence in various cell types, including endothelial cells and fibroblasts via the induction of splicing factors like *HNRNPD* and posttranslational modification of Keap1 (17, 20). In the present study, we demonstrate a causal relationship between the induction of senescence by inhibiting H_2S production and the (partial) reversal of stellate cell activation: inhibition of CTH reverses activation of stellate cells and induces a senescent phenotype, whereas H_2S donors promote stellate cell activation and (partially) reverse the senescent phenotype. Moreover, we demonstrate that the induction of the senescent phenotype in HSCs by inhibition of H_2S is dependent on PI3K-Akt signaling, since an inhibitor of PI3K is capable to partially reverse the senescent phenotype and restore the fibrogenic phenotype.

TGFβ1 plays a central role in fibrogenesis: it promotes stellate cell activation and increases the production of extracellular matrix (ECM) (3). We previously reported that expression of CTH/H_2S is increased during transdifferentiation of quiescent HSCs into activated stellate cells (16). In addition, previous studies reported that H_2S shows anti-fibrotic effects via pro-apoptotic, anti-oxidant and anti-inflammatory effects in HSC-T6 cells and in rat primary HSCs (21, 22). However, in these studies a rather high concentration of the fast releasing NaHS donor was used, which could be toxic. In another study,the natural compound diallyl trisulfide (DATS) was used as a H_2S donor, which could be different fromH_2S alone (23). Furthermore, accumulating evidences support the notion that H_2S slow releasing donors better reflect endogenous H_2S levels within biological systems over a longer time course (24).

In the present study we demonstrate that TGFβ1 time-dependently stimulated the protein and mRNA expression of CTH. In contrast, TGFβ1 did not change CBS and MPST expression. We did not observe increased production of H_2S in response to TGFβ1 treatment, probably because endogenous H_2S production was already at a high level in the culture-activated HSCs or the lack of sensitivity of our method. Our observation of increased expression of CTH upon stimulation with TGFβ1 is in line with several reports on the effect

of growth factors (PDGF) on fibrogenic markers and proliferation in fibroblasts during skin wound healing and overexpression of CTH in proliferating cancer cells (25-27). These results suggest that CTH has the potency to regulate cell proliferation and activation via endogenous H_2S production in fibroblasts and cancer cells as well as in HSCs.

PI3K-dependent signaling has been demonstrated to be an essential regulator of cellular senescence (6). Activation of the PI3K-Akt axis permits the induction of $P21^{Cip1}$ dependent senescence (8, 18, 28). As downstream target and substrate of Akt, Ser9-phosphorylated GSK3β stabilizes $P21^{Cip1}$ and Ser9 phosphorylation of GSKβ is positively correlated with the proportion of senescent cells (29, 30). The PI3K inhibitor LY294002 inhibits Akt kinase activity, phosphorylation of GSK3β and restores the proliferation ability of oncogene Ras-induced senescent fibroblasts (8, 30). In our present study, a similar effect of LY294002 was observed in DL-PAG-treated senescent HSCs. LY294002 downregulated the cell cycle arrest marker Cdkn1a, the number of SA-β-Gal positive cells and SASP in DL-PAG treated HSCs. Furthermore, LY294002 reversed the downregulation of the fibrogenic marker *Acta2* in DL-PAG-treated HSCs. These results demonstrate that the inactivation of HSCs results from the induction of HSC senescence. Nevertheless, neither the senescent phenotype and proliferation arrest induced by DL-PAG nor the downregulation of CTH was completely rescued by the PI3K inhibitor. This suggests that the PI3K-Akt signaling pathway accounts for part of the senescent phenotype. In addition to PI3K-Akt signaling, mitochondrial dysfunction may be a driving factor in the induction of cellular senescence (31). This is in line with our previous observation that H_2S improves mitochondrial function and hence, the lack of the H_2S may contribute to mitochondrial dysfunction and senescence (17).

To date, several studies have reported that H_2S shows anti-senescence and anti-aging effects via splicing factors *HNRNPD*, *SRSF2* and upregulation of SIRT1 in endothelial cells (17, 32, 33). In addition, Yang et al., reported that CTH knockout mice display increased senescence, whereas exogenous H_2S posttranslationally S-sulfhydrates the transcription factor Keap1 to stimulate anti-oxidant systems and reverse senescence in fibroblasts (20). In line with these reports, the DL-PAG-increased senescence markers $P21^{cip1}$, β-gal staining and decreased HSCs proliferation were dose-dependently and partially reversed by the H_2S slow releasing donor GYY4137. Since the senescent phenotype is the integrative effect of both senescent and non-senescent cells, the modulation of single signaling pathways may affect both cell populations and lead to a partially reversed phenotype. The restoration of DNA synthesis by DL-PAG can be attributed to H_2S, a phenomenon we reported before (16). These results demonstrate that H_2S has a central role in HSCs senescence and inhibition of H_2S signaling shows anti-fibrotic effects via induction of senescence.

In summary, our results suggest that CTH and endogenous H_2S generation are increased during fibrogenesis. Inhibition of CTH shows anti-fibrotic effects through increased cellular senescence and this cellular senescence is regulated through PI3K-Akt pathways.

References

1. Kasparek MS, Linden DR, Kreis ME, Sarr MG. Gasotransmitters in the gastrointestinal tract. Surgery 2008;143:455-459.

2. Geerts A. History, heterogeneity, developmental biology, and functions of quiescent hepatic stellate cells. Semin Liver Dis 2001;21:311-335.

3. Dewidar B, Meyer C, Dooley S, Meindl-Beinker AN. TGF-beta in Hepatic Stellate Cell Activation and Liver Fibrogenesis-Updated 2019. Cells 2019;8:1419.

4. Jin H, Lian N, Zhang F, Bian M, Chen X, Zhang C, Jia Y, et al. Inhibition of YAP signaling contributes to senescence of hepatic stellate cells induced by tetramethylpyrazine. Eur J Pharm Sci 2017;96:323-333.

5. Schrader J, Fallowfield J, Iredale JP. Senescence of activated stellate cells: not just early retirement. Hepatology 2009;49:1045-1047.

6. Gorgoulis V, Adams PD, Alimonti A, Bennett DC, Bischof O, Bishop C, Campisi J, et al. Cellular Senescence: Defining a Path Forward. Cell 2019;179:813-827.

7. Sharpless NE, Sherr CJ. Forging a signature of in vivo senescence. Nat Rev Cancer 2015;15:397-408.

8. Kim YY, Jee HJ, Um JH, Kim YM, Bae SS, Yun J. Cooperation between p21 and Akt is required for p53-dependent cellular senescence. Aging Cell 2017;16:1094-1103.

9. Krizhanovsky V, Yon M, Dickins RA, Hearn S, Simon J, Miething C, Yee H, et al. Senescence of activated stellate cells limits liver fibrosis. Cell 2008;134:657-667.

10. Aravinthan AD, Alexander GJ. Senescence in chronic liver disease: Is the future in aging? J Hepatol 2016;65:825-834.

11. Jin H, Jia Y, Yao Z, Huang J, Hao M, Yao S, Lian N, et al. Hepatic stellate cell interferes with NK cell regulation of fibrogenesis via curcumin induced senescence of hepatic stellate cell. Cell Signal 2017;33:79-85.

12. Kim KH, Chen CC, Monzon RI, Lau LF. Matricellular protein CCN1 promotes regression of liver fibrosis through induction of cellular senescence in hepatic myofibroblasts. Mol Cell Biol 2013;33:2078-2090.

13. Huang YH, Chen MH, Guo QL, Chen YX, Zhang LJ, Chen ZX, Wang XZ. Interleukin10 promotes primary rat hepatic stellate cell senescence by upregulating the expression levels of p53 and p21. Mol Med Rep 2018;17:5700-5707.

14. Kong X, Feng D, Wang H, Hong F, Bertola A, Wang FS, Gao B. Interleukin-22 induces hepatic stellate cell senescence and restricts liver fibrosis in mice. Hepatology 2012;56:1150-1159.

15. Wu D-D, Wang D-Y, Li H-M, Guo J-C, Duan S-F, Ji X-Y. Hydrogen Sulfide as a Novel Regulatory Factor in Liver Health and Disease. Oxid Med Cell Longev 2019;2019:1-16.

16. Damba T, Zhang M, Buist-Homan M, van Goor H, Faber KN, Moshage H. Hydrogen sulfide stimulates activation of hepatic stellate cells through increased cellular bio-energetics. Nitric Oxide 2019;92:26-33.

17. Latorre E, Torregrossa R, Wood ME, Whiteman M, Harries LW. Mitochondria-targeted hydrogen sulfide attenuates endothelial senescence by selective induction of splicing factors HNRNPD and SRSF2. Aging (Albany NY) 2018;10:1666-1681.

18. Huy H, Song HY, Kim MJ, Kim WS, Kim DO, Byun JE, Lee J, et al. TXNIP regulates AKT-mediated cellular senescence by direct interaction under glucose-mediated metabolic stress. Aging Cell 2018;17:e12836.

19. Tsuchida T, Friedman SL. Mechanisms of hepatic stellate cell activation. Nat Rev Gastroenterol Hepatol 2017.

20. Yang G, Zhao K, Ju Y, Mani S, Cao Q, Puukila S, Khaper N, et al. Hydrogen sulfide protects against cellular senescence via S-sulfhydration of Keap1 and activation of Nrf2. Antioxid Redox Signal 2013;18:1906-1919.

21. Fan HN, Wang HJ, Yang-Dan CR, Ren L, Wang C, Li YF, Deng Y. Protective effects of hydrogen sulfide on oxidative stress and fibrosis in hepatic stellate cells. Mol Med Rep 2013;7:247-253.

22. Zhang F, Jin H, Wu L, Shao J, Zhu X, Chen A, Zheng S. Diallyl Trisulfide Suppresses Oxidative Stress-Induced Activation of Hepatic Stellate Cells through Production of Hydrogen Sulfide. Oxid Med Cell Longev 2017;2017:1406726.

23. Rao PS, Midde NM, Miller DD, Chauhan S, Kumar A, Kumar S. Diallyl Sulfide: Potential Use in Novel Therapeutic Interventions in Alcohol, Drugs, and Disease Mediated Cellular Toxicity by Targeting Cytochrome P450 2E1. Curr Drug Metab 2015;16:486-503.

24. Rose P, Dymock BW, Moore PK: Chapter Nine - GYY4137, a Novel Water-Soluble, H2S-Releasing Molecule. In: Cadenas E, Packer L, eds. Methods in Enzymology. Volume 554: Academic Press, 2015; 143-167.

25. Hassan MI, Boosen M, Schaefer L, Kozlowska J, Eisel F, von Knethen A, Beck M, et al. Platelet-derived growth factor-BB induces cystathionine gamma-lyase expression in rat mesangial cells via a redox-dependent mechanism. Br J Pharmacol 2012;166:2231-2242.

26. Wang YH, Huang JT, Chen WL, Wang RH, Kao MC, Pan YR, Chan SH, et al. Dysregulation of cystathionine gamma-lyase promotes prostate cancer progression and metastasis. EMBO Rep 2019;20:e45986.

27. Goren I, Kohler Y, Aglan A, Pfeilschifter J, Beck KF, Frank S. Increase of cystathionine-gamma-lyase (CSE) during late wound repair: Hydrogen sulfide triggers cytokeratin 10 expression in keratinocytes. Nitric Oxide 2019;87:31-42.

28. Qiu T, Tian Y, Gao Y, Ma M, Li H, Liu X, Wu H, et al. PTEN loss regulates alveolar epithelial cell senescence in pulmonary fibrosis depending on Akt activation. Aging (Albany NY) 2019;11:7492-7509.

29. Iwagami Y, Huang CK, Olsen MJ, Thomas JM, Jang G, Kim M, Lin Q, et al. Aspartate beta-hydroxylase modulates cellular senescence through glycogen synthase kinase 3beta in hepatocellular carcinoma. Hepatology 2016;63:1213-1226.

30. Rossig L, Badorff C, Holzmann Y, Zeiher AM, Dimmeler S. Glycogen synthase kinase-3 couples AKT-dependent signaling to the regulation of $p21^{Cip1}$ degradation. J Biol Chem 2002;277:9684-9689.

31. Wiley CD, Velarde MC, Lecot P, Liu S, Sarnoski EA, Freund A, Shirakawa K, et al. Mitochondrial Dysfunction Induces Senescence with a Distinct Secretory Phenotype. Cell Metab 2016;23:303-314.

32. Zheng M, Qiao W, Cui J, Liu L, Liu H, Wang Z, Yan C. Hydrogen sulfide delays nicotinamide-induced premature senescence via upregulation of SIRT1 in human umbilical vein endothelial cells. Mol Cell Biochem 2014;393:59-67.

33. Suo R, Zhao ZZ, Tang ZH, Ren Z, Liu X, Liu LS, Wang Z, et al. Hydrogen sulfide prevents H(2)O(2)-induced senescence in human umbilical vein endothelial cells through SIRT1 activation. Mol Med Rep 2013;7:1865-1870.

Chapter 6

Pirfenidone Inhibits Cell Proliferation and Collagen I Production of Primary Human Intestinal Fibroblasts

Yingying Cui [1], Mengfan Zhang [1], Changsen Leng [2], Tjasso Blokzijl [1,3],

Bernadien H. Jansen [1], Gerard Dijkstra [1,†] and Klaas Nico Faber [1,3,†]

[1]Department of Gastroenterology and Hepatology, University of Groningen, University Medical Center Groningen, Groningen, The Netherlands. [2]Department of Biomedical Sciences of Cells and Systems, section Molecular Cell Biology, University of Groningen, University Medical Center Groningen, Groningen, the Netherlands. [3]Department of Laboratory Medicine, University of Groningen, University Medical Center Groningen, Groningen, The Netherlands.

† These authors contributed equally.

Published in *Cells*. 2020 Mar 22;9(3)

Abstract

Intestinal fibrosis is a common complication of inflammatory bowel disease. So far, there is no safe and effective drug for intestinal fibrosis. Pirfenidone is an anti-fibrotic compound available for the treatment of idiopathic pulmonary fibrosis. Here, we explored the anti-proliferative and anti-fibrotic properties of pirfenidone on primary human intestinal fibroblasts (p-hIFs). p-hIFs were cultured in the absence and presence of pirfenidone. Cell proliferation was measured by a real-time cell analyzer (xCELLigence) and BrdU incorporation. Cell motility was monitored by live cell imaging. Cytotoxicity and cell viability were analyzed by Sytox green, Caspase-3 and Water Soluble Tetrazolium Salt-1 (WST-1) assays. Gene expression of fibrosis markers was determined by quantitative reverse transcription PCR (RT-qPCR). The mammalian target of rapamycin (mTOR) signaling was analyzed by Western blotting and type I collagen protein expression additionally by immunofluorescence microscopy. Pirfenidone dose-dependently inhibited p-hIF proliferation and motility, without inducing cell death. Pirfenidone suppressed mRNA levels of genes that contribute to extracellular matrix production, as well as basal and TGF-β1-induced collagen I protein production, which was associated with inhibition of the rapamycin-sensitive mTOR/p70S6K pathway in p-hIFs. Thus, pirfenidone inhibits the proliferation of intestinal fibroblasts and suppresses collagen I production through the TGF-β1/mTOR/p70S6K signaling pathway, which might be a novel and safe anti-fibrotic strategy to treat intestinal fibrosis.

Keywords: intestinal fibrosis; pirfenidone; mTOR; TGF-β1; collagen; fibroblast; inflammatory bowel disease

Introduction

Inflammatory bowel diseases (IBD), e.g., Crohn's Disease and ulcerative colitis, are complex diseases, characterized by chronic and recurrent inflammation in the intestine (1). Typically diagnosed in early adulthood, patients require life-long disease management without a curative therapy available at this moment. The prevalence of IBD has increased significantly in the past decades and is expected to increase even further, especially in countries adopting a Western lifestyle (2). Intestinal fibrosis is a severe and common complication of IBD and is increasingly recognized as a therapeutic problem (3). Chronic inflammation leads to damage to the intestinal tissue. In response, intestinal myofibroblasts become activated and secrete extracellular matrix (ECM) such as collagen and fibronectins under the regulation of TGF-β1 and several other pro-fibrotic and anti-fibrotic factors. Intestinal fibrosis develops when the ECM production exceeds the co-induced ECM degradation and may lead to organ stenosis and malfunction (3,4). Despite the introduction of novel therapeutics for IBD in the past two decades, the incidence of fibrosis-induced intestinal strictures has not significantly changed in these patients (5). Up to 30–60% of Crohn's disease patients experience intestinal stenosis and bowel obstruction. Short strictures can be dilated by endoscopic balloon dilatation, but approximately 75% of subjects need redilatation and 30–40% require surgical resection (5–8). While this improves quality of life directly after surgery, stenotic bowel obstruction is bound to recur in approximately 50% of the patients within 20 years (9). Thus, there is an urgent need to elucidate the pathophysiological mechanisms of intestinal fibrosis at the cellular and molecular level in order to develop safe and effective drugs to prevent and treat intestinal fibrosis. TGF-β1 has been identified as an important factor during fibrogenesis as it promotes ECM protein synthesis and inhibits ECM degradation (10). Also, TGF-β1 is known to activate mTORC1 signaling pathway, which is a central regulator of cell metabolism, proliferation, and protein synthesis (11,12). Important downstream execution proteins are 4E-BP1, a translation repressor protein, and p70S6K that targets the S6 ribosomal protein (13,14).

Pirfenidone is a pyridone compound with anti-fibrotic properties in idiopathic pulmonary fibrosis (IPF), liver cirrhosis, and cardiac fibrosis (15–17). Moreover, pirfenidone significantly suppressed TGF-β1-induced ECM synthesis in a mouse model with renal fibrosis (18). In a phase III randomized, double-blind, placebo-controlled, and multinational clinical trial (ASCEND), pirfenidone significantly improved progression-free survival and reduced the number of IPF patients who had a decline in forced vital capacity (17).

In this study, we investigated the effect of pirfenidone on primary human intestinal fibroblasts (p-hIFs), including its effect on TGF-β1-mediated mTOR-p70S6K1 signaling.

Materials and Methods

Primary human Intestinal Fibroblast (p-hIFs) Isolation and Culture

The procurement of a part of the colon for research was approved by the National Discussion of the Procurement Teams (Landelijk OveRleg Uitname Teams) from the Dutch Transplantation Association (Nederlandse Transplantatie Vereniging) and performed after written informed consent from the relatives. All the procedures were performed according to Helsinki Declaration. Primary human colon fibroblasts were isolated and cultured as previously described (19). Fresh transplantation surgical specimens from morphological normal ascending colon tissue were obtained from the donor. Colon tissue was cut into small pieces and placed in T25 cell culture flasks with culture medium: Dulbecco's Modified Eagle Medium containing 20% heat-inactivated fetal calf serum, 1X MEM Non-Essential Amino Acid, 100 µg/mL gentamycin, 200 u/mL of penicillin, 200 µg/mL of streptomycin, and 2.5 µg/mL of Amphotericin B (all Gibco™ by Life technologies, Bleiswijk, The Netherlands) in a humidified incubator at 37 °C and 5% CO_2. After p-hIFs grew from the tissue, the tissue was removed from the flask. The confluency of the p-hIFs reached up to 70–80% after approximately 3–4 weeks. All experiments were performed with at least 3 independent p-hIF isolates.

Proliferation Assays

Real-Time Cell Analysis (RCTA)

Experiments of p-hIF proliferation were performed using the xCELLigence Real-Time Cell Analysis (RTCA, xCELLigence RTCA DP, ACEA Biosciences Inc., San Diego, CA, USA) as previous described (20). p-hIFs were seeded in an E-16 plate with a density of 2500 cells/well in 200 µL culture volume. E-16 plates carry sensor microelectrodes to measure electronic impedance that represents the cell confluency. The impedance of electron flow caused by adherent cells is reported using a unitless parameter called Cell Index (CI), where CI = (impedance at time point n – impedance in the absence of cells)/nominal impedance value. The impedance was recorded at 15 min intervals to continuously monitor the proliferation of p-hIFs. p-hIFs were refreshed with new medium and treated with different concentrations of pirfenidone after 18 h. Results were analyzed by RTCA Software (Version 1.2, ACEA Biosciences Inc.).

BrdU Assay

The BrdU assay was performed according to the standard protocol of the manufacturer (Roche, Mannheim, Germany). p-hIFs were seeded in a 96-well plate overnight and were treated with pirfenidone (0, 0.5, 1, 2 mg/mL) for 72 h. BrdU (10 μmol/L) was added and incubated in the final 24 h. After fixation, p-hIFs were incubated with 100 μL/well anti-BrdU-POD working solution for 90 min at room temperature. After 15 min of incubation with the substrate solution, the proliferation measurement was conducted using the BrdU incorporation ELISA kit (all from Roche, Mannheim, Germany).

p-hIFs Cell Counting

p-hIFs were seeded in 6-well plates with a density of 8×10^5 cells/well. After exposure to various concentrations of pirfenidone for 72 h, wells were washed with PBS and p-hIFs were dissociated using trypsin. Then p-hIFs were centrifuged and resuspended in a small volume of culture medium. Numbers of p-hIFs were quantified using a TC20 cell counter (Bio-Rad Laboratories, Inc., Hercules, CA, USA).

Real-Time Imaging of Cell Motility

p-hIFs were seeded in a 8-well chamber plate (Lab-Tek II, 155409, Thermo Scientific, Waltham, MA, USA) in 250 μL medium at a density of 1000 cells/well and cultured overnight, after which they were exposed to 0, 1, and 2 mg/mL pirfenidone for 24 h. Next, the plate containing the p-hIFs was transferred to a live cell imaging platform in a DeltaVision microscope (GE Healthcare Bio-sciences, Marlborough, MA, USA) and p-hIF motility was monitored for 15 h. Images were taken every 5 min using a 40 × oil objective with DIC channels and cell motility was analyzed with Imaris software (Version 8.0, Oxford Instruments, Zurich, Switzerland; https://imaris.oxinst.com/downloads).

Cytotoxicity and Cell Viability Assays

Sytox Green Assay

p-hIFs were seeded in the 96-well plate with a density of 2500 cells/well. p-hIFs were exposed to pirfenidone for 72 h. p-hIFs exposed to H_2O_2 (5 mmol/L) were included as positive (necrotic) control group (21). Sytox Green (10 μM; Life Technologies) nucleic acid stain was added to tested wells for 15 min, followed by fluorescence microscopy using a Leica DMI6000 microscope (Leica Microsystems GmbH, Wetzlar, Germany).

Caspase-3 Assay

Caspase-3 activity (as marker for apoptosis) was quantified as described earlier (22). After 72 h of treatment with pirfenidone, p-hIFs were scraped and cell lysates were obtained after three times of freezing (−80 °C) and thawing (37 °C) followed by centrifugation for 5 min at 12,000× g. 20 μg protein per sample was used to quantify caspase-3 activity.

WST-1 Assay

The p-hIF cell viability assay was quantified using the Cell Proliferation Reagent Water Soluble Tetrazolium Salt-1 (WST-1, 11644807001 Roche) according to the manufacturer's protocol. p-hIFs were seeded in a 12-well plate with a density of 4×10^4 cells/well and were exposed to pirfenidone for 72 h. Thus, 10 μL of WST-1 solution per 100 μL medium was added to the growing p-hIFs and was next incubated at 37 °C for 90 min after which the WST-1-containing medium was transferred to a new 96-well plate for analysis.

Quantitative Real–Time PCR (RT-qPCR)

p-hIFs were seeded in 6-well plates with a density of 8×10^5 cells/well and were exposed to pirfenidone with or without TGF-β1 for 72 h. Total mRNA was extracted from scraped p-hIFs using TRIzol reagent (Sigma-Aldrich, Zwijndrecht, The Netherlands). RNA concentrations were determined with a NanoDrop 1000 spectrophotometer (Thermo Fisher Scientific, Wilmington, DE, USA). RT-qPCR was performed using 7900HT fast Real-Time PCR system (Applied Biosystems, Bleiswijk, The Netherlands) as previously described (23). The TaqMan primers and probes and SYBR green primers used are shown in Supplementary Table S1 and S2. *18S* was used to normalize the mRNA level.

Immunofluorescence Microscopy (IF)

p-hIFs were seeded in 12-well plates (4×10^5 cells/well) containing coverslips. After 72 h of different treatments, coverslips were rinsed with PBS, fixed with 4% paraformaldehyde for 10 min, and permeabilized with 0.1% Triton X-100 for 10 min at room temperature. Non-specific antibody binding was blocked with 3% bovine serum albumin/PBS solution for 30 min. Then, coverslips were incubated with primary collagen I antibody (1:1000, 1310-01, Southern Biotech, Birmingham, UK) for 1 h at 37 °C. Afterward, coverslips were rinsed with PBS three times and incubated with Alexa-Fluor488-conjugated rabbit anti-goat secondary antibodies (1:400 A11008; Molecular Probes, Leiden, The Netherlands) for 30 min. Nuclei were stained with Mounting Medium with 4',6-diamidino-2-phenylindole (DAPI H-1200 Vector Laboratories, Peterborough, UK). Images were taken using a Leica DMI6000 fluorescence microscope (Leica Microsystems GmbH).

Western Blotting

p-hIFs were lysed with cell lysis buffer containing 25 mM HEPES, 150 mM KAc, 2 mM EDTA, and 0.1% NP-40 (all from Sigma-Aldrich) supplemented with protease inhibitors on ice. Protein concentrations were quantified using the Bio-Rad protein assay (Bio-Rad). Equal quantities of protein were separated by 5–12% gradient sodium dodecyl sulfate polyacrylamide gel electrophoresis. Proteins were transferred to membranes with the Trans-Blot Turbo transfer system (Bio-Rad). After 1 h of blocking using 2% bovine serum albumin/PBS-Tween, membranes were incubated with the primary antibody (antibodies catalog numbers and dilutions supplied in Supplementary Table S3) at 4 °C overnight. Then membranes were washed with three times of PBS-Tween and incubated with horseradish-peroxidase conjugated secondary antibody for 1 h. Glyceraldehyde 3-phosphate dehydrogenase (GAPDH) was used as the reference protein. The signals were detected by chemidoc XRS system and Image Lab version 3.0 (Bio-Rad).

Statistical Analysis

Statistical analyses were performed with Graphpad Prism 7 (Graphpad Software, San Diego, CA, USA). All data presented as mean ± SEM. Statistical differences between two groups were analyzed by using unpaired t-test. If more than two groups were evaluated, the groups were analyzed by using one-way ANOVA with Dunnett or Turkey test. A p-value < 0.05 was considered as statistically significant.

Results

Pirfenidone Suppresses the Proliferation of p-hIFs, Which is Reversible

Primary hIFs (p-hIFs) were cultured in a real-time cell analysis (RTCA, xCELLigence) to analyze the effect of pirfenidone on cell proliferation. The p-hIFs were allowed to attach to the culture plate for 18 h, represented by stabilization of the Cell Index (CI). Next, the p-hIFs were treated with increasing concentrations of pirfenidone (0, 0.5, 1, and 2 mg/mL) for 72 h, which revealed that pirfenidone dose-dependently reduced the increase in CI (green, purple and blue lines) when compared to untreated control p-hIFs (red line in Figure 1A). In line, pirfenidone dose-dependently reduced BrdU incorporation (Figure 1B; all **** $p < 0.0001$ when compared to untreated control p-hIFs) and cell numbers (-34%, -72%, and -97% at 0.5, 1.0, and 2.0 mg/mL, respectively; Figure 1C, all **** $p < 0.0001$). Video-assisted imaging of p-hIFs revealed that pirfenidone also suppressed the motility of individual p-hIF, albeit only significantly at the highest concentration of 2 mg/mL (Figure 1E,F). Pirfenidone treatment did not evidently affect the typical spindle-shaped cell morphology of p-hIFs (Figure 1D,E). Moreover, pirfenidone did not induce significant levels of necrotic p-hIF cell death (Figure 2A), nor did it induce caspase-3 activity as a measure of apoptotic cell death (Figure 2B). Still, 72 h pirfenidone treatment dose-dependently reduced the metabolic activity of p-hIFs, as quantified in WST-1 assays (Figure 2C; **** $p < 0.0001$ for at all tested concentrations). As pirfenidone did not appear cytotoxic for p-hIFs, we next analyzed whether p-hIFs proliferation is reversible after cessation of pirfenidone treatment. p-hIFs were pre-treated for 72 h with 2 mg/mL pirfenidone inhibiting cell proliferation and upon refreshing the medium without pirfenidone the p-hIFs regained normal proliferation rates after a lag-phase of approximately 48 h (Figure 2D). Notably, the cell index of pirfenidone pre-treated p-hIFs reached the same level after 96 h as compared to non-treated p-hIFs (see for reference Figure 1A).

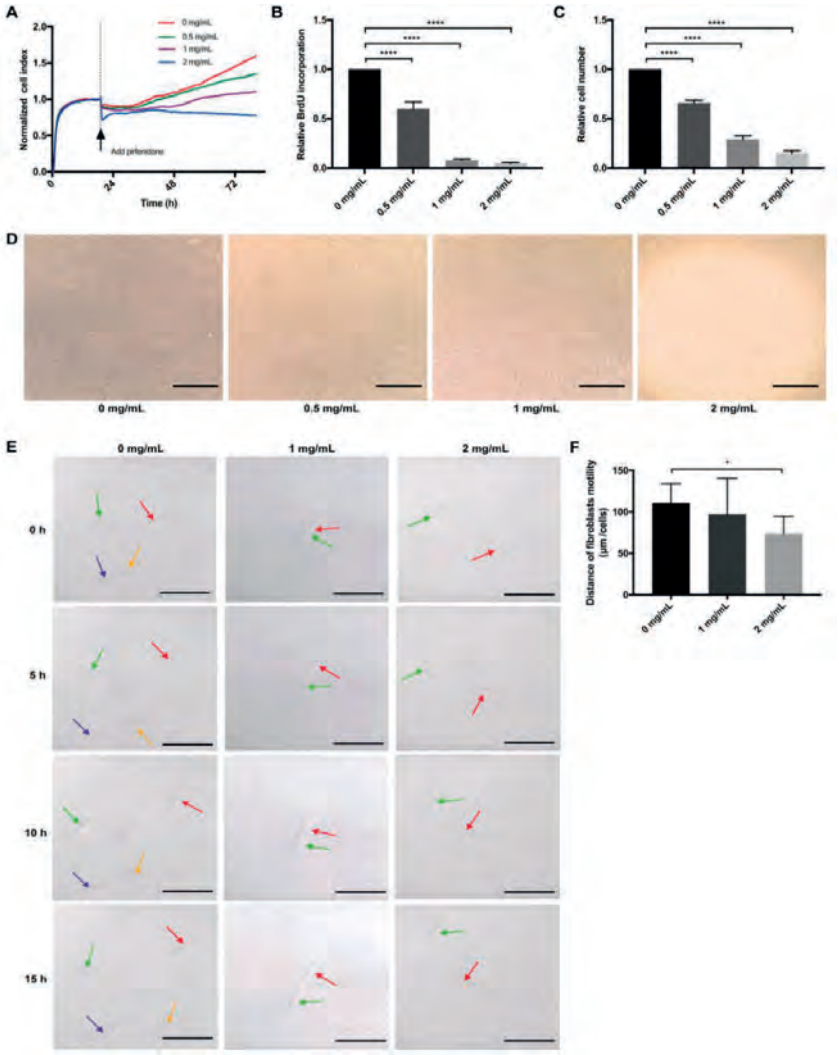

Figure 1. Pirfenidone suppresses the proliferation of primary human intestinal fibroblasts (p-hIFs).

(**A**) Intestinal fibroblasts were seeded in the xCELLigence system for 18 h and were then exposed to increasing concentrations of pirfenidone (0, 0.5, 1, and 2 mg/mL) for 72 h. Cell index curves showed pirfenidone dose-dependently inhibited the proliferation of fibroblasts. (**B**) Pirfenidone dose-dependently decreased BrdU incorporation (n=3, **** $p < 0.0001$ for all groups) and (**C**) p-hIF cell numbers (n = 3, **** $p < 0.0001$ for all groups) after 72 h exposure. (**D**) Bright field images showing pirfenidone inhibited the proliferation of p-hIFs, while maintaining their spindle like morphology. (**E**) Stills of real-time cell imaging tracking the movement of individual p-hIFs after 0, 5, 10 and 15 h in the absence or presence of pirfenidone. (**F**) Quantification of p-hIF motility in each group shown in E. Motility was tracked every 5 min for 15 h in total. * $p < 0.05$; Data are shown in mean ± SEM. Scale bars = 100 μm.

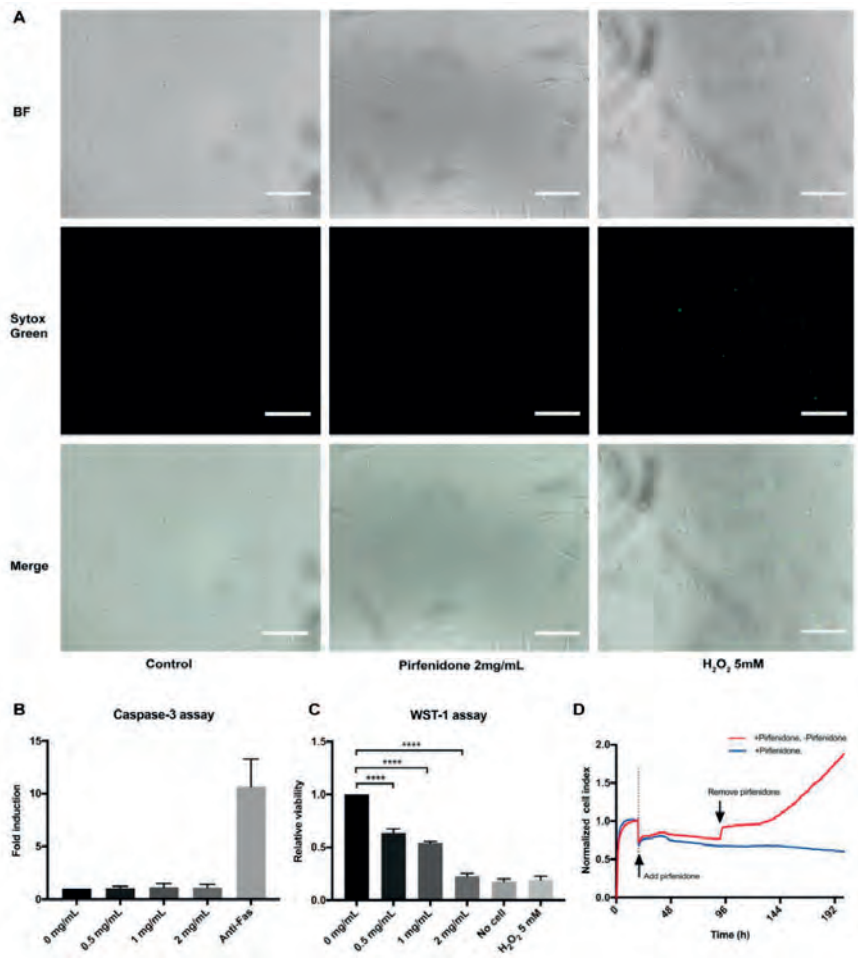

Figure 2. Pirfenidone does not induce cell death and reversibly suppresses the proliferation of human primary intestinal fibroblasts.

(**A**) Bright field (top panels), Sytox Green nucleic staining (middle panels) and overlay images (bottom panels) of p-hIFs exposed for 72 h to 2 mg/mL pirfenidone or for 24 h to 5 mmol/L H_2O_2 (positive control for necrosis) showing that less than 1% of pirfenidone-exposed p-hIFs were necrotic (representative image of n = 3). (**B**) Pirfenidone did not induce caspase-3 activity compared to anti-Fas-exposed (1 ug/mL for 9 h) p-hIFs (positive control for apoptotic cell death) (n = 3). (**C**) Water Soluble Tetrazolium Salt-1 (WST-1) assay showed pirfenidone dose-dependently suppressed the total metabolic activity of p-hIFs as proxy for total cell number (**** $p < 0.0001$, n = 3). (**D**) Pirfenidone (2 mg/mL for 72 h)-induced inhibition of p-hIF proliferation was reversible even refreshing the cells with pirfenidone-free medium, as analyzed in real-time in the xCELLigence. Scale bars = 50 µm.

Pirfenidone Suppresses Extracellular Matrix Protein (ECM) Expression in p-hIFs

In order to determine whether pirfenidone also affects ECM production, p-hIFs were exposed to pirfenidone for 72 h and mRNA levels of genes encoding ECM proteins, as well as collagen I protein production were analyzed by RT-qPCR, IF, and Western blot analysis (Figure 3). Pirfenidone dose-dependently reduced *COL1A1*, *COL3A1*, *COL4A1*, *COL6A1*, *FN1* (encoding fibronectin 1) and *ELN* (encoding elastin) mRNA levels, while it did not affect *ACTA2* (encoding alpha-smooth muscle actin; α-SMA) expression (Figure 3A–G). Untreated p-hIFs contained high levels of (intracellular) collagen I, which was dose-dependently reduced by pirfenidone and was virtually absent after 72 h exposure with 2 mg/mL pirfenidone (Figure 3H), also when analyzed by Western blotting (Figure 3I,J). When 72 h-pirfenidone treated p-hIFs were exposed to normal medium again, collagen I protein reappeared (Figure 3K), but even after 96 h collagen I protein levels were still clearly lower compared to p-hIFs that were not pretreated with pirfenidone (Figure 3I,L).

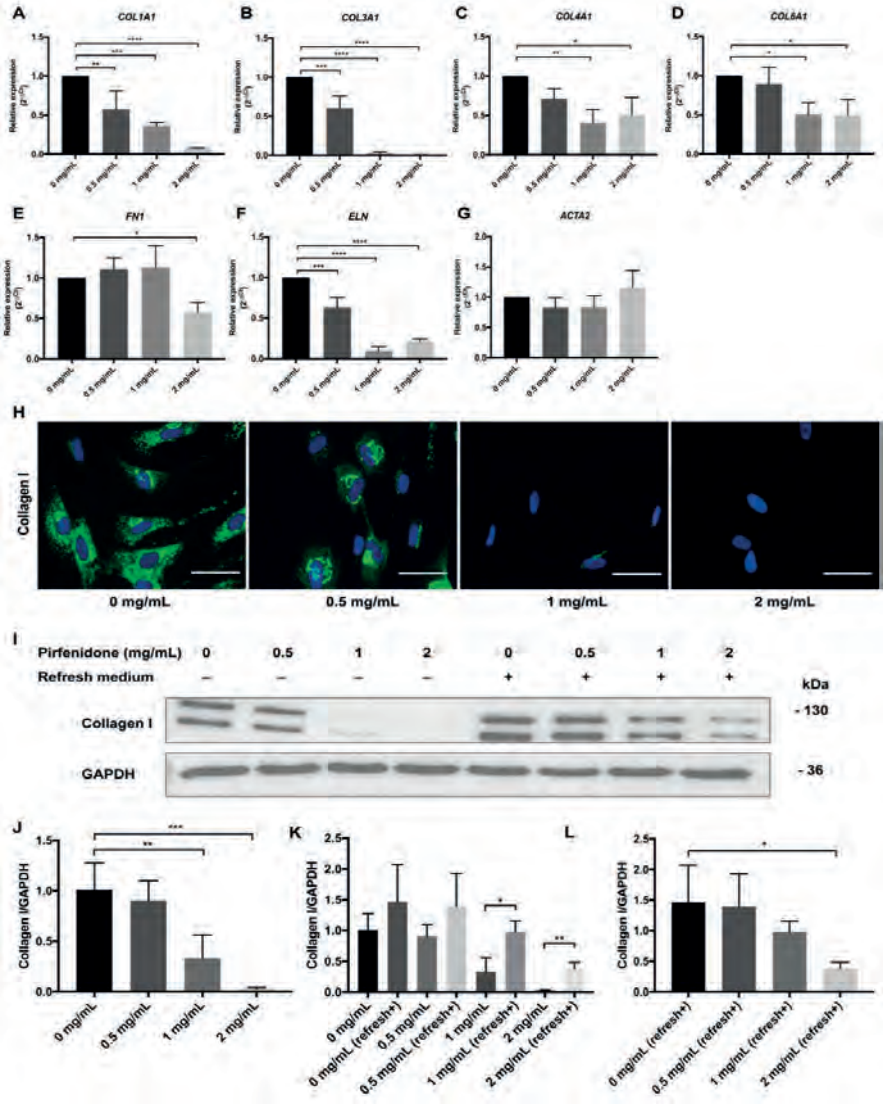

Figure 3. Pirfenidone inhibits Extracellular Matrix Protein (ECM) production. (A–G)

Intestinal fibroblasts were treated with increasing (maximum 2 mg/mL) concentrations of pirfenidone for 72 h. Pirfenidone suppressed *COL1A1*, *COL3A1*, *COL4A1*, *COL6A1*, *FN1*, and *ELN* mRNA levels, but not *ACTA2* levels (* $p < .05$, n = 3). (**H**) Immunofluorescent images showing that pirfenidone dose-dependently suppressed intracellular levels of collagen I. (**I**) p-hIFs were exposed for 72 h to pirfenidone (Lanes 1–4) and subsequently cultured in pirfenidone-free medium for 96 h (Lanes 5–8). (**J–L**) Western blot analysis showed that pirfenidone concentration-dependently and reversibility suppressed collagen I protein levels in p-hIFs. The relative abundance of the tested proteins was normalized to that of Glyceraldehyde 3-phosphate dehydrogenase (GAPDH). ** $p < 0.01$, *** $p < 0.001$, **** $p < 0.0001$; Data are presented as mean ± SEM. Scale bars = 50 μm. Refresh+, refresh medium.

Pirfenidone Reduces TGF-β1-Induced COL1A1 mRNA Expression and Collagen I Synthesis

Exposure of p-hIFs to TGF-β1 (2.5 ng/mL for 72 h) strongly increased *COL1A1* mRNA levels (>4-fold; Figure 4A), which was accompanied by increased collagen I protein levels (Figure 4B–D). Co-treatment with pirfenidone completely blocked the TGF-β1-induced expression of collagen 1, both at mRNA (pirfenidone at 1 and 2 mg/mL) and protein level (pirfenidone at 1 mg/mL) (Figure 4A–C). IF revealed that TGF-β1 induced collagen I protein accumulation in intestinal fibroblasts. Collagen I remained detectable in TGF-β1 + pirfenidone cotreated p-hIFs but it appeared to accumulate perinuclear, in comparison to more evenly distributed throughout the cellular cytoplasm in TGF-β1-only treated p-hIFs (Figure 4D).

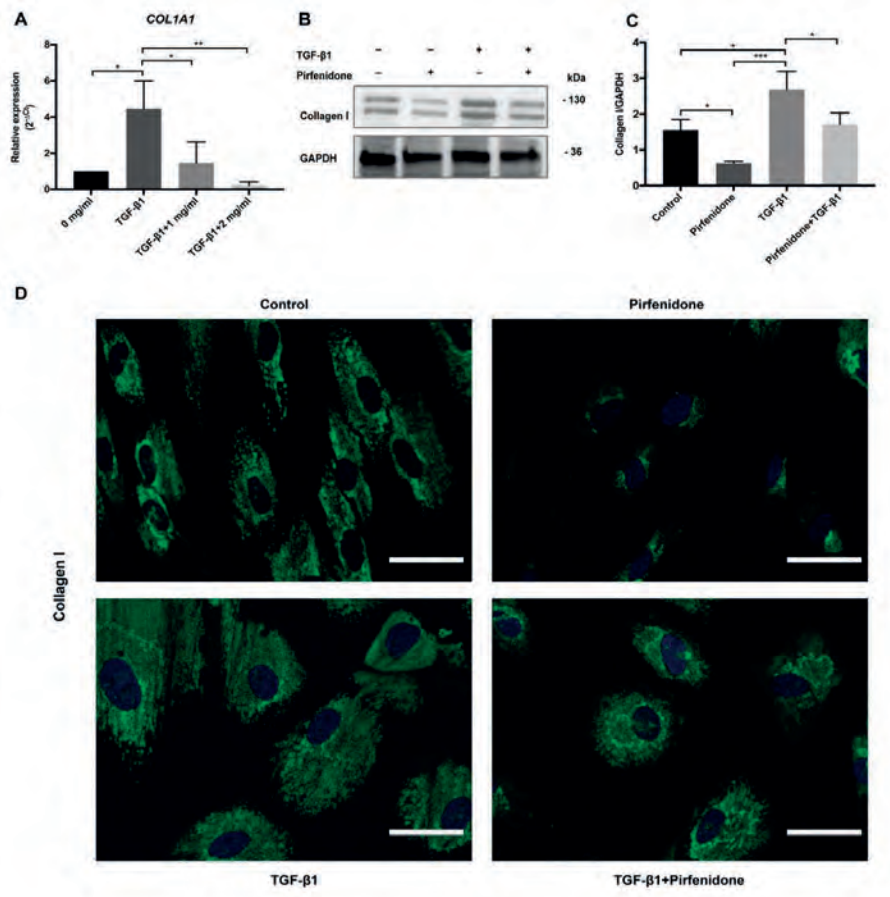

Figure 4. Pirfenidone suppresses basal and TGF-β1-induced collagen I expression in p-hIFs.

(**A**) TGF-β1 (2.5 ng/mL) induces *COL1A1* mRNA levels. Pirfenidone dose-dependently suppresses TGF-β1-induced *COL1A1* mRNA levels (* $p < 0.05$, n = 3) which was accompanied with a reduction in collagen I protein expression levels (**B–C**). (* $p < 0.05$, n = 3; GAPDH is included as protein loading control) (**D**) Immunofluorescence microscopy revealed that TGF-β1 enhanced the cellular surface area positive for collagen I, which was reduced again by pirfenidone leading to a perinuclear location of collagen I. ** $p < 0.01$, *** $p < 0.001$; Data are presented as mean ± SEM. Scale bars = 50 μm.

Pirfenidone Inhibits TGF-β1-Mediated Phosphorylation of TGF-β1/mTOR/p70S6K Signaling Pathway in p-hIFs

In order to delineate the molecular signaling pathways that underlie the anti-proliferative/anti-fibrotic effects of pirfenidone, we analyzed its effect on Smad2/3, p38 MAPK and mTOR phosphorylation in p-hIFs in the presence and absence of TGF-β1. As shown in Supplementary Figure S1, both TGF-β1 and pirfenidone did not significantly affect phosphorylation of Smad2/3 and p38 MAPK in p-hIFs. Besides activation of the Smad-signaling (24–29), TGF-β1 may also signal via mTOR (30,31), the latter not being studied earlier in intestinal fibroblasts. Indeed, TGF-β1 enhanced mTOR phosphorylation (at 6 h) in p-hIFs, as well as downstream signaling factor p70S6K (at 6 and 12 h) (Figure 5A). In contrast, TGF-β1 did not affect the levels of phosphorylated 4E-BP1 at any of the analyzed time points (6, 12, and 24 h TGF-β1 exposure) (Figure 5A). Pirfenidone (1 mg/mL) strongly suppressed both basal and TGF-β1-induced phosphorylation of mTOR and p70S6K, while it hardly affected 4E-BP1 phosphorylation (Figure 5B). Similar effects were observed for rapamycin (100 nmol/L, Figure 5B), the classical mTOR signaling pathway inhibitor. In line, rapamycin (100 nmol/L) also suppressed basal and TGF-β1-induced expression of collagen I in p-hIFs (Figure 5C).

Taken together, our data show that pirfenidone suppressed proliferation of p-hIFs and collagen I production by p-hIFs. Pirfenidone inhibits TGF-β1-induced mTOR signaling that may aid in the inhibition of p-hIFs proliferation and collagen production.

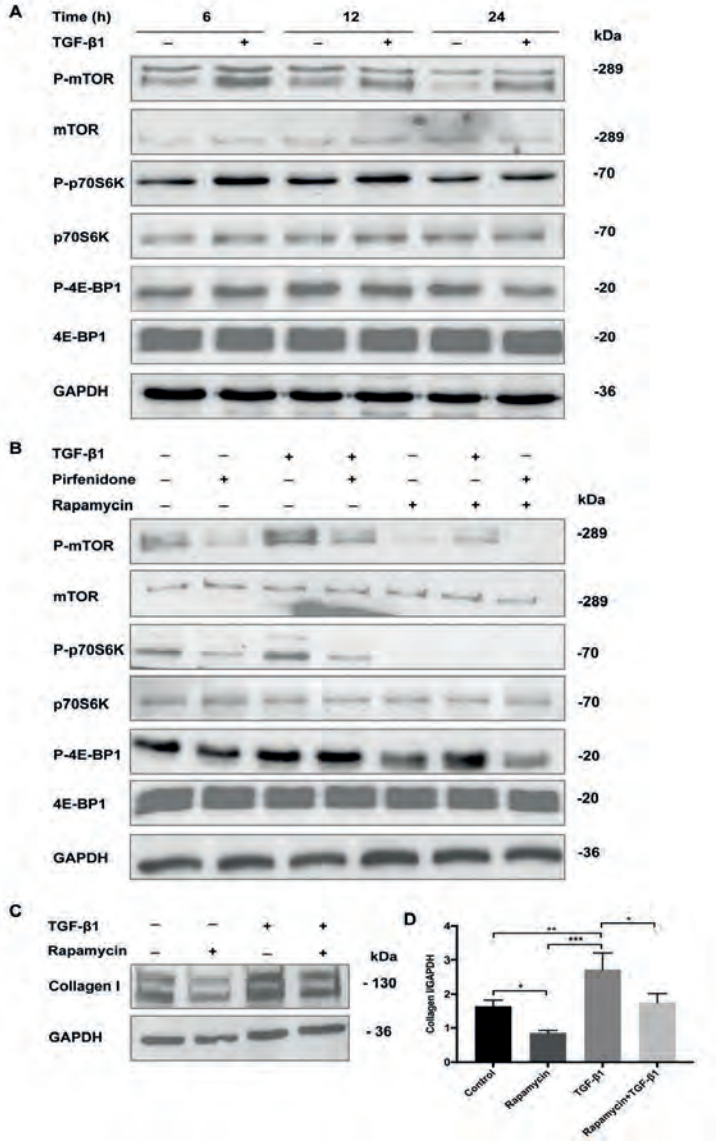

Figure 5. Pirfenidone suppresses the TGF-β1/mTOR/p70S6K signaling pathway.

(**A**) p-hIFs were cultured for 6, 12, and 24 h in the absence or presence of TGF-β1 (2.5 ng/mL). Levels of total and phosphorylated mTOR, p70S6K, and 4E-BP1 were assessed by Western blot analysis. TGF-β1 enhanced the levels of p-mTOR (at 6 h) and p-p70S6K (at 6–12 h). (**B**) p-hIFs were exposed to TGF-β1 (2.5 ng/mL), pirfenidone (1 mg/mL), rapamycin (100 nmol/L), or combinations of those compounds for 6 h and analyzed by Western blotting. Pirfenidone and rapamycin inhibited basal and TGF-β1-induced phosphorylation of mTOR and p70S6K. (**C–D**) Rapamycin (100 nmol/L for 72 h) inhibited basal and TGF-β1-induced collagen I production in p-hIFs. * $p < 0.05$, ** $p < 0.01$, *** $p < 0.001$, n = 3; GAPDH is

included as protein loading control.

Discussion

In this study, we show that pirfenidone dose-dependently and reversibly inhibits the proliferation and excessive production of ECM components, in particular collagen I. We show for the first time that pirfenidone suppresses basal and TGF-β1-induced mTOR signaling in p-hIFs, a pathway known to contribute to organ fibrosis. Thus, pirfenidone is a relevant drug to explore further for the treatment of intestinal fibrosis, a condition often associated with chronic intestinal diseases, such as IBD.

Intestinal inflammation triggers the activation of myofibroblasts that are central players in tissue repair, as they migrate into damaged tissue and control production and turnover of the extracellular matrix in support of all the other tissue-resident cell types. However, chronic inflammation leads to overactivation and proliferation of myofibroblasts that produce excessive amounts of ECM causing fibrosis (32,33). Therefore, suppressing myofibroblast proliferation and/or ECM production is an important therapeutic target to control and prevent intestinal fibrosis. An earlier study analyzed p-hIFs from CD patients and found that pirfenidone inhibited cell proliferation, but did not affect collagen (I-V) production (34). The p-hIFs were exposed to the same concentrations of pirfenidone as we did, however, only for 24 h. Moreover, only secreted collagen (in the medium) was quantified and no difference were found for untreated and pirfenidone-treated p-hIFs. Given the fact that pirfenidone did not affect collagen production in their study, they concluded that it may be of limited clinical value for treating intestinal fibrosis. We, however, found that pirfenidone dose-dependently suppresses *COL1A1*, *COL3A1*, *ELN* (all >90%) and *COL4A1*, *COL6A1* and *FN1* (>50%) mRNA levels, as well as collagen I protein production by p-hIFs, along with inhibiting cell proliferation. The key difference probably is that we treated the p-hIF for 72 h and the most pronounced effect of pirfenidone, also on cell proliferation, is observed only 24 h after the treatment started, especially at the lower concentrations of pirfenidone (Figure 1A). In addition, we show that TGF-β1-induced collagen I production is effectively suppressed by pirfenidone. Our results are largely in line with earlier observations using human intestinal fibroblast cell lines and rat and mouse primary intestinal fibroblasts. Pirfenidone was shown to suppress TGF-β1-induced *COL1A1* and *ACTA2* expression in a human intestinal myofibroblast cell lines either by activating the transient receptor potential ankyrin 1 channel (24), by inhibiting Smad/PI3K/AKT (27) signaling or the MAPK pathway (25). Many studies have analyzed the effect of pirfenidone on tissue fibrosis in organs other than the intestine, and multiple pathways have been implicated with most focus on Smad-related signaling pathways (summarized in Figure 6) (18,24–30,36,37). However, compared to the earlier

studies using intestinal fibroblasts, we found that a 6 h exposure to TGF-β1 (2.5 ng/mL) did not significantly induce phosphorylation of Smad 2/3 or p38-MAPK in p-hIFs. This may be because we exposed the p-hIFs to lower concentrations TGF-β1 compared to the other studies (5-10 ng/mL; (24–27)). TGF-β1 induces Smad2/3 phosphorylation within minutes (24) and elevated levels are still detectable after 24–48 h exposure (25–27). Still, the extent of Smad2/3 phosphorylation is time-dependent and the time-point we chose (6 h of TGF-β1 treatment) may not have been optimal. Sun et al. also examined the effect of pirfenidone on "untreated" human intestinal fibroblasts and found that this did not lower Smad 2/3 phosphorylation, which is in line with our data. Notably, phosphorylated Smad2/3 and p38 MAPK were detectable in control-cultured p-hIFs, which may indicate a higher basal activation state compared to CCD-Co18 (25), InMyoFib (24) and HUM-CELL-d022 (27) fibroblasts. A possible effect of pirfenidone on mTOR signaling has so far not been studied for intestinal fibrosis. We show that 2.5 ng/mL TGF-β1 quickly enhances mTOR phosphorylation, followed by downstream p70S6K phosphorylation. This suggests that the mTOR pathway was more sensitive to the stimulation of TGF-β1 than Smad 2/3 and p38-MAPK pathways in p-hIFs. Rapamycin-sensitive mTOR signaling plays an important role in regulating cell growth, cell proliferation, protein synthesis, transcription and autophagy (38). p70S6K is one of the main key substrates of mTOR and promotes protein synthesis at the ribosome (39). Pirfenidone inhibited both basal and TGF-β1-induced mTOR and p70S6K phosphorylation which may suppress collagen production. Indeed, treating p-hIFs with rapamycin, the prototypical inhibitor on mTOR (40) also suppressed both basal and TGF-β1-induced collagen I production in p-hIFs. This supports the relationship between mTOR signaling and collagen I production in p-hIFs and suggests that pirfenidone, at least in part, acts via mTOR to suppress ECM production and p-hIF proliferation.

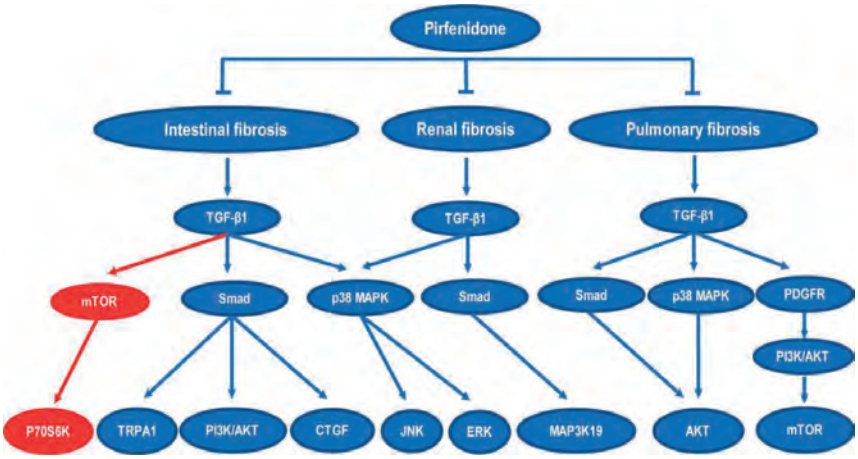

Figure 6. Overview of signaling pathways involved in the development of tissue fibrosis that are affected by pirfenidone.

Previously reported pathways are presented in blue. The mTOR pathways studied in this work is presented in red.

It is important to note that besides anti-fibrotic activity, pirfenidone has also been shown to act as an anti-inflammatory and an anti-oxidant agent in IPF patients (41,42). Here, we specifically focused on the potential anti-fibrotic action of p-hIFs, but the anti-inflammatory and anti-oxidant activities of pirfenidone may synergize in its therapeutic effect in patients with IBD. One important aspect of pirfenidone has to considered, as it has been reported to cause some gastrointestinal side effects in IPF patients, including nausea, vomiting, dyspepsia and diarrhea (43,44). Current therapies for IBD, however, are also pursuing intestine-specific delivery of drugs. The ColoPulse technology is such a novel approach which allows controlled release of drugs at the terminal ileum and colon (45). Systemic and gastrointestinal side effects of pirfenidone may be minimized using such approach, concomitant with a higher drug-efficacy of pirfenidone on intestinal inflammation and fibrosis (46).

In this study, we made use of p-hIFs from healthy tissue, which were exposed to TGF-β1, being a “master cytokine” in the development of tissue fibrosis. It remains to be determined to what level this exactly resembles the phenotype of fibroblasts residing in stenotic intestinal tissue in vivo. In addition, future studies need to establish the interindividual, as well as location-specific differences between intestinal fibroblasts and their value as in vitro models to study intestinal fibrosis.

In summary, we show that pirfenidone suppresses the proliferation and collagen production of primary intestinal fibroblasts, and it does so, at least in part, by inhibiting

mTOR/p70S6K signaling. This study suggests that pirfenidone might be a potential new therapeutic drug for the treatment of intestinal fibrosis.

Supplementary Materials: Figure S1: Pirfenidone does not suppress Smad2/3 and p38 MAPK phosphorylation in p-hIFs, Table S1: TaqMan primers and probes for Real-time Quantitative PCR analysis, Table S2: SYBR green primer sequences used for Real-time Quantitative PCR Analysis, Table S3: Antibodies catalog numbers and dilutions.

Author Contributions: Conceptualization, Y.C., G.D. and K.N.F.; Funding acquisition, G.D. and K.N.F.; Investigation, Y.C., M.Z., C.L., T.B. and B.H.J.; Methodology, Y.C., T.B. and B.H.J.; Project administration, Y.C., T.B., B.H.J., G.D. and K.N.F.; Resources, G.D. and K.N.F.; Supervision, G.D. and K.N.F.; Validation, Y.C., M.Z., C.L. and T.B.; Visualization, Y.C.; Writing – original draft, Y.C. and K.N.F.; Writing – review & editing, M.Z., C.L., T.B., B.H.J., G.D. and K.N.F.

Acknowledgements: We thank Peter Olinga and Ruud Bank for providing materials for analyzing transcriptional effects on fibrosis markers.

Conflicts of Interest: The authors declare no conflict of interest.

References

1. Baumgart, D.C.; Carding, S.R. Inflammatory bowel disease: Cause and immunobiology. Lancet 2007, 369, 1627–1640, doi:10.1016/S0140-6736(07)60750-8.

2. Kaplan, G.G. The global burden of IBD: From 2015 to 2025. Nat. Rev. Gastroenterol. Hepatol. 2015, 12, 720–727, doi:10.1038/nrgastro.2015.150.

3. Latella, G.; Di Gregorio, J.; Flati, V.; Rieder, F.; Lawrance, I.C. Mechanisms of initiation and progression of intestinal fibrosis in IBD. Scand. J. Gastroenterol. 2015, 50, 53–65, doi:10.3109/00365521.2014.968863.

4. Bettenworth, D.; Rieder, F. Pathogenesis of Intestinal Fibrosis in Inflammatory Bowel Disease and Perspectives for Therapeutic Implication. Dig. Dis. 2017, 35, 25–31, doi:10.1159/000449079.

5. Lawrance, I.C.; Rogler, G.; Bamias, G.; Breynaert, C.; Florholmen, J.; Pellino, G.; Reif, S.; Speca, S.; Latella, G. Cellular and Molecular Mediators of Intestinal Fibrosis. J. Crohns Colitis 2017, 11, 1491–1503, doi:10.1016/j.crohns.2014.09.008.

6. Rieder, F.; Fiocchi, C. Mechanisms of tissue remodeling in inflammatory bowel disease. Dig. Dis. 2013, 31, 186–193, doi:10.1159/000353364.

7. Allocca, M.; Fiorino, G.; Bonifacio, C.; Peyrin-Biroulet, L.; Danese, S. Noninvasive Multimodal Methods to Differentiate Inflamed vs Fibrotic Strictures in Patients With Crohn's Disease. Clin. Gastroenterol. Hepatol. 2019, 12, 2397–2415, doi:10.1016/j.cgh.2019.04.025.

8. Bettenworth, D.; Gustavsson, A.; Atreja, A.; Lopez, R.; Tysk, C.; van Assche, G.; Rieder, F. A Pooled Analysis of Efficacy, Safety, and Long-term Outcome of Endoscopic Balloon Dilation Therapy for Patients with Stricturing Crohn's Disease. Inflamm. bowel dis. 2017, 23, 133–142, doi:10.1097/MIB.0000000000000988.

9. van Loo, E.S.; Dijkstra, G.; Ploeg, R.J.; Nieuwenhuijs, V.B. Prevention of postoperative recurrence of Crohn's disease. J. Crohns Colitis 2012, 6, 637–646, doi:10.1016/j.crohns.2011.12.006.

10. Isaka, Y. Targeting TGF-beta Signaling in Kidney Fibrosis. Int. J. Mol. Sci. 2018, 19, doi:10.3390/ijms19092532.

11. Laplante, M.; Sabatini, D.M. mTOR signaling at a glance. J. Cell Sci. 2009, 122, 3589–3594, doi:10.1242/jcs.051011.

12. Lamouille, S.; Derynck, R. Cell size and invasion in TGF-beta-induced epithelial to mesenchymal transition is regulated by activation of the mTOR pathway. J. Cell Biol. 2007, 178, 437–451, doi:10.1083/jcb.200611146.

13. Richter, J.D.; Sonenberg, N. Regulation of cap-dependent translation by eIF4E inhibitory proteins. Nature 2005, 433, 477–480, doi:10.1038/nature03205.

14. Chung, J.; Kuo, C.J.; Crabtree, G.R.; Blenis, J. Rapamycin-FKBP specifically blocks growth-dependent activation of and signaling by the 70 kd S6 protein kinases. Cell 1992, 69, 1227–1236, doi:10.1016/0092-8674(92)90643-q.

15. Li, C.; Han, R.; Kang, L.; Wang, J.; Gao, Y.; Li, Y.; He, J.; Tian, J. Pirfenidone controls the feedback loop of the AT1R/p38 MAPK/renin-angiotensin system axis by regulating liver X receptor-alpha in myocardial infarction-induced cardiac fibrosis. Sci. Rep. 2017, 7, doi:10.1038/srep40523.

16. Armendariz-Borunda, J.; Islas-Carbajal, M.C.; Meza-Garcia, E.; Rincon, A.R.; Lucano, S.; Sandoval, A.S.; Salazar, A.; Berumen, J.; Alvarez, A.; Covarrubias, A.; et al. A pilot study in patients with established advanced liver fibrosis using pirfenidone. Gut 2006, 55, 1663–1665, doi:10.1136/gut.2006.107136.

17. King, T.E., Jr.; Bradford, W.Z.; Castro-Bernardini, S.; Fagan, E.A.; Glaspole, I.; Glassberg, M.K.; Gorina, E.; Hopkins, P.M.; Kardatzke, D.; Lancaster, L.; et al. A phase 3 trial of pirfenidone in patients with idiopathic pulmonary fibrosis. N. Engl. J. Med. 2014, 370, 2083–2092, doi:10.1056/NEJMoa1402582.

18. Li, Z.; Liu, X.; Wang, B.; Nie, Y.; Wen, J.; Wang, Q.; Gu, C. Pirfenidone suppresses MAPK signalling pathway to reverse epithelial-mesenchymal transition and renal fibrosis. Nephrology 2017, 22, 589–597, doi:10.1111/nep.12831.

19. Herrera, M.; Islam, A.B.; Herrera, A.; Martin, P.; Garcia, V.; Silva, J.; Garcia, J.M.; Salas, C.; Casal, I.; de Herreros, A.G.; et al. Functional heterogeneity of cancer-associated fibroblasts from human colon tumors shows specific prognostic gene expression signature. Clin. Cancer Res. 2013, 19, 5914–5926, doi:10.1158/1078-0432.CCR-13-0694.

20. Roshan Moniri, M.; Young, A.; Reinheimer, K.; Rayat, J.; Dai, L.J.; Warnock, G.L. Dynamic assessment of cell viability, proliferation and migration using real time cell analyzer system (RTCA). Cytotechnology 2015, 67, 379–386, doi:10.1007/s10616-014-9692-5.

21. Conde de la Rosa, L.; Schoemaker, M.H.; Vrenken, T.E.; Buist-Homan, M.; Havinga, R.; Jansen, P.L.; Moshage, H. Superoxide anions and hydrogen peroxide induce hepatocyte death by different mechanisms: Involvement of JNK and ERK MAP kinases. J. Hepatol. 2006, 44, 918–929, doi:10.1016/j.jhep.2005.07.034.

22. Schoemaker, M.H.; Conde de la Rosa, L.; Buist-Homan, M.; Vrenken, T.E.; Havinga, R.; Poelstra, K.; Haisma, H.J.; Jansen, P.L.; Moshage, H. Tauroursodeoxycholic acid protects rat hepatocytes from bile acid-induced apoptosis via activation of survival pathways. Hepatology 2004, 39, 1563–1573, doi:10.1002/hep.20246.

23. Blokzijl, H.; Vander Borght, S.; Bok, L.I.; Libbrecht, L.; Geuken, M.; van den Heuvel, F.A.; Dijkstra, G.; Roskams, T.A.; Moshage, H.; Jansen, P.L.; et al. Decreased P-glycoprotein (P-gp/MDR1) expression in inflamed human intestinal epithelium is independent of PXR protein levels. Inflamm. Bowel Dis. 2007, 13, 710–720, doi:10.1002/ibd.20088.

24. Kurahara, L.H.; Hiraishi, K.; Hu, Y.; Koga, K.; Onitsuka, M.; Doi, M.; Aoyagi, K.; Takedatsu, H.; Kojima, D.; Fujihara, Y.; et al. Activation of Myofibroblast TRPA1 by Steroids and Pirfenidone Ameliorates Fibrosis in Experimental Crohn's Disease. Cell. Mol. Gastroenterol. Hepatol. 2018, 5, 299–318, doi:10.1016/j.jcmgh.2017.12.005.

25. Li, G.; Ren, J.; Hu, Q.; Deng, Y.; Chen, G.; Guo, K.; Li, R.; Li, Y.; Wu, L.; Wang, G.; et al. Oral pirfenidone protects against fibrosis by inhibiting fibroblast proliferation and TGF-beta signaling in a murine colitis model. Biochem. Pharmacol. 2016, 117, 57–67, doi:10.1016/j.bcp.2016.08.002.

26. Sun, Y.W.; Zhang, Y.Y.; Ke, X.J.; Wu, X.J.; Chen, Z.F.; Chi, P. Pirfenidone prevents radiation-induced intestinal fibrosis in rats by inhibiting fibroblast proliferation and differentiation and suppressing the TGF-beta1/Smad/CTGF signaling pathway. Eur. J. Pharmacol. 2018, 822, 199–206, doi:10.1016/j.ejphar.2018.01.027.

27. Sun, Y.; Zhang, Y.; Chi, P. Pirfenidone suppresses TGFβ1induced human intestinal fibroblasts activities by regulating proliferation and apoptosis via the inhibition of the Smad and PI3K/AKT signaling pathway. Mol. Med. Rep. 2018, 18, 3907–3913, doi:10.3892/mmr.2018.9423.

28. Conte, E.; Gili, E.; Fagone, E.; Fruciano, M.; Iemmolo, M.; Vancheri, C. Effect of pirfenidone on proliferation, TGF-beta-induced myofibroblast differentiation and fibrogenic activity of primary human lung fibroblasts. Eur. J. Pharm. Sci. 2014, 58, 13–19, doi:10.1016/j.ejps.2014.02.014.

29. Boehme, S.A.; Franz-Bacon, K.; DiTirro, D.N.; Ly, T.W.; Bacon, K.B. MAP3K19 Is a Novel Regulator of TGF-β Signaling That Impacts Bleomycin-Induced Lung Injury and Pulmonary Fibrosis. PLoS One 2016, 11, doi:10.1371/journal.pone.0154874.

30. Kurita, Y.; Araya, J.; Minagawa, S.; Hara, H.; Ichikawa, A.; Saito, N.; Kadota, T.; Tsubouchi, K.; Sato, N.; Yoshida, M.; et al. Pirfenidone inhibits myofibroblast differentiation and lung fibrosis development during insufficient mitophagy. Respir. Res. 2017, 18, doi:10.1186/s12931-017-0600-3.

31. Woodcock, H.V.; Eley, J.D.; Guillotin, D.; Plate, M.; Nanthakumar, C.B.; Martufi, M.; Peace, S.; Joberty, G.; Poeckel, D.; Good, R.B.; et al. The mTORC1/4E-BP1 axis represents a critical signaling node during fibrogenesis. Nat. Commun. 2019, 10, 6, doi:10.1038/s41467-018-07858-8.

32. Latella, G.; Rieder, F. Intestinal fibrosis: Ready to be reversed. Curr. Opin. Gastroenterol. 2017, 33, 239–245, doi:10.1097/MOG.0000000000000363.

33. Rockey, D.C.; Bell, P.D.; Hill, J.A. Fibrosis- A common pathway to organ injury and failure. N. Engl. J. Med. 2015, 372, 1138–1149, doi:10.1056/NEJMra1300575.

34. Kadir, S.I.; Wenzel Kragstrup, T.; Dige, A.; Kok Jensen, S.; Dahlerup, J.F.; Kelsen, J. Pirfenidone inhibits the proliferation of fibroblasts from patients with active Crohn's disease. Scand. J. Gastroenterol. 2016, 51, 1321–1325, doi:10.1080/00365521.2016.1185146.

35. Pan, C.; Kumar, C.; Bohl, S.; Klingmueller, U.; Mann, M. Comparative proteomic phenotyping of cell lines and primary cells to assess preservation of cell type-specific functions. Mol. Cell. Proteomics 2009, 8, 443–450, doi:10.1074/mcp.M800258-MCP200.

36. Ji, X.; Naito, Y.; Weng, H.; Ma, X.; Endo, K.; Kito, N.; Yanagawa, N.; Yu, Y.; Li, J.; Iwai, N. Renoprotective mechanisms of pirfenidone in hypertension-induced renal injury: through anti-fibrotic and anti-oxidative stress pathways. Biomed. Res. 2013, 34, 309–319.

37. Molina-Molina, M.; Machahua-Huamani, C.; Vicens-Zygmunt, V.; Llatjos, R.; Escobar, I.; Sala-Llinas, E.; Luburich-Hernaiz, P.; Dorca, J.; Montes-Worboys, A. Anti-fibrotic effects of pirfenidone and rapamycin in primary IPF fibroblasts and human alveolar epithelial cells. BMC Pulm. Med. 2018, 18, doi:10.1186/s12890-018-0626-4.

38. Lipton, J.O.; Sahin, M. The neurology of mTOR. Neuron 2014, 84, 275–291, doi:10.1016/j.neuron.2014.09.034.

39. Saxton, R.A.; Sabatini, D.M. mTOR Signaling in Growth, Metabolism, and Disease. Cell 2017, 168, 960–976, doi:10.1016/j.cell.2017.02.004.

40. Li, J.; Kim, S.G.; Blenis, J. Rapamycin: One drug, many effects. Cell Metab. 2014, 19, 373–379, doi:10.1016/j.cmet.2014.01.001.

41. Lopez-de la Mora, D.A.; Sanchez-Roque, C.; Montoya-Buelna, M.; Sanchez-Enriquez, S.; Lucano-Landeros, S.; Macias-Barragan, J.; Armendariz-Borunda, J. Role and New Insights of Pirfenidone in Fibrotic Diseases. Int. J. Med. Sci. 2015, 12, 840–847, doi:10.7150/ijms.11579.

42. Fois, A.G.; Posadino, A.M.; Giordo, R.; Cossu, A.; Agouni, A.; Rizk, N.M.; Pirina, P.; Carru, C.; Zinellu, A.; Pintus, G. Antioxidant Activity Mediates Pirfenidone Antifibrotic Effects in Human Pulmonary Vascular Smooth Muscle Cells Exposed to Sera of Idiopathic Pulmonary Fibrosis Patients. Oxid. Med. Cell. Longev. 2018, 2018, doi:10.1155/2018/2639081.

43. Noble, P.W.; Albera, C.; Bradford, W.Z.; Costabel, U.; Glassberg, M.K.; Kardatzke, D.; King, T.E., Jr.; Lancaster, L.; Sahn, S.A.; Szwarcberg, J.; et al. Pirfenidone in patients with idiopathic pulmonary fibrosis (CAPACITY): Two randomised trials. Lancet 2011, 377, 1760–1769, doi:10.1016/S0140-6736(11)60405-4.

44. Noble, P.W.; Albera, C.; Bradford, W.Z.; Costabel, U.; du Bois, R.M.; Fagan, E.A.; Fishman, R.S.; Glaspole, I.; Glassberg, M.K.; Lancaster, L.; et al. Pirfenidone for idiopathic pulmonary fibrosis: analysis of pooled data from three multinational phase 3 trials. Eur. Respir. J. 2016, 47, 243–253, doi:10.1183/13993003.00026-2015.

45. Gareb, B.; Dijkstra, G.; Kosterink, J.G.W.; Frijlink, H.W. Development of novel zero-order release budesonide tablets for the treatment of ileo-colonic inflammatory bowel disease and comparison with formulations currently used in clinical practice. Int. J. Pharm. 2019, 554, 366–375, doi:10.1016/j.ijpharm.2018.11.019.

46. Khanna, D.; Albera, C.; Fischer, A.; Khalidi, N.; Raghu, G.; Chung, L.; Chen, D.; Schiopu, E.; Tagliaferri, M.; Seibold, J.R.; et al. An Open-label, Phase II Study of the Safety and Tolerability of Pirfenidone in Patients with Scleroderma-associated Interstitial Lung Disease: The LOTUSS Trial. J. Rheumatol. 2016, 43, 1672–1679, doi:10.3899/jrheum.151322.

Supplementary tables:

Table S1. TaqMan primers and probes for Real-time Quantitative PCR analysis.

Gene	TaqMan primers and probes
18S	Forward: CGGCTACCACATCCAAGGA
	Reverse: CCAATTACAGGGCCTCGAAA
	Probe: CGCGCAAATTACCCACTCCCGA
COL1A1	Forward: GGCCCAGAAGAACTGGTACATC
	Reverse: CCGCCATACTCGAACTGGAA
	Probes: CCCCAAGGACAAGAGGCATGTCTG
ACTA2	Forward: GGGACGACATGGAAAAGATCTG
	Reverse: CAGGGTGGGATGCTCTTCA
	Probe: CACTCTTTCTACAATGAGCTTCGTGTTGCCC

Table S2. SYBR green primer sequences used for Real-time Quantitative PCR Analysis.

Gene	SYBR green primers
COL3A1	Forward: CTGGACCCCAGGGTCTTC
	Reverse: CATCTGATCCAGGGTTTCCA
COL4A1	Forward: AGGAGAGAAGGGCGCTGT
	Reverse: TCCAGGTAAGCCGTCAACA
COL6A1	Forward: GAAGAGAAGGCCCCGTTG
	Reverse: CGGTAGCCTTTAGGTCCGATA
FN1	Forward: CTGGCCGAAAATACATTGTAAA
	Reverse: CCACAGTCGGGTCAGGAG
ELN	Forward: CGGGAGTAGTTGGTGTCCC
	Reverse: AGCTGCTTCTGGTGACACAA

Table S3. Antibodies catalog numbers and dilutions.

Antibody	Cat no. (dilution)	Company
GAPDH	CB1001 (1:1000)	Calbiochem
Phospho-mTOR	2971 (1:1000)	Cell Signaling
mTOR	2983T (1:1000)	Cell Signaling
Phospho-p70S6K Thr389	9205 (1:1000)	Cell Signaling
p70S6K	9202S (1:1000)	Cell Signaling
Phospho-4E-BP1 Ser65	9451 (1:1000)	Cell Signaling
4E-BP1	9644T (1:1000)	Cell Signaling
Phosho-Smad2 (S465/467)/3 (S423/425)	8828 (1:1000)	Cell Signaling
Smad2/3	3120 (1:1000)	Cell Signaling
Phosho-p38 MAPK	9211 (1:1000)	Cell Signaling
p38 MAPK	9212 (1:1000)	Cell Signaling
Polyclonal Rabbit Anti-Mouse Immunoglobulins	P0260 (1:2000)	DAKO
Polyclonal Rabbit Anti-Goat Immunoglobulins	P0160 (1:2000)	DAKO
Polyclonal Goat Anti-Rabbit Immunoglobulins	P0448 (1:2000)	DAKO

Supplementary Figure:

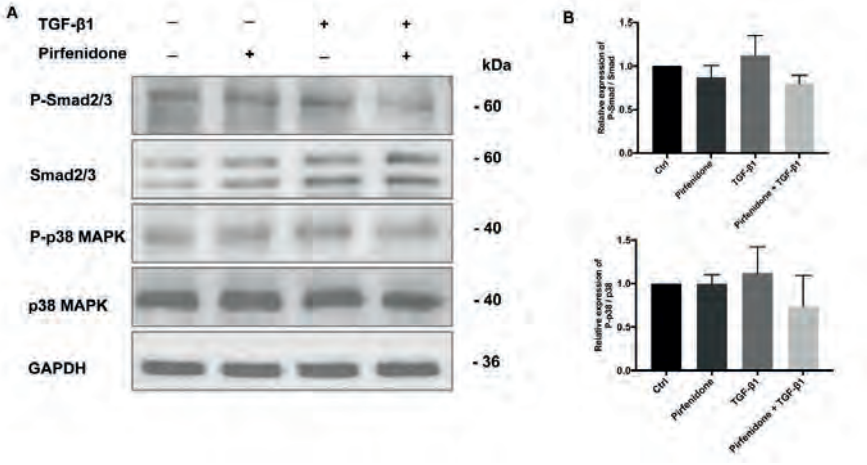

Figure S1. Pirfenidone does not suppress Smad2/3 and p38 MAPK phosphorylation in p-hIFs.

(**A**) p-hIFs were exposed to pirfenidone (1 mg/ml) and/or, TGF-β1 (2.5 ng/ml) for 6 h. Total and phosphorylated Smad2/3 and p38 MAPK were assessed by Western blot analysis. Compared with the control group, TGF-β1 or pirfenidone did not pronouncedly change levels of phosphorylated Smad2/3 or p38 MAPK in p-hIFs. (**B**) Shows the quantification of the signal intensity-ratios of P‐Smad2/3 to Smad2/3 and P-p38 MAPK to p38 MAPK of 3 independent experiments. GAPDH is included as protein loading control.

Supplementary References for Figure 6:

1. Kurahara LH, Hiraishi K, Hu Y, et al. Activation of Myofibroblast TRPA1 by Steroids and Pirfenidone Ameliorates Fibrosis in Experimental Crohn's Disease. Cellular and molecular gastroenterology and hepatology. 2018;5(3):299-318.

2. Sun Y, Zhang Y, Chi P. Pirfenidone suppresses TGFbeta1induced human intestinal fibroblasts activities by regulating proliferation and apoptosis via the inhibition of the Smad and PI3K/AKT signaling pathway. Molecular medicine reports. 2018;18(4):3907-3913.

3. Li G, Ren J, Hu Q, et al. Oral pirfenidone protects against fibrosis by inhibiting fibroblast proliferation and TGF-beta signaling in a murine colitis model. Biochemical pharmacology. 2016;117:57-67.

4. Sun YW, Zhang YY, Ke XJ, Wu XJ, Chen ZF, Chi P. Pirfenidone prevents radiation-induced intestinal fibrosis in rats by inhibiting fibroblast proliferation and differentiation and suppressing the TGF-beta1/Smad/CTGF signaling pathway. European journal of pharmacology. 2018;822:199-206.

5. Li Z, Liu X, Wang B, et al. Pirfenidone suppresses MAPK signalling pathway to reverse epithelial-mesenchymal transition and renal fibrosis. Nephrology. 2017;22(8):589-597.

6. Ji X, Naito Y, Weng H, et al. Renoprotective mechanisms of pirfenidone in hypertension-induced renal injury: through anti-fibrotic and anti-oxidative stress pathways. Biomedical research. 2013;34(6):309-319.

7. Conte E, Gili E, Fagone E, Fruciano M, Iemmolo M, Vancheri C. Effect of pirfenidone on proliferation, TGF-beta-induced myofibroblast differentiation and fibrogenic activity of primary human lung fibroblasts. European journal of pharmaceutical sciences : official journal of the European Federation for Pharmaceutical Sciences. 2014;58:13-19.

8. Boehme SA, Franz-Bacon K, DiTirro DN, Ly TW, Bacon KB. MAP3K19 Is a Novel Regulator of TGF-beta Signaling That Impacts Bleomycin-Induced Lung Injury and Pulmonary Fibrosis. PloS one. 2016;11(5):e0154874.

9. Kurita Y, Araya J, Minagawa S, et al. Pirfenidone inhibits myofibroblast differentiation and lung fibrosis development during insufficient mitophagy. Respiratory research. 2017;18(1):114.

10. Molina-Molina M, Machahua-Huamani C, Vicens-Zygmunt V, et al. Anti-fibrotic effects of pirfenidone and rapamycin in primary IPF fibroblasts and human alveolar epithelial cells. BMC pulmonary medicine. 2018;18(1):63.

Chapter 7

Increased arginase-1 expression during hepatic stellate cell activation promotes fibrogenesis

Mengfan Zhang, Zongmei Wu, Manon Buist-Homan, Han Moshage

Department of Gastroenterology and Hepatology, University Medical Center Groningen, University of Groningen, Groningen, the Netherlands

Correspondence: Han Moshage; a.j.moshage@umcg.nl

Abstract

Background Activation of hepatic stellate cells (HSC) is one of the essential pathogenetic mechanisms of liver fibrosis. Unresolved excessive extracellular matrix deposition (ECM) characteristic of liver fibrosis can exacerbate to cirrhosis. Collagen is the most abundant constituent of ECM and proline is the most abundant amino acid of collagen. Arginine is a non-essential amino acid. It is the precursor in the biosynthetic pathway of proline. Arginine is the exclusive substrate of both nitric oxide synthase (NOS) and arginase. NOS is an M1 (pro-inflammatory) marker of macrophage polarization whereas arginase-1 (Arg1) is an M2 (pro-fibrogenic) marker of macrophage polarization. Differential expression of NOS and Arg1 has not been studied in HSCs yet. The aim of this study was to identify the expression profile of arginine catabolic enzymes during HSC activation and to investigate the possibility to inhibit HSC activation and fibrogenesis via targeting arginine metabolism. **Methods** Isolated primary rat HSCs were culture for 7 days to achieve complete activation, and transcription and translation of iNOS and Arg1 were investigated. The arginase inhibitor Nor-NOHA was used to investigate the effect of Arg1 inhibition on collagen production and cell proliferation in activated HSCs. **Results** I During HSC activation, iNOS expression decreased whereas Arg1 expression increased. Inhibition of Arg1 in activated HSCs efficiently inhibited collagen production while cell proliferation remained unchanged. **Conclusion:** HSC activation is accompanied by a switch of arginine catabolism from iNOS to Arg1. Inhibition of Arg1 decreases collagen synthesis. Arg1 can be a therapeutic target for the inhibition of liver fibrogenesis.

Key words: Arginine, proline, iNOS, Arg1, Hepatic stellate cell, Fibrosis

Introduction

Liver fibrosis is the result of an uncontrolled wound healing response in chronic liver diseases of various etiology. Liver fibrosis is characterized by the accumulation of excessive amounts of extracellular matrix (ECM) in the liver (1). Although liver fibrosis is still reversible, advanced liver fibrosis has a high probability to progress to cirrhosis and even hepatocellular carcinoma (2). In these terminal stages, scar tissue formed by unresolved ECM deposition segments hepatic lobules, causing architectural changes that eventually cause hepatic failure with severe complications (1). In view of the poor prognosis of cirrhosis, therapy is aimed at the stages preceding cirrhosis including (reversible) fibrosis. However, no medication to treat liver fibrosis is currently approved for clinical application.

Fibrogenesis is the key pathogenetic mechanism of liver fibrosis and is attributed to excessive production of ECM by myofibroblasts. In chronic liver diseases of various etiology, hepatic stellate cells are the major source of myofibroblasts (3). The hepatic stellate cell is the most abundant non-parenchymal cell type in the liver. In the healthy liver, hepatic stellate cells (HSC) maintain a quiescent state and store retinoids. Upon continuous liver injury, the quiescent hepatic stellate cells (qHSC) transdifferentiates into the activated hepatic stellate cell (aHSC) and acquire the ability to proliferate, migrate and contract. Furthermore, they secrete large amounts of various ECM components to contribute to wound repair (4, 5). In the pathological condition, ECM secretion by aHSC is uncontrolled and ECM accumulates in the perisinusoidal space (6). The grade of liver fibrosis correlates with the long term prognosis of patients (7). Preclinical evidence suggests that reversal of the activated state of aHSCs to reduce the deposition of ECM is a promising strategy to slow down or even reverse liver fibrosis (4). Collagen is one of the major components of ECM (8). Collagen contains a relatively high proportion of the amino acids arginine, proline and glycine and the availability of these amino acids is the limiting factor in the synthesis of collagen (9). This phenomenon permits to target amino acid metabolism to reduce fibrogenesis.

The metabolism of the non-essential amino acid arginine is closely related to the metabolism of proline. L-arginine is the exclusive substrate of the enzymes nitric oxide synthase (NOS) and arginase (9).NOS has three isoforms: neuronal NOS (nNOS), inducible NOS (iNOS) and endothelial NOS (eNOS) which are encoded by NOS1, NOS2 and NOS3, respectively. Arginase has two isoforms: Arg1 and Arg2. Arg1 is predominantly expressed in the cytoplasm of liver cells, whereas Arg2 is localized in mitochondria of kidney cells(10). NOS converts arginine into nitric oxide (NO) and citrulline. NO is an important gasotransmitter and activates soluble guanylate cyclase (sGC). Some studies suggest that activation of sGC attenuates fibrosis (11). In addition, NO can serve as a reductant to scavenge ROS and to inhibit the proliferation of aHSCs (12). Arginase catalyzes the reaction arginine + H_2O → ornithine + urea. Ornithine can be converted by ornithine aminotransferase (OAT) into proline and by ornithine decarboxylase (ODC) into polyamines. Proline is essential for collagen synthesis. Polyamines are necessary for progression through the cell cycle and proliferation (10). It has been demonstrated that arginine promotes the synthesis of proline and collagen in vascular smooth muscle cells, a cell type which could be considered the myofibroblast in vascular tissue (13). Since the catabolism of arginine by NOS and arginase are likely to induce opposite effects in HSCs, the metabolic fate of arginine is hypothesized to be associated with the transdifferentiation of HSCs. However, there is currently little evidence to support the hypothesis that (increased) arginase promotes fibrosis and (increased) NOS is attenuates fibrosis.

The differential expression of iNOS and Arg1 is associated with M1 and M2 polarization in macrophages, respectively (10). It has not been elucidated whether activation of HSCs is associated with a similar metabolic shift of arginine catabolism. Our hypothesis in this study is that the activation of HSC is accompanied by a metabolic shift in arginine catabolism. Primary rat HSCs are an established *in vitro* model to study the activation of hepatic stellate cells and were used in this study to test the hypothesis.

Materials and methods

Hepatic stellate cell isolation and culture

Primary rat hepatic stellate cells were isolated as previously described (14). Following isolation, HSCs were cultured in Iscove's Modified Dulbecco's Medium supplemented with Glutamax (Thermo Fisher Scientific, Waltham, MA, USA), 20% heat inactivated fetal calf serum (Thermo Fisher Scientific), 1% MEM Non Essential Amino Acids (Thermo Fisher Scientific), 1% Sodium Pyruvate (Thermo Fisher Scientific) and antibiotics: 50 µg/mL gentamycin (Thermo Fisher Scientific), 100 U/mL Penicillin (Lonza, Verviers, Belgium), 10 µg/mL streptomycin (Lonza) and 250 ng/mL Fungizone (Lonza) in an incubator containing 5% CO_2 at 37°C. HSCs were culture-activated for seven days on tissue culture plastic.

Quantitative Real-Time Polymerase Chain Reaction

Total RNA was isolated by Tri-reagent (Sigma Aldrich) according to manufacturer's protocol and then used for preparation of cDNA. cDNA was diluted in RNAse-free water and used for real-time polymerase chain reaction on the QuantStudioTM 3 system (Thermo Fisher Scientific). All samples were analyzed in duplicate using 36b4 as housekeeping gene. The genes were quantified by TaqMan probes and primers. Relative gene expression was calculated via the $2^{-\Delta\Delta Ct}$ or $2^{-\Delta Ct}$ method. The primers and probes are shown in Table 1.

Table1.

Gene	Sense 5'-3'	Antisense 5'-3'	Probe 5'-3'
36b4	GCTTCATTGTGGGAGCAGACA	CATGGTGTTCTTGCCCATCAG	TCCAAGCAGATGCAGCAGATCCGC
Col1α1	TGGTGAACGTGGTGTACAAGGT	CAGTATCACCCTTGGCACCAT	TCCTGCTGGTCCCCGAGGAAACA
Acta	GCCAGTCGCCATCAGGAAC	CACACCAGAGCTGTGC	CTTCACACATAGCTGGAGCA

2		TGTCTT	GCTTCTCGA
Nos 2	CTATCTCCATTCTACTACTAC CAGATCGA	CCTGGGCCTCAGCTTC TCAT	CCCTGGAAGACCCACATCTG G CAG
Arg1	AGCTGGGAATTGGCAAAGT G	TCCAGTCCATCAACATC AAAACTC	AATGGGCCTTTTCTTCCTTCC CAGCAG

Cell proliferation assays

Cell proliferation was determined by BrdU incorporation assay (Roche Diagnostic Almere, the Netherlands) and Real-Time xCelligence assay (RTCA DP; ACEA Biosciences, Inc., CA, USA). Cells were seeded in 96-well plates and treated as described. Incorporation of BrdU was detected by chemiluminescence using Synergy-4 (Bio-Tek).

Western blot analysis

Cells were seeded and treated as described. Protein lysates were prepared by scraping in cell lysis buffer (HEPES 25 mmol/L, KAc 150 mmol/L, EDTA pH 8.0 2 mmol/L, NP-40 0.1%, NaF 10 mmol/L, PMSF 50 mmol/L, aprotinin 1 µg/µL, pepstatin 1 µg/µL, leupeptin 1 µg/µL, DTT 1 mmol/L). 10-20 µg protein was loaded on SDS-PAGE gels and transferred to nitrocellulose transfer membranes using Trans-Blot Turbo Blotting System for tank blotting. Proteins were detected using the primary antibodies listed in table 2. Protein band intensities were determined and detected using the Chemidoc MR (Bio-Rad) system.

Table2.

Protein	Species	Dilution	Company
β-Actin	Polyclonal rabbit	1:1000	4970, Cell Signaling
Collagen type 1	Polyclonal goat	1:2000	1310-01, Southern Biotech
αSMA	Monoclonal mouse	1:5000	A5228, Sigma Aldrich
iNOS	Monoclonal mouse	1:2000	610432, BD Bioscience
Arg1	Monoclonal rabbit	1:2000	ab233548, Abcam

Statistical analysis

Data are presented as mean ± standard deviation (mean ± SD) or mean ± standard error of mean (mean ± sem) of at least three independent experiments. Statistical significance was analyzed by Mann-Whitney test between the two groups. $P<0.05$ was considered statistically significant. Analysis was performed using GraphPad Prism 7 (GraphPad Software, San Diego, CA, USA).

Results

Differential transcription of inducible nitric oxide synthase (iNOS) and arginase-1 (Arg1) during activation of hepatic stellate cells

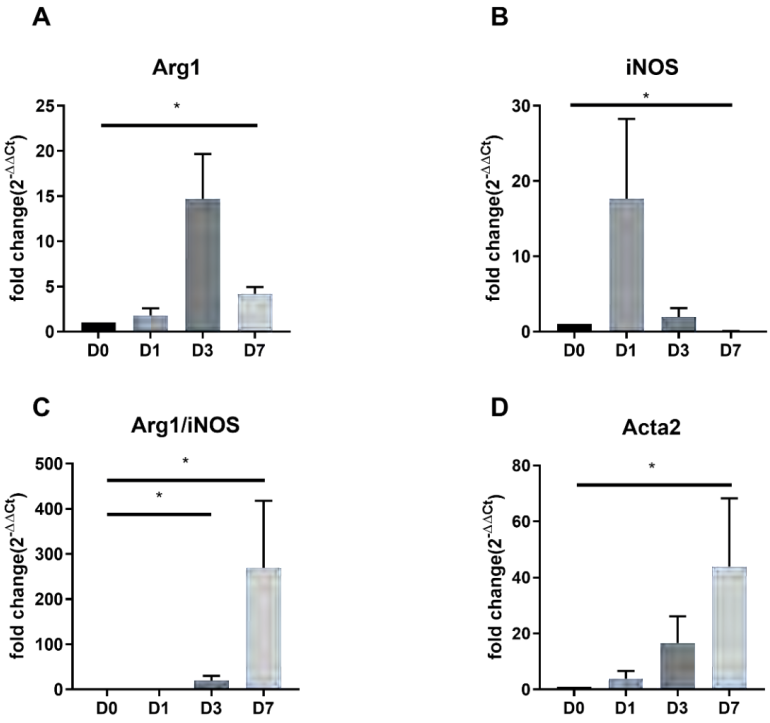

Figure 1. mRNA expression of iNOS, Arg1 and Acta2 during activation of primary rat HSCs.

Panel A: mRNA expression of Arg1. Panel B: mRNA expression of iNOS. Panel C: Ratio of mRNA expression of Arg1 to iNOS. Panel D: mRNA expression of Acta2. Data are shown as mean ± sem. n = 3, *p < 0.05.

mRNA level of Arg1 was increased up to 5 fold in aHSCs compared to qHSCs (Figure 1A). In contrast, mRNA level of iNOS was strongly diminished in activated HSCs (Fig. 1B) B. To illustrate the differential expression of Arg1 and iNOS, the ratio of Arg1 to iNOS was calculated. The ratio of Arg1 to iNOS was sharply increased during activation. These results demonstrate that arginine catabolizing enzymes exhibit differential transcription profiles in qHSCs and aHSCs. Activation of stellate cells at day 7 was confirmed by

measuring mRNA level of Acta2, an established marker of HSC activation (Fig. 1D).

Protein expression of arginine catabolizing enzymes

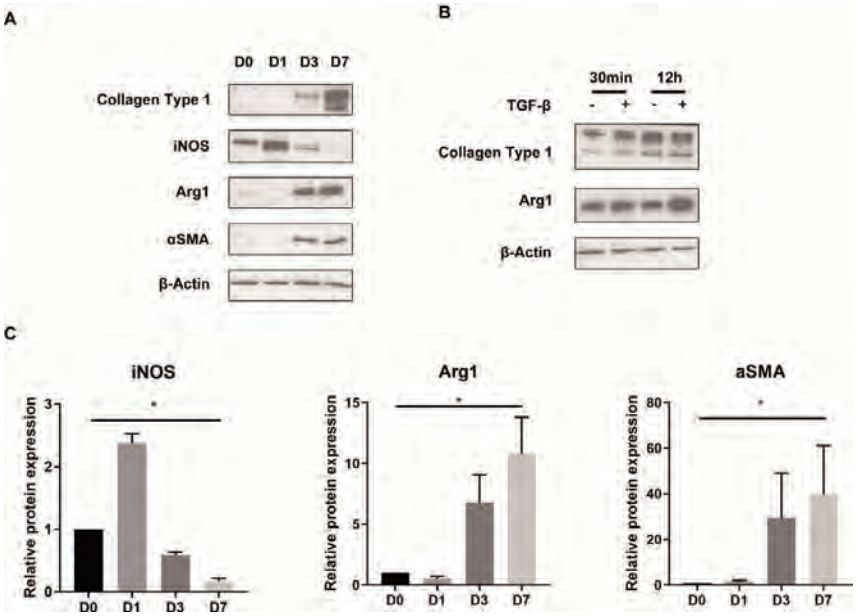

Figure 2. Panel A: Protein levels of the arginine catabolizing enzymes iNOS and Arginase 1 (Arg1) and the stellate cell activation makers α-smooth muscle actin (αSMA) and collagen

type 1. β-actin was used as loading control. n=3. Panel B: Protein expression of collagen type 1 and Arg1 in activated hepatic stellate cells treated with or without 5 ng/ml TGF-β. Panel C: Relative protein expression of iNOS, Arg1 and aSMA. Intensity of protein signals from repeated Western blotting was quantified and analyzed. Data are shown as mean ± sem, n =3.

In line with the mRNA levels, the protein level of iNOS was increased at day1 but strongly reduced at day 7 (Fig. 2A, C). Protein expression of Arg1 was increased at day 3 and appeared to be even more increased at day 7 (Fig. 2A, C). As expected, the protein levels of the activation markers collagen type 1 and αSMA were strongly induced in activated HSCs. In addition, in aHSCs (D7) treated with the pro-fibrogenic cytokine TGF-β demonstrated increased expression of Arg1 (Fig. 2B).

Inhibition of Arginase 1 reduces collagen production in activated hepatic stellate cells without affecting proliferation

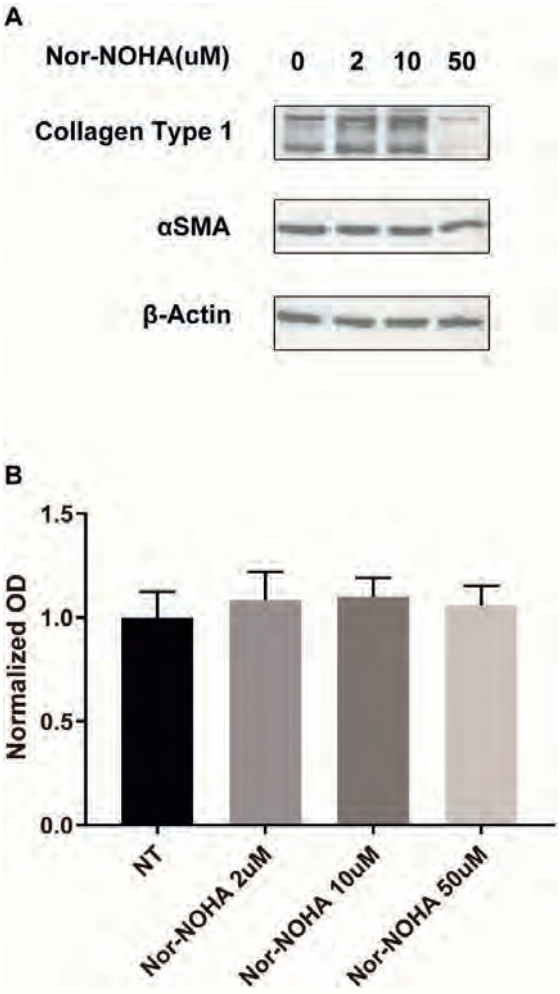

Figure 3. Effect of the Arg1 inhibitor Nor-NOHA on aHSCs.

Panel A: Western blot for collagen type 1 and αSMA in aHSCs treated with Nor-NOHA for 72h. Panel B. BrdU incorporation into aHSCs treated with Nor-NOHA for 72h. n=2.

Nor-NOHA is a reversible and specific inhibitor of arginase. Nor-NOHA was used to demonstrate the necessity of Arg1 for collagen production and proliferation of aHSCs. Nor-NOHA at 50 μmol/L significantly inhibited collagen type 1 protein level, but had no effect on αSMA protein expression (Fig. 3A). BrdU proliferation assay was performed to

verify the effect of Nor-NOHA on aHSCs. As shown in Fig. 3B Nor-NOHA at 2 μmol/L to 50 μmol/L did not affect HSC proliferation. These data demonstrate that arginase specifically affects collagen protein synthesis in HSCs.

Arginase inhibition reduces arginine-stimulated proliferation of hepatic stellate cells

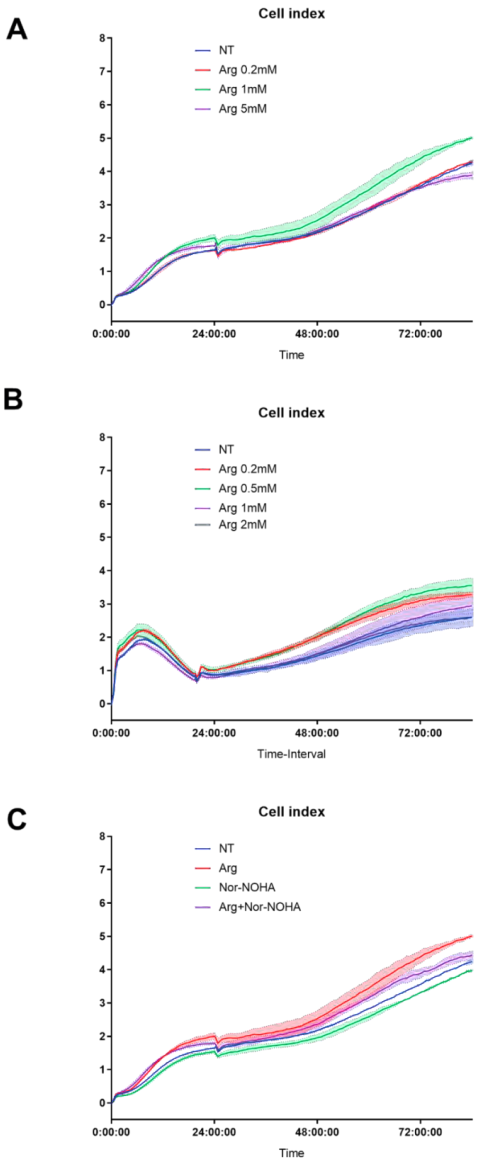

Figure 4. Cell proliferation of hepatic stellate cells treated with arginine and/or Nor-NOHA.

Panel A: Cell index of HSCs treated with different concentrations of arginine. Arginine (Arg) was added 24h after cell seeding. Panel B: HSCs cultured in arginine-deficient medium for 20h followed by culture in

low serum (1% FCS) medium with different concentrations of arginine. Panel C: Cell index of HSCs treated with arginine and/or Nor-NOHA. The concentrations of arginine and Nor-NOHA were 1 mmol/L and 100 μmol/L, respectively.

Polyamine synthesis is dependent on arginase catalyzing the conversion of arginine into ornithine. Therefore, addition of exogenous arginine may increase the synthesis of polyamines and promote cell proliferation. To verify this hypothesis, cell proliferation was analyzed in real-time in HSCs treated with 0.2-5 mmol/L L-arginine (Fig. 4A). Only 1 mmol/L arginine increased proliferation of HSCs. Since serum-containing culture medium contains significant amounts of arginine, we performed experiments using arginine starvationfollowed by low-serum containing culture medium (Fig. 4B). After arginine starvation, aHSCs appeared to be more sensitive to exogenous arginine with 0.5 mmol/L exogenous arginine maximally increased proliferation. Next, we investigated the effect of the arginase inhibitor nor-NOHA on the proliferation of HSCs (Fig. 4C). HSCs were treated with 1 mmol/L arginine with or without 100 μmol/L Nor-NOHA and the cell proliferation was analyzed. The arginase inhibitor only decreased proliferation of HSCs treated with arginine. The results indicate that exogenous arginine promotes cell proliferation of HSCs in an arginase-dependent manner.

Discussion

Activation of HSCs is a key pathogenetic mechanism in liver fibrosis. It has been demonstrated that clearance and/or inactivation of aHSCs is a therapeutic mechanism to alleviate or resolve liver fibrosis(4, 15). The activation of HSCs is driven by endogenous and exogenous factors. Extracellular mitogens, including TGF-β, PDGF, and FGF,activate qHSCs(4, 16). Upon activation, HSCs acquire the ability to secrete pro-fibrogenic mitogens and cytokines, causing a positive feedback loop in fibrogenesis (17). Endogenous factors that affect HSC activation include dysregulated intracellular processes like mitochondrial function, signal transduction pathways, autophagy etc. (18-20). Spontaneous activation of isolated primary HSCs on tissue culture plastic is well known model for HSC activation (21). Even though the exact mechanism of spontaneous activation is not fully elucidated yet, primary aHSCs share a highly similar phenotype with pathogenetic aHSCs (22). Increased expression of ACTA2 and COL1A1 and reduced expression of the quiescence-associated transcription factor PPARG and LRAT are characteristic for the transcription profile of aHSCs and is identical in culture activated HSCs and *in situ* activated HSCs (3, 22).

ECM deposition by aHSCs is the key mechanism of liver scar tissue formation. Arginine is a non-essential amino acid but it is conditionally essential during wound healing (23). Arginine is the exclusive substrate of NOS and arginase. NOS consists of three isoforms including iNOS, eNOS and nNOS. iNOS is an inducible NOS widely expressed in many cell types while eNOS and nNOS are specifically expressed in endothelium and neurons, respectively. Arginase has two isoforms Arg1 and Arg2. Arg1 is dominantly expressed in liver while Arg2 is dominantly expressed in kidney (10). NOS and arginase play opposite roles in the polarization of macrophages, with NOS promoting the M1 phenotype and Arginase the M2 phenotype (10). NO has been demonstrated to inhibit the proliferation of aHSCs and alleviate liver fibrosis (24). Activation of sGC, the downstream target of NO, has been demonstrated to suppress activation of HSCs as well (25). Ornithine, which is synthesized from arginine by arginase, is subsequently converted

by ODC and OAT into putrescine and proline, respectively. Putrescine is the main substrate for polyamine biosynthesis and is essential for cell cycle progression (26). Proline is the most abundant amino acid of collagen. The opposite roles of NOS and arginase on macrophage polarization is well-known. However, a shift in arginine catabolism between NOS and Arginase in the activation of HSCs has not been demonstrated. In this study, we have demonstrated that during activation of primary HSCs, the dominant catabolic enzyme of arginine shifts from iNOS to Arg1. The differential expression of iNOS and Arg1 was demonstrated both at the transcriptional (mRNA) and translational (protein) level. The differential expression of iNOS and Arg1 in HSC activation is in accordance with the function of proline in collagen production and polyamines in proliferation of aHSCs. Inhibition of NOS has been demonstrated to promote activation of fibroblasts and to prevent resolution of liver fibrosis (27, 28). In a rat model of wound healing induced by experimental surgical trauma, oral administration of arginine increased the systemic concentration of hydroxyproline, a marker of collagen production (29). Likewise, inhibition of Arg1 or OAT decreased the concentration of intracellular proline and reduces collagen synthesis in vascular smooth muscle cells and colonic epithelial cell (13, 30). Based on these studies, we hypothesized that the downregulation or inhibition of iNOS and the upregulation of Arg1 induces a switch in arginine catabolism that promotes activation of HSCs.

Since arginase activity determines proline and collagen synthesis and cell proliferation, inhibition of Arg1 could be a therapeutic method to alleviate hepatic fibrosis. N(omega)-hydroxy-nor-L-arginine (nor-NOHA) is a specific arginase inhibitor without inhibitory effects on NOS (31). Our results demonstrated that inhibition of Arg1 by Nor-NOHA reduced collagen production but did not affect cell proliferation at the same concentration. However, supplementation of arginine did increase proliferation of HSCs. Ornithine is an amino acid that is not present in proteins. It is synthesized from arginine by arginase. It has been observed that polyamine synthesis remains intact even when ornithine concentrations are reduced by the arginase inhibitor Nor-NOHA (32). Since ODC is the key enzyme in polyamine synthesis, we assumed that the ODC activity of aHSCs

was not as sensitive as OAT when intracellular concentration of ornithine is decreased by Nor-NOHA.

In conclusion, the activation of HSC is accompanied by a switch in arginine catabolism resulting from downregulation of iNOS and upregulation of Arg1. Inhibition of Arg1 can be an anti-fibrotic target for the treatment of liver fibrosis.

References

1. Schuppan D, Afdhal NH. Liver Cirrhosis. Lancet 2008;371:838-851.

2. Simeone JC, Bae JP, Hoogwerf BJ, Li Q, Haupt A, Ali AK, Boardman MK, et al. Clinical course of nonalcoholic fatty liver disease: an assessment of severity, progression, and outcomes. Clin Epidemiol 2017;9:679-688.

3. Kisseleva T. The origin of fibrogenic myofibroblasts in fibrotic liver. Hepatology 2017;65:1039-1043.

4. Tsuchida T, Friedman SL. Mechanisms of hepatic stellate cell activation. Nat Rev Gastroenterol Hepatol 2017;14:397-411.

5. Friedman SL. Hepatic stellate cells: protean, multifunctional, and enigmatic cells of the liver. Physiol Rev 2008;88:125-172.

6. Bedossa P, Patel K. Biopsy and Noninvasive Methods to Assess Progression of Nonalcoholic Fatty Liver Disease. Gastroenterology 2016;150:1811-1822.e1814.

7. Angulo P, Kleiner DE, Dam-Larsen S, Adams LA, Bjornsson ES, Charatcharoenwitthaya P, Mills PR, et al. Liver Fibrosis, but No Other Histologic Features, Is Associated With Long-term Outcomes of Patients With Nonalcoholic Fatty Liver Disease. Gastroenterology 2015;149:389-397 e310.

8. Frantz C, Stewart KM, Weaver VM. The extracellular matrix at a glance. J Cell Sci 2010;123:4195-4200.

9. Li P, Wu G. Roles of dietary glycine, proline, and hydroxyproline in collagen synthesis and animal growth. Amino Acids 2018;50:29-38.

10. Bronte V, Zanovello P. Regulation of immune responses by L-arginine metabolism. Nat Rev Immunol 2005;5:641-654.

11. Sandner P, Stasch JP. Anti-fibrotic effects of soluble guanylate cyclase stimulators and activators: A review of the preclinical evidence. Respir Med 2017;122 Suppl 1:S1-S9.

12. Svegliati-Baroni G, Saccomanno S, van Goor H, Jansen P, Benedetti A, Moshage H. Involvement of reactive oxygen species and nitric oxide radicals in activation and proliferation of rat hepatic stellate cells. Liver 2001;21:1-12.

13. Durante W, Liao L, Reyna SV, Peyton KJ, Schafer AI. Transforming growth factor-beta(1) stimulates L-arginine transport and metabolism in vascular smooth muscle cells: role in polyamine and collagen synthesis. Circulation 2001;103:1121-1127.

14. Damba T, Zhang M, Buist-Homan M, van Goor H, Faber KN, Moshage H. Hydrogen sulfide stimulates activation of hepatic stellate cells through increased cellular bio-energetics. Nitric Oxide 2019;92:26-33.

15. Troeger JS, Mederacke I, Gwak GY, Dapito DH, Mu X, Hsu CC, Pradere JP, et al. Deactivation of hepatic stellate cells during liver fibrosis resolution in mice. Gastroenterology 2012;143:1073-1083 e1022.

16. Liu C, Li J, Xiang X, Guo L, Tu K, Liu Q, Shah VH, et al. PDGF receptor-alpha promotes TGF-beta signaling in hepatic stellate cells via transcriptional and posttranscriptional regulation of TGF-beta receptors. Am J Physiol Gastrointest Liver Physiol 2014;307:G749-759.

17. Li HY, Ju D, Zhang DW, Li H, Kong LM, Guo Y, Li C, et al. Activation of TGF-beta1-CD147 positive feedback loop in hepatic stellate cells promotes liver fibrosis. Sci Rep 2015;5:16552.

18. Thoen LF, Guimaraes EL, Dolle L, Mannaerts I, Najimi M, Sokal E, van Grunsven LA. A role for autophagy during hepatic stellate cell activation. J Hepatol 2011;55:1353-1360.

19. Gajendiran P, Vega LI, Itoh K, Sesaki H, Vakili MR, Lavasanifar A, Hong K, et al. Elevated mitochondrial activity distinguishes fibrogenic hepatic stellate cells and sensitizes for selective inhibition by mitotropic doxorubicin. J Cell Mol Med 2018;22:2210-2219.

20. Du Z, Lin Z, Wang Z, Liu D, Tian D, Xia L. SPOCK1 overexpression induced by platelet-derived growth factor-BB promotes hepatic stellate cell activation and liver fibrosis through the integrin alpha5beta1/PI3K/Akt signaling pathway. Lab Invest 2020.

21. Zhai X, Wang W, Dou D, Ma Y, Gang D, Jiang Z, Shi B, et al. A novel technique to prepare a single cell suspension of isolated quiescent human hepatic stellate cells. Sci Rep 2019;9:12757.

22. Liu X, Rosenthal SB, Meshgin N, Baglieri J, Musallam SG, Diggle K, Lam K, et al. Primary Alcohol-Activated Human and Mouse Hepatic Stellate Cells Share Similarities in Gene-Expression Profiles. Hepatol Commun 2020;4:606-626.

23. Wu G, Bazer FW, Davis TA, Kim SW, Li P, Marc Rhoads J, Carey Satterfield M, et al. Arginine metabolism and nutrition in growth, health and disease. Amino Acids 2009;37:153-168.

24. Failli P, De FR, Caligiuri A, Gentilini A, Romanelli RG, Marra F, Batignani G, et al. Nitrovasodilators inhibit platelet-derived growth factor-induced proliferation and migration of activated human hepatic stellate cells. Gastroenterology 2000;119:479-492.

25. Hall KC, Bernier SG, Jacobson S, Liu G, Zhang PY, Sarno R, Catanzano V, et al. sGC stimulator praliciguat suppresses stellate cell fibrotic transformation and inhibits fibrosis and inflammation in models of NASH. Proc Natl Acad Sci U S A 2019;116:11057-11062.

26. Mandal S, Mandal A, Johansson HE, Orjalo AV, Park MH. Depletion of cellular polyamines, spermidine and spermine, causes a total arrest in translation and growth in mammalian cells. Proc Natl Acad Sci U S A 2013;110:2169-2174.

27. Sciacca M, Belgorosky D, Zambrano M, Gomez Escalante JI, Roca F, Langle YV, Sandes EO, et al. Inhibition of breast tumor growth by N(G)-nitro-l-arginine methyl ester (l-NAME) is accompanied by activation of fibroblasts. Nitric Oxide 2019;93:34-43.

28. Lukivskaya O, Patsenker E, Lis R, Buko VU. Inhibition of inducible nitric oxide synthase activity prevents liver recovery in rat thioacetamide-induced fibrosis reversal. Eur J Clin Invest 2008;38:317-325.

29. Shi HP, Wang SM, Zhang GX, Zhang YJ, Barbul A. Supplemental L-arginine enhances wound healing following trauma/hemorrhagic shock. Wound Repair Regen 2007;15:66-70.

30. Singh K, Coburn LA, Barry DP, Boucher JL, Chaturvedi R, Wilson KT. L-arginine uptake by cationic amino acid transporter 2 is essential for colonic epithelial cell restitution. Am J Physiol Gastrointest Liver Physiol 2012;302:G1061-1073.

31. Pudlo M, Demougeot C, Girard-Thernier C. Arginase Inhibitors: A Rational Approach Over One Century. Med Res Rev 2017;37:475-513.

32. Reid KM, Tsung A, Kaizu T, Jeyabalan G, Ikeda A, Shao L, Wu G, et al. Liver I/R injury is improved by the arginase inhibitor, N(omega)-hydroxy-nor-L-arginine (nor-NOHA). Am J Physiol Gastrointest Liver Physiol 2007;292:G512-517.

Chapter 8

General Discussion

General Discussion

Decompensating cirrhosis is the final outcome of progressive liver fibrosis. As the most advanced stage of chronic liver disease, decompensated cirrhosis causes more than 1 million deaths per year globally. Liver fibrosis is the intermediate stage of chronic liver disease. Liver fibrosis is still reversible, but can also progress to cirrhosis, deteriorating the prognosis of patients. To minimize the incidence of cirrhosis, liver fibrosis is targeted as the last interventional phase due to the reversibility of this stage (1). Liver resident cells, including hepatocytes, macrophages, sinusoidal endothelial cells, hepatic stellate cells (HSC) and infiltrating inflammatory cells all contribute to the pathogenesis of fibrogenesis. Uncontrolled fibrogenesis caused by activated HSC disrupts the normal architecture of the liver and exacerbates liver dysfunction, thus constituting a vicious cycle advancing to the final stages of chronic liver diseases (2).

The characteristic histology of liver fibrosis is fibrous expansion ranging from perisinusoidal fibrosis to bridging fibrosis (3). HSCs are the most important cells that produce ECM in the fibrotic liver. Upon chronic injury, quiescent HSCs (qHSCs) transdifferentiate into myofibroblasts, a process termed activation (2). Compared to qHSCs, activated HSC (aHSC) proliferate and synthesize large amounts of ECM components, notably collagens. (4). Recent preclinical evidence has demonstrated that targeting HSC to reduce the number of aHSCs or decrease HSC activation is a way to attenuate liver fibrosis (5, 6). In addition, liver fibrosis can be spontaneously reversed when the injurious stimuli are removed (7). Activated HSCs that are “inactivated” to a quiescence-like phenotype have a transcriptomic profile that is different from qHSCs and aHSCs (8). This type of HSCs is termed inactivated HSCs (iHSCs).

Various mechanisms are involved in the activation and inactivation of HSC. In this dissertation, a few promising mechanisms and therapeutic targets were investigated and elucidated. In **chapter 2**, biomarkers, mechanisms and consequences of cellular senescence were reviewed and the concept of therapy-induced senescence was introduced as a promising strategy to alleviate fibrogenesis. In **chapter 3**, the bioactive

compound esculetin was shown to decrease the activation of HSC by inducing senescence via a mechanism that involves the PI3K-Akt-GSK3β pathway. In **chapter 4**, the bioenergetic effect of H_2S was demonstrated to promote the activation of HSC. In **chapter 5,** we demonstrated that inhibition of H_2S induces HSC senescence and decreases HSC activation and fibrogenesis. In **chapter 6**, the broad-spectrum anti-fibrotic drug pirfenidone was shown to inhibit proliferation and collagen production in primary intestinal fibroblasts via the TGF-β/mTOR axis. In **chapter 7**, differential expression of the arginine-metabolizing enzymes inducible Nitric Oxide Synthase (iNOS) and Arginase1 (ARG1) in activating HSC was investigated and it was shown that the increased expression of Arg1 was associated with HSC activation and inhibition of Arg1 decreased collagen synthesis. Details of the results and their implications for future research and therapy are discussed in the next paragraphs.

Cellular Senescence of Hepatic Stellate Cells in Liver Fibrosis: A Review of Characteristics, Mechanisms and Consequences

Cellular senescence is defined as a state of permanent cell cycle arrest (9). Senescent cells have been identified in fibrotic livers (10). Senescent cells cultured *in vitro* have a different morphology: cells become flattened and nuclei are enlarged. In addition, senescent cells exhibit increased senescence-associated beta-galactosidase (SA-β-Gal) activity, shortened or dysfunctional telomeres, elevated expression levels of $P21^{CIP1}$ and $P16^{INK4A}$ and hypophosphorylated Retinoblastoma protein (RB), senescence-associated heterochromatin foci (SAHF) and a senescence-associated secretory phenotype (SASP) (9). These characteristic biomarkers are commonly used to identify senescent cells, but it should be noted that not all the biomarkers are simultaneously detectable in all senescent cells.

Several mechanisms are involved in cellular senescence. The DNA damage response can trigger the initiation of cellular senescence (11). NF-κB activation is essential for senescence progression and SASP secretion (12, 13). Persistent PI3K-Akt

activation, associated with GSK3β and mTOR kinases, regulates the negative cell cycle regulators $P21^{CIP1}$ and SASP (14-16). Furthermore, mTOR complexes, including mTORC1 and mTORC2, autophagy, oxidative stress, gasotransmitters like hydrogen sulfide, the STAT3 signaling pathway, all impact on senescence as discussed in detail in **chapter 2**.

HSCs are the main source of senescent cells in experimental models of fibrosis (17). Senescent HSC are characterized by a defective ability to proliferate and reduced fibrogenic properties, as well as enhanced chemotaxis to natural killer cells (17). It has been shown that the ability of HSCs to enter senescence is essential to slow down the progression of liver fibrosis (17, 18). In addition to HSCs, hepatocytes can also undergo cellular senescence in chronic liver diseases (10). In general, senescence is a tumor-suppressing mechanism. However, senescent hepatocytes can escape the senescent state and re-enter the cell cycle, becoming pre-malignant and promote tumorigenesis (19).

Therapy-induced senescence has been described in the response of tumor cells to CDK4/6 inhibitors (20). Recently, it has been demonstrated that bioactive compounds and cytokines, including curcumin and interleukin-22, can trigger HSC senescence to alleviate liver fibrosis (18, 21). Inducing transient senescence of HSC to treat liver fibrosis could be an attractive therapeutic strategy, but more studies are needed to completely elucidate the role of senescence in the pathogenesis of liver fibrosis. Important remaining issues are detrimental effects of inducing senescence on other liver cell types, notably hepatocytes, and the clearance of senescent HSCs by immune cells, notably NK cells.

The heterogeneous phenotype of senescent cells and the limited availability of specific biomarkers is a barrier to translate *in vitro* results to the *in vivo* situation (9). SA-β-Galactosidase staining is the most common method to detect senescent cells *in vivo*. However, the constitutive expression of β-Galactosidase in macrophages may be a confounder and lead to an overestimation of senescent cells on histological screening (22, 23). Senescent cells may contribute to the maintenance of the function of injured tissue and (acute) elimination of senescent cells might disrupt this delicate balance (24). The

dynamics of elimination of senescent cells and regeneration of non-senescent cells may therefore be an important factor in the outcome of integrative therapy. A thorough study of the timing of administration of inducers of senescence and senolytics is therefore very important.

Bioactive coumarin-derivative esculetin decreases HSC activation via induction of cellular senescence via the PI3K-Akt-GSK3β pathway

Esculetin is a bioactive compound, which has been shown to attenuate high fat diet-induced hepatic steatosis and inflammation (25) and to arrest cell proliferation of tumor cells (26). In **chapter 2**, therapy-induced senescence was proposed as a possible therapeutic strategy to treat liver fibrosis. In **chapter 3**, esculetin was investigated as a candidate to induce HSC senescence. Esculetin increased markers of senescence in both qHSCsand aHSCs: the number of SA-β-Gal positive cells and mRNA transcription of *Cdkn1a* and *Il6* were both increased by esculetin treatment. SA-β-Gal staining is a well-established marker of senescent cells *in vitro* and *in vivo*. *Cdkn1a* encodes the cell cycle negative regulator $P21^{Cip1}$, which is a downstream target of P53. IL-6 is one of the SASP molecules. Esculetin-treated HSCs also showed reduced expression of activation and fibrogenic markers, including αSMA and Collagen type 1. Interestingly, esculetin-induced senescence was not accompanied by restoration of the expression of the quiescence marker *Lrat*, demonstrating that senescent HSCs are not identical to qHSCs.

Serum contains growth factors that induce cell cycle progression and cell division. Senescent cells have lost the ability to respond to growth factors. Non-proliferating esculetin-treated aHSCs remain unresponsive to serum-derived growth factors as shown by the wash-out studies in **chapter 3**. We used PCNA, a scaffold protein that allows DNA polymerase to bind to DNA and initiates DNA replication, as a marker of an intact cell cycle. (27). Esculetin treatment dramatically reduced PCNA expression in the subsequent wash-out incubation, demonstrating that the arrested cell proliferation of aHSCs was

irreversible. In line with this, SA-β-Gal staining and transcription of *Cdkn1a*, *Il6* and *Mmp9*, all indicators of HSC senescence, were also not reversed after esculetin wash-out, indicating the long-lasting effect of esculetin in decreasing the activation of HSCs. It has been demonstrated that co-culture of senescent cells and non-senescent cells will induce senescence in the non-senescent cells(28). This phenomenon in which progression of cellular senescence is independent of its inducer has been termed cell-non-autonomous senescence. It is driven by the paracrine action of released SASP molecules. The phenomenon might favor a stable and long-lasting effect on the inhibition of HSC activation and fibrogenesis.

PI3K-Akt activity has been demonstrated to be involved in cellular senescence. Phosphorylation of Ser9 on GSK3β, a well-established downstream target of Akt, is positively correlated with cellular senescence (15, 29). Inhibition of Akt and GSK3β exerts an inhibitory effect on the induction of cellular senescence. In line with this, we demonstrated that esculetin-induced senescence is dependent on an intact PI3K-Akt-GSK3β axis. As expected, non-selective inhibition of PI3K restored the ability of collagen synthesis and cell proliferation. These results demonstrate the causal association between induction of HSC senescence and deficient fibrogenesis. Hence, therapy-induced senescence may be a promising strategy in the treatment of liver fibrosis.

As a coumarin derivative, esculetin may have effects on Vitamin K-dependent enzymes. This has been well-described for the coumarin-derivative warfarin. Vitamin K is involved in various essential physiological process. Vitamin K serves as a co-factor in the posttranslational modification executed by γ-glutamyl carboxylase (GGCX) in which specific glutamic acid residues (Glu) are converted into γ-carboxyglutamate (Gla).(30). Warfarin is widely used as anti-coagulation medication in cardiovascular diseases because of its powerful inhibitory effect on the hepatic synthesis of coagulation factors II, VII, IX, X and the anticoagulant proteins C and S (31). In addition, Vitamin K has anti-inflammatory and anti-oxidant properties independent of GGCX, which implies that Vitamin K may have effects on aging and senescence (30). A subclinical deficiency of Vitamin K has been demonstrated in patients with cystic fibrosis (32). However, the role of

Vitamin K in liver fibrosis is not clear. Furthermore, excessive exposure to the Vitamin K analog menadione induces oxidative stress in hepatocytes (33). Therefor it is important to elucidate the effect of esculetin on Vitamin K metabolism and to consider potential side effects. Esculetin can be converted into scopoletin and isoscopoletin by Catechol-O-methyltransferase (COMT) (34). Some studies demonstrated that scopoletin can attenuate hepatic steatosis, but its effect on fibrosis is not clear (35, 36). Unpublished data from our laboratory demonstrated that scopoletin has no anti-proliferative or anti-fibrogenic effects on rat HSCs *in vitro*. COMT degrades catecholamines, such as dopamine and epinephrine. Inhibitors of COMT are used in the treatment of Parkinson's disease (37). Considering the relation between COMT and esculetin, (genetic) variations in the expression of COMT may influence the pharmacokinetic half-life of esculetin and its anti-fibrotic effects. However, the pattern of expression and activity of COMT in the natural history of liver fibrosis has not been elucidated yet. High-fat diet decreases protein expression of COMT in the liver and COMT inhibitors enhance hepatic steatosis, which suggests a role for COMT in this metabolic disorder (38). Therefore, various experimental models of chronic liver disease may be needed to identify indications for the clinical use of esculetin. The potential effect of esculetin on catecholamine metabolism also needs to be investigated.

Hydrogen sulfide stimulates activation of hepatic stellate cells through increased cellular bio-energetics

Hydrogen sulfide is an essential gasotransmitter involved in various (patho)physiological processes. E.g. H_2S mediated S-sulfhydration of Kelch-like ECH-associated protein (KEAP1) facilitates dissociation of Nuclear erythroid 2-related factor 2 (Nrf2) from KEAP1(39). In **chapter 4**, the association between hydrogen sulfide-stimulated mitochondrial bioenergetics and HSC activation was investigated. During the activation of HSC, the expression of the hydrogen sulfide-synthesizing enzymes Cystathionine gamma-lyase (*Cth*) and Mercaptopyruvate sulfurtransferase

(*Mpst*) were increased, while expression of *Cbs* was reduced. Despite the reduced expression of *Cbs,* the net result was increased endogenous hydrogen sulfide production. Hydrogen sulfide donors release H_2S with different kinetics. Fast-releasing donors are represented by NaHS and slow-releasing donors by GYY4137. Proliferation of HSC was increased by H_2S donors and decreased by H_2S inhibitors. Inhibition of endogenous production of H_2S decreased collagen synthesis. However, hydrogen sulfide donors did not affect transcription and translation of collagen type 1. These results indicate that local production of H_2S in HSCs promotes fibrogenesis, probably by stimulating mitochondrial bioenergetics.

In general, H_2S is regarded as a redox regulator that activates the Nrf2-dependent anti-oxidant pathway (40, 41). Oxidative stress (ROS) causes hepatocyte damage and death and contributes to fibrosis. Therefore, it was expected that H_2S was anti-fibrogenic. However, our results revealed a HSC-specific profibrogenic effect of H_2S. We speculate that the decreased H_2S production of hepatocytes during fibrogenesis outweighs the increased H_2S production of HSCs. To support this hypothesis, mRNA expression of H_2S-producing enzymes was measured and the results supported our hypothesis: mRNA expression of *Cth*, *Cbs* and *Mpst* was decreased in fibrotic liver tissue. TGF-β is a well-known cytokine known to promote liver fibrosis. Interestingly, TGF-β decreased the expression of all H_2S-producing enzymes in hepatocytes, but it increased *Cth* expression in aHSCs. The opposite response to TGF-β between HSCs and hepatocytes could be due to cell-specific metabolic effects of H_2S. Since H_2S has a pro-fibrogenic effect on HSCs, specific inhibition of H_2S production in HSCs may be a therapeutic strategy to alleviate liver fibrosis.

Inhibition of endogenous hydrogen sulfide reduces hepatic stellate cells activation via induction of cellular senescence

Induction of HSC senescence decreased the activation of HSC as reported in **chapter 3**. In **chapter 4,** we demonstrated that H_2S promotes HSC proliferation via

improving mitochondrial bioenergetics. In addition, inhibitors of H_2S production exhibited anti-proliferative effects on aHSCs. Therefore, we hypothesized that inhibition of H_2S production could induce HSC senescence. TGF-β is the well-established pro-fibrotic cytokine that activates HSC. In **chapter 4**, we demonstrated that *Cth* expression wasincreased by TGF-β. The CTH inhibitor DL-PAG was used to inhibit the activity of CTH and block the production of H_2S. Interestingly, DL-PAG also inhibited the expression of CTH. DL-PAG reduced both mRNA transcription and protein production of collagen type 1 in aHSCs. Senescence markers were increased in aHSCs treated with DL-PAG. In addition, DL-PAG permanently arrested proliferation of aHSCs. GYY4137, the slow-releasing H_2S donor, restored the proliferation ability of aHSCs and decreased markers of cellular senescence. Moreover, we demonstrated that DL-PAG-induced HSC senescence was dependent on an intact PI3K-Akt pathway, in accordance with the mechanism of esculetin-induced senescence, described in **chapter 3**.

Knockout of the *Cth* gene in mouse embryonic myofibroblasts leads to lack of H_2S generation and initiates cellular senescence (41). In line with this, DL-PAG, the inhibitor of Cth, decreases CTH expression and H_2S production of aHSCs and leads to senescence. The anti-senescence effect of H_2S has been demonstrated in senescent endothelial cells to be the result of mitochondrial dysfunction (42). H_2S is capable to increase NAD^+ levels to improve mitochondrial activity (43). In **chapter 4**, we also demonstrated that H_2S improved the bioenergetics of HSC mitochondria. H_2S has been demonstrated to increase Akt activity in cell lines and to modulate cell proliferation. In our results, the effect of H_2S was also shown to be mediated by the PI3K-Akt pathway. These results indicate the association between PI3K-Akt signaling and mitochondrial activity in cellular senescence. The causal association between HSC senescence and decreased fibrogenesis supports the idea that the H_2S-synthesizing enzyme CTH can be a HSC-specific target for drug development to alleviate liver fibrosis.

Hepatocytes contain much higher levels of H_2S producing enzymes than HSCs and are therefore also the major cell type responsible for hepatic H_2S production. On the other hand, CTH is the key enzyme accounting for H_2S production in aHSCs, but HSCs are not

the major H_2S producing cell type in the liver (44). DL-PAG is an amino acid analog of glycine which irreversibly inhibits the enzyme CTH. CTH knock-out mice as well as DL-PAG-treated wildtype mice have a delayed onset of diabetes (45). Likewise, CTH deletion protects mice against inflammation and acute liver injury and maintains the fenestration of liver sinusoidal endothelial cells (46). In addition, our results demonstrate that CTH inhibition induces HSC senescence but this cannot be completely reversed by supplementation of H_2S. Therefore, CTH may have effects that are independent of H_2S. The evidence indicates that the products of CTH, including α-ketobutyrate, cysteine and H2S, may have different targets and effects. α-Ketobutyrate administration has been shown to increase autophagy and attenuate aging-induced hair loss in mice (47). Interestingly, α-ketobutyrate maintains cell proliferation when mitochondrial respiration is inhibited (48). However, the role of α-ketobutyrate in chronic liver diseases remains to be elucidated. It can be hypothesized that endogenous α-ketobutyrate, in conjunction with H_2S, maintains mitochondrial respiration. These data suggest that CTH may also be an interesting therapeutic target in the treatment of chronic liver diseases.

Pirfenidone Inhibits Cell Proliferation and Collagen I Production of Primary Human Intestinal Fibroblasts

Pirfenidone is a broad-spectrum anti-fibrotic drug, which has been demonstrated to reduce fibrogenesis in lung, liver and kidney. It has been approved for the treatment of idiopathic pulmonary fibrosis (49). Both in experimental models of liver fibrosis and in clinical practice, pirfenidone is sufficient to reduce fibrogenesis and attenuate inflammation (50, 51). Intestinal fibrosis is correlated with the deterioration of inflammatory bowel disease (IBD). Anti-fibrotic treatments have been shown to alleviate IBD in preclinical models (52). In line with this, pirfenidone has been suggested to be a potential therapeutic candidate in the treatment of IBD.

Pirfenidone decreases fibrogenesis via inhibition of the TGF-β signaling pathway (53). TGF-β is known to induce fibrogenesis in various organs and to regulate the inflammatory

response in chronic diseases. TGF-β has been shown to activate SMAD3 to promote collagen synthesis in various models of fibrosis. In addition, TGF-β has been shown to modulate additional signaling pathways, including P38/MAPK, ERK/JNK and mTOR (54).

To fully understand the anti-fibrotic mechanism of pirfenidone in intestinal fibrosis, primary human intestinal fibroblasts were used as an *in vitro* model. We show that pirfenidone dose-dependently inhibited proliferation and collagen synthesis of intestinal fibroblasts. The effect of pirfenidone is not associated with cellular senescence since pirfenidone did not induce irreversible cell cycle arrest in intestinal fibroblasts. Pirfenidone did reduce mTOR/P70S6K signaling, which was activated by TGF-β. Similarly, rapamycin, an established mTOR inhibitor, decreased TGF-β-increased collagen production. We concluded that the effect of pirfenidone was associated with inhibiting the TGF-β/mTOR/P70S6K axis.

Increased arginase-1 expression during hepatic stellate cell activation promotes fibrogenesis

Arginine is a non-essential amino acid in adults, but conditionally essential in infants. It is the exclusive substrate of two enzymes: Nitric Oxide Synthase (NOS) and arginase. NOS converts arginine into citrulline and nitric oxide (NO), whereas arginase converts arginine into ornithine. In turn, ornithine is the substrate for both Ornithine Decarboxylase (ODC), which leads to the production of polyamines and Ornithine Aminotransferase (OAT) ,which leads to the production of proline (55). NO is a well-known gasotransmitter that activates soluble guanylate cyclase (sGC). It has been demonstrated that activation of the NO-sGC pathway decreases the activation of HSCs and prevents liver fibrosis (56). Polyamines are necessary for cell cycle progression. Proline is the most abundant amino acid in collagen and therefore essential for collagen biosynthesis. The concentration of proline is tightly controlled by arginase activity. Intracellular synthesis of proline is dependent on arginase activity (57, 58). Dietary supplementation of L-arginine increases plasma concentration of proline (59). In contrast, deficient Arg1 activity decreases plasma

concentration of proline (60). Differential expression of iNOS and Arg1 is a well-known characteristic of macrophage polarization with high iNOS expression being associated with the pro-inflammatory M1 phenotype and high Arg1 expression with the pro-fibrogenic M2 phenotype. (61). In view of the opposite effect of their metabolites, the arginine catabolizing enzymes are likely to modulate transdifferentiation of HSCs. Our results show that during transdifferentiation/activation, HSCs increase mRNA and protein expression of Arg1 and gradually decrease the expression of iNOS, resulting in a strong increase in the ratio of Arg1 to iNOS in fully activated HSCs. This increased Arg1/iNOS ratio correlated with increased expression of the activation markers αSMA and Collagen type 1 in aHSCs. The change of arginine catabolism promotes proliferation and collagen synthesis of HSCs. To verify whether arginase activity is necessary for cell proliferation and collagen synthesis in HSCs, the arginase inhibitor, Nor-NOHA, was used to block the arginase activity. As expected, the arginase inhibitor decreased collagen synthesis. However, the arginase inhibitor only decreased cell proliferation in conditions of extra arginine supplementation. These results indicate different sensitivities of OAT and ODC in response to decreased ornithine concentrations. Collectively, the results demonstrate that the arginine metabolic pathway is a promising therapeutic target to treat liver fibrosis.

Conclusions

Hepatic stellate cells are the main effector cells in the formation of fibrous tissue in liver injury caused by various etiologies. Induction of HSC senescence, e.g. by esculetin, could be a therapeutic strategy to attenuate progression of liver fibrosis. Intact Akt activity is essential to induce senescence. H_2S is an important gasotrasmitter that promotes bioenergetics of HSCs and decreases cellular senescence. Conversely, inhibition of H_2S-producing enzymes induces HSC senescence in an Akt-dependent manner. The TGF-β/mTOR signaling pathway is the target of pirfenidone in the inhibition of proliferation and collagen synthesis in intestinal fibroblasts. During HSC activation, the arginine metabolism is profoundly altered by a change in the ratio of the arginine metabolizing

enzymes iNOS and Arg1 in aHSCs. Inhibition of arginase decreases collagen synthesis and arginine-dependent cell proliferation in HSCs.

References

1. Schuppan D, Afdhal NH. Liver Cirrhosis. Lancet 2008;371:838-851.

2. Tsuchida T, Friedman SL. Mechanisms of hepatic stellate cell activation. Nat Rev Gastroenterol Hepatol 2017.

3. Goodman ZD. Grading and staging systems for inflammation and fibrosis in chronic liver diseases. J Hepatol 2007;47:598-607.

4. Shang L, Hosseini M, Liu X, Kisseleva T, Brenner DA. Human hepatic stellate cell isolation and characterization. J Gastroenterol 2018;53:6-17.

5. Zhang J, Li Y, Liu Q, Huang Y, Li R, Wu T, Zhang Z, et al. Sirt6 alleviated liver fibrosis by deacetylating conserved lysine 54 on Smad2 in hepatic stellate cells. Hepatology 2020.

6. Choi YY, Seok JI, Hwang JI, Kim DS. Co-administration of everolimus and N-acetylcysteine attenuates hepatic stellate cell activation and hepatic fibrosis. Am J Transl Res 2020;12:2627-2639.

7. Ellis EL, Mann DA. Clinical evidence for the regression of liver fibrosis. J Hepatol 2012;56:1171-1180.

8. Liu X, Xu J, Rosenthal S, Zhang LJ, McCubbin R, Meshgin N, Shang L, et al. Identification of Lineage-Specific Transcription Factors That Prevent Activation of Hepatic Stellate Cells and Promote Fibrosis Resolution. Gastroenterology 2020;158:1728-1744 e1714.

9. Sharpless NE, Sherr CJ. Forging a signature of in vivo senescence. Nat Rev Cancer 2015;15:397-408.

10. Paradis V, Youssef N, Dargere D, Ba N, Bonvoust F, Deschatrette J, Bedossa P. Replicative senescence in normal liver, chronic hepatitis C, and hepatocellular carcinomas. Hum Pathol 2001;32:327-332.

11. d'Adda di Fagagna F, Reaper PM, Clay-Farrace L, Fiegler H, Carr P, Von Zglinicki T, Saretzki G, et al. A DNA damage checkpoint response in telomere-initiated senescence. Nature 2003;426:194-198.

12. Shao AW, Sun H, Geng Y, Peng Q, Wang P, Chen J, Xiong T, et al. Bclaf1 is an important NF-kappaB signaling transducer and C/EBPbeta regulator in DNA damage-induced senescence.

Cell Death Differ 2016;23:865-875.

13. Salminen A, Kauppinen A, Kaarniranta K. Emerging role of NF-kappaB signaling in the induction of senescence-associated secretory phenotype (SASP). Cell Signal 2012;24:835-845.

14. Huy H, Song HY, Kim MJ, Kim WS, Kim DO, Byun JE, Lee J, et al. TXNIP regulates AKT-mediated cellular senescence by direct interaction under glucose-mediated metabolic stress. Aging Cell 2018;17:e12836.

15. Kim YY, Jee HJ, Um JH, Kim YM, Bae SS, Yun J. Cooperation between p21 and Akt is required for p53-dependent cellular senescence. Aging Cell 2017;16:1094-1103.

16. Astle MV, Hannan KM, Ng PY, Lee RS, George AJ, Hsu AK, Haupt Y, et al. AKT induces senescence in human cells via mTORC1 and p53 in the absence of DNA damage: implications for targeting mTOR during malignancy. Oncogene 2012;31:1949-1962.

17. Krizhanovsky V, Yon M, Dickins RA, Hearn S, Simon J, Miething C, Yee H, et al. Senescence of activated stellate cells limits liver fibrosis. Cell 2008;134:657-667.

18. Kong X, Feng D, Wang H, Hong F, Bertola A, Wang FS, Gao B. Interleukin-22 induces hepatic stellate cell senescence and restricts liver fibrosis in mice. Hepatology 2012;56:1150-1159.

19. Wang C, Chen WJ, Wu YF, You P, Zheng SY, Liu CC, Xiang D, et al. The extent of liver injury determines hepatocyte fate toward senescence or cancer. Cell Death Dis 2018;9:575.

20. Yoshida A, Diehl JA. CDK4/6 inhibitor: from quiescence to senescence. Oncoscience 2015;2:896-897.

21. Jin H, Jia Y, Yao Z, Huang J, Hao M, Yao S, Lian N, et al. Hepatic stellate cell interferes with NK cell regulation of fibrogenesis via curcumin induced senescence of hepatic stellate cell. Cell Signal 2017;33:79-85.

22. Amor C, Feucht J, Leibold J, Ho YJ, Zhu C, Alonso-Curbelo D, Mansilla-Soto J, et al. Senolytic CAR T cells reverse senescence-associated pathologies. Nature 2020;583:127-132.

23. Lee BY, Han JA, Im JS, Morrone A, Johung K, Goodwin EC, Kleijer WJ, et al. Senescence-associated beta-galactosidase is lysosomal beta-galactosidase. Aging Cell 2006;5:187-195.

24. Grosse L, Wagner N, Emelyanov A, Molina C, Lacas-Gervais S, Wagner KD, Bulavin DV. Defined p16(High) Senescent Cell Types Are Indispensable for Mouse Healthspan. Cell Metab

2020;32:87-99 e86.

25. Pandey A, Raj P, Goru SK, Kadakol A, Malek V, Sharma N, Gaikwad AB. Esculetin ameliorates hepatic fibrosis in high fat diet induced non-alcoholic fatty liver disease by regulation of FoxO1 mediated pathway. Pharmacol Rep 2017;69:666-672.

26. Turkekul K, Colpan RD, Baykul T, Ozdemir MD, Erdogan S. Esculetin Inhibits the Survival of Human Prostate Cancer Cells by Inducing Apoptosis and Arresting the Cell Cycle. J Cancer Prev 2018;23:10-17.

27. Boehm EM, Gildenberg MS, Washington MT. The Many Roles of PCNA in Eukaryotic DNA Replication. Enzymes 2016;39:231-254.

28. Nelson G, Wordsworth J, Wang C, Jurk D, Lawless C, Martin-Ruiz C, von Zglinicki T. A senescent cell bystander effect: senescence-induced senescence. Aging Cell 2012;11:345-349.

29. Iwagami Y, Huang CK, Olsen MJ, Thomas JM, Jang G, Kim M, Lin Q, et al. Aspartate beta-hydroxylase modulates cellular senescence through glycogen synthase kinase 3beta in hepatocellular carcinoma. Hepatology 2016;63:1213-1226.

30. Simes DC, Viegas CSB, Araújo N, Marreiros C. Vitamin K as a Powerful Micronutrient in Aging and Age-Related Diseases: Pros and Cons from Clinical Studies. International Journal of Molecular Sciences 2019;20:4150.

31. Lurie Y, Loebstein R, Kurnik D, Almog S, Halkin H. Warfarin and vitamin K intake in the era of pharmacogenetics. British Journal of Clinical Pharmacology 2010;70:164-170.

32. Hatziparasides G, Loukou I, Moustaki M, Douros K. Vitamin K and cystic fibrosis: A gordian knot that deserves our attention. Respiratory Medicine 2019;155:36-42.

33. Conde de la Rosa L, Vrenken TE, Buist-Homan M, Faber KN, Moshage H. Metformin protects primary rat hepatocytes against oxidative stress-induced apoptosis. Pharmacol Res Perspect 2015;3:e00125.

34. Zhao Y, Wang N, Sui Z, Huang C, Zeng Z, Kong L. The Molecular and Structural Basis of O-methylation Reaction in Coumarin Biosynthesis in Peucedanum praeruptorum Dunn. International Journal of Molecular Sciences 2019;20:1533.

35. Lee HI, Yun KW, Seo KI, Kim MJ, Lee MK. Scopoletin prevents alcohol-induced hepatic lipid accumulation by modulating the AMPK-SREBP pathway in diet-induced obese mice.

Metabolism 2014;63:593-601.

36. Choi R-Y, Ham JR, Lee H-I, Cho HW, Choi M-S, Park S-K, Lee J, et al. Scopoletin Supplementation Ameliorates Steatosis and Inflammation in Diabetic Mice. Phytotherapy Research 2017;31:1795-1804.

37. Silva TB, Borges F, Serrão MP, Soares-da-Silva P. Liver says no: the ongoing search for safe catechol O-methyltransferase inhibitors to replace tolcapone. Drug Discovery Today 2020.

38. Kanasaki M, Srivastava SP, Yang F, Xu L, Kudoh S, Kitada M, Ueki N, et al. Deficiency in catechol-o-methyltransferase is linked to a disruption of glucose homeostasis in mice. Scientific Reports 2017;7.

39. Zhao S, Song T, Gu Y, Zhang Y, Cao S, Miao Q, Zhang X, et al. Hydrogen sulfide alleviates liver injury via S-sulfhydrated-Keap1/Nrf2/LRP1 pathway. Hepatology 2020.

40. Corsello T, Komaravelli N, Casola A. Role of Hydrogen Sulfide in NRF2- and Sirtuin-Dependent Maintenance of Cellular Redox Balance. Antioxidants (Basel) 2018;7.

41. Yang G, Zhao K, Ju Y, Mani S, Cao Q, Puukila S, Khaper N, et al. Hydrogen sulfide protects against cellular senescence via S-sulfhydration of Keap1 and activation of Nrf2. Antioxid Redox Signal 2013;18:1906-1919.

42. Latorre E, Torregrossa R, Wood ME, Whiteman M, Harries LW. Mitochondria-targeted hydrogen sulfide attenuates endothelial senescence by selective induction of splicing factors HNRNPD and SRSF2. Aging (Albany NY) 2018;10:1666-1681.

43. Sanokawa-Akakura R, Akakura S, Tabibzadeh S. Replicative Senescence in Human Fibroblasts Is Delayed by Hydrogen Sulfide in a NAMPT/SIRT1 Dependent Manner. PLoS One 2016;11:e0164710.

44. Damba T, Zhang M, Buist-Homan M, van Goor H, Faber KN, Moshage H. Hydrogen sulfide stimulates activation of hepatic stellate cells through increased cellular bio-energetics. Nitric Oxide 2019;92:26-33.

45. Yang G, Tang G, Zhang L, Wu L, Wang R. The pathogenic role of cystathionine gamma-lyase/hydrogen sulfide in streptozotocin-induced diabetes in mice. Am J Pathol 2011;179:869-879.

46. Gaddam RR, Fraser R, Badiei A, Chambers S, Cogger VC, Le Couteur DG, Ishii I, et al.

Cystathionine-Gamma-Lyase Gene Deletion Protects Mice against Inflammation and Liver Sieve Injury following Polymicrobial Sepsis. PLoS One 2016;11:e0160521.

47. Chai M, Jiang M, Vergnes L, Fu X, de Barros SC, Doan NB, Huang W, et al. Stimulation of Hair Growth by Small Molecules that Activate Autophagy. Cell Rep 2019;27:3413-3421 e3413.

48. Sullivan LB, Gui DY, Hosios AM, Bush LN, Freinkman E, Vander Heiden MG. Supporting Aspartate Biosynthesis Is an Essential Function of Respiration in Proliferating Cells. Cell 2015;162:552-563.

49. Marcos Ribes B, Sancho-Chust JN, Talens A, Arlandis M, Herraiz P, Chiner E, Aznar T. Effectiveness and safety of pirfenidone for idiopathic pulmonary fibrosis. European Journal of Hospital Pharmacy 2019:ejhpharm-2018-001806.

50. Flores-Contreras L, Sandoval-Rodriguez AS, Mena-Enriquez MG, Lucano-Landeros S, Arellano-Olivera I, Alvarez-Alvarez A, Sanchez-Parada MG, et al. Treatment with pirfenidone for two years decreases fibrosis, cytokine levels and enhances CB2 gene expression in patients with chronic hepatitis C. BMC Gastroenterol 2014;14:131.

51. Garcı´a L, Hernández I, Sandoval A, Salazar A, Garcia J, Vera J, Grijalva G, et al. Pirfenidone effectively reverses experimental liver fibrosis. Journal of Hepatology 2002;37:797-805.

52. Latella G, Rieder F. Intestinal fibrosis: ready to be reversed. Curr Opin Gastroenterol 2017;33:239-245.

53. Stahnke T, Kowtharapu BS, Stachs O, Schmitz KP, Wurm J, Wree A, Guthoff RF, et al. Suppression of TGF-beta pathway by pirfenidone decreases extracellular matrix deposition in ocular fibroblasts in vitro. PLoS One 2017;12:e0172592.

54. Biernacka A, Dobaczewski M, Frangogiannis NG. TGF-beta signaling in fibrosis. Growth Factors 2011;29:196-202.

55. Wu G, Bazer FW, Davis TA, Kim SW, Li P, Marc Rhoads J, Carey Satterfield M, et al. Arginine metabolism and nutrition in growth, health and disease. Amino Acids 2009;37:153-168.

56. Hall KC, Bernier SG, Jacobson S, Liu G, Zhang PY, Sarno R, Catanzano V, et al. sGC stimulator praliciguat suppresses stellate cell fibrotic transformation and inhibits fibrosis and inflammation in models of NASH. Proc Natl Acad Sci U S A 2019;116:11057-11062.

57. Durante W, Liao L, Reyna SV, Peyton KJ, Schafer AI. Transforming growth factor-beta(1) stimulates L-arginine transport and metabolism in vascular smooth muscle cells: role in polyamine and collagen synthesis. Circulation 2001;103:1121-1127.

58. Singh K, Coburn LA, Barry DP, Boucher JL, Chaturvedi R, Wilson KT. L-arginine uptake by cationic amino acid transporter 2 is essential for colonic epithelial cell restitution. Am J Physiol Gastrointest Liver Physiol 2012;302:G1061-1073.

59. Yang Y, Wu Z, Jia S, Dahanayaka S, Feng S, Meininger CJ, McNeal CJ, et al. Safety of long-term dietary supplementation with L-arginine in rats. Amino Acids 2015;47:1909-1920.

60. Sin YY, Ballantyne LL, Mukherjee K, St Amand T, Kyriakopoulou L, Schulze A, Funk CD. Inducible arginase 1 deficiency in mice leads to hyperargininemia and altered amino acid metabolism. PLoS One 2013;8:e80001.

61. Murray PJ. Macrophage Polarization. Annu Rev Physiol 2017;79:541-566.

Appendices

Abbreviations

Summary and Nederlandse Samenvatting

Acknowledgement

About the author

Abbreviations

aHSC	Activated HSC
aHSCs	Activated HSCs
αSMA	Alpha-smooth muscle actin
ARG1	Arginase-1
ARG2	Arginase-2
ACTA2	Alpha actin 2
ATM	Ataxia-Telangiectasia Mutated
ATR	ATM- and Rad3-related
ALD	Alcoholic liver disease
BDL	Bile duct ligation
Bio-Rad	Bio-Rad protein assay
COL1A1	Collagen type 1 alpha-1
CTGF	Connective tissue growth factor
CSE	Cystathionine γ-lyase
CBS	Cystathionine β-synthase
CMA	Chaperone-mediated autophagy
CBS	Cystathionine β-synthase
CTH/CSE	Cystathionine -lyase
CCl4	Carbon tetrachloride
CBS	Cystathionine β-synthase
CTH	Cystathionine γ-lyase
CO	Carbon monoxide
COMT	Catechol-O-methyltransferase
CDKs	Cyclin dependent kinases
cGMP	Cyclic guanosine monophosphate
DDR	DNA-damage response

DL-PAG	DL-propargylglycine
DATS	Diallyl trisulfide
eNOS	Endothelial NOS
ECM	Extracellular matrix
ECAR	Extra-Cellular Acidification Rate
ECM	Excessive extracellular matrix
GFAP	Glial fibrillary acidic protein
GSK3	Glycogen Synthase Kinase 3
G-CSF	Granulocyte colony-stimulating factor
GAPDH	Glyceraldehyde 3-phosphate dehydrogenase
GGCX	γ -glutamyl carboxylase
Glu	Glutamic acid residues
Gla	γ-carboxyglutamate
HSCs	Hepatic stellate cells
HMGA	High-mobility group A
H3K4me3	Histone 3 lysine 4 trimethylation
H_2S	Hydrogen sulfide
iHSCs	Inactivated HSCs
IBD	Inflammatory bowel diseases
IPF	Idiopathic pulmonary fibrosis
iNOS	Inducible nitric oxide synthase
IBD	Inflammatory bowel disease
IKK	IKB kinase
KEAP1	Kelch-like ECH-associated protein
LRAT	Lecithin retinol acyltransferase
LADs	Lamin-associated domains
LAMP2a	Lysosomeassociated membrane protein type 2a
mTOR	Mammalian target of rapamycin
MSCs	Mesenchymal stromal cells

mean± SD	Mean ± standard deviation
mean± sem	Mean ± standard error of means
MPST	3-mercaptopyruvate sulfur transferase
mTOR	The mammalian target of rapamycin
Mpst	Mercaptopyruvate sulfurtransferase
MAFLD	Metabolic Associated Fatty Liver Disease
MRN	Mre11-Rad50-Nbs1
NAFLD	Non-alcoholic fatty liver disease
NAS CRN	Non-alcoholic Steatohepatitis Clinical Research Network
NASH CRN	NASH Clinical Research Network
NAD+	Nicotinamide adenine dinucleotide
NAFLD	Non-alcoholic fatty liver disease
NO	Nitric oxide
NOS	Nitric Oxide Synthases
Nrf2	Nuclear factor E2-related factor 2
NF-κB	Nuclear factor kappa B
Nrf2	Nuclear erythroid 2-related factor 2
nor-NOHA	N(omega)- hydroxy-nor-L-arginine
nNOS	Neuronal NOS
ODC	Ornithine decarboxylase
OPTN	Optineurin
OCR	Oxygen Consumption Rate
ODC	Ornithine Decarboxylase
OAT	Ornithine Aminotransferase
PDGF	Platelet-derived growth factor
PI3K	Phosphoinositide 3-kinases
PKC	Protein kinase C
PFs	Portal fibroblasts
PDGFRβ	Platelet-derived growth factor receptor-β

PPARG	Peroxisome proliferator-activated receptor gamma
PARP	Poly (ADP)ribose polymerase
PI3K	Phosphatidylinositol-3-kinase
pS473	Phospho-Ser473
pT308	Phospho Thr308
PIKK	PI3K-related kinase
PLP-	pyridoxal-5'-phosphate-
PCNA	Proliferating cell nuclear antigen
PDGF-BB	Platelet-derived growth factor BB
PDGF	Growth factors
p-hIFs	Primary human intestinal fibroblasts
qHSCs	Quiescent hepatic stellate cells
RB	Retinoblastoma protein
RCTA	Real-Time Cell Analysis
ROS	Reactive oxygen species
RT-qPCR	Reverse transcription PCR
ROS	Oxidative stress
STAT	Signal Transducers and Activators of Transcription
SA-β-Gal	Senescence Associated β-Galactosidase
SASP	Senescence-Associated Secretory Phenotype
SAHF	Senescence-Associated heterochromatin foci
SGC	Soluble guanylate cyclase
SOX	SRY-related HMG-box
SOCS3	Suppressor of cytokine signaling 3
SREBP	Sterol responsive element binding protein
TGF-β	Transforming growth factor beta
TGFβ	Transforming growth factor
3-MST	3-mercaptopyruvate sulfurtransferase
UPR	Unfolded protein response

WST-1	Water Soluble Tetrazolium Salt-1

Summary

In chapter 1, the essential role of hepatic stellate cell activation in the pathogenesis of live fibrosis was introduce. The activated hepatic stellate cells are the main precursor of myofibroblasts. Targeting hepatic stellate cells can be the way to prevent or reverse liver fibrosis.

In chapter 2, senescence of hepatic stellate cells was interpreted as a protective mechanism against liver fibrosis progression. The biomarkers, signaling pathways and probable effects of hepatic stellate cells senescence was elucidated. Among various biomarkers, we proposed that P21 (cell-cycle arrest), Senescence-associated β Galactosidase (lysosomal mass), Interleukin-6 (senescence-associated secretory phenotype) could be used as biomarkers to identify senescent hepatic stellate cells. The pathogenic role of hepatic stellate cell senescence was not fully elucidated. Therapy-induced senescence of hepatic stellate cells followed by senolytics may be an optimized strategy to attenuate liver fibrosis.

In chapter 3, a coumarin derivative, esculetin was demonstrated to induce senescence in hepatic stellate cells. With increased senescent hepatic stellate cells, collagen production and cell proliferation were inhibited. Senescent hepatic stellate cells acquired resistance to be reverted to active proliferation. The effect of esculetin was dependent on PI3K-Akt-GSK3β signaling pathway.

In chapter 4, differential expression of H_2S producing enzymes were determined during the activation of hepatic stellate cells and determined in bile duct ligation rats. The cystathionine γ-lyase (CTH) was increased accompanied by activation of hepatic stellate cells, while the other enzymes cystathionine β-synthase (CBS) and 3-mercaptopyruvate sulfur transferase (MPST) were decreased in vitro and in vivo. However, the endogenous H_2S was demonstrated to be increased in activated hepatic stellate cells. The H_2S inhibitor was shown to decrease cell proliferation and collagen synthesis whereas H_2S donor was shown to increase cell proliferation. The mechanism of H_2S promoting hepatic stellate cell activation was associated with improvement of mitochondrial bioenergetics.

In chapter 5, The hypothesis of inducing senescence via inhibiting H_2S to decrease fibrogenic potential of hepatic stellate cells was investigated. CTH inhibitor DL -Propargylglycine (PAG) was demonstrated to decrease cell proliferation and collagen synthesis of hepatic stellate cells via inducing senescence. The senescent phenotype of hepatic stellate cells can be partially decreased via exogenos H_2S and PI3K inhibitor.

In chapter 6, the broad-spectrum anti-fibrotic drug pirfenidone was investigated the anti-fibrotic effect on primary human intestinal fibroblasts. Pirfenidone was demonstrated to reversibly decrease cell proliferation and collagen production of intestinal fibroblasts. The mechanism of pirfenidone was not associated with induction of cellular senescence or apoptosis. The mechanism of pirfenidone was demonstrated to be associated with TGF-β1/mTOR/p70S6K signaling pathway.

In chapter 7, differential expression of arginine metabolizing enzymes iNOS (inducible Nitric Oxide Synthase) and ARG1 (Arginase-1) were determined during activation of hepatic stellate cells. iNOS was decreased and ARG1 was increased during the activation of hepatic stellate cells. ARG1 inhibitor Nor-NOHA was shown to decrease collagen production and cell proliferation in arginine-dependent manner.

In chapter 8, the results and further steps of research were discussed. Therapy-induced senescence of hepatic stellate cells may be a promising strategy to alleviate liver fibrosis. But senolytics should be considered as combination therapy to avoid potential pro-inflammatory effect of senescent hepatic stellate cells. To further investigate the effect of esculetin in vivo, Vitamin K-dependent coagulation factors should be investigated to determine the potential side effect and Catechol-O-methyltransferase (COMT) dependent metabolism may dampen effect of esculetin via influencing its pharmacokinetics. Among H_2S producing enzymes, CTH may be a promising target for the treatment of liver fibrosis. And the byproduct of CTH α-ketobutyrate needs to be further investigated. Pirfenidone has been verified to alleviate intestinal fibrosis in vitro. But various model of liver fibrosis should be considered to testify the effect of pirfenidone before clinical application. Arginine metabolizing change was demonstrated in the activation of hepatic stellate cells. Increased expression of ARG1 can be a promising

therapy target for the treatment of liver fibros

Nederlandse Samenvatting

Hoofdstuk 1 introduceert de cruciale rol van de activatie van stellaatcellen in de lever bij het ontstaan van leverfibrose. Geactiveerde lever-stellaatcellen zijn de belangrijkste precursors van myofibroblasten. Therapie gericht op lever-stellaatcellen kan leverfibrose voorkomen of omkeren.

In hoofdstuk 2 wordt de veroudering van lever-stellaatcellen geïnterpreteerd als een mechanisme dat beschermt tegen de progressie van leverfibrose. De biomarkers, signaalroutes en waarschijnlijke effecten van de veroudering van lever-stellaatcellen worden toegelicht. We stellen voor dat de biomarkers P21 (stilstand van de celcyclus), senescentie-geassocieerd β-galactosidase (lysosomale inhoud), en interleukine-6 (senescentie-geassocieerd secretoir fenotype) gebruikt kunnen worden omverouderde lever-stellaatcellen te identificeren. Ondanks dat de veroudering van lever-stellaatcellen nog niet volledig is opgehelderd, kan therapie-geïnduceerde veroudering van lever-stellaatcellen, gevolgd door senolytica, een optimale strategie zijn voor het tegengaan van leverfibrose.

In hoofdstuk 3 wordt aangetoond dat esculetine, een cumarine-derivaat, de veroudering van lever-stellaatcellen veroorzaakt en blijkt dat bij verouderde lever-stellaatcellen, de collageenproductie en celproliferatie zijn verminderd. Verouderde lever-stellaatcellen ontwikkelen bovendien resistentie tegen een terugkeer naar actieve proliferatie. Het effect van esculetine blijkt afhankelijk van de PI3K/AKT/GSK3β-signaalroute.

In hoofdstuk 4 is de differentiële expressie van H_2S-producerende enzymen bepaald tijdens de activatie van lever-stellaatcellen in ratten die aan ligatie van de galgang zijn onderworpen. Tijdens dit proces nam de expressie van cystathionine γ-lyase (CTH) toe, en ging gepaard met de activatie van lever-stellaatcellen; de expressie van de enzymen cystathionine β-synthase (CBS) en 3-mercaptopyruvaat zwaveltransferase (MPST) nam juist af, zowel in vitro als in vivo. In geactiveerde lever-stellaatcellen bleek echter een endogene H_2S-toename. Daarnaast bleek dat de H_2S-remmer celproliferatie en

collageensynthese verminderde, terwijl de H_2S-donor celproliferatie verhoogde. Het mechanisme dat de activatie van lever-stellaatcellen door H_2S bevordert, kan leiden tot een verbeterde mitochondriale bio-energetica.

In hoofdstuk 5 wordt de hypothese onderzocht dat veroudering van lever-stellaatcellen door middel van H_2S-remming hun fibrogene potentie kan verminderen. Zo blijkt dat de CTH-remmer DL-propargylglycine (PAG), door veroudering te induceren, de celproliferatie van en collageensynthese door lever-stellaatcellen verminderde. Het verouderd fenotype van lever-stellaatcellen kan gedeeltelijk verminderd worden door exogeen H_2S en een PI3K-remmer.

In hoofdstuk 6 wordt het effect van het breedspectrum antifibrotischgeneesmiddel pirfenidon op primaire humane darmfibroblasten bestudeerd. Zo blijkt dat pirfenidon de celproliferatie van en de collageenproductie door darmfibroblasten reversibel vermindert. De werking van pirfenidon blijkt niet samen te hangen met de inductie van cellulaire veroudering of apoptose, maar wel met de TGF-β1/mTOR/p70S6K signaal-route.

In hoofdstuk 7 wordt de differentiële expressie van de arginine-metaboliserende enzymen iNOS (induceerbaar stikstofmonoxide synthase) en ARG1 (arginase-1) tijdens de activatie van lever-stellaatcellen bepaald. Hieruit blijkt dat de expressie van iNOS was verlaagd en die van ARG1 verhoogd. Daarnaast blijkt dat de ARG1-remmer nor-NOHA de collageenproductie en celproliferatie op een arginine-afhankelijke wijze verlaagt.

In hoofdstuk 8 worden de resultaten besproken evenals stappen om het onderzoek voort te zetten. Therapie-geïnduceerde veroudering van lever-stellaatcellen kan een veelbelovende strategie zijn om leverfibrose te verlichten. Daarbij moeten senolytica overwogen worden als combinatietherapie om potentiële pro-ontstekingseffecten van verouderde lever-stellaatcellen te voorkomen. Om het effect van esculetine in vivo nader te bestuderen, moeten vitamine K-afhankelijke stollingsfactoren onderzocht worden om zo mogelijke bijwerkingen vast te stellen. Tegelijkertijd moet er rekening mee worden gehouden dat metabolisme afhankelijk van catechol-O-methyltransferase (COMT) het effect van esculetine kan verzwakken omdat dit de farmacokinetiek hiervan beïnvloedt. Van de H_2S-producerende enzymen is CTH een veelbelovend target voor de behandeling

van leverfibrose. Het bijproduct van CTH, α-ketobutyraat, moet echter nog nader onderzocht worden. Het is in ieder geval aangetoond dat pirfenidon darmfibrose in vitro verbetert. Er moeten echter meerdere leverfibrosemodellen overwogen worden om het effect van pirfenidon te bevestigen voordat er sprake kan zijn van klinische toepassing. Dit onderzoek toont ook een arginine-metaboliserende verandering tijdens de activatie van lever-stellaatcellen aan. Een verhoogde expressie van ARG1 kan eveneens een veelbelovend target zijn voor de behandeling van leverfibrose.

Acknowledgement

It is a great challenge for me to obtain a PhD degree. The whole journey turns out to be a team work after four years. In the end I must say I can't finish it without great effort and support from my mentors, colleagues, friends and family. Hereby, I want to express my deepest gratitude to all of you.

First of all, I want to express my sincere appreciation to Prof. dr. Han Moshage. Thank you for leading me the way to biological research. In the beginning of PhD program, I was worried about whether I could manage it. During the four years, you have been always kind to support and encourage me to try my ideas, even though most of them turned out to be naïve and pointless. Supervised by you, I have gained much more fun than frustration from research.

I would also like to express my gratitude to Prof. dr. Klaas Nico Faber. I can sense your enthusiasm to scientific research. Your questions and ideas help me a lot to improve the quality of my research and learn to interpret the results and phenomenon in the scientific world.

My sincere appreciation to the members of assessment committee and Prof. dr. Marco Demaria, Prof. dr. Janette Burgess and Prof. dr. Derek Mann for reading and approving my thesis.

Dear MDLers, thanks for your support over the years. Manon, most of time I suddenly bothered you, but you were always kind to lend a hand. And my grateful thanks for the help and support from Dianne, Tjasso, Janette and Sofie. Turu, it was my fortune that we worked and learnt together over the years. Sandra, thanks a lot for the help with isolating hepatic stellate cells. Zongmei, thank you for helping me continuing the uncompleted projects. Fabio, it was very nice to have you around to share the ideas. Johanna, you were always ready to give your helping hand. Yana, it was nice working with you. Yingying, I must say I also leant a lot from your questions. And I express my gratitude to Natalia, Ali, Rapheal, Defu, Emilia and Erick. And I also express my thanks to Archie, Sandra, Herson, Rumei and Tian in the Y2.117 for the pleasant cookies and memories.

I gratefully thank my dear friends. Turu, Fabio and Angela, thank you for distracting me from my monotonous life style. Yingying and Changsen, I could always have authentic Henan recipe at your home. That really eased my nostalgia. Yang, it was great fun we gathered at your houseboat. Weiteng and Yukun, it was a pleasant time we lived in a very nice house together. Qingqing, thanks for your concern and I appreciated you sharing delicious food and excellent games with me. Yuan, I appreciated we shared similar interest about the classical music and your advices helped me a lot. Yi, you were so kind helping me. My heartful thanks also belongs to my dear friends Chenghao Yang, Huifang Yin, Yanyan Fu, Yuxin Fu, Xiaodong Feng, Zheng Wang, Shipeng Chen, Mengfei Cai, Tian Xie, Peng Wang, Hong Lian, Yan Zhou, Lin Chen, Wenze Guo, Jin Li, Yingying Wu and Wangzhao Song. It was my great luck to meet you and share joyful moments with you in Groningen.

My dear paranymphs Zongmei and Sandra, thanks for your help with the defense.

My deepest gratitude belongs to my family. My dear father, mother and sister, thanks for your concerning all the time. If not in such pandemic situation, I would have you all here to join my ceremony.

After four years, I can still recall the feeling I had when I first step on the land of the Netherlands. That was a mixture of curiosity, excitement and a bit fear. When I reflect on the days of being a PhD candidate in Groningen, that feeling has been unconsciously knitted into my four-year memory. I am fortunate that people around always help me and care about me during the time. With your help, I can overcome the difficulties in the journey. With your care, I can bear the loneliness in the life. With sincere gratitude, I thank all of you.

About the author

Mengfan Zhang was born on July 15, 1989 in Henan. From Sep, 2008 to July, 2013, he studied medicine in Zhengzhou University and obtained a bachelor of medicine. He continued to obtain a master of medicine in the First Affiliated Hospital of Zhengzhou University on July, 2016. During the master program, he focused on the clinical research about efficacy of interventional radiological procedures on hepatocellular carcinoma and portal hypertension. With a scholarship from China Scholarship Council, He was enrolled in a PhD program from Nov, 2016 in the Department of Gastroenterology and Hepatology, University Medical Center Groningen, University of Groningen. His research was focused on the targeting molecular mechanisms of hepatic stellate cells in the pathogenesis of liver fibrosis. From Dec, 2020, He will work as a junior physician in the Department of Interventional Radiology, the First Affiliated Hospital of Zhengzhou University.

List of publications

1. Y. Cui, **M. Zhang**, C. Leng, T. Blokzijl, B.H. Jansen, G. Dijkstra, K.N. Faber, Pirfenidone Inhibits Cell Proliferation and Collagen I Production of Primary Human Intestinal Fibroblasts, Cells 9 (2020).

2. T. Damba, **M. Zhang**, M. Buist-Homan, H. van Goor, K.N. Faber, H. Moshage, Hydrogen sulfide stimulates activation of hepatic stellate cells through increased cellular bio-energetics, Nitric Oxide 92 (2019) 26-33.

3. X.H. Duan, **M.F. Zhang**, J.Z. Ren, X.W. Han, P.F. Chen, K. Zhang, Z.L. Jia, Urgent transcatheter arterial embolization for the treatment of ruptured renal angiomyolipoma with spontaneous hemorrhage, Acta Radiol 57 (2016) 1360-1365.

4. J.Z. Ren, **M.F. Zhang**, A.M. Rong, X.J. Fang, K. Zhang, G.H. Huang, P.F. Chen, Z.Y. Wang, X.H. Duan, X.W. Han, Y.J. Liu, Lower gastrointestinal bleeding: role of 64-row computed tomographic angiography in diagnosis and therapeutic planning, World J Gastroenterol 21 (2015) 4030-7.

5. T.F. Li, G.H. Huang, Z. Li, C.F. Hao, J.Z. Ren, X.H. Duan, K. Zhang, C. Chen, X.W. Han, D.C. Jiao, **M.F. Zhang**, Y.L. Wang, Percutaneous transhepatic cholangiography and intraductal radiofrequency ablation combined with biliary stent placement for malignant biliary obstruction, J Vasc Interv Radiol 26 (2015) 715-21.

6. T.F. Li, X.H. Duan, Z. Li, J.Z. Ren, K. Zhang, G.H. Huang, X.W. Han, D.C. Jiao, **M.F. Zhang**, Endovascular embolization for managing anastomotic bleeding after stapled digestive tract anastomosis, Acta Radiol 56 (2015) 1368-72.

7. X. Duan, K. Zhang, X. Han, J. Ren, M. Xu, G. Huang, **M. Zhang**, Comparison of percutaneous transhepatic variceal embolization (PTVE) followed by partial splenic embolization versus PTVE alone for the treatment of acute esophagogastric variceal massive hemorrhage, J Vasc Interv Radiol 25 (2014) 1858-65.